AN OSTEOLOGICAL DOCUMENTATION OF HYBRID WILDEBEEST AND ITS BEARING ON BLACK WILDEBEEST (*CONNOCHAETES GNOU*) EVOLUTION

By

Bonita De Klerk

A dissertation submitted to the Faculty of Science, University of the Witwatersrand, Johannesburg, in fulfilment of the requirements for the degree of Master of Science.

Johannesburg, 2007.

DECLARATION

I declare that this dissertation is my own, unaided work. It is submitted for the Degree of Master of Science at the University of the Witwatersrand, Johannesburg. It has not been submitted before for any degree or examination in any other University.

Signature: _____

Date: _____

ABSTRACT

Wildebeest are part of the sub family Alcelaphinae and the genus *Connochaetes*. There are two extant species of wildebeest namely *Connochaetes gnou* (black wildebeest) and *Connochaetes taurinus* (blue wildebeest). From fossil evidence, it is thought that co-generic blue and black wildebeest diverged *ca*. 1Ma. Historically, geographic ranges of these two species have overlapped, but different social behaviour and habitat preference prevented sexual interaction. It has been proposed that reproductive isolation between *C. taurinus* and *C. gnou* may have disappeared due to artificial management. This has caused mate choice to change in the absence of species-specific mates, resulting in hybridisation. Most documented cases of hybridisation have occurred from dispersing blue wildebeest bulls introgressing into black herds however, the opposite has been observed. Genetic studies on a population where the blue males have introgressed with black females, show that the blue wildebeest populations are "pure" and that the black wildebeest populations are receiving an influx of blue alleles. In this research, 14 skeletons of modern hybrid *Connochaetes taurinus* and *Connochaetes gnou,* from more than one post-hybridisation generation from the Spioenkop reserve, were morphologically as well as metrically compared with a sample of ten modern "pure" blue and 15 black wildebeest. This project showed that univariate, bivariate statistical analyses of selected measurements of the skeletons were successful in identifying all of the Spioenkop individuals as hybrids. Morphologically, the hybrids exhibit a general increase in body size, and

have unusual horns. The auditory bullae of the Spioenkop specimens are highly deformed, as are some axes. There is unusual bone growth on most of the post crania, morphological differences are observed on the distal ends of the metapodials, and the radius and ulna are fused in many specimens.

TABLE OF CONTENTS

ACKNOWLEDGEMENTS

I would like to thank my supervisors, Dr James Brink and Dr Lucinda Backwell, for all their guidance, support and contributions to my study.

Thank you James Brink for taking time out to teach me faunal identification and osteological comparison techniques. It was invaluable to this study.

I thank Christine Steininger for all her help this year and for her helpful insight on my project. Thanks to Rodrigo Lacruz for his explanation and guidance with statistics used in this study. Thanks to Lee Berger, for all his help and guidance with this project.

I am indebted to Malcolm Fenner for all his help in the layout of this thesis. Thanks Mal for giving me an engineer's perspective on palaeontology and for the skills you taught me in working 'word'.

The staff at the Florisbad Quaternary Research Station for all their help with the collections.

Thanks to Patrick Ahern, for all your support during this year.

Thanks to Carol Varga, for coming to my rescue when my computer became mutinous, thank you for saving my project! Thank you to Melanie Beck for your help with printing.

I am grateful to Joe and Marie Morau for helping fund my Masters and for always taking an interest in my studies. Thank you to PAST for awarding me a bursary without which I would not have been able to study and do what I love.

Finally, thank you to my mom, Sharaine, my dad, Deon and brothers, Thomas and Jason for all your moral support. Thank you for allowing me to follow my passion and for showing a real interest in palaeontology.

This is dedicated to my parents:

Deon & Sharaine De Klerk

LIST OF FIGURES

LIST OF TABLES

ABBREVIATIONS

Bd:	Breadth of the distal end
BFcr:	Breadth of the facies articularis cranialis
BG:	Breadth of the glenoid process
Bp:	Breadth of the proximal end
BPacd:	Breadth across the processus articularis caudales
BPtr:	Breadth across the processus transversi
BT:	Greatest breadth of the trochlea
D:	Distance between the anterior and posterior tuberosities
DD:	Smallest depth of the diaphysis
Dda	Depth of the achsial part of the medial condyle
Ddp	Depth of the peripheral part of the medial condyle
DHA:	Diagonal height
Dwa:	Width between the anterior tuberosities
Dwp:	Width between the posterior tuberosities
Dp:	Depth of the proximal end
GL:	Greatest length
GLC:	Greatest length of the caput
GLP:	Greatest length of the processus articularis
H:	Height

HS:	Height along the spine
LAPa:	(Greatest) length of the arch
LCDe:	(Greatest) length in the region of the corpus
LG:	Length of the glenoid process
Lngth:	Length
n.	Number of possible hybrids
SBV:	Smallest breadth of the vertebrae
SD:	Smallest breadth of the diaphysis
SLC:	Smallest length of the column scapulae
STD:	Standard

1 INTRODUCTION

There are two extant species of wildebeest, *Connochaetes gnou* (black wildebeest) and *Connochaetes taurinus* (blue wildebeest). Black wildebeest are morphologically distinct from blue wildebeest and are endemic to southern Africa. From both fossil and genetic evidence, the split between blue and black wildebeest can be placed at 1Ma (Brink 2005, Corbet *et al.* 1994). Although genetically these two groups are still closely related, they are considered separate species. The black wildebeest lineage evolved from an early form of *C. taurinus*. The evolution of the black wildebeest is characterised by a general reduction in body size, and cranial adaptation reflecting a territorial behaviour in open grassland (Kok & Vrahimis 1995).

In recent times, hybridisation between blue and black wildebeest has occurred mainly due to management (Grobler *et al*. 2005). The sample specimens for this study were taken from the Spioenkop Nature Reserve in KwaZulu-Natal. The first documented cases of hybridisation on the Spioenkop Nature Reserve was in 1995, (Langley 1995) and again in 2000 when Dr James Brink (National Museum) collected the skeletons from a herd of wildebeest that were culled due to reports of hybridisation occurring at Spioenkop Nature Reserve. It appears that one/a few males from a neighbouring population of blue wildebeest mated with

the black wildebeest cows. When the first hybridisation took place is unknown and it is not known for how many generations this occurred.

Due to the body size differences, and distinct cranial morphology of the blue and black wildebeest, it would be expected that there may be increased 'abnormalities' in the hybrids, in areas of the skeleton which are diagnostic for black wildebeest.

1.1 Aims

The aim of this study is to test whether it is possible to identify hybrid wildebeest based on morphology and metric comparison with pure blue and black animals. Identification of hybrids is important for conservation of the black wildebeest species. The Spioenkop specimens are used because the sample was taken from a reserve on which hybridisation is known to occur.

This project has developed out of the ongoing work of Dr. J Brink on wildebeest evolution. According to Brink (2005), no cases of hybridization are known from the fossil record.

2 BACKGROUND

2.1 Introduction

Bovidae is a very diverse mammal family, owing to its adaptation to arid and open areas (Gentry 1978). Bovids are found on all continents with the exception of South America, Australia and Antarctica. Distinguishing features of this family are the unbranched horns, which consist of a keratinised sheath that fits over a bony core (Gentry 1978). As the horns are distinct, it is a common characteristic utilised in the identification of this family (Gentry 1978). All ruminants lack the upper incisors as well as the upper and lower first premolars (Gentry 1978).

Alcelaphines are medium to large antelope presently confined to the African continent (Gentry 1978). Typical features of this sub-family are a long skull, horns in both sexes. There are four living genera: *Alcelaphus, Damaliscus, Connochaetes* and *Beatragus.*

Wildebeest form part of the subfamily Alcelaphinae (Vrba 1985, Gentry 1992) and the genus *Connochaetes*. There are two extant species of wildebeest, *C. gnou* (black wildebeest) and *C. taurinus* (blue wildebeest). Wildebeest are large antelope, which are classically characterised by high shoulders, a broad muzzle and cow-like horns in both sexes (Smithers 1986) that are unridged and thick (Estes 1991). They have short glossy coats and their colouration varies with geographic occurrence, as well as between individuals (Estes 1991).

Connochaetes gnou are limited to terrains that are void of trees, such as karroid areas of the Cape Province and the Highveld temperate grasslands of southern Africa (Estes 1991, Smithers 1986). They are typically a buffy brown colour with long white hair on the tail. The horns 'arise from expanded bases and sweep downward and forward to curve upward about the end of the muzzle' (Smithers 1986). Social behaviour is linked to ecology (Brink 2005). Black wildebeest are permanently territorial and need open habitats to visually patrol and maintain breeding territories (Von Richter 1974). In black wildebeest, the dominant male will form territorial networks, which receptive females will approach (Brink 2005). This breeding behaviour can only function in an open habitat and is the reason why this species remains historically confined to the Highveld and Karoo areas.

C. taurinus is found in the central, northern and Northeastern parts of South Africa (Plug & Badenhorst 2001) in regions associated with open woodland where there is water (Smithers 1986). The males are dark grey in colour with a silvery sheen and have long black hair on the tail (Smithers 1986). Their lower legs are often tan in colour and they have a white to tan coloured beard. Blue wildebeest manes are often upstanding (Estes 1991). Both sexes have horns that are unridged and rise from swollen bosses (Smithers 1986). The horns are directed outwards and slightly downwards before curving up (Smithers 1986).

Blue wildebeest have a degree of territoriality but can be flexible and this often depends on external factors.

Classification of Wildebeest (Gentry 1978):

Family:	Bovidae
Sub family:	Alcelaphinae
Tribe:	Alcelaphini
Genus:	*Connochaetes*
Species:	*gnou* (black wildebeest)
	taurinus (blue wildebeest).

2.2 Wildebeest fossil record

From fossil evidence, it was thought that congeneric blue and black wildebeest diverged *ca*. 2Ma (Gentry 1978). This date has been revised by Brink (2005) to *ca.* 1Ma, a date that is also suggested by genetic studies (Corbet *et al.* 1994).

Connochaetes gnou is a species endemic to South Africa. Fossils of this species are found at Elandsfontein, Cornelia and Florisbad (Vrba 1979). The earliest form of wildebeest is thought to be *Oreonagor tournoueri* (Gentry 1978). The wide separation of the horn core insertions as well as the basal swelling of the

horn cores set *O. tournoueri* apart from the genus *Megalotragus* and indicates a closer relationship with *Connochaetes* (Brink 2005).

Connochaetes gnou antiquus (Broom 1913) has been found at Florisbad. The horn cores pass less markedly forward from the base, and the tips are less recurved than in *C. gnou* (Gentry 1978). *Connochaetes gnou laticornutus* is an earlier type from Cornelia and Elandsfontein, and is thought by Brink (2005) to represent the earliest form of the black wildebeest. However, Gentry (1978) proposed *C. africanus* as the earliest form. *Connochaetes africanus* resembles *C. gnou* with regard to facial features rather more than *C. taurinus*. This species had rather small horn cores, which were inserted extremely far apart (Gentry 1978). However, Brink (1993) concluded that since no black wildebeest fossil material has been found outside of southern Africa, that it is a southern endemic species of Middle Pleistocene age. This means that *C. africanus* which is of early Pleistocene age is an unlikely ancestor to modern black wildebeest. Pleistocene aged *C. gnou* species from Cornelia show that cranial changes preceded other skeletal modifications (Brink 2005).

Connochaetes taurinus is widely spread relative to *C. gnou* and covers a wide area of southern Africa as well as eastern Africa. Fossil evidence for the presence of *C. taurinus* antecedents found in east Africa dates to 2.5 million years (Harris 1991). The earliest form of *C. taurinus* is from the Nachukui Formation (west of

Lake Turkana) and dates between 3.0 and 2.5 million years (Harris 1991). Gentry and Gentry (1978) have identified *C. gentryi* in Olduvai Beds I and II and *C. taurinus* in Middle Bed II and Bed IV. The Peninj Formation in Tanzania contains *C. taurinus prognu* that dates to 1.1 Ma (Vrba 1979). *Connochaetes taurinus prognu* has horn cores that are less posteriorly inserted and less downwardly curved than *C. taurinus* (Brink 2005).

The antecedents of *C. taurinus* also occur in southern Africa. Evidence for the presence of *C. taurinus prognu* has been found in the hominid bearing caves of South Africa (Vrba 1979). It is thought that the blue wildebeest has remained relatively unchanged and is presently found as the extant *C. taurinus taurinus* of southern Africa (Brink 2005). Blue wildebeest are considered unchanged descendants of an ancestral population from which black wildebeest evolved (Gentry & Gentry 1978). *Connochaetes taurinus prognu* is thought to be the earlier form of blue wildebeest from which *C. gnou* evolved (Brink 2005). The evolution of the endemic *C. gnou* in the Pleistocene is proposed by Brink (2005) to be associated with a shift towards a more specialised territorial breeding behaviour.

The natural distribution of black wildebeest was focused on the central plateau of southern Africa (Brink 2005). In the southern open grasslands, there is evidence for this periodic overlap in ranges of blue and black wildebeest in the past this is indicated in fossil records in places such as Spitskop, Mahemspan, Rose Cottage

Cave and Sunnyside Pan (Brink *et al.* 1999, Plug and Engela 1992, Plug and Badenhorst 2001, Brink 2005).

2.3 Modern wildebeest osteology

Alcelaphinae share derived osteological features that include long skull with a short braincase, and horns in both sexes. Horn cores of wildebeest are inserted wide apart (Gentry 1978). The braincase is dorso-ventrally shallow (Gentry 1978). Gentry (1978) notes that the zygomatic bars usually deepen anteriorly under the orbits. Modern alcelaphines do not have goat folds. The upper molars are widely out-bowed and ribs are present. P_2 is reduced or absent in the short premolar rows (Gentry 1978).

In spite of differences in body size, skull shape, and colouration, black wildebeest are closely related to the blue in that they have similar body proportions (Gentry & Gentry 1978). Typical osteological features of *C. taurinus* are a large, wide skull with a long face (Gentry 1978). Horn cores in this species do not have large bases and do not pass forward (Gentry 1978). *Connochaetes gnou* has a lower and wider cranium, with broad bases on the horn cores. These horn cores pass forward to end in a sharply recurved tip (Gentry 1978). The most recent study to compare blue and black wildebeest anatomy was undertaken by Brink (2005).

2.4 Crania

The following section on comparative osteology will concentrate on the main differences between blue and black wildebeest. Table 1 shows the differences in cranial morphology between blue and black wildebeest, the most obvious of which is horn curvature and facial length. The forward positioning and basal inflation of the horns and fusion of the frontal suture in *C. gnou* are proposed by Brink (2005) to be associated with territorial behaviour.

Table 1: Comparison of blue and black wildebeest cranial morphology (Adapted from Brink 2005, p95-96)

Feature	*C. gnou*	*C. taurinus*
Horn curvature	Horns curve down and then forward	Horns grow sideways and the upwards
Basal bosses	Enlarged basal bosses, horns positioned more posteriorly than in *C. taurinus*.	Basal bosses are not as large as *C. gnou.*
Frontal profile of the forehead	Frontal and nasals are often flat or concave.	Frontal is convex.
Facial length	Short.	Long.
Frontal suture	Suture fuses in early in life.	Frontal suture remains unfused.
Orbits	Enlarged and laterally projecting relative to *C. taurinus*	Are less laterally projected relative to *C. gnou*
Paracondylar processes	Small	Larger than *C. gnou*

2.5 Post-crania

Comparison of the post crania is vital in order to study hybrids. It is important to understand the differences between the blue and black wildebeest in order to know which of the unique traits are present in the Spioenkop specimens.

2.5.1 Axis

The axis and atlas were the only vertebral elements collected during the sampling of the Spioenkop specimens. The axis is thought to be useful in this study for the following reasons: the length of the axis reflects in the overall size of the neck, while the smallest width of the body (SBV) is a function of the stoutness of the neck (Brink 1993, 2005). The axis of the extant black wildebeest is short and compact while the blue tends to be more elongated and less wide across the corpus of the vertebrae (Brink 2005). In *C. taurinus*, the axis is more elongated (Brink 1993) with a more pronounced waist compared to that of *C. gnou.*

2.5.2 Humerus

The humerus of the blue wildebeest is less robust than that of the black (Brink 2005). Brink (2005) found that the caudal part of the tuberculum maius is occasionally enlarged when compared to *C. gnou*. In the midline of the fossa

radialis there tends to be a longitudinal ridge present in *C. gnou* but is absent in *C. taurinus* (Brink 2005).

2.5.3 Radius

There are three main difference discussed by Brink (2005) concerning the radius. Firstly, the dorsal view of the attachment for the collateral ligament of *C. gnou* tends to be on the same level as the rest of the proximal articular surface. In *C. taurinus* this attachment is slightly offset distally (Brink 2005). In *C. gnou* the incision in the proximal radius approaches a right angle, 'while in *C. taurinus* it is often an intermediate between two extremes'. In the distal radius, the dorso-lateral edge of the facet for the *os carpi radiale* is used for differentiation (Brink 2005). In the black wildebeest, it tends to be flat while in the blue wildebeest it tends to be dorsally extended (Brink 2005).

2.5.4 Metacarpal

Changes in the metacarpus have been attributed by Brink (2005 & 1993) to be associated with the horns becoming progressively lighter in the Quaternary.

2.5.5 Metatarsal

In the metapodials, the distal parts of *C. gnou* tend to be flatter and narrower, which causes a sharper angle. ‘In the distal and volar view, the lateral and medial margins of the distal part of the shaft in *C. taurinus* do not flow evenly into the distal articulation as it does in *C. gnou*, but tends rather to form an angle (Brink 2005)’. In *C. gnou* the shaft at the distal end is flatter and causes a flair, which is not so in the blue wildebeest (Brink 2005). The metapodials are a useful palaeo-environmental indicator, as the morphology indicates the type of environment the animal occupies (Kappelman *et al.* 1997, Plummer & Bishop 1994). It is, however, noted that *C. gnou* and *C. taurinus* are often grouped together under the same environment in these studies.

2.5.6 Femur

In the genus *Connochaetes,* the trochlea of the femur has a pronounced medial ridge (Brink 2005). Brink (2005) found that when viewed laterally this medial ridge manifested as a strong dorsal projection, which in the case of *C. gnou* ended in a thickened tubercle. He noted that this derived feature evolved independently in the black wildebeest. In *C. taurinus* the fossa supracondylaris is deeper than in *C. gnou* this feature is related to the larger body size of the blue wildebeest.

2.5.7 Tibia

The first difference between the two genera noted by Brink (2005) is that the corpus of the tibia in *C. gnou* is unique in that it is recurved. The proximal fibula of the black wildebeest is less well developed than it is in the blue wildebeest. In a lateral view, it was found that the angle of the tuberositas tibiae is less steep in *C. gnou* than in *C. taurinus* (Brink 2005).

2.6 Hybridisation

Hybrids are the offspring produced from mating different species or genotypes, (Rhymer & Simberloff. 1996). Hybridisation is problematic for rare species that encounter a more abundant species (Rhymer & Simberloff. 1996). Hybrids in nature are rare. Hybrids often result due to human interference (Rhymer & Simberloff. 1996), and change in habitat can play a big role in promoting hybridisation.

Historically, geographic ranges of the two *Connochaetes* species have overlapped but different social behaviour and habitat preference of *C. gnou* and *C. taurinus* prevented interbreeding. Under these conditions, blue wildebeest males can become dominant in a black wildebeest breeding territory due to larger body size. This results in blue wildebeest males mating with black wildebeest females. The

loss of habitat essentially opens up a ‘permanent corridor’ that allows the continual movement of one taxon into the range if another, allowing for hybridisation (Rhymer & Simberloff. 1996). In the case of the wildebeest, hybridisation is currently occurring in South African game farms and nature reserves. There is also introgression; this is when there is gene flow between the hybrids and the parent species (also called backcrossing), (Rhymer & Simberloff. 1996).

There are documented cases of hybridisation between these two genetically distinct populations (Fabricius *et al.* 1988, Grobler *et al.* 2005). All known cases of hybridisation have occurred from dispersing blue wildebeest bulls introgressing into black herds, although the inverse may occur. The genetic study by Grobler *et al.* (2005) showed that the blue wildebeest populations are “pure” and that the black wildebeest populations are receiving an influx of blue alleles as a result of hybridisation with the blue (Grobler *et al.* 2005). Genetically the two extant wildebeest species share the same number of chromosomes and many morphological similarities (Grobler *et al.* 2005). The close genetic relationship between the blue and black wildebeest allows for interbreeding and results in fertile offspring being produced (Grobler *et al.* 2005). Black and blue wildebeest have been kept side by side at many localities (Brink pers comm.). This means that there is potentially a high percentage of blue wildebeest genes introgressed with the black wildebeest.

The first documented case of hybridisation on the Spioenkop nature reserve was in 1995 (Langley 1995). Blue wildebeest bulls crossed to the upper reaches of the dam during a period of drought and established themselves in an area favoured by black wildebeest (Langley 1995, Internet reference 1). The larger size of the blue wildebeest is considered the reason for the blue wildebeest dominating the smaller black wildebeest and mating with black wildebeest females (Langley 1995, Internet reference 1). These blue wildebeest were removed several years later as soon as a hybrid male was discovered (Internet reference 1). However, this lowered the hybridisation risk at the Spioenkop nature reserve, but did not remove it. In 2000, Dr James Brink (National Museum) collected the skeletons from a herd of wildebeest that were culled due to reports of hybridisation occurring at Spioenkop nature reserve. This was done in collaboration with the Dr. Ian Rushworth (KZN Parks Board) and Mr. Savvas Vrahimis (Department of Tourism, Environment and Economic affairs, Free State).

2.7 Species Concepts

The presence of hybrids sparks an interest in the various species concepts. A question of interest is whether a hybrid qualifies as a new species or sub-species. Linnaeus (1758) introduced the classification of organisms into groups; the lowest of which is the species level. Species are further split into sub-species,

defined as ‘a taxonomic subdivision of a species consisting of an interbreeding, usually geographically isolated population of organisms’. Debates concerning what constitutes a species often concern reproductive connectedness and morphological resemblance (Eldredge 1993). The following section outlines a few of the better-known species concepts considered in this project.

2.7.1 Biological species concept (BSC)

The leaders in the promotion of the biological species concept are Dobzhansky (1937) and Mayr (1942). The definition of the biological species concept states, “Species are groups of actually or potentially interbreeding populations which are reproductively isolated from other such populations” (Mayr 1942). This concept, however, deals with sexually reproducing organisms (Vrba 1985). Organisms are recognised as the same species under the BSC if interbreeding results in viable offspring being produced (Vrba 1985), however, this idea is not commonly held today (Brink pers. Comm.). Reproductive isolation is achieved when a species buds off from its ancestor or a single species divides into two reproductively independent descendants (Szalay 1993).

The biological species concept is the first modern attempt to define species, but there are numerous problems with this concept, on both theoretical and practical grounds. Because this concept only deals with reproductive isolation, asexual

species and fossil species do not fit into this concept (Alexander 2004, pers. comm., Vrba 1985) and therefore cannot be applied to the wildebeest.

2.7.2 Evolutionary species concept

This is the broadest concept in that it covers both sexually and asexually reproducing organisms (Vrba 1985). Simpson (1951) stated that both lineage splitting and change in a single unbranching lineage could result in a new species (Vrba 1985). This concept combines the idea that 'species are historical lineages with the concept of their evolutionary and ecological role' (Mallet 2001). At some point in the progress of the species, members may diverge from one another. When such a divergence becomes sufficiently clear, as in the case of the wildebeest, the two populations become separate (Internet reference 2). Lineages may separate, become separate species and come back together in the future which means they will no longer be different species (Internet reference 2).

2.7.3 Mate recognition concept

This concept was developed by Patterson (1978), species are identified as "the most inclusive population of individual biparental organisms which share a common fertilisation mechanism" (Patterson 1978). This concept is also termed Specific Mate Recognition System or SMRS. Under this concept, pre-mating and

post mating isolation mechanisms do exist but are never a product of selection but rather a secondary by-product of divergence (Patterson 1978). SMRS essentially maintains successful mating within isolated populations (Eldredge 1993). Most authors now feel that the recognition concept actually falls within the definition of the biological species concept (Eldredge 1993 & Szalay 1993).

2.7.4 Ecological species concept

In this concept, the true definition of a species is seen as the 'occupancy of an ecological niche rather than interbreeding' (Mallet 2001).

No species concept yet proposed is entirely unbiased, or applied in all cases without resorting to judgement. Given the complexity of species, such an objective definition is in all likelihood impossible.

2.8 Origin of species

This topic covered by Vrba (1985), stated that speciation is associated with change in two kinds of characters, namely 'those that initiate the cause of speciation and those that come along for the ride'. Genetic as well as phenotypic characters of organisms are involved in divergence of species (Vrba 1985). With

phenotypic change come isolation mechanisms (Vrba 1985). Mayer (1963) separating these mechanisms into pre-mating and post-mating mechanisms.

Premating isolation mechanisms include seasonal and habitat isolation, where potential mates do not meet (Mayr 1963). Ethological isolation is where potential mates meet but do not mate. Finally, mechanical isolation, where there is copulation but there is no transfer of sperm (Mayr 1963). Post-mating mechanism includes gamete mortality, zygote mortality, hybrid inviability and hybrid sterility (Mayr 1963).

2.8.1 Speciation of Connochaetes gnou from Connochaetes taurinus

Speciation of *C. gnou* from *C. taurinus* is linked to the appearance of permanently open Highveld grasslands (Brink 2005). Morphological changes in the earliest fossil populations of black wildebeest are linked to a shift towards a fixed territorial breeding behaviour (Brink 2005) which is dependant on an open habitat that is visually unobstructed (Brink 2005). The speciation of black wildebeest from a blue wildebeest like ancestor was marked by a major genetic change due to the shift in reproductive behaviour (Brink 2005). Oppenheimer (2004) found that behavioural innovations could become genetically set and as a result develop into the driving force of evolution (Brink 2005).

3 MATERIALS

3.1 Introduction

The modern materials used in this study are outlined in the first section of this chapter. In the second section, the methods used in measurement-taking as well as statistical data analysis are covered.

3.2 Specimens

3.2.1 Hybrids

The study sample is from the Spioenkop Nature reserve. This sample is thought to be hybrids of *C. taurinus* and *C. gnou*. There are 14 specimens consisting of both males and females (see Table 3). It is likely that the specimens are from more than one post-hybridisation generation. Table 2 shows the order in which the specimens were studied, as well as the sexes of the individuals.

Specimens were chosen randomly from the collection, currently housed at the Florisbad Quaternary Research Centre. In this study the Spioenkop sample, presumed to be that of hybrids, will be referred to in the text as such.

3.2.2 Connochaetes gnou and Connochaetes taurinus

Modern material of *C. gnou* and *C. taurinus* from the National Museum (Bloemfontein) was used in the osteological comparison. Brink (2005) stated that the black wildebeest underwent two population bottlenecks (Brink (2005) pers. comm. with Savvas Vrahimis), one that occurred at the turn of the century and the other in the 1930's (Brink 2005). The sample at Florisbad collected by Von Hoepen (Brink 2005), predates the 1930's bottleneck and can be considered a true representation of a 'Pre-20th Century black wildebeest population' (Brink 2005). The eleven blue and fourteen black wildebeest used in this study are all part of the modern faunal collection at the Florisbad Quaternary Research Station.

Postcranial measurements for blue and black wildebeest were taken from the study by Brink (2005). This sample reflects the range for each species per skeletal element.

3.2.3 Equipment

A 30cm slide gauge with a vernier scale was used to take the large measurements. For smaller measurements, a 15cm digital calliper was used. Due to the shape of the skull, a measuring box was used to measure awkward lengths. In order to

assure little error in the measurements taken, random measurements were re-taken at the start of each collection session.

Specimens were photographed using a Nikon digital camera. Statistics on measurements were run using STATVIEW®.

4 METHODS

4.1 Introduction

This project required training in osteological comparison and taking of measurements. Morphological deviations in the hybrid specimens were noted and statistical analysis was used to determine the nearness of the Spioenkop specimens to the parent populations, as well as the extent of deviation of from the parent populations.

Due to the size differences between blue and black wildebeest, it would be expected that hybrid measurements would plot between the plots of *C. gnou* and *C. taurinus.* The author is assuming the hybrids will be larger then the black wildebeest because of the hybridization with the larger blue wildebeest.

4.2 Measurements

To take the measurements, von den Driesch (1976) was used as a guideline. Measurements are important as it often reveals morphology that is not immediately visible to the eye (Brink *et al.* 1999).

4.3 Cranial measurements

Figure 1, Figure 2, Figure 3, Figure 4 and Figure 5 (von den Driesch 1978). Indicate the measurements taken on the skull.

The following measurements are taken on the skull in addition to the von den Driesch measurements:

D: Distance from the anterior to the posterior tuberosities (Tubercula muscularia). For this measurement the distance was taken from the inner edge of one tuberosity to the other

Dwa: Width between the anterior tuberosities. This measurement was taken from the inner edge of one anterior tuberosity to the other.

Dwp: Width between the posterior tuberosities. See Dwa for measurement.

E Diameter of the earhole. For this measurement, the back part of the vernier was placed inside the earhole until the edges of the calliper touched the edges of inner part of the earhole.

F: Auditory bullar thickness, this measurement was taken across the width of the bulla for each specimen.

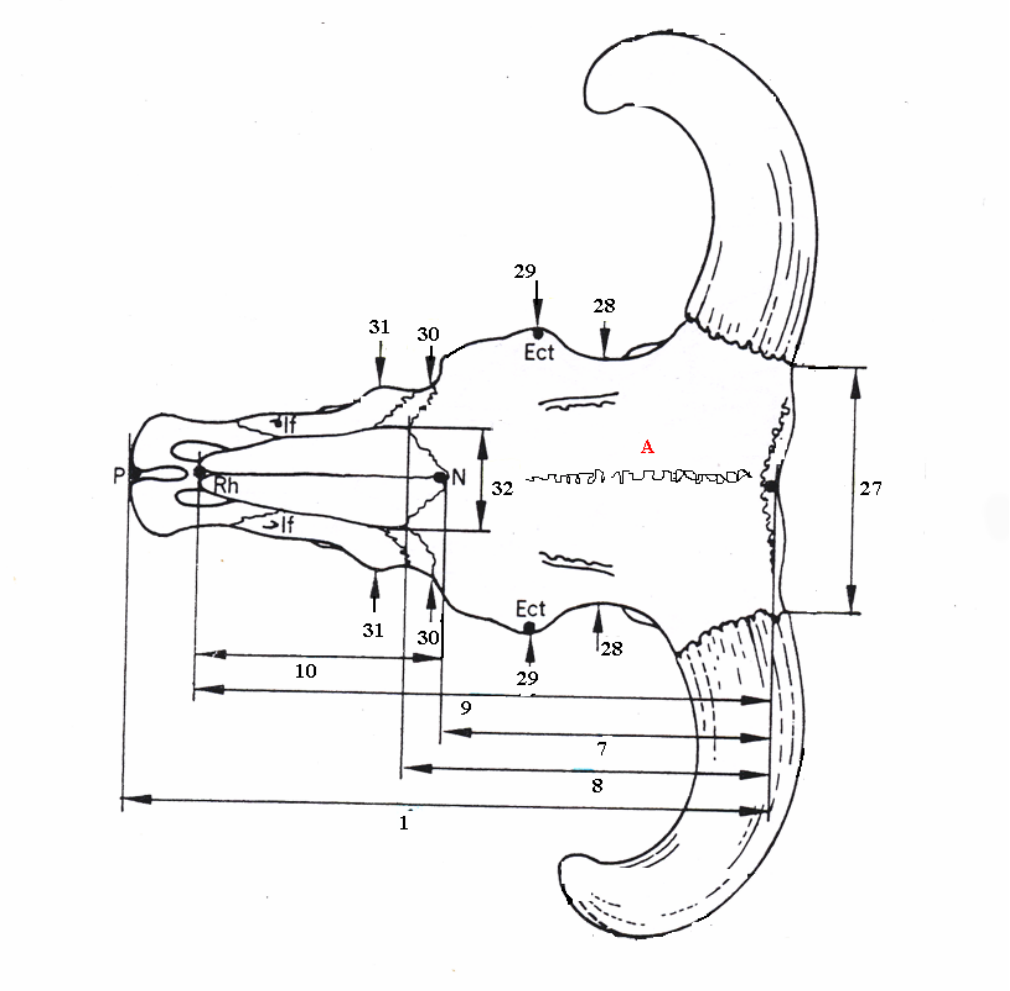

Figure 1: Dorsal view of the cranium, the numbers relate to measurements taken, (after Von den Driesch, 1976)

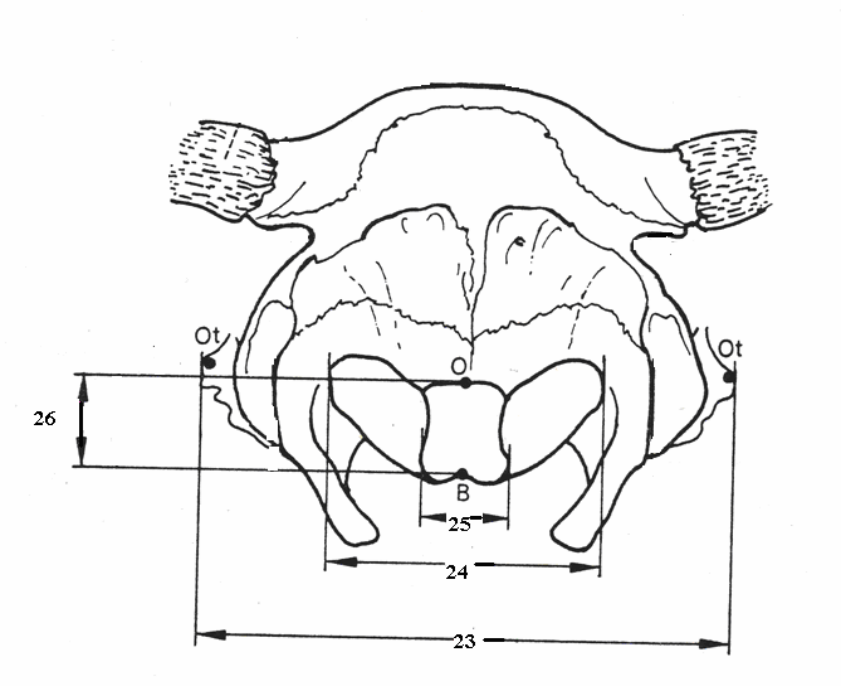

Figure 2: Cranium nuchal view, (after von den Driesch 1976)

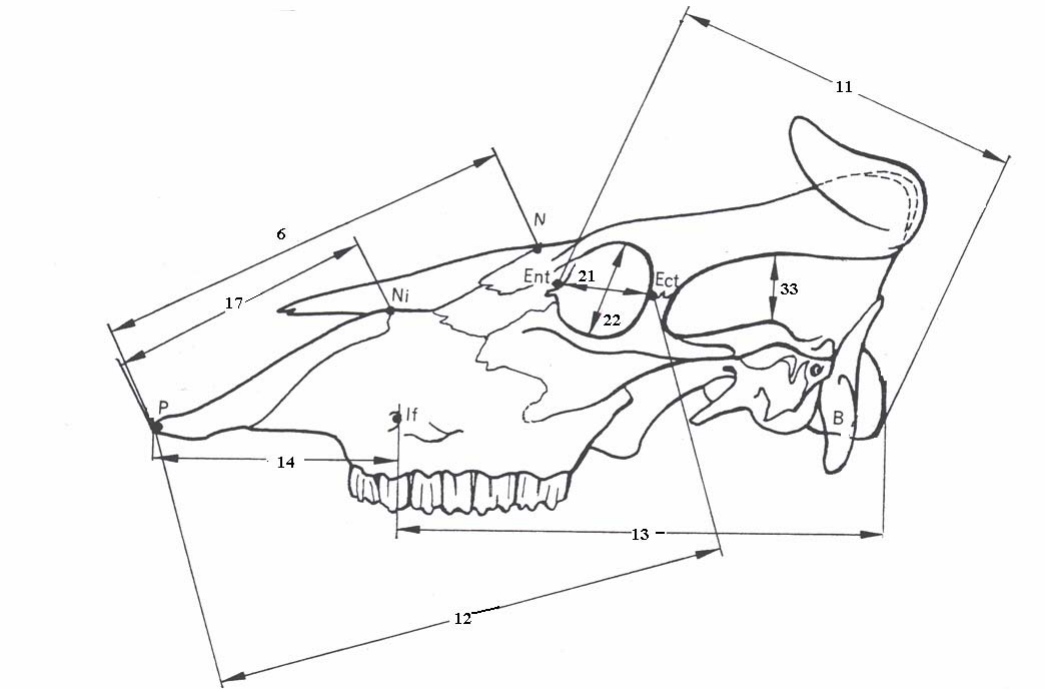

Figure 3: Cranium, left side (After von den Driesch 1976)

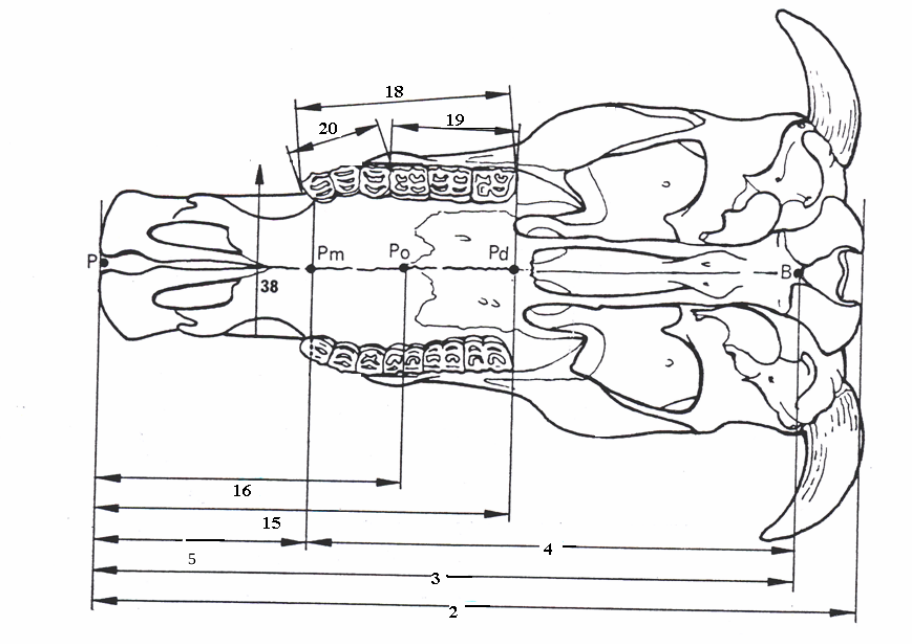

Figure 4: Cranium, basal view (after von den Driesch, 1976)

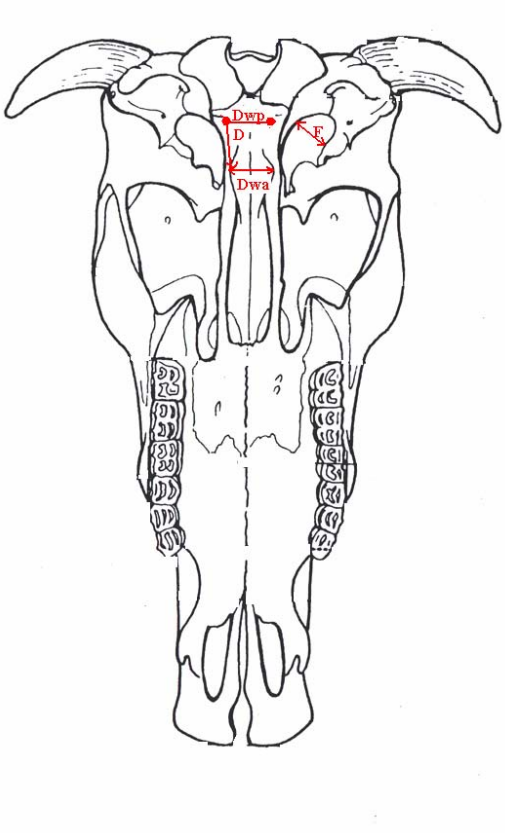

Figure 5: Basal view showing measurements of features thought to be different in each wildebeest species, (after von den Driesch edit by B. de Klerk)

4.3.1 Lower jaw

For measurements of the mandible, see Figure 6. The length and breadth of the second molar was also measured in this study.

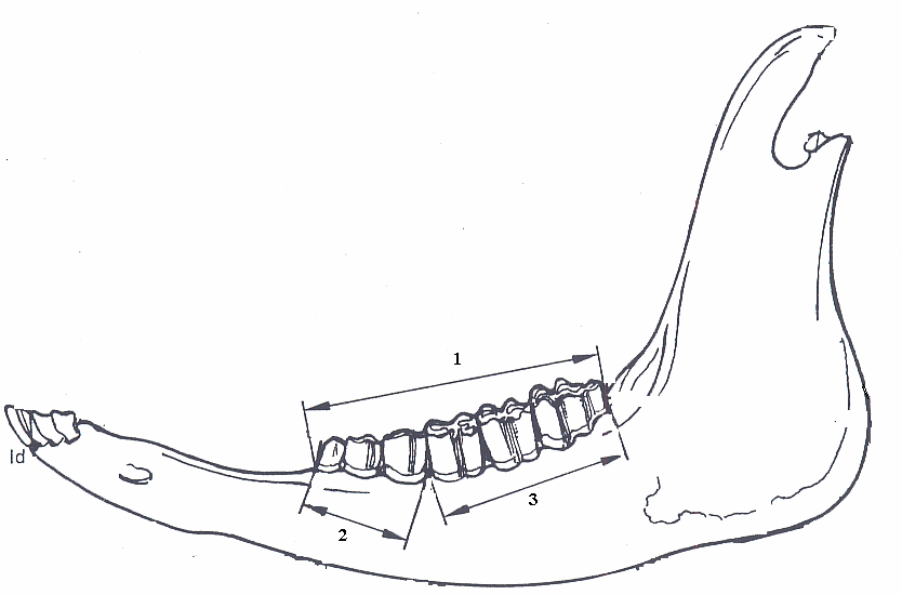

Figure 6: Lower Jaw measurements (After von den Driesch (1976). Measurements edited by B. de Klerk).

4.4 Postcranial measurements

4.4.1 Axis

Figure 7 and Figure 8-indicate all measurements taken on the axis.

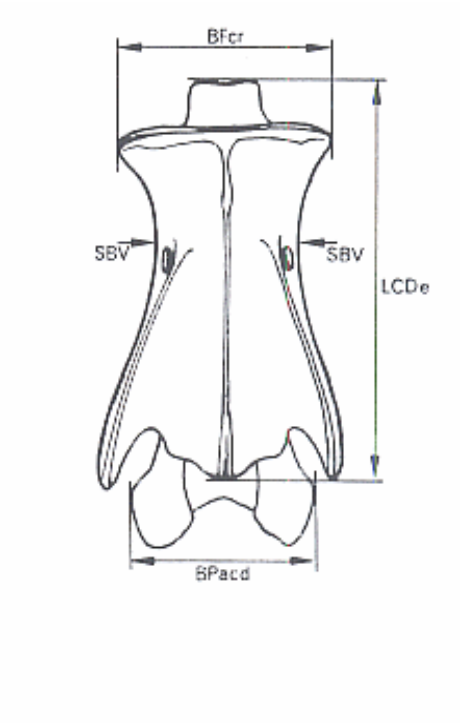

Figure 7: Ventral view of a *Cervus* axis showing various measurements taken. This picture was used as a guideline for the measurements taken on the wildebeest axes (after von den Driesch 1976).

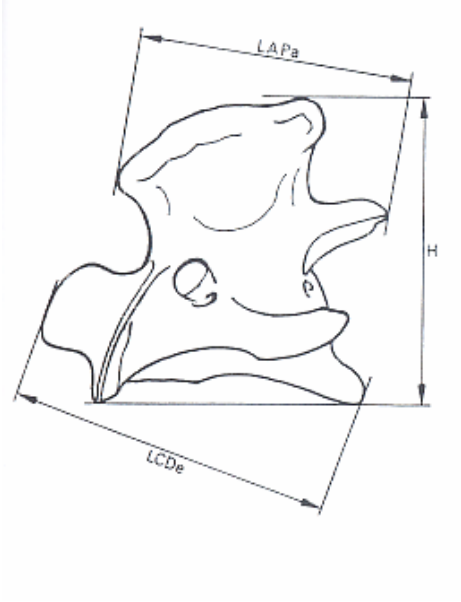

Figure 8: Axis, Left side view showing measurements taken (after von den Driesch 1976).

4.4.2 Scapula

Figure 9 and Figure 10 indicate measurements used in this study.

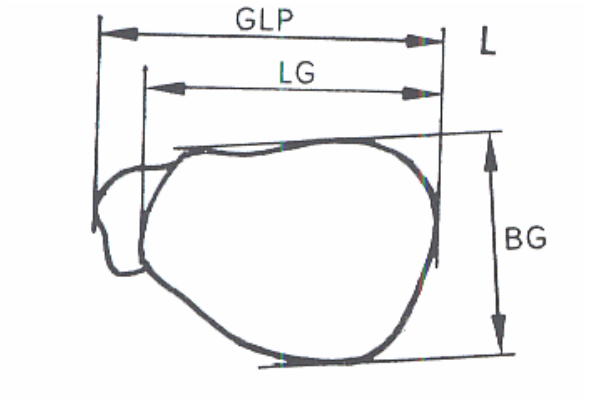

Figure 9: Distal view of the scapula (after von den Driesch 1976).

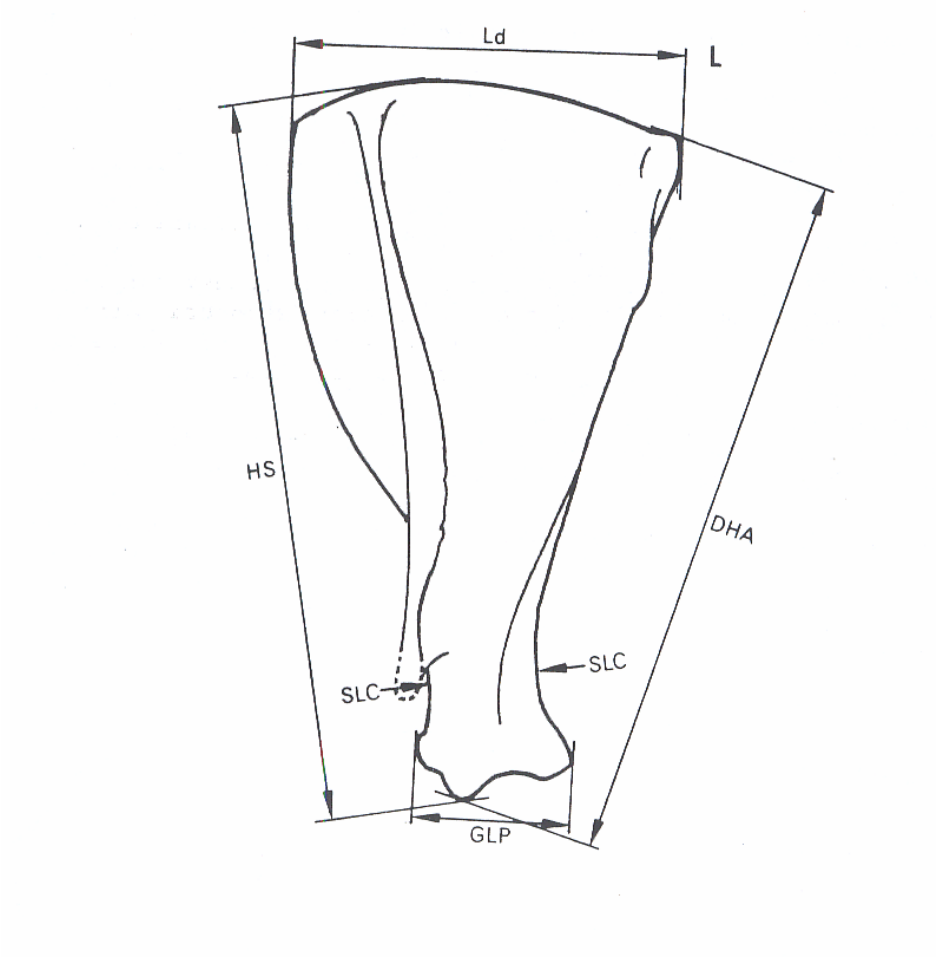

Figure 10: Lateral view of the scapula (after von den Driesch 1976).

4.4.3 Humerus

See Figure 11 for measurements taken on the humerus

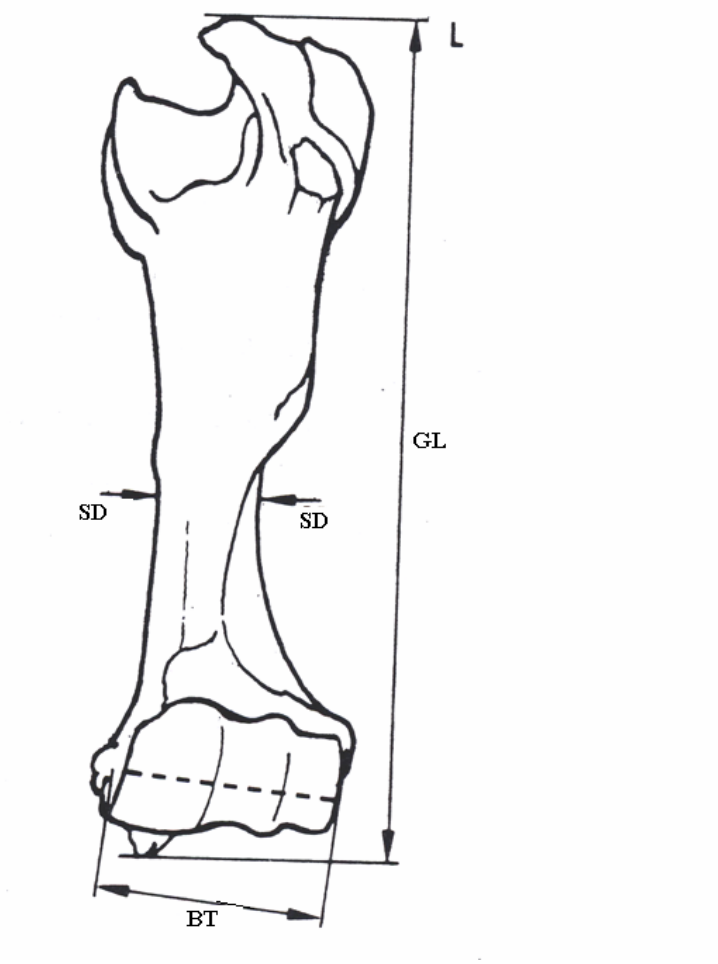

Figure 11: Cranial view of the humerus (after, von den Driesch 1976).

4.4.4 Radius

See Figure 12 for measurements taken on the radius

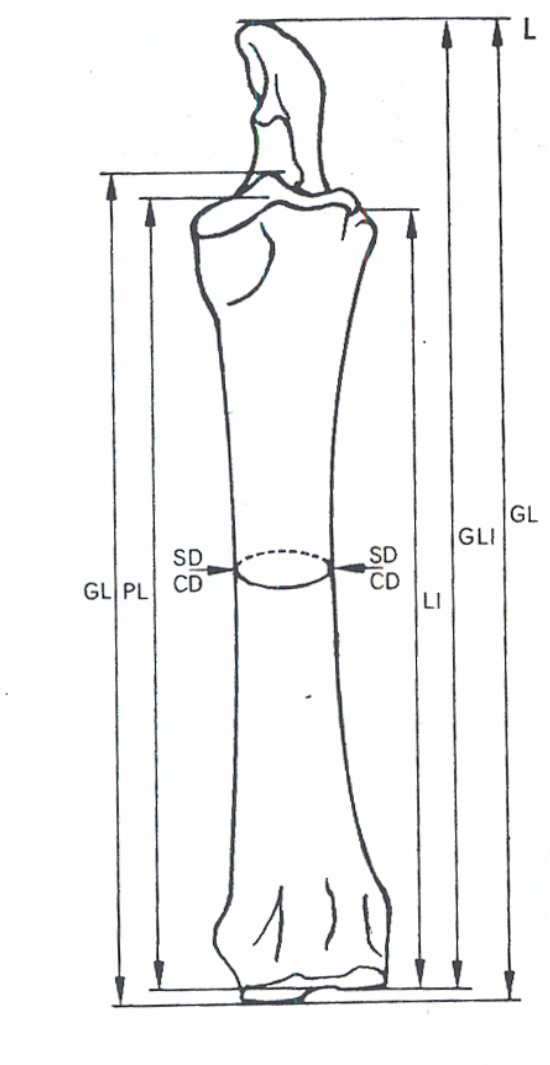

Figure 12: Dorsal view of the radius and ulna of an equid, indicating measurements taken on the ulna, (after von den Driesch 1976).

4.4.5 Femur

See Figure 13 for measurements taken on the femur.

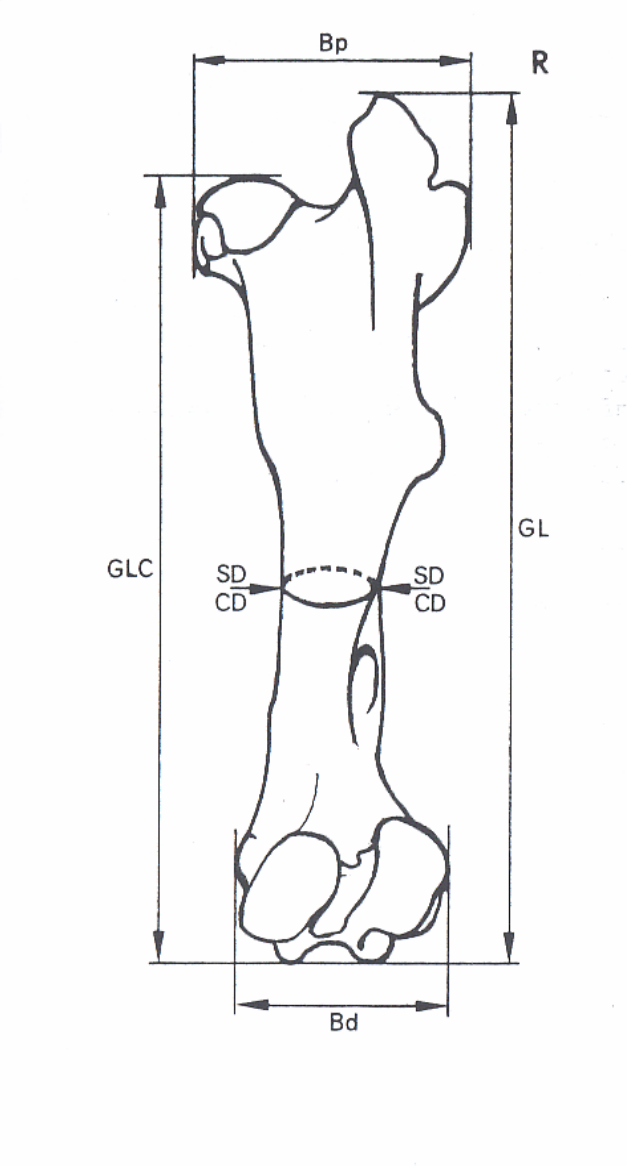

Figure 13: Caudal view of the equid femur. This was used as a guideline when taking measurements on the wildebeest femur (after von den Driesch 1976).

4.4.6 Tibia

For measurements taken on the tibia, refer to von den Driesch (1976).

4.4.7 *Metapodials*

Figure 14 and Figure 15 indicate measurements taken on both the metacarpal and the metatarsal. The depth of the achsial and peripheral part of the medial condyle for both the metacarpal and the metatarsal were taken, (Brink *et al.* 1999).

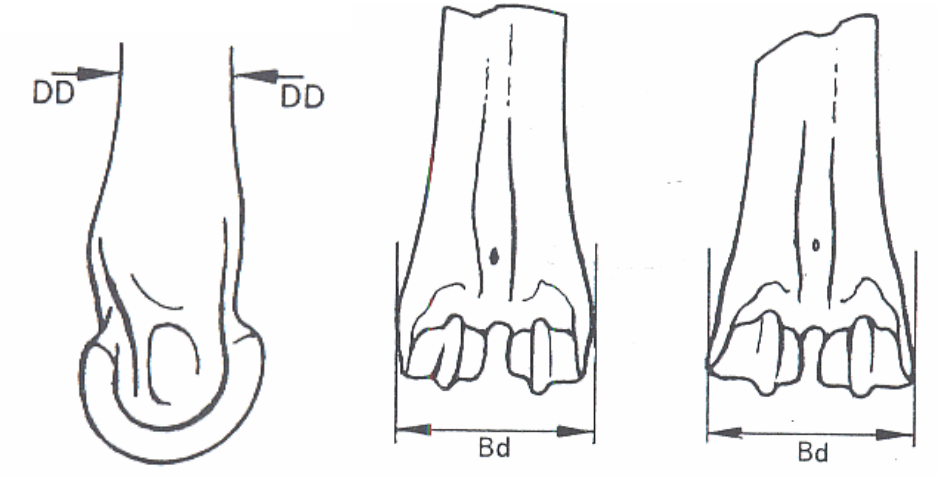

Figure 14: Dorsal and side view of the metatarsus, indicating measurements taken (after von den Driesch 1976).

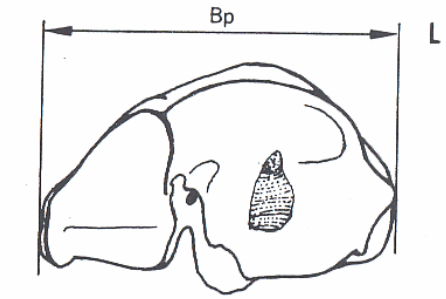

Figure 15: Dorsal view of the metacarpal (after von den Driesch 1976).

4.5 Statistical analysis

Statistical analysis of the measurements was done using the STATVIEW® program. All data were entered into matrices and transferred into STATVIEW®. Univariate analysis was used on each measurement to establish the relationships that may exist between the blue, black and hybrid specimens used in this study.

Standard deviation provides an average of the differences for each mean of the wildebeest. The standard deviation is related to the range. Range is the distribution between the lowest and the highest measurement taken. A low standard deviation indicates that there is little spread of the measurements around the mean for that species. A high standard deviation indicates a large spread of the measurements around the mean (Brown 1988).

The standard error gives an indication of the difference between the species. This is an indication of the dispersion of the sampling errors when estimating a population mean from a sample mean. These standard error plots indicate the range where the mean should probably lie and not necessarily, where it does (Townsend, 2002). Standard error bars represent this. In all cases, the graphs represent ± 1 standard error.

Statistics should establish which features the Spioenkop specimens might share with the black and blue wildebeest. This may also be useful in determining any unique features within this population. However, in this case it may be used to support an observed morphology (Brink 2005, Eisenmann & Brink 2000).

Hybrids will be defined as those individuals that lie outside the 95% confidence intervals for the measurements taken on the black wildebeest. It is expected that hybrids should plot above the upper limit for black wildebeest. In addition, if the specimens are indeed hybrids, it is expected that for some features the hybrids should plot within the blue wildebeest range. Any Spioenkop specimens that plot in the blue wildebeest range, for features in which there is no overlap between the black and blue range, will be regarded as hybrids.

4.6 Morphology

The comparative morphological approach used in this study is the same technique used by osteoarchaeologists to distinguish between domestic sheep and goats and the process of domestication (von den Driesch 1976, Boessneck & von den Driesch 1978, Brink 2005). This methodology is used in South Africa in archaeozoological studies (Plug and Peters 1991, Plug and Badenhorst 2001) and it is used in this study to record morphological changes due to hybridisation. The black wildebeest will be used as the standard to which the hybrids will be

compared using Brink (2005) as a guideline. For deviation in the hybrids, blue wildebeest will be used to see if the deviation resembles blue wildebeest or if in fact the morphology is unique.

5 RESULTS 1: MORPHOLOGY

In this section any observed morphological deviation in the Spioenkop specimens will be noted.

5.1 The skull

5.1.1 Introduction

The skull is more complex than the other skeletal elements and thus requires more attention (Brink 2005). The morphology discussed in this chapter is based on the author's observations and bivariate analysis. The morphological differences of the blue and black wildebeest (Chapter 2, Table 1), will be the basis on which cranial morphology is assessed. This chapter will evaluate which parent species (*C. gnou* or *C. taurinus*) the hybrid most resembles, or if, it has its own unique morphology.

5.1.2 Horn curvature

The overall horn curvature for the Spioenkop specimens have some resemblance to the black wildebeest in that the horns curve down and then forward. However, Spioenkop specimen horn curvature varies from one individual to the next. Figure 17 shows all horn curvatures for the Spioenkop specimens.

The following individuals' horn morphology resembles that of *C. gnou* 12042, 12044, 12047, 12048, 12051 and 12060, these specimens have horns that curve down and then forward (see Figure 17).

Specimens 12046 and 12049 have a horn curvature that shows a tendency toward blue wildebeest horn curvature. The horns in these specimens form a wider angle with the skull than the horns in a black wildebeest.

Specimen 12053 has extreme deformity in the horns, they are asymmetrical and the right horn has irregular bends in it.

Specimens 12043, 12049, 12050 and 12052 have strong ‘kink’ morphology. This is when the horns start by having a wide angle to the skull and then there is a sudden change in the angle as the horns curve more forward (see Figure 16). This causes a sharp bend or kink in the horn.

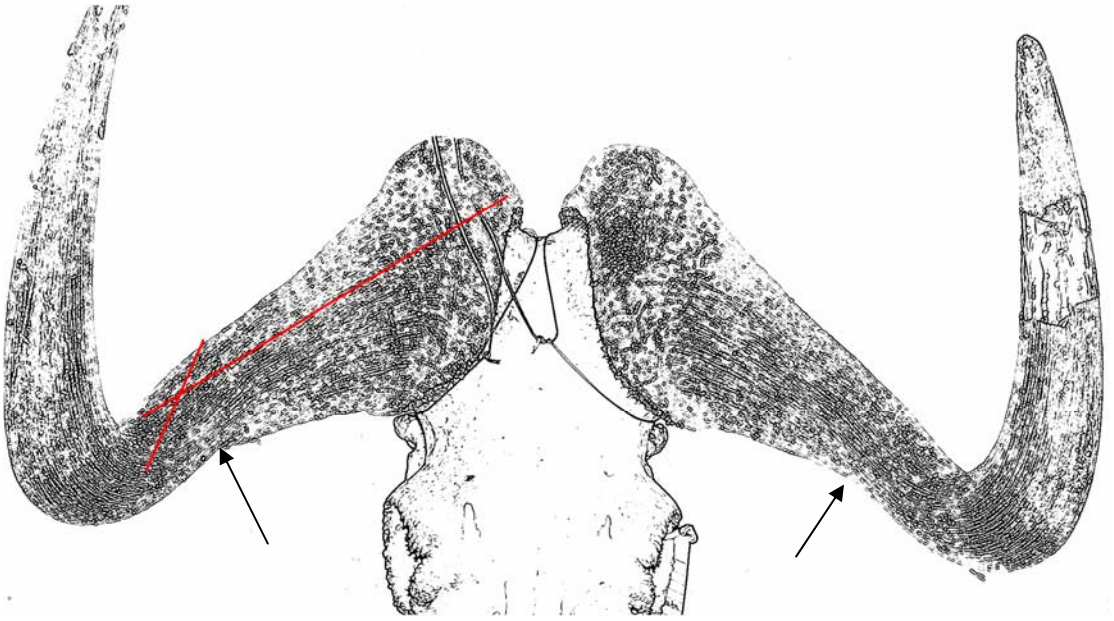

Figure 16: Horn morphology showing the sharp bend that occurs in some of the hybrid specimens. Diagram based on horn morphology of NMB 12043.

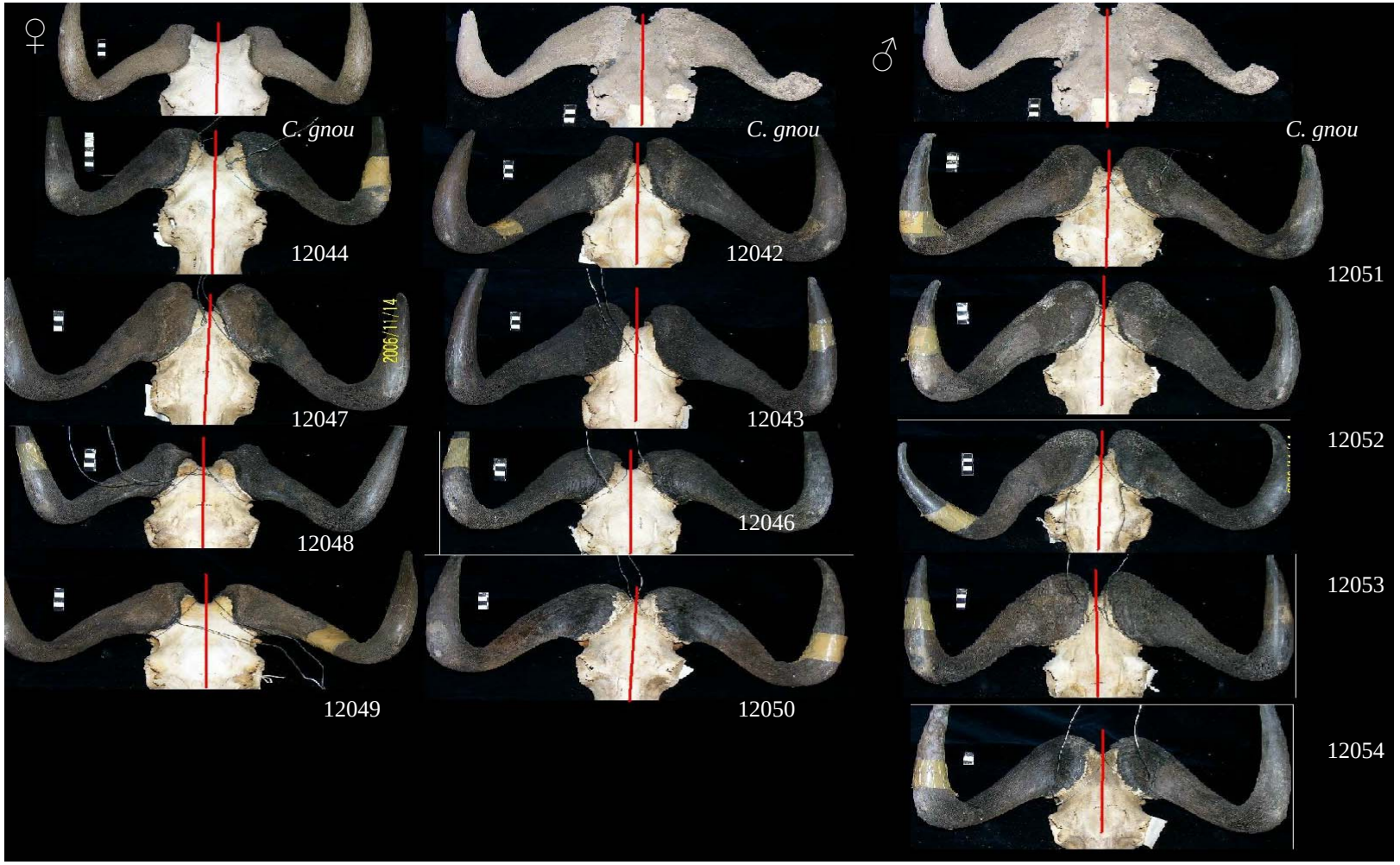

Figure 17: Horn curvature of the Spioenkop specimens in comparison to NMB 1930 (female) and C438 (male). The left column is female specimens and the middle and right hand columns are males.

5.1.3 Basal bosses

The Spioenkop specimens have large basal bosses typical of black wildebeest and this is seen through the entire sample. However, many individuals display excessive bone growth in the areas of basal bosses (see Figure 18). While this is known to occur in black wildebeest, the bone growth in the hybrids is extreme, and in many cases, the basal bosses almost touch in nuchal view, (see Figure 19). Excessive bone growth can be seen in 12 out of the 13 specimens (12043, 12044, 12046, 12047, 12048, 12050, 12051, 12052, 12053, 12054 and 12060). With the basal bosses a small distance apart in 12050, 12052, 12053, and 12060. NMB 1930 and M84 were used as the comparative black wildebeest samples for this feature.

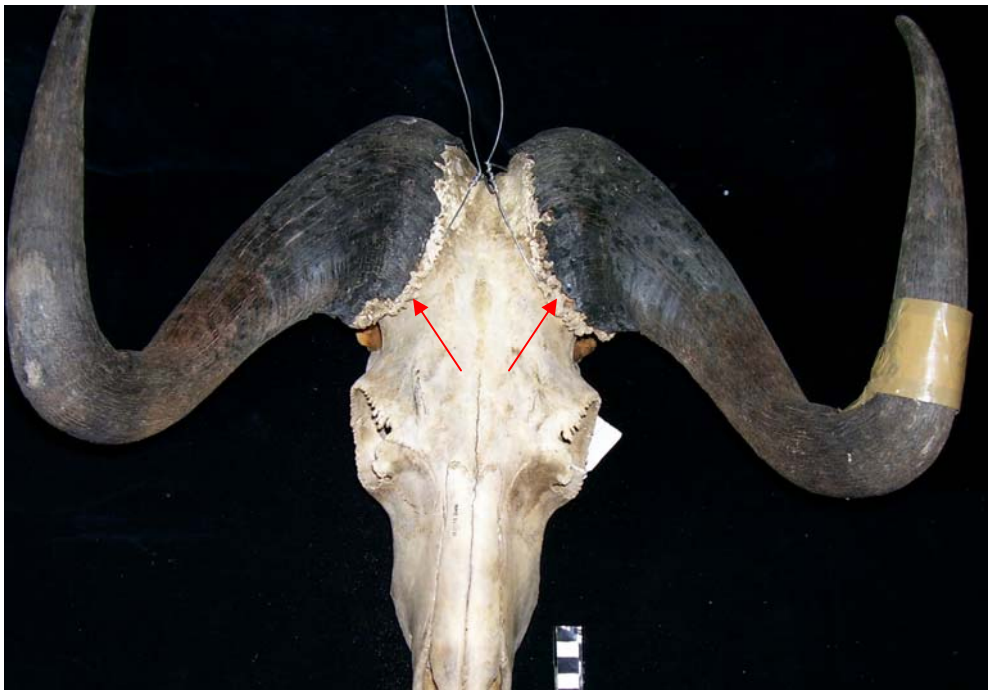

Figure 18: Example of excessive bone growth in the basal bosses of 12050, indicated by the red arrows.

Figure 19: Nuchal view illustrating the distance between basal bosses of a black wildebeest male, M84 (left) and 12060 (right) a young hybrid male from Spioenkop nature reserve.

5.1.4 The frontal and nasals

In lateral view, the area of the junction between the frontal and nasal of the black wildebeest often forms a straight line or is concave. In the Spioenkop specimens, the same concave morphology is noted. However, the frontal does have a unique morphology for the Spioenkop population. The frontal of the Spioenkop specimens, on either side of the midline (frontal suture), is raised and forms two ridges. Between these two ridges is a longitudinal depression. Although a similar morphology has been noted in black wildebeest specimens, the ridges are slight if at all present. This ridge and valley formation is seen on more than half of the Spioenkop specimens (7 out of 13) with the exception of 12044, 12050, 12051, 12052, 12054 and 12060, in which the frontal resembles that of the black wildebeest.

5.1.5 The face

Brink (2005) found that the face of *C. gnou* is short due to shortening of the premaxilla and nasals. From univariate statistics conducted in this study, the premolar to prosthion measurements of the Spioenkop sample show a trend of slight lengthening when compared to *C. gnou* while the nasals are of equal length in the hybrids and in *C. gnou*.

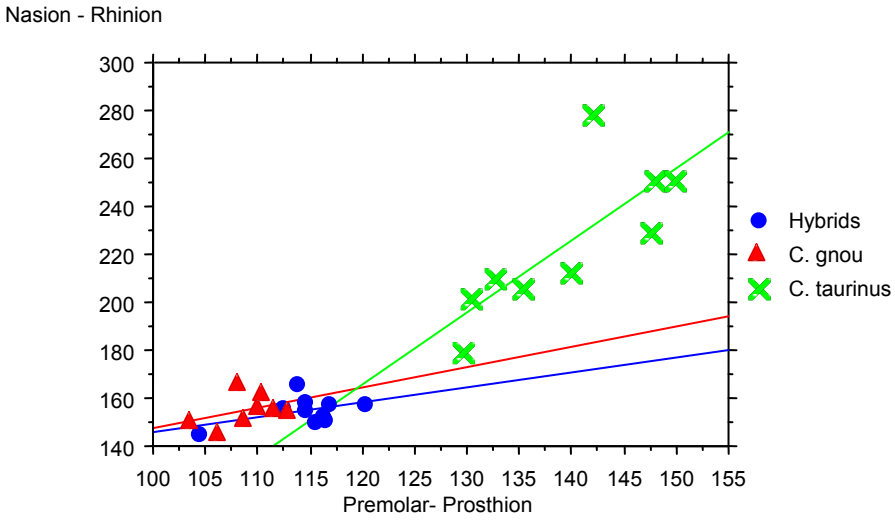

Figure 20: Bivariate plot of nasion to the rhinion measurements versus the premolar to the prosthion showing a regression line for each group.

Bivariate plots (Figure 20 and Figure 21) show this trend towards an elongation of the face in the Spioenkop specimens.

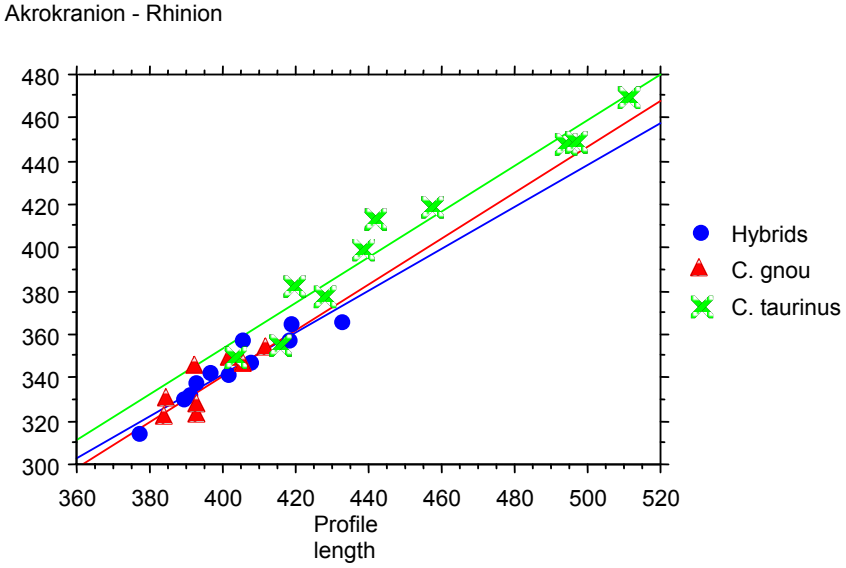

Figure 21: Bivariate plot of akrokranion to the rhinion measurements versus the skull profile length, regression lines are shown for each group.

5.1.6 Frontal sutures

In black wildebeest, the frontal sutures fuse early in life. This morphology reflects the aggressive behaviour associated with defending territories (Brink 2005), while in blue wildebeest they do not fuse at all (see Figure 22).

Figure 22: Photos illustrating the presence of an unfused frontal suture in *C. taurinus* (left) and the fused frontal suture in *C. gnou* (right).

A large number of Spioenkop individuals have their sutures fused. Evidence of hybridization with blue wildebeest is evident in some individuals where there are unfused sutures and remnants of the sutures. This can be seen in hybrids 12042, 12044, 12046 and 12048 (see Figure 23).

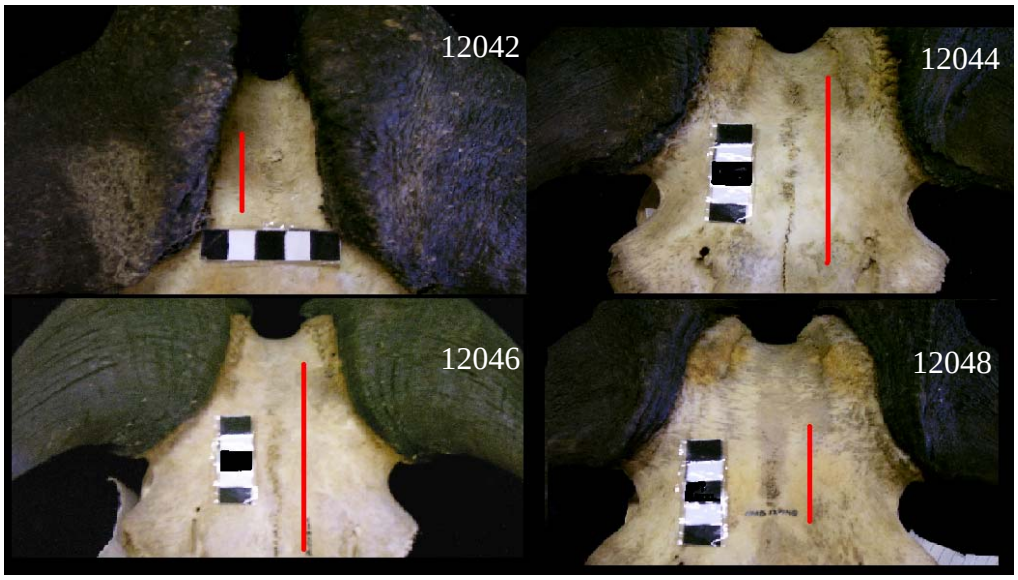

Figure 23: Photos showing frontal sutures present in the Spioenkop specimens.

The sutures present in 12042 and 12048 show that while some fusion has occurred, some sections remained unfused. 12044 and 12046 have unfused frontal sutures. Fusion of the frontal suture is a normal occurrence in black wildebeest. Some hybrid individuals show extreme fusion of sutures in that the entorbitale (suture leading from the nasal toward the eye) as well as nasal sutures become fused (see Figure 24 and Table 2). It is an over compensation against the blue gene which codes for unfused sutures.

Figure 24: Left (NMB 1930), *C. gnou* female with unfused nasal sutures and entorbitale, and right Spioenkop male (12043), with fused nasal sutures.

Table 2: Table Indicating which of the sutures related with the frontal are fused for the Spioenkop specimens.

Specimen #	Frontal Suture	Entorbitale	Nasal
12042	Remnants remain. Excessive bone growth forming a ridge where frontal suture should be.	Fused	unfused
12043	Fused	Fused	Fused
12044	Unfused	Unfused	Unfused
12046	Unfused	Unfused	Unfused
12047	Fused, but has a large deformity between the basal bosses	Unfused	Fused
12048	Remnants of the suture remain	Entorbitale fused on one side	Unfused
12049	Fused	Unfused	Unfused
12050	Fused	Unfused	Unfused
12051	Fused	Fused	Fused
12052	Fused	Fused	Fused
12053	Remnant suture remain	Fused	unfused
12054	Fused, but has sharp ridge where the suture was.	Fused	Fused
12060	Fused	Unfused	Unfused

5.1.7 Orbits

The Spioenkop specimens have large orbits, which is typical of both *C. gnou* and *C. taurinus*. However, the hybrids resemble the black wildebeest in that their orbits also project laterally.

5.1.8 Tubercula muscularia

In blue wildebeest, the valley between the tubercula muscularia is well defined while in black wildebeest this feature tends to be flattened. In the hybrids, this feature tends to be flattened with the exception of 12047, which has a well-defined valley.

5.1.9 Bullae tympanicae

From the univariate statistics, we know that there is very little difference in the size of the auditory bullae of black and hybrid wildebeest. Morphologically the hybrids have a large number of individuals with one or both bullae deformed (see Figure 25). One would expect the larger diameter of the earhole seen in the univariate plots to be related to larger auditory bullae. Instead, the high number of deformities could be related to the larger auditory bullae having to fit into a

smaller cranial space. There is no common morphology seen in the hybrid wildebeest auditory bullae and they are highly variable throughout the sample.

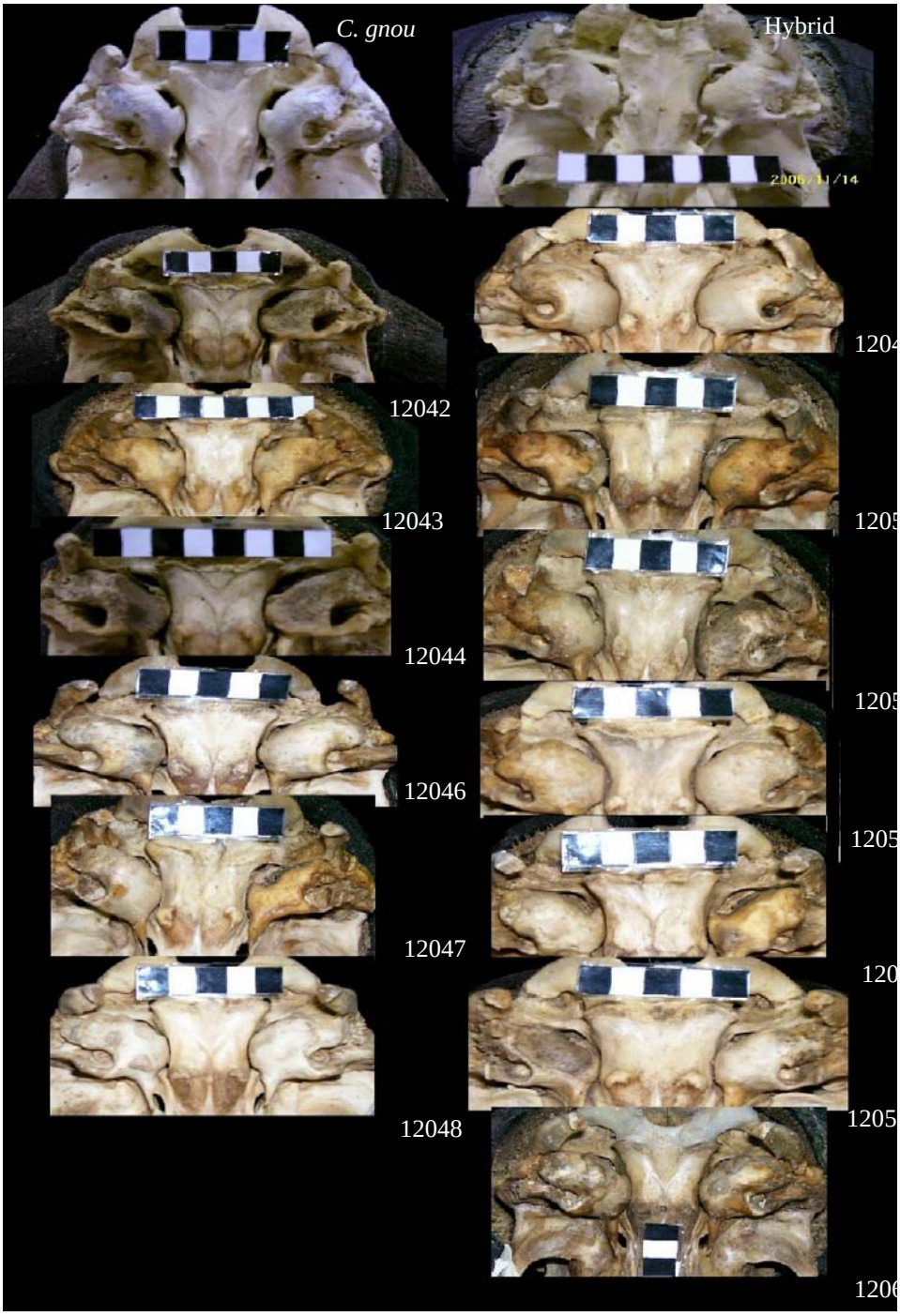

Figure 25: Photos of the auditory bullae of the Spioenkop specimens (labelled) compared to *C. gnou* (top left).

5.2 Morphology of the post crania

Bivariate plots give an indication of the shape of various postcranial elements by the ratios produced. Due to the univariate plots showing no clear separation for individual measurements, a bivariate analysis was used. For the postcranial elements, the greatest length measurements were plotted against the proximal or distal end. Also for the metacarpal and metatarsal, the dimensions of the medial condyle of the distal end were evaluated due to the large number of outliers. This section documents any morphological deviation the Spioenkop specimens may have in the post crania relative to *C. gnou*. It is important to note that 12050 and 12060 are young individuals and many of the articulation surfaces have not yet fused. However, their morphology was evaluated to see if they might have a similar trend in morphological deviation as the rest of the Spioenkop specimens.

5.2.1 Axis

Brink (2005) found that the axis of *C. taurinus* had a more pronounced waist than *C. gnou*. The Spioenkop samples all have waists that resemble black wildebeest. The hybrids have a large number of deformations in the axis as well as exostosis on various parts of the axis. Because the irregularities vary in each specimen, they will be discussed individually.

Specimen 12044 has a deformed caudal articulation facies (see Figure 26). This facies is short and there is an extra growth on the left hand side. See

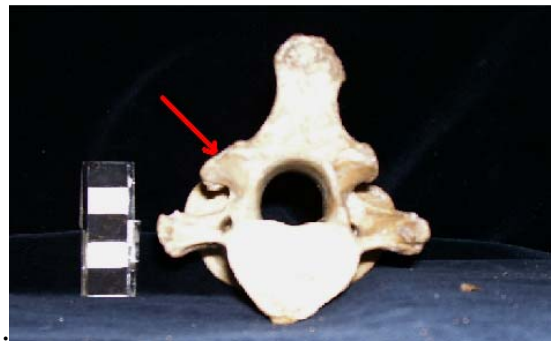

Figure 26: Caudal view of Spioenkop specimen 12044 showing deformity on the caudal articulation facet.

Specimen 12045 has exostosis on the spine of the axis and one caudal articulation facet (see Figure 27).

Figure 27: Caudal view of Spioenkop specimen 12045 showing exostosis on the spine and transverse process.

The axis of specimen 12047 has a rounded spine with excessive exostosis. There is general asymmetry in both the caudal articulation facets and the facies cranialis (see Figure 28).

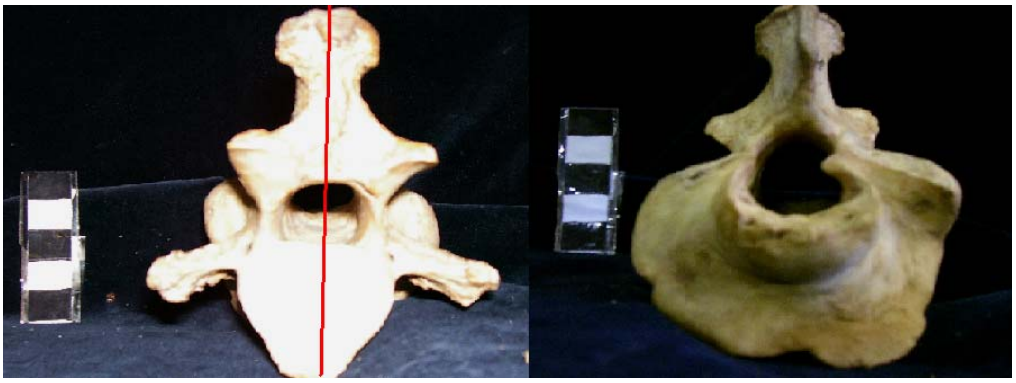

Figure 28: Spioenkop specimen 12047, in caudal and cranial view. Both views show extreme asymmetry and exostosis.

Specimens 12051, 12052 12054 all have some degree of excessive bone growth on the spine of the axis. All other Spioenkop specimens (12042, 12043, 12044, 12046, 12048 and 12049) display normal black wildebeest morphology.

5.2.2 Scapula

From univariate plots, it was noted that the measurements of the scapula showed a clear outlying of the hybrid measurement in relation to the measurements of *C. gnou* and *C. taurinus*. Due to the small sample size, these elements did not give a clear indication of where the hybrids plot in relation to *C. gnou* and *C. taurinus*.

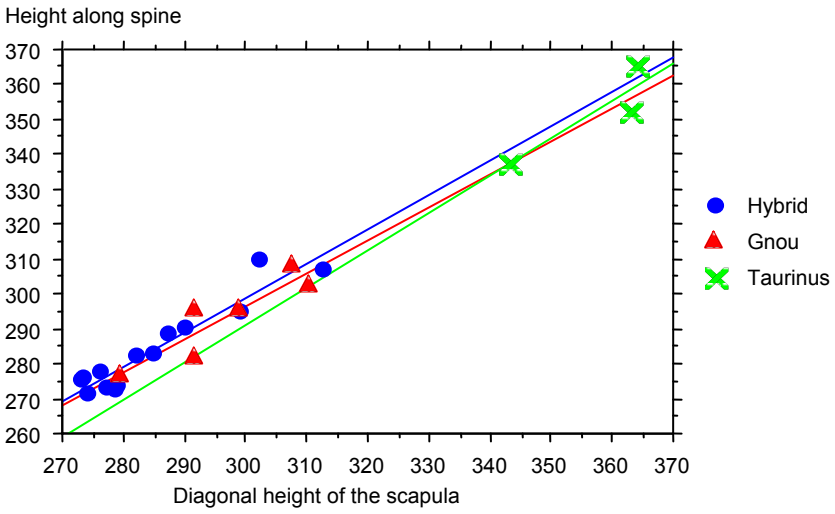

Figure 29: Bivariate scattergram showing height along spine versus diagonal height.

Figure 29 shows that the linear regression of the height along the spine and the diagonal height of the black and hybrid wildebeest are closely related, indicating not much difference in the shape of the scapula. There are however, individuals that are much smaller than the black wildebeest.

5.2.3 Humerus

Brink (2005) found three differences in the humerii of blue and black wildebeest. Firstly that the humerus of *C. taurinus* is slender compared to black wildebeest, secondly, the caudal part of the tuberculum maius is sometimes enlarged and lastly that in the fossa radialis there is a longitudinal ridge which is absent in *C. taurinus*. In respect to the first two features, the Spioenkop specimens' morphology resembles the black wildebeest. Using a univariate plot of the ratio of

greatest length against the smallest depth of the diaphysis shows that blue wildebeest humerii are more slender (see Figure 30). Here we see that the Spioenkop samples plot within black wildebeest range. Specimen 12053 had some exostosis on the trochlea.

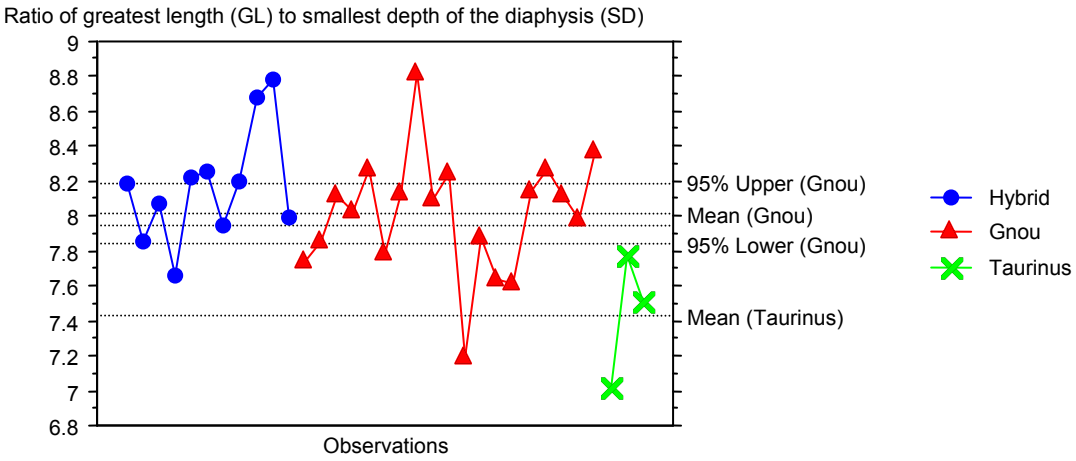

Figure 30: Univariate plot indicating the slenderness of the humerus.

For the ridge in the fossa radialis, the results were more varied. Specimens 12043, 12044, 12046, 12051 12052 and 12053 all have longitudinal ridges. The remaining specimens 12042, 12045, 12047 12048 and 12054 do not have the ridge, however, the depth of the fossa in these specimens varies. Specimens 12042, 12047 and 12048 have shallow fossae that resemble blue wildebeest, and 12045 and 12054 both resemble black wildebeest. This feature of the humerus is variable within black wildebeest and cannot be used for the identification of hybrids.

The bivariate analysis of the humerus shows the hybrid wildebeest plotting within the black wildebeest range for the general dimensions of the humerus. There are also similar regression lines for the black and hybrid wildebeest (see Figure 31).

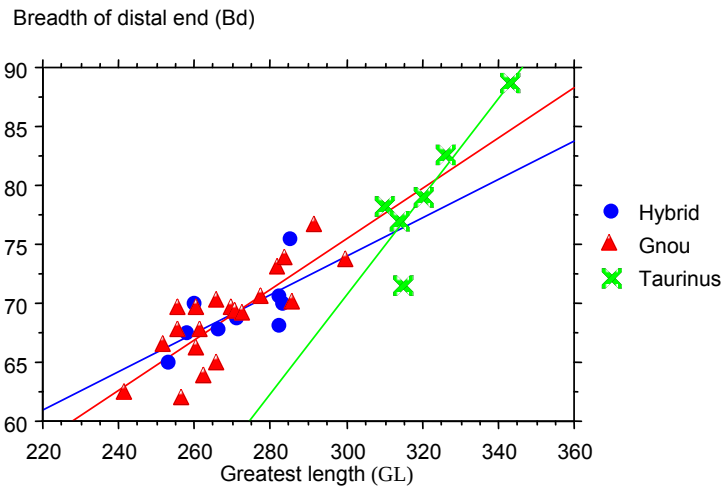

Figure 31: Bivariate analysis for the humerus. Greatest length versus the breadth of the distal end of the humerus.

5.2.4 Radius

The radii of the Spioenkop sample did not vary morphologically from that of the black wildebeest. The incision in the proximal radius for the lateral coronoid process of the ulna is sharp and deep in the hybrid specimens. Just as in black wildebeest, this incision forms a 90° angle in most of the Spioenkop samples. The incisions on specimens 12044 and 12053 do not form a 90° angle, instead the angle is more obtuse. In specimens 12042, 12043, 12046, 12047, 12048, 12049, 12052, and 12054 (7 out of 14 samples) the radius and ulna were fused together

(see Figure 32). This does not occur in either the blue or the black wildebeest, and is unique to the Spioenkop sample.

Figure 32: Lateral view of Spioenkop specimen 12043 radius and ulna. The arrow indicates fusion of these bones.

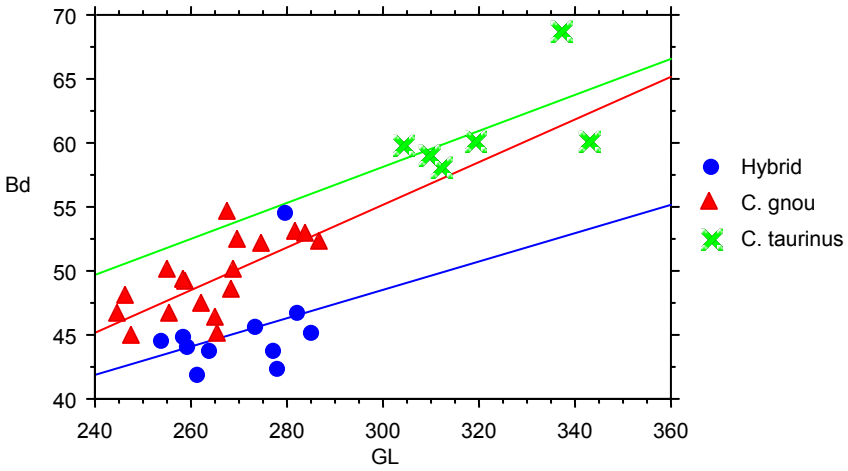

Figure 33: Scattergram for greatest length versus the breadth of the distal end of the radius.

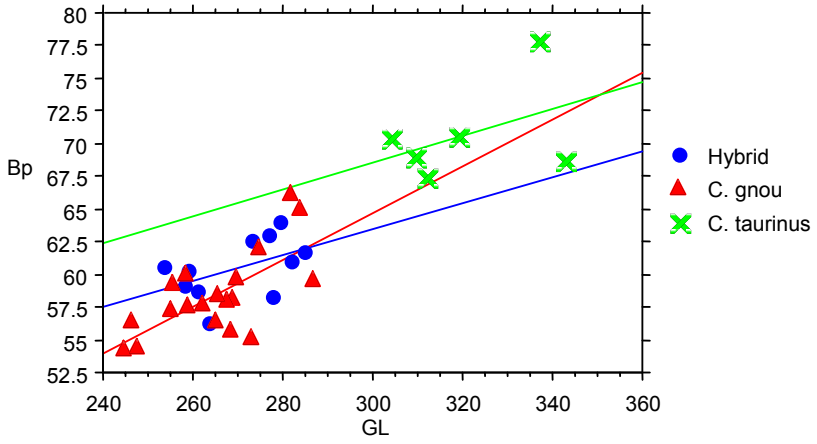

Figure 34: Scattergram showing greatest length versus the breadth of the proximal end of the radius.

In Figure 33, the hybrids fall well below the black wildebeest. The sample size is large enough to assume that the black wildebeest range is well represented. Figure 34, however, does not show this same pattern and hybrids plot within the black wildebeest range. This Spioenkop group has a trend of being smaller than both *C. gnou* and *C. taurinus* in the distal ends of the radius.

5.2.5 Metacarpal

For this feature, black and blue wildebeest are differentiated in two ways; firstly, medially on the proximal articular surface the facet for the os carpale II an angle is formed that is more accentuated in *C. gnou* than in *C. taurinus*. Secondly, in dorsal and volar view the lateral margins of the distal part of the shaft of *C. taurinus* does not flow evenly in the distal articulation but forms an angle. These

were the two features examined while studying the metacarpal of the Spioenkop samples.

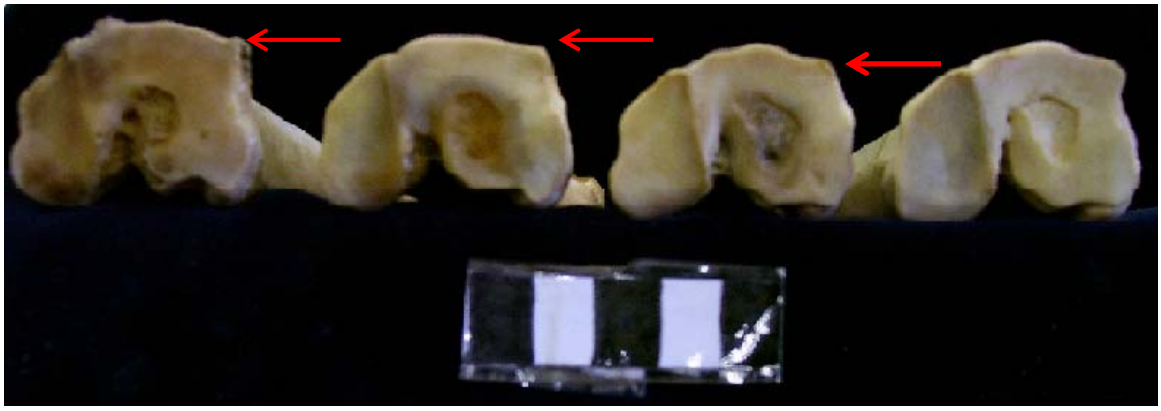

Figure 35: Spioenkop specimens 12042 (left), 12043 (centre left), 12047 (centre right) and 12054 (right) all showing sharp angles in the proximal articular facets of the os carpale.

In Figure 35, the sharp angle of the os carpale facet is indicated by the red arrows. Specimens 12042, 12043, 12047 and 12054 had the only irregularities in this regard while the rest of the specimens resembled black wildebeest.

Three specimens had lateral margins that did not flow evenly into the distal articulation they are: 12045, 12047 and 12054 (see Figure 36). These specimens resembled blue wildebeest. It is also noted that while 12060 is a young individual, it too displayed irregularities in the angle of the os carpale facet and distal articulation of the metacarpal. All the Spioenkop specimens had extra irregular bone growth on the shafts of the metacarpal.

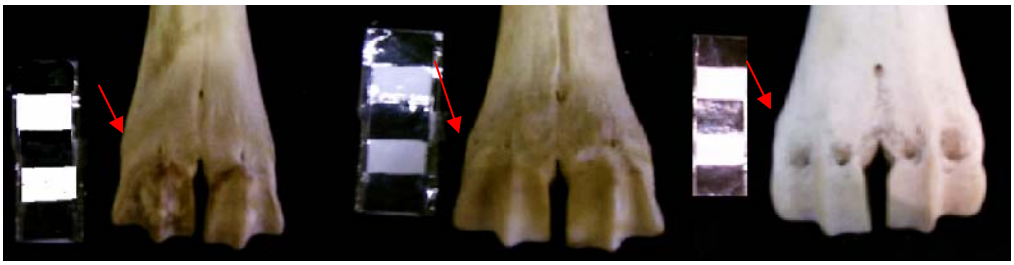

Figure 36: Dorsal view of the distal metacarpal showing irregularities in the lateral margins. Spioenkop specimens 12045 (left), 12047 (center) and 12054 (right).

For the metacarpal, Figure 37 shows little difference in the dimensions of the hybrid and black wildebeest.

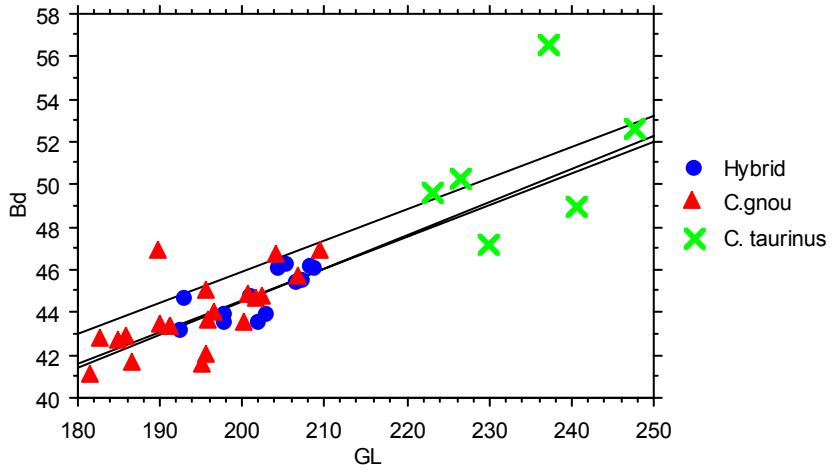

Figure 37: Bivariate scattergram of the greatest length versus the breadth distal end of the metacarpal.

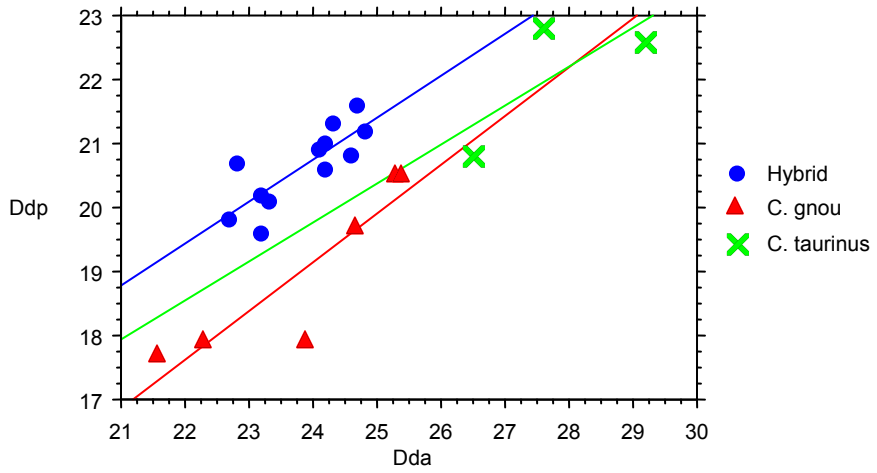

Figure 38: Bivariate plot showing depth of the peripheral part of the medial condyle against the depth of the achsial part of the medial condyle of the metacarpal.

In Figure 38, there is clear separation between the blue, black and Spioenkop wildebeest for the dimensions of the medial condyle. This same trend is seen in the metatarsal. For this feature, the hybrids have their own unique morphology.

5.2.6 Femur

Morphologically there is little difference in the morphology of *C. taurinus* and *C. gnou.* The fossa supracondylaris is noted by Brink to be deeper in *C. taurinus* than in *C. gnou,* and that this may be related to body size (see Figure 39). There is one deviation in the Spioenkop specimens from a black wildebeest femur. In the following individuals: 12042, 12043, 12045, 12046, 12047, 12048, 12049 and 12051 the fossa supracondylaris is very shallow compared to both parent species

an example of this is seen in Figure 40. The angles of the photographs differ in Figure 39 and Figure 40 due to the shallow depth of the fossa in the hybrid specimens, a proximal view of the femur showed this shallow fossa clearer than it would it caudal view.

Figure 39: Caudal view of the distal ends of *C. gnou* (left) and *C. taurinus* (right). Arrows indicate the fossa supracondylaris.

Figure 40: Proximal view of the femur of Spioenkop specimens 12042 and 12047 indicating shallow fossa supracondylaris.

Figure 41: Femur of Spioenkop specimen 12046 in the cranial view showing extreme exostosis.

Specimen 12046 has a large amount of exostosis on the femur (see Figure 41).

There is unusual wear pattern on the trochlea of the Spioenkop femurs (see Figure 42). This wear pattern is caused by friction with the patella on this joint surface. This wear pattern is seen on specimens 12042, 12043, 12045, 12046, 12047, 12049, 12051, 12052 and 12054.

Figure 42: Cranial view of the distal end of the femur of Spioenkop specimen 12046. The red lines outline the irregular wear pattern seen on this surface.

For the femur, Figure 43 shows little difference in the dimensions of the hybrid and black wildebeest.

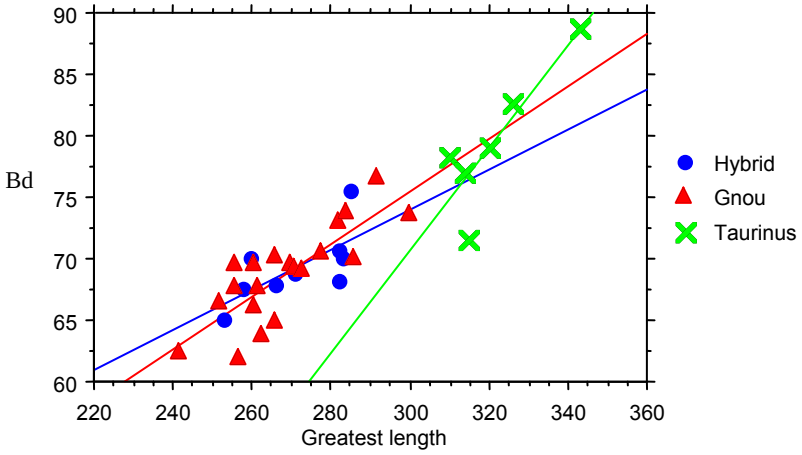

Figure 43: Greatest length versus the breadth of the distal end of the femur.

5.2.7 Tibia

The corpus in the hybrid specimens are recurved resembling the black wildebeest. The only deviation found in some Spioenkop specimens was that the proximal fibula was more developed compared to *C. gnou.* This was seen in 12042, 12043 and 12044 (see Figure 44). There was excessive bone growth on 12044 and 12046 (see Figure 45).

Figure 44: Spioenkop specimen 12042 in medial view showing a more developed proximal fibula than *C. gnou.*

Figure 45: Spioenkop specimen 12046 in lateral view showing exostosis on the proximal ends of the tibia.

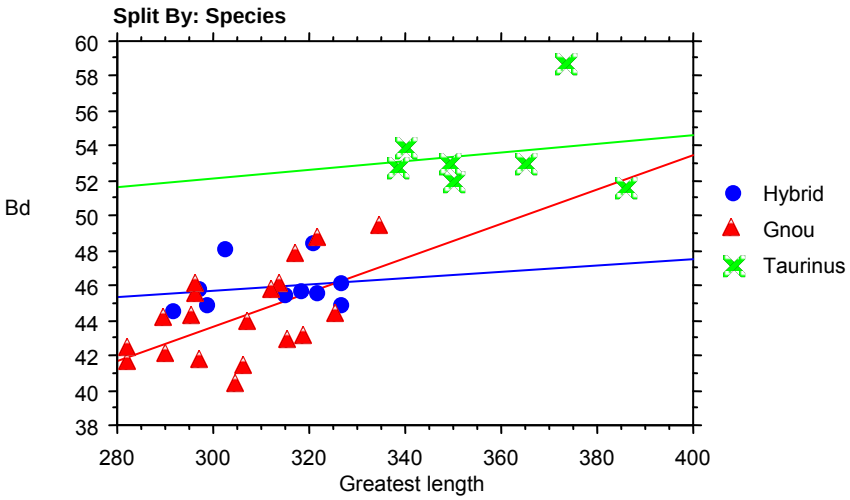

Figure 46: Bivariate scattergram for greatest length versus the breadth of the distal end of the tibia.

Figure 46, shows little difference in the dimensions of the hybrid tibia and that of the black wildebeest. The 95% regression line for the hybrids shows a similar gradient to the blue wildebeest. This could change by increasing the sample size of the blue and hybrid wildebeest.

5.2.8 Metatarsal

There is no difference other than size between *C. gnou* and *C. taurinus* for the metatarsal. Only one hybrid (12050) shows morphological deviation and that is in the plantar view. Specimen 12050 has a deep longitudinal groove along the metatarsal (see Figure 47). Specimens 12042, 12043, 12045, 12047, 12048, 12049, 12050, 12051, 12052, 12053 and 12054 all have varying degrees of extra bone growth on the metatarsal. This bone growth is often observed on the shafts and proximal ends of the metatarsals.

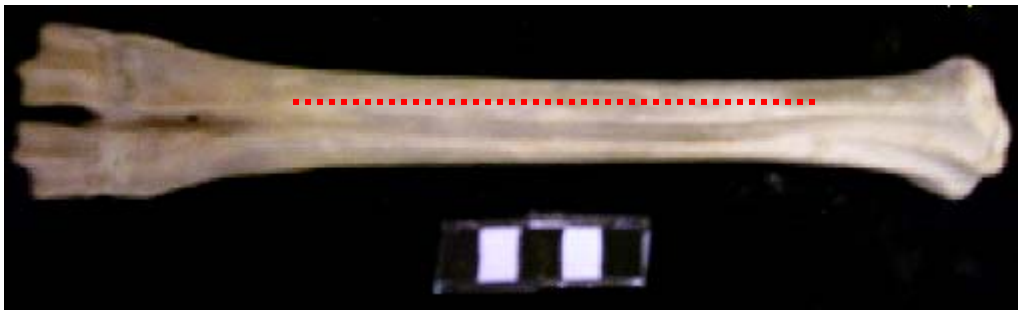

Figure 47: Plantar view of the metatarsal of Spioenkop specimen 12050, the red line indicates the deep longitudinal groove.

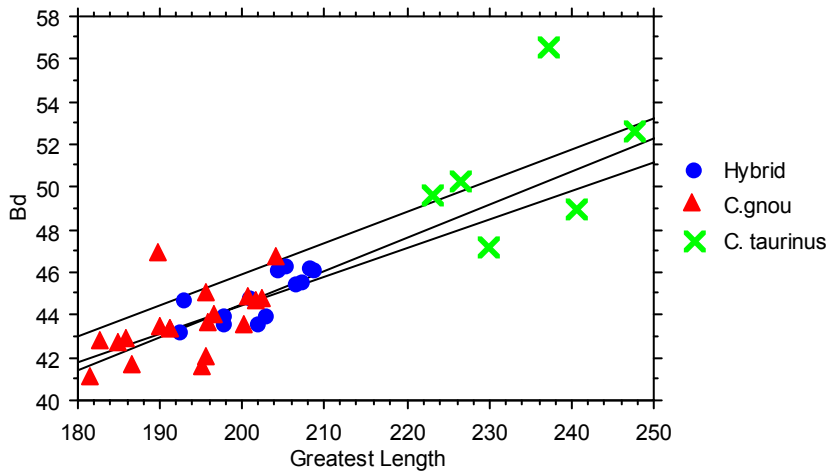

Figure 48: Bivariate scattergrams of the greatest length versus the breadth of the distal end of the metatarsal.

For the metatarsal, Figure 48 shows that the dimensions of the Spioenkop specimens fall within the black wildebeest range. There is overlap between the blue, black and hybrid wildebeest. The hybrid measurements cluster similarly to the blue wildebeest.

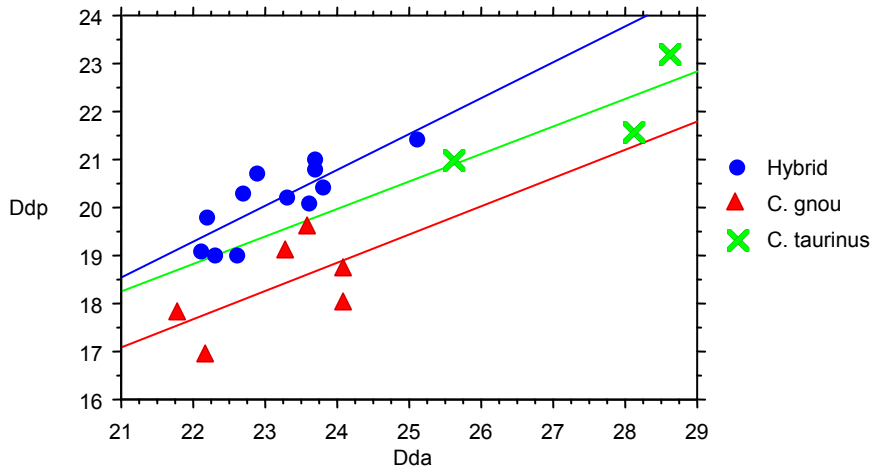

Figure 49: Bivariate plot showing depth of the peripheral part of the medial condyle against the depth of the achsial part of the medial condyle of the metatarsal.

Figure 49 shows that in the distal ends of the metatasals the Spioenkop specimens have their own unique dimensions in relation to *C. gnou* and *C. taurinus.*

5.2.9 Summary of morphology

The Bivariate analysis shows that dimensionally the hybrids have unique trends in the scapula, radius, metacarpal and metatarsal. For the scapula, there is a trend for smaller scapula relative to *C. gnou* and *C. taurinus*. The radius and the metapodials of the hybrids have their own unique dimensions relative to *C. gnou* and *C. taurinus.* There is no consistency in the trending of the Spioenkop specimens.

Morphologically there are a large number of deformities in this group. There are no consistent deviations in the morphology and the features are highly variable between individuals.

6 RESULTS 2: STATISTICS

6.1 Introduction

In this chapter, the statistical results for measurements taken will be examined.

The Spioenkop specimens are evaluated using bivariate analysis. This is to give an accurate indication of the dimensions of skeletal elements. In addition, the univariate plots, blue represents the hybrids, red represents the black wildebeest and green represents the blue wildebeest. The species plots were joined by straight lines in order to show clear separation between the three separate groups of plots. Figure 50 indicates the order in which the samples were plotted, the standard order for the entire project. Spioenkop specimen 12045 did not have a skull available for measurement and will only be used in the postcranial analysis.

Table 3: Table indicating specimen numbers used and the sex of that individual. Highlighted number indicates the order in which the specimens were entered into the statistical plots.

	Specimen number		Specimen number		Specimen number	
	Spioenkop	Sex	*C. gnou*	Sex	*C. taurinus*	Sex
1	12042	♂	M84	♀	Unknown #	♂
2	12043	♂	NMB92	♂	NMB57	♀
3	12044	♀	NMB81	♀	NMB12172	♀
4	12045	♀	NMB96	♀	NMB77	♀
5	12046	♂	NMB93	♀	NMB12209	♂
6	12047	♀	NMB1930	♀	NMB12088	♂
7	12048	♀	M89	♂	NMB9355	♂
8	12049	♀	M90	♂	NMB12066	♂
9	12050	♂	NMB80	♂	NMB12064	♂
10	12051	♂	Sub fossil C1464	♂	NMBF64	♂
11	12052	♂	Sub fossil C438	♂	NMB73	♂
12	12053	♂	C1463	♂		
13	12054	♂	C1463	♂		
14	12060	♂				

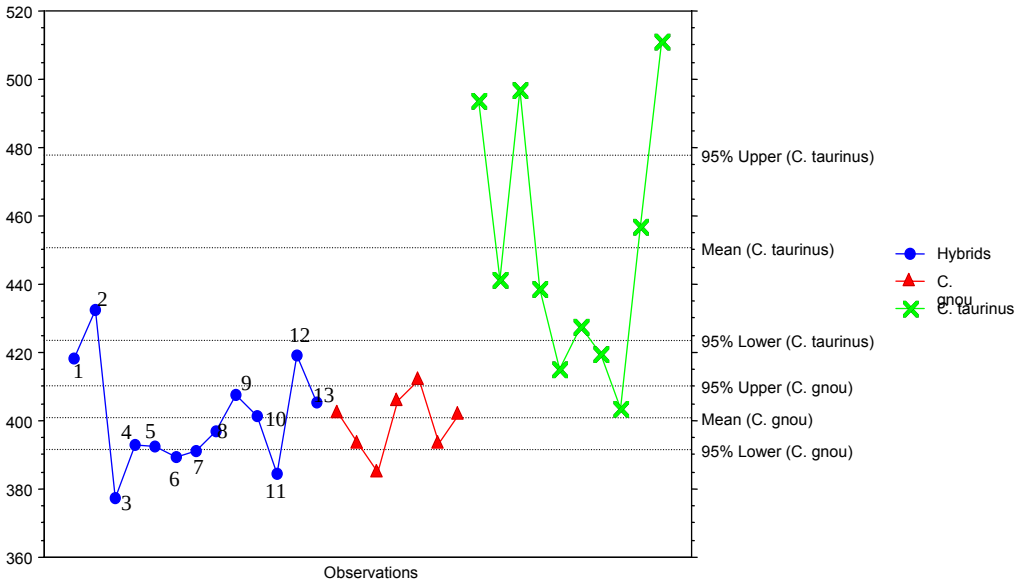

Figure 50: Example plot showing the order in which hybrids plot. The numbers next to the blue plots correlate with the numbers highlighted in yellow in Table 3. The Spioenkop specimens were plotted in this particular order for all statistical plots done in this study.

6.2 Univariate analysis for the cranium

6.2.1 Skull profile length

(See Figure 1, measurement 1).

Table 4: Descriptive statistics for skull profile length.

	Profile lngth, Total	Profile lngth, Hybrids	Profile lngth, C.Gnou	Profile lngth, C.Taurinus
Mean	416.940	400.731	399.143	450.470
Std. Dev.	33.832	15.541	9.076	37.898
Std. Error	6.177	4.310	3.430	11.984
Count	30	13	7	10
Minimum	377.400	377.400	385.100	403.400
Maximum	511.200	432.500	412.000	511.200
# Missing	5	0	5	0
Variance	1144.629	241.531	82.370	1436.251
Coef. Var.	.081	.039	.023	.084
Range	133.800	55.100	26.900	107.800

In Table 4, the mean of black wildebeest and that of the Spioenkop specimens are very similar for skull profile length. The standard deviation shows that the spread of the data from the mean is greater in the Spioenkop specimens than in the black wildebeest. The standard deviation for the Spioenkop specimens lies between the blue and black wildebeest.

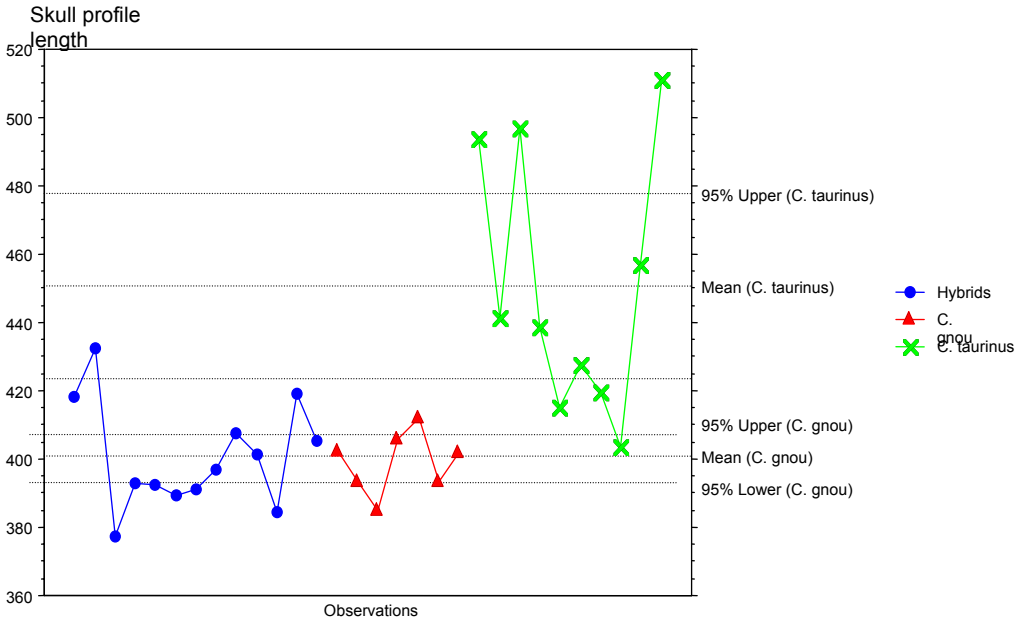

Figure 51: Univariate analysis of skull profile length.

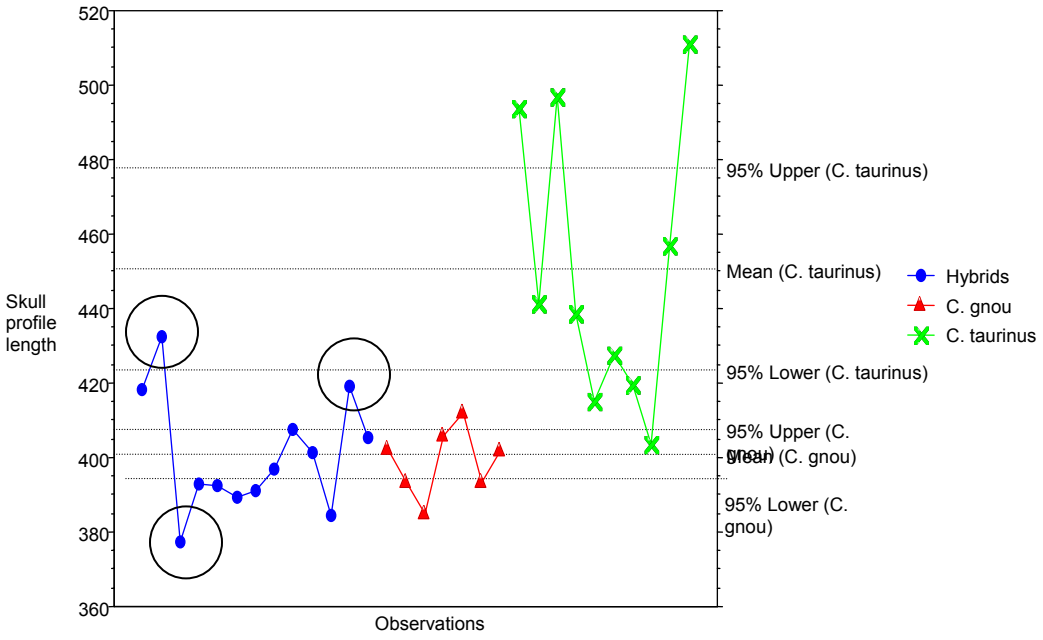

Figure 52: Examples of outliers for skull profile length

In Figure 51, a general overlap can be seen between *C. gnou* and the Spioenkop specimen plots. For skull profile length, *C. gnou* plot tightly together, showing very little deviation in the measurements. For *C. taurinus* the measurements spread, while *C. gnou* measurements cluster together. For the Spioenkop specimens, the plots are random and unpredictable.

In Figure 52, three specimens appear to be hybrids. They lie outside of the *C. gnou* confidence interval and plot further than any of the *C. gnou* specimens. Two specimens fall above the upper limit of the black wildebeest, while one specimen plots well below the range of black wildebeest. This trend is unexpected.

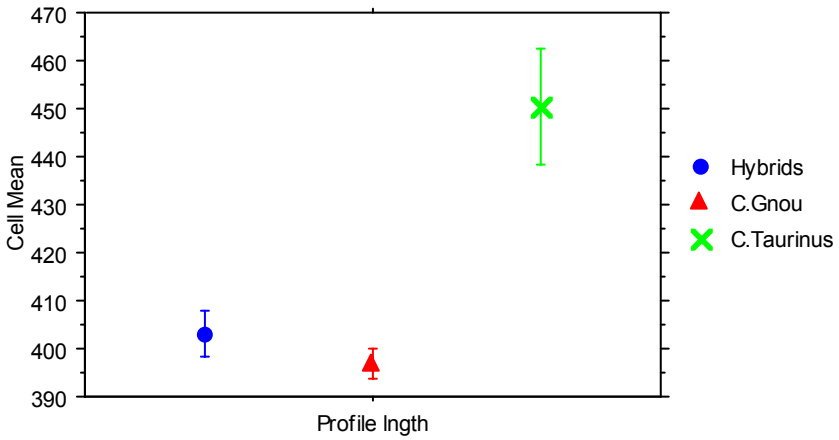

Figure 53: Standard error for skull profile length (error bars: ±1 STD error).

From Figure 53 we see that the Spioenkop specimens plot extremely close to *C. gnou*, with the blue wildebeest outlying. In standard error, the upper limit for Spioenkop specimens is slightly higher than that of the black wildebeest.

6.2.2 Condylobasal length

(See Figure 4, measurement 2).

Table 5: Descriptive statistics for condylobasal length.

	Condylobasal lngth, Total	Condylobasal lngth, Hybrids	Condylobasal lngth, C.Gnou	Condylobasal lngth, C.Taurinus
Mean	401.617	382.315	378.557	442.850
Std. Dev.	35.692	11.051	6.072	32.813
Std. Error	6.516	3.065	2.295	10.376
Count	30	13	7	10
Minimum	365.700	365.700	370.200	401.700
Maximum	494.600	398.600	390.200	494.600
# Missing	5	0	5	0
Variance	1273.937	122.118	36.870	1076.716
Range	128.900	32.900	20.000	92.900

Table 5 shows the differences in mean, standard deviation and range between the three species. The Spioenkop specimen measurements for condylobasal length fall between the measurements of *C. gnou* and *C. taurinus*.

In Table 5, a general overlap can be seen between *C. gnou* and the Spioenkop specimens. For Condylobasal length, *C. gnou* plot tightly together showing very little deviation in the measurements. For *C. taurinus* the measurement are more spread than the measurements of *C. gnou*. The Spioenkop specimen plots spread more than the black wildebeest. There are six outliers in the condylobasal plots, these plots lie just out of the black wildebeest range.

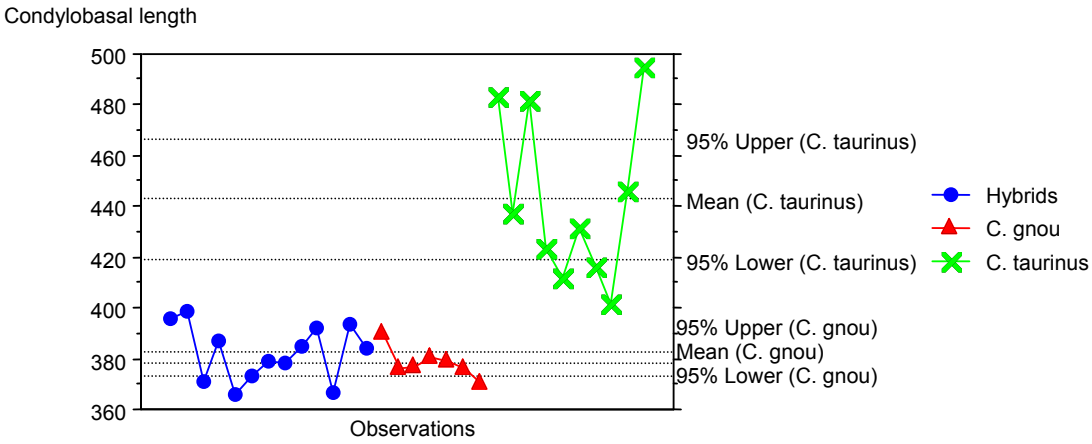

Figure 54: Univariate line chart for condylobasal length.

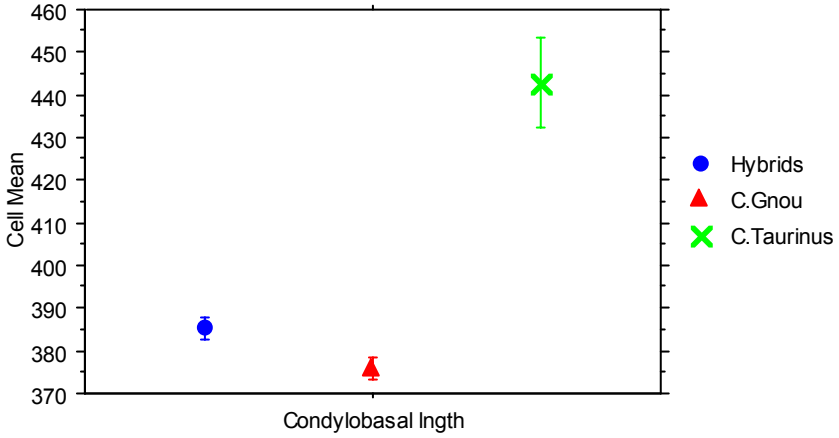

Figure 55: Standard error cell plot for condylobasal length (error bars: ±1 STD error).

Figure 55 shows that a there is a separation between the black wildebeest and the Spioenkop specimens with respect to standard error, but that some specimens still fall within range of black wildebeest.

6.2.3 Basal length of the skull

(See Figure 4, measurement 3).

Table 6: Descriptive statistics for basal length of the skull.

	Basal length, Total	Hybrids	C. gnou	C. taurinus
Mean	372.576	357.423	354.671	408.389
Std. Dev.	29.723	11.039	4.112	28.288
Std. Error	5.519	3.062	1.554	9.429
Count	29	13	7	9
Minimum	341.500	341.500	349.900	371.300
Maximum	452.900	377.800	361.800	452.900
# Missing	6	0	5	1
Variance	883.478	121.870	16.906	800.186
Range	111.400	36.300	11.900	81.600

Observations made from Table 6 are that the means of the Spioenkop sample and black wildebeest are very similar, while the range for the Spioenkop specimens is much larger than the black. The standard deviation for Spioenkop specimens is larger than that of black.

Figure 56 shows that black wildebeest and the Spioenkop specimens share a lower limit, but there are Spioenkop specimens that plot much further than the upper limit of black wildebeest. The Spioenkop specimen plots are spread, while the black plots cluster over a small interval. There are eight outliers for basal length of the skull.

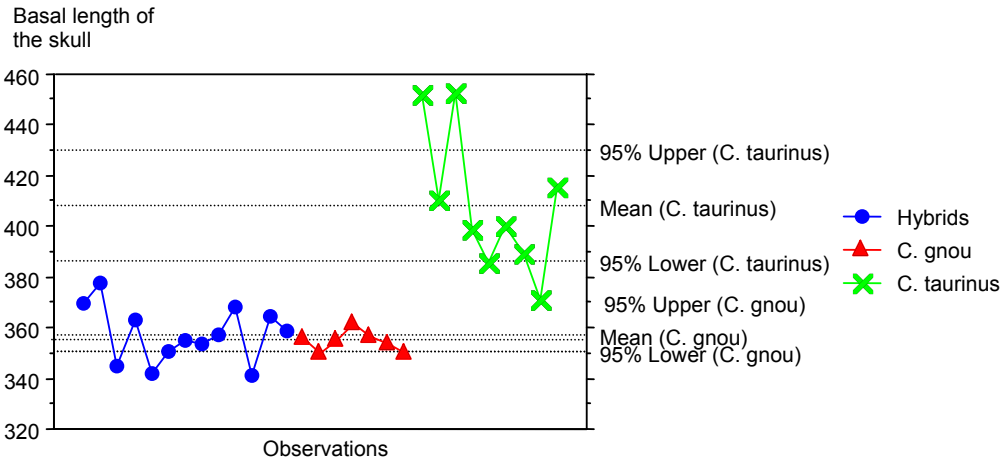

Figure 56: Univariate line plot for basal length of the skull.

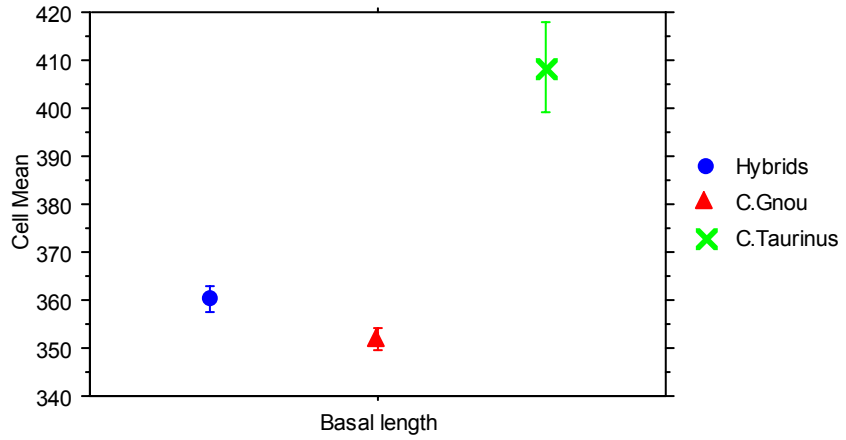

Figure 57: Standard error cell plot for basal length of the skull (error bars: ±1 STD error).

Standard error in both condylobasal length of the skull and basal length of the skull are almost identical (Figure 55 and Figure 57) in that the Spioenkop specimens plot outside the range of black wildebeest, with some individuals falling within range.

6.2.4 Short skull length, measured from the basion to the premolar.

(See Figure 4, measurement 4).

Table 7: Descriptive statistics for short skull length.

	Short skll lngth, Total	Short skll lngth, Hybrids	Short skll lngth, C.Gnou	Short skll lngth, C.Taurinus
Mean	253.922	246.454	245.180	274.422
Std. Dev.	17.224	8.501	5.799	18.557
Std. Error	3.045	2.358	1.834	6.186
Count	32	13	10	9
Minimum	231.200	232.800	231.200	257.700
Maximum	304.700	259.200	250.700	304.700
# Missing	3	0	2	1
Variance	296.660	72.273	33.624	344.369
Range	73.500	26.400	19.500	47.000

Table 7 shows that while the mean for the Spioenkop specimens is almost equal to the black wildebeest, the standard deviation and standard error are much larger for the Spioenkop specimens. The maximum value for the Spioenkop specimens lies out of the black wildebeest range. In Figure 58 we see the Spioenkop specimens and the black wildebeest share the lower confidence interval and that many of the Spioenkop specimens plot slightly higher than the black wildebeest plots. However, none of the specimens lies outside of the range of black wildebeest on the lower interval, but five lie outside of the upper interval for the black. Two individuals plot within range of blue wildebeest.

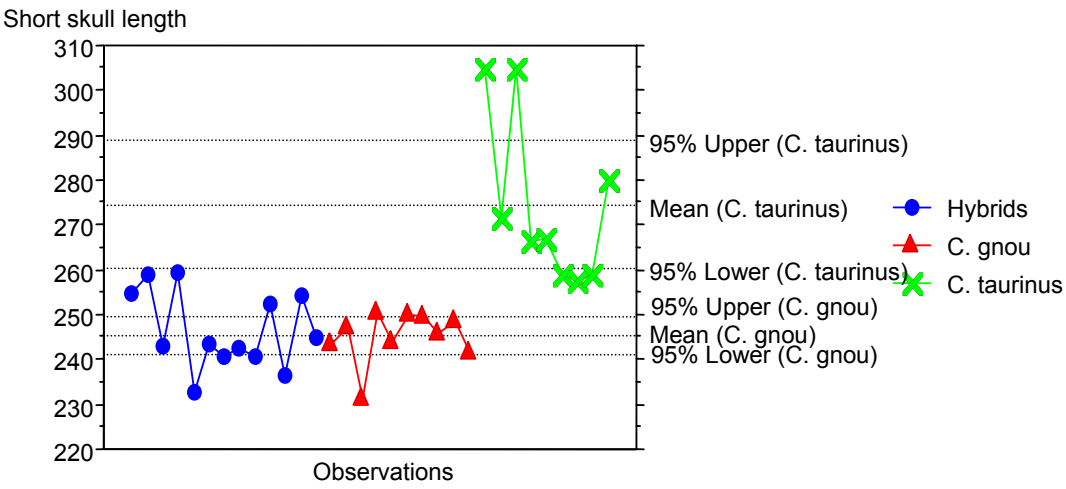

Figure 58: Univariate line plot for short skull length.

In Figure 59, most of the Spioenkop specimens plot similar to black wildebeest, with the exception of a few individuals.

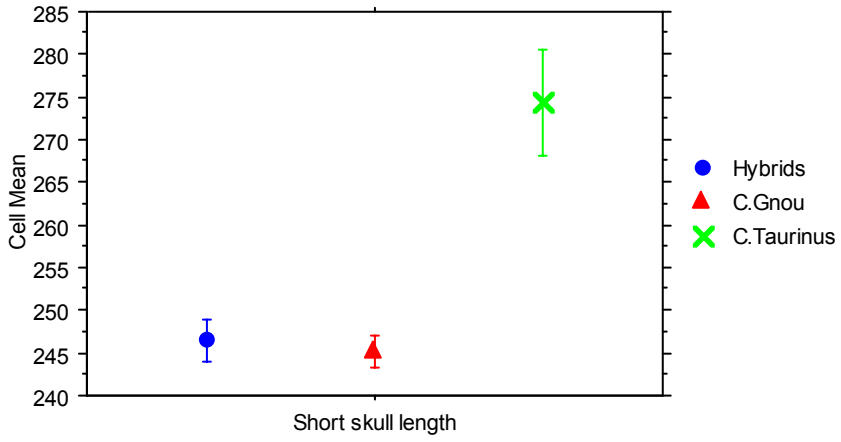

Figure 59: Standard error cell plot for short skull length (error bars: ±1 STD error).

6.2.5 Premolar to the prosthion

(See Figure 4, measurement 5).

Table 8: Descriptive statistics for the distance from the premolar to the prosthion.

	Premol- Prosthion, Total	Premol- Prosthion, Hybrids	Premol- Prosthion, C.Gnou	Premol- Prosthion, C.Taurinus
Mean	120.613	113.892	108.271	137.990
Std. Dev.	14.058	4.654	4.072	8.810
Std. Error	2.567	1.291	1.539	2.786
Count	30	13	7	10
Minimum	102.000	104.300	102.000	124.600
Maximum	149.900	120.200	113.000	149.900
# Missing	5	0	5	0
Variance	197.618	21.659	16.582	77.614
Range	47.900	15.900	11.000	25.300

Table 8 shows that the main difference between the Spioenkop specimens and the black wildebeest are the means and range. The values show that the Spioenkop specimens are slightly larger than the black wildebeest with regard to Premolar to Prosthion measurements. The standard deviation and standard error values are similar.

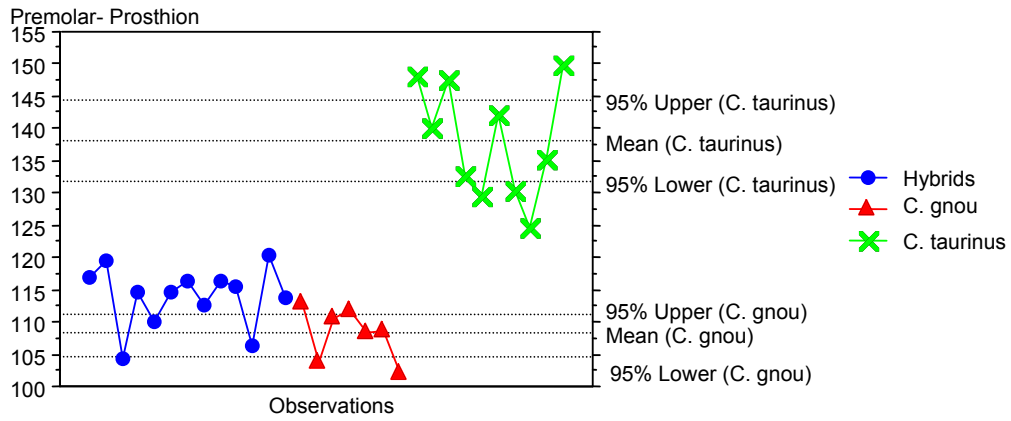

Figure 60: Univariate line plot for the distance from the premolar to the prosthion.

Figure 60 shows that there is a marked difference in the means as well as the intervals for the premolar to prosthion measurements. Nine Spioenkop specimen measurements fall out of range of the black wildebeest. None falls within the blue wildebeest range.

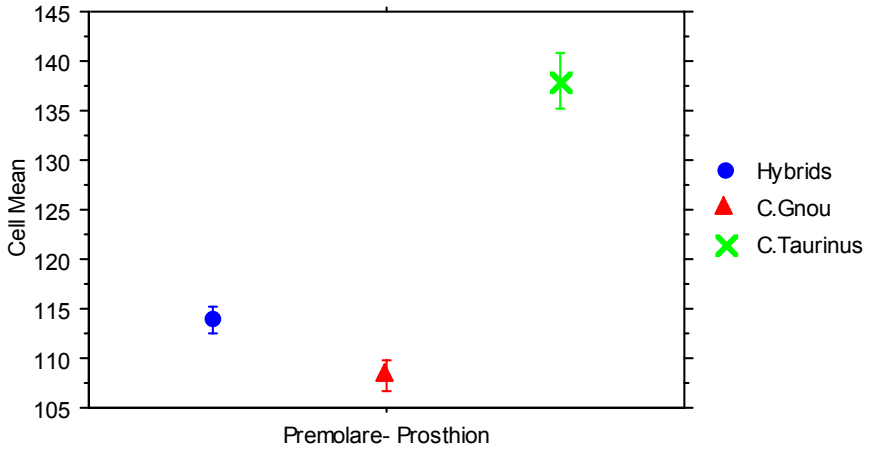

Figure 61: Standard error cell plot of premolar to the prosthion (error bars: ±1 STD error).

The standard errors in Figure 61 show that the Spioenkop specimens plot clear of the black wildebeest. There is no overlap in the standard errors.

6.2.6 Viscerocranium length.

(See Figure 3, measurement 6).

This measurement is taken from the nasion to the prosthion.

Table 9: Descriptive statistics of the distance from the nasion to the prosthion.

	Nasion - Prosthion, Total	Nasion - Prosthion, Hybrids	Nasion - Prosthion, C.Gnou	Nasion - Prosthion, C.Taurinus
Mean	254.155	236.862	234.950	288.160
Std. Dev.	30.732	6.615	3.794	30.155
Std. Error	5.707	1.835	1.549	9.536
Count	29	13	6	10
Minimum	225.800	225.800	229.400	251.700
Maximum	334.000	250.200	240.100	334.000
# Missing	6	0	6	0
Variance	944.474	43.759	14.391	909.332
Range	108.200	24.400	10.700	82.300

Table 9 shows that the Spioenkop specimens have a larger range and standard deviation than the black. The mean of the Spioenkop specimens still falls within the range of black wildebeest.

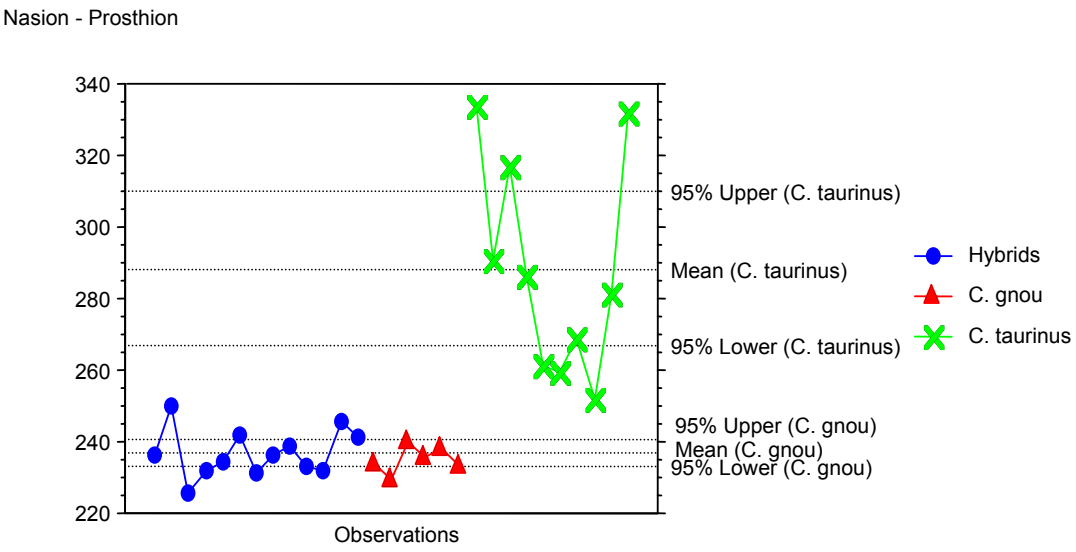

Figure 62: Univariate line plot of the distance from the nasion to the prosthion.

In Figure 62, the Spioenkop specimens and the black wildebeest plots cluster in a very similar way and the Spioenkop specimens seem to have a slightly wider spread. Only five specimens lie outside the range of black wildebeest (one below the lower limit and four above the upper limit).

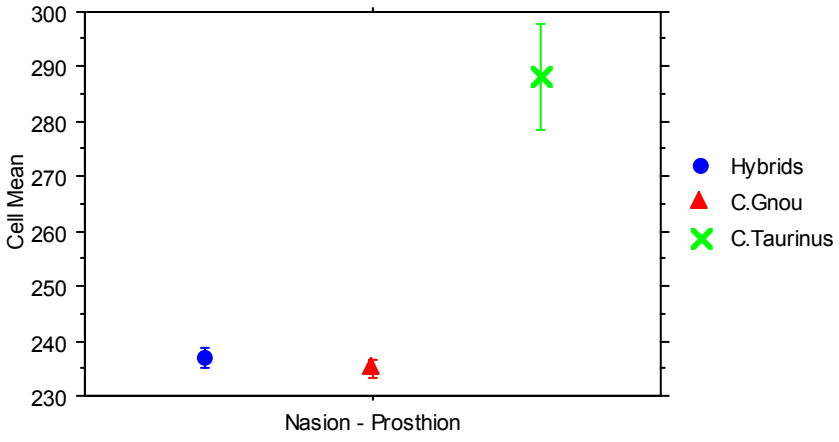

Figure 63: Standard error cell plot of the distance from the nasion to the prosthion (error bars: ±1 STD error).

Figure 63 shows that the standard error ranges for both Spioenkop specimens and black wildebeest are narrow, but that the Spioenkop specimens plot just out of the range of black wildebeest. Narrow range indicates the measurements are very similar within the species for all individuals.

6.2.7 Median frontal length

This measurement is taken from the akrokranion to the nasion.

(See Figure 1, measurement 7).

Table 10: Descriptive statistics for the distance from the akrokranion to the nasion.

	Akro - nasion, Total	Akro - nasion, Hybrids	Akro - nasion, C.Gnou	Akro - nasion, C.Taurinus
Mean	189.300	183.833	183.020	201.744
Std. Dev.	14.223	9.205	7.715	16.549
Std. Error	2.688	3.068	2.440	5.516
Count	28	9	10	9
Minimum	168.000	168.000	172.600	180.000
Maximum	229.100	195.900	193.800	229.100
# Missing	7	4	2	1
Variance	202.281	84.725	59.520	273.875
Coef. Var.	.075	.050	.042	.082
Range	61.100	27.900	21.200	49.100
Sum	5300.400	1654.500	1830.200	1815.700
Skew ness	1.219	-.278	.107	.591

Table 10 shows that for this particular trait the hybrid specimens have the same mean as the black wildebeest. There is a larger range for the Spioenkop

specimens and the minimum and maximum values are larger. The range for blue wildebeest is larger and the lower range fall within range of black wildebeest.

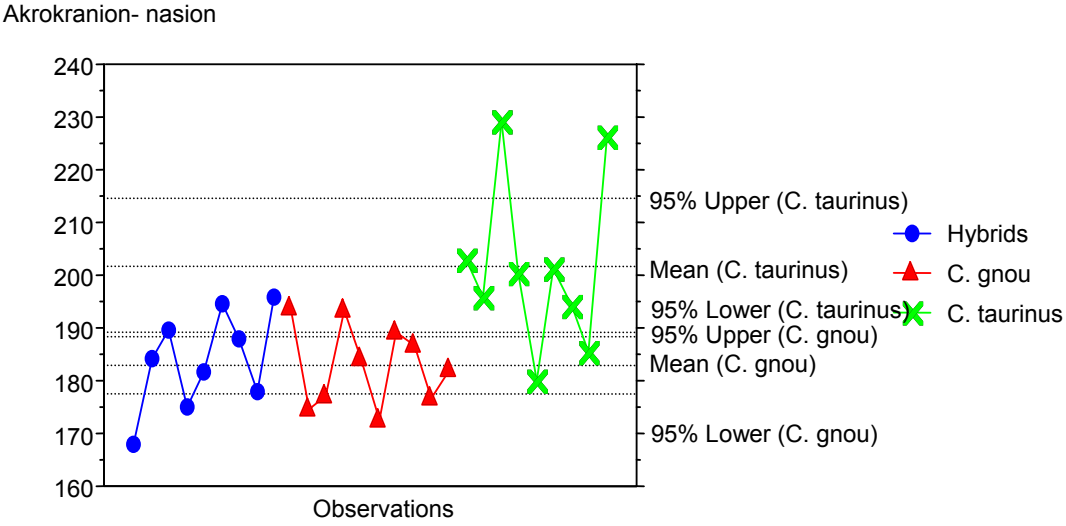

Figure 64: Univariate line plot for the distance from the akrokranion to the nasion showing a 95% confidence interval.

The confidence interval plots in Figure 64 show plotting and spread of measurements are similar for both the Spioenkop specimens and black wildebeest. The large range for the blue wildebeest is noted and there is overlap with the black wildebeest range. Two blue individuals fall within the black wildebeest range.

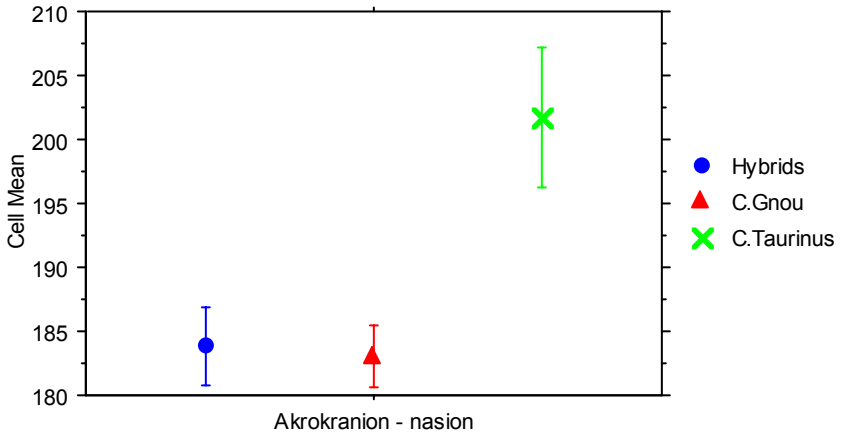

Figure 65: Standard error cell plot for the distance from the akrokranion to the nasion (error bars: ±1 STD error).

The standard errors in Figure 65 show a clearer separation between the blue and black wildebeest. There is a close relationship in the measurements for the Spioenkop specimens and black wildebeest. However, the Spioenkop specimens lie just outside the range of black wildebeest.

6.2.8 Greatest frontal length of the skull

(See Figure 1, measurement 8).

Table 11: Descriptive statistics for greatest frontal length of the skull.

	greatst frontal length, Total	greatst frontal length, Hybrids	greatst frontal length, C.Gnou	greatst frontal length, C.Taurinus
Mean	206.610	204.273	198.944	216.080
Std. Dev.	14.725	11.097	6.340	19.000
Std. Error	2.688	3.346	2.113	6.008
Count	30	11	9	10
Minimum	184.900	185.500	187.900	184.900
Maximum	242.400	230.000	207.400	242.400
# Missing	5	2	3	0
Variance	216.816	123.146	40.200	360.984
Coef. Var.	.071	.054	.032	.088
Range	57.500	44.500	19.500	57.500
Sum	6198.300	2247.000	1790.500	2160.800

In Table 11, each species mean differs, with the Spioenkop specimens plotting between the blue and black wildebeest. The minimum values are all very similar. Interestingly, blue wildebeest have a very large range with the minimum measurement taken for this species being smaller than both the Spioenkop specimens and black wildebeest. Black wildebeest have the smallest range of the three species.

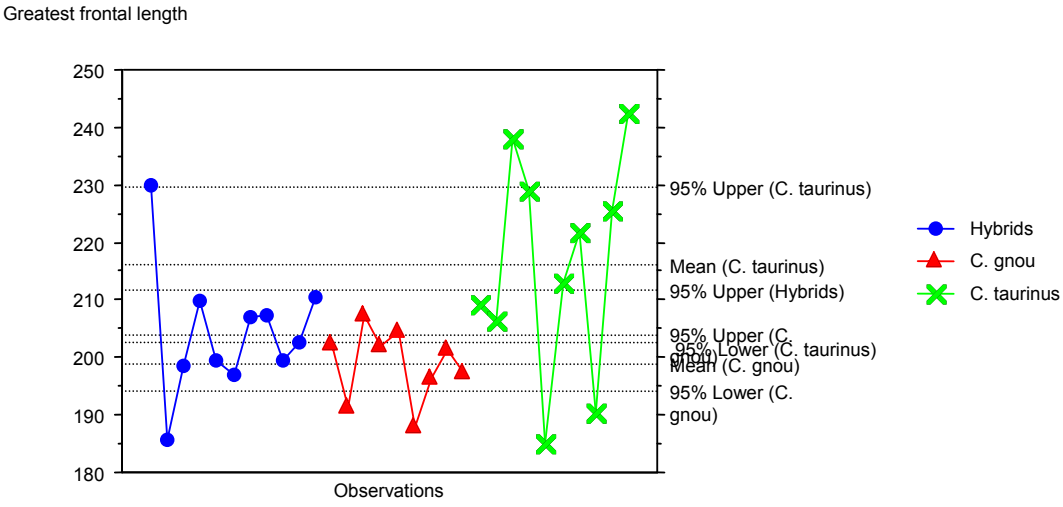

Figure 66: Univariate line plot for greatest frontal length of the skull showing a 95% confidence interval.

In Figure 66, the interval is large for black wildebeest. Black wildebeest have the narrowest range and the Spioenkop specimens plot in a similar fashion, with the exception of two individuals that are 'extreme' outliers. One outlier plots outside the upper 95% confidence interval for blue wildebeest. Four Spioenkop specimens meet the requirements characteristic of true hybrids.

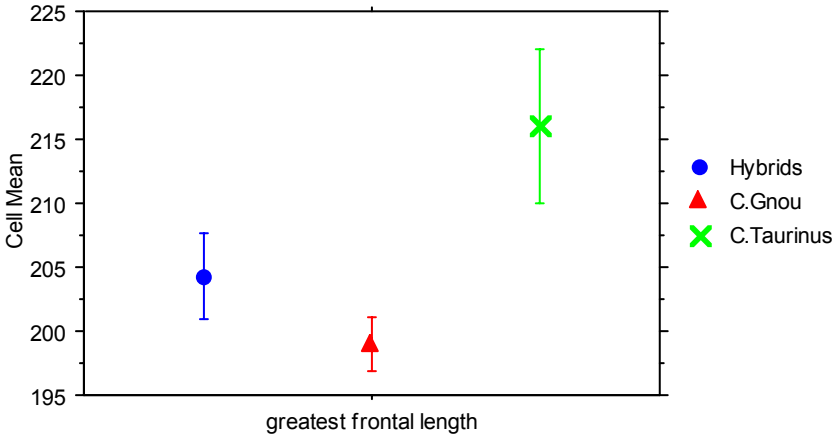

Figure 67: Standard error cell plot for greatest frontal length of the skull (error bars: ±1 STD error).

Standard error seen in Figure 67 shows a clear separation between the black wildebeest and Spioenkop specimens. This trait's standard error for Spioenkop specimens plots between black and blue wildebeest, with the Spioenkop specimens sharing a lower limit with the black wildebeest upper limit.

6.2.9 Akrokranion to the rhinion

(Short upper cranium length; see Figure 1, measurement 9).

Table 12: Descriptive statistics for akrokranion to the rhinion.

	Akro - Rhinion, Total	Akro - Rhinion, Hybrids	Akro - Rhinion, C.Gnou	Akro - Rhinion, C.Taurinus
Mean	363.020	342.738	338.643	406.450
Std. Dev.	40.427	16.010	12.047	40.934
Std. Error	7.381	4.440	4.553	12.944
Count	30	13	7	10
Minimum	313.700	313.700	322.100	350.100
Maximum	470.100	365.800	353.200	470.100
# Missing	5	0	5	0
Variance	1634.333	256.318	145.140	1675.581
Coef. Var.	.111	.047	.036	.101
Range	156.400	52.100	31.100	120.000

Table 12 shows a clear difference in the means of all three species. The Spioenkop specimens mean plots between the means of the parent species. The Spioenkop specimens minimum and maximum fall below and above that of the black wildebeest. The standard error for black wildebeest and the Spioenkop specimens are almost identical.

In Figure 68, there is similarity in the clustering of the Spioenkop specimens and black wildebeest. The Spioenkop specimens have a wider spread than that of the black wildebeest. Five individuals plot outside of the range of black wildebeest.

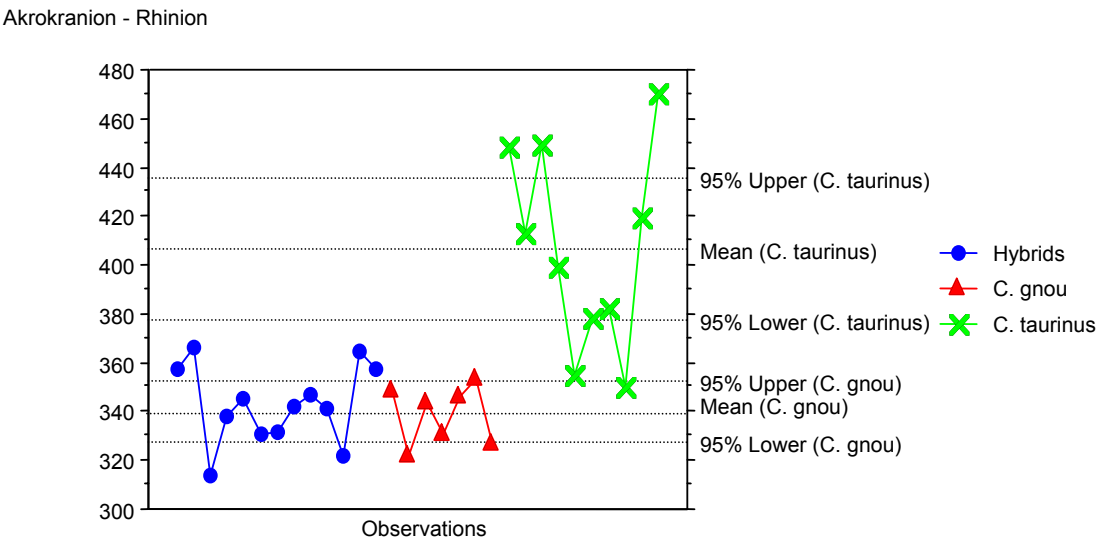

Figure 68: Univariate line chart for the measurements of the akrokranion to the rhinion showing a 95% confidence interval.

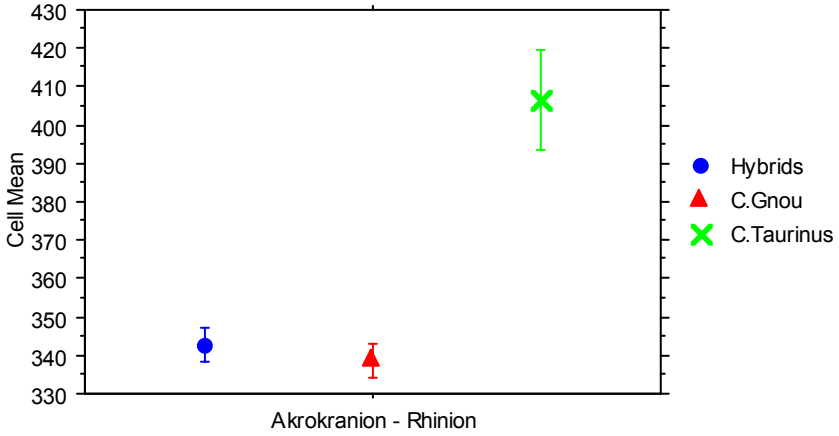

Figure 69: Standard error cell plot for the measurements from the akrokranion to the rhinion (error bars: ±1 STD error).

Figure 69 shows there is overlap in the standard error of black wildebeest and Spioenkop specimens. The mean for Spioenkop specimens falls within the range of black wildebeest, but the upper limit for Spioenkop specimens falls outside the upper limit of black wildebeest.

6.2.10 Distance from the nasion to the rhinion

(See Figure 1, measurement 10).

Table 13: Descriptive statistics for the distance from the nasion to the rhinion.

	Nasion - Rhinion, Total	Nasion - Rhinion, Hybrids	Nasion - Rhinion, C.Gnou	Nasion - Rhinion, C.Taurinus
Mean	177.036	154.167	155.529	224.256
Std. Dev.	37.395	5.941	6.048	30.758
Std. Error	7.067	1.715	2.286	10.253
Count	28	12	7	9
Minimum	144.900	144.900	150.400	179.300
Maximum	278.300	166.200	166.100	278.300
# Missing	7	1	5	1
Variance	1398.418	35.292	36.579	946.045
Coef. Var.	.211	.039	.039	.137
Range	133.400	21.300	15.700	99.000

In Table 13, the Spioenkop specimens and black wildebeest have similar means and share a maximum value. The standard deviation values are also relatively small for the Spioenkop specimens and black wildebeest, when compared to the blue wildebeest.

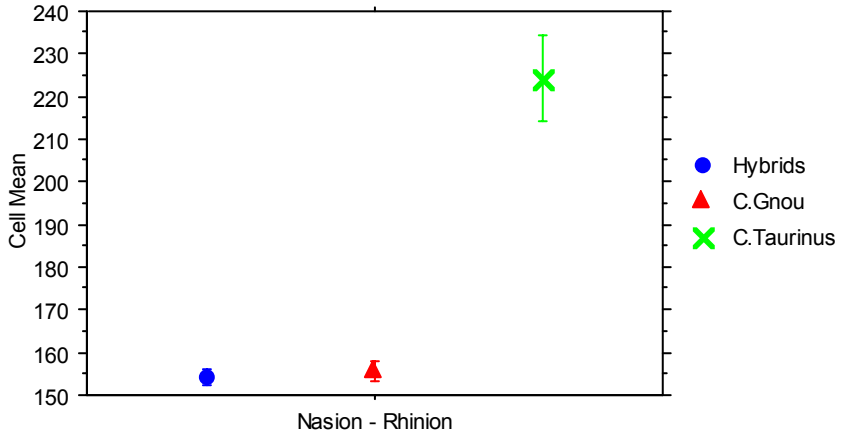

Figure 70: Standard error cell plot for the distance from the nasion to the rhinion (error bars: ±1 STD error).

Figure 71 shows that while blue wildebeest have a wide range, the black wildebeest and Spioenkop specimens have a narrower range. Both black and Spioenkop specimen plots cluster in a similar way. In Figure 71, two individuals fall outside of the range of black wildebeest.

In Figure 70, the black and Spioenkop wildebeest have a small range for standard error and the plots overlap one another. The lower limit for the Spioenkop specimens fall just below the lower limit of black wildebeest.

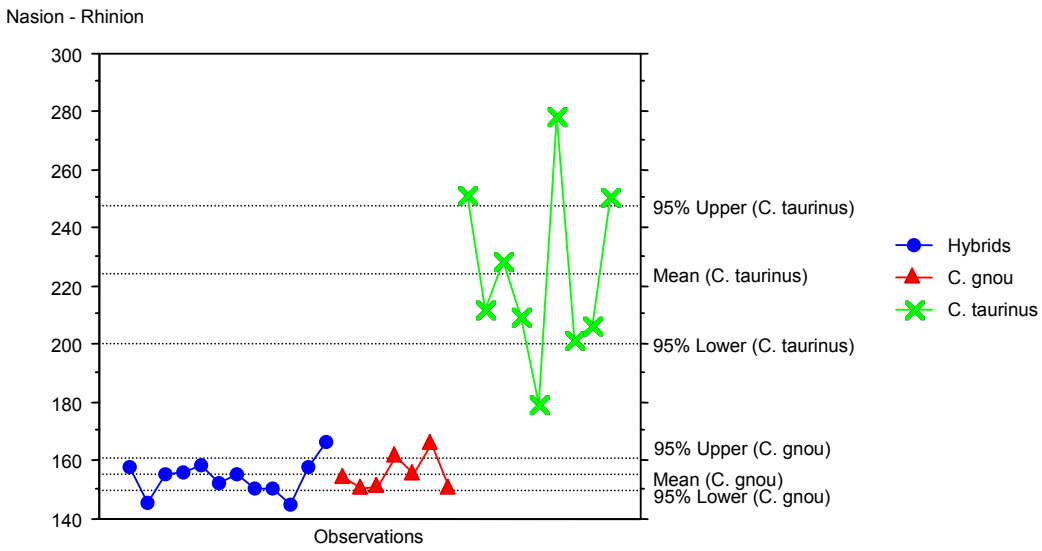

Figure 71: Univariate line plot for the distance from the nasion to the rhinion, showing a 95% confidence interval.

6.2.11 Distance from the arboral border occipital condyle to the entorbitale

(See Figure 3, measurement 11).

Table 14: Descriptive statistics for the distance from the arboral border of the occipital condyle to entorbitale of the same side.

	Arboral -enorbit, Total	Arboral -enorbit, Hybrids	Arboral -enorbit, C.Gnou	Arboral -enorbit, C.Taurinus
Mean	193.123	187.870	183.190	208.310
Std. Dev.	21.785	7.867	5.585	32.243
Std. Error	3.977	2.488	1.766	10.196
Count	30	10	10	10
Minimum	172.900	174.700	172.900	183.500
Maximum	290.600	202.900	192.400	290.600
# Missing	5	3	2	0
Variance	474.600	61.889	31.197	1039.621
Coef. Var.	.113	.042	.030	.155
Range	117.700	28.200	19.500	107.100

Table 14 shows clear differences in mean, standard deviation and range for all three species. The range for the Spioenkop specimens is larger than black wildebeest, evident in the larger minimum and maximum ranges relative to black.

In Figure 72, there is an over lap in confidence interval for both *C. gnou* and *C. taurinus*. The lower limit for blue wildebeest falls within the upper 95% confidence interval of black wildebeest. The mean for blue wildebeest is still much larger than that of black wildebeest. The blue wildebeest have a large range. The Spioenkop specimens have a small range and the plots cluster in a similar way to that of the black wildebeest. There is one Spioenkop specimen that plots outside the range of black wildebeest.

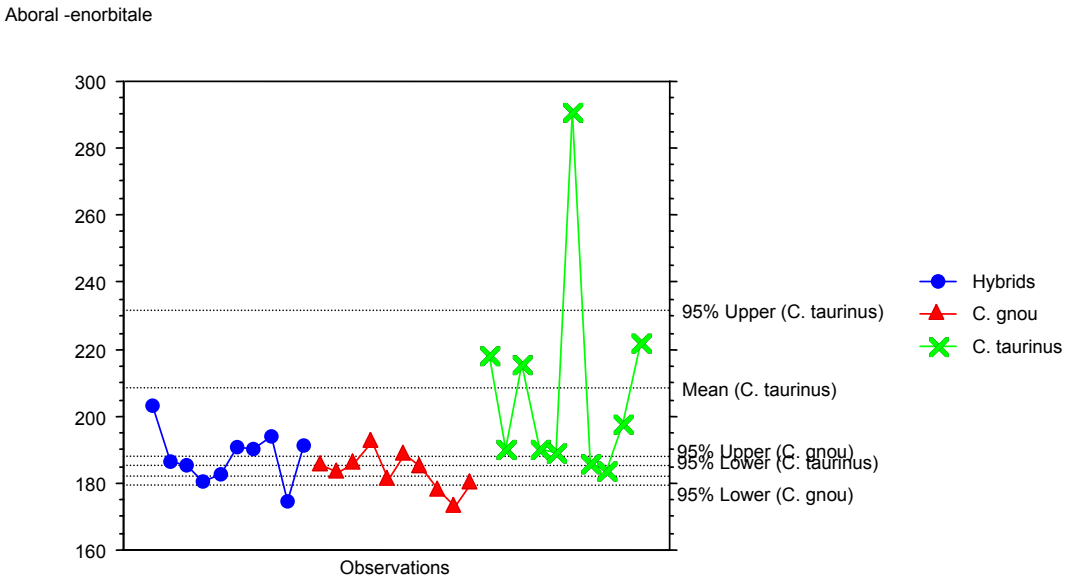

Figure 72: Univariate line plot for the distance from the aboral border of the occipital condyle to the entorbitale, showing the 95% confidence intervals.

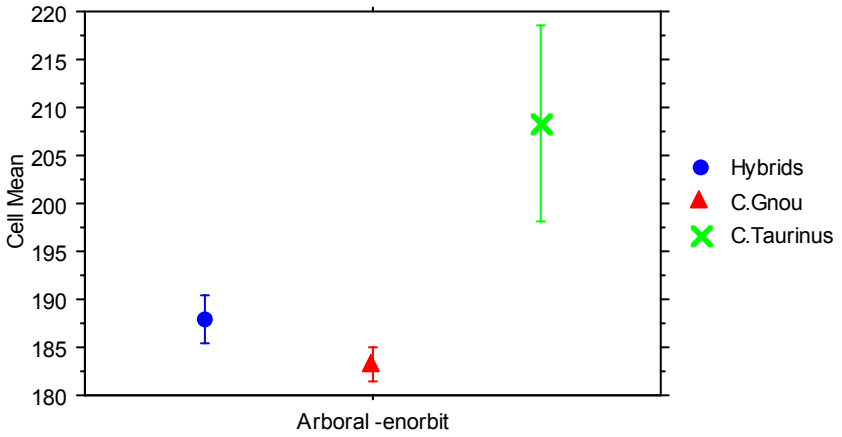

Figure 73: Standard error cell plot for the distance from the aboral border of the occipital condyle to the entorbitale (error bars: ±1 STD error).

Figure 73 shows a clear separation in standard errors between the three species. The Spioenkop specimens plot inbetween the blue and black wildebeest.

6.2.12 Distance from the ectorbitale to the prosthion

(See Figure 3, measurement 12).

Table 15: Descriptive statistics for the distance from the ectorbitale to the prosthion.

	Ectorb - Prosthi, Total	Ectorb - Prosthi, Hybrids	Ectorb - Prosthi, C.Gnou	Ectorb - Prosthi, C.Taurinus
Mean	289.890	269.842	264.071	332.020
Std. Dev.	34.880	8.166	11.576	24.243
Std. Error	6.477	2.357	4.375	7.666
Count	29	12	7	10
Minimum	245.600	254.100	245.600	298.300
Maximum	365.600	281.000	273.000	365.600
# Missing	6	1	5	0
Variance	1216.640	66.686	134.012	587.724
Coef. Var.	.120	.030	.044	.073
Range	120.000	26.900	27.400	67.300

Table 15 shows that while the Spioenkop wildebeest have a similar range to black wildebeest there are significant differences in means and minimum and maximum values, with Spioenkop specimens being larger. Standard deviation for the Spioenkop specimens is smaller than that of the black wildebeest.

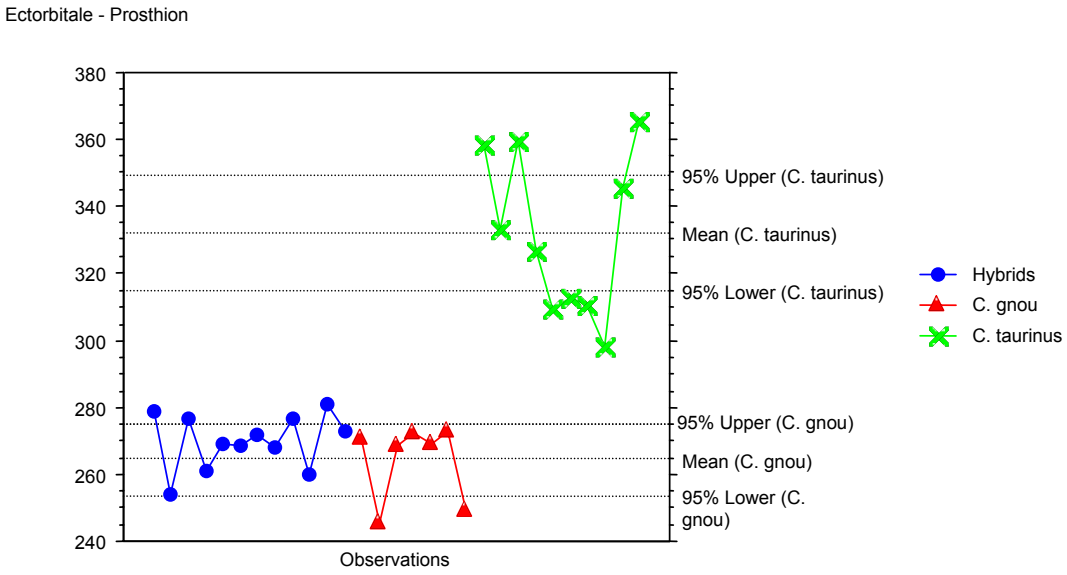

Figure 74: Univariate line plot for the distance from ectorbitale to the prosthion showing the 95% confidence intervals.

Figure 74 shows, that the blue wildebeest have a large range while the black and Spioenkop wildebeest cluster similarly. The range of black wildebeest is wider than that of the Spioenkop specimens. From the Univariate plots, four individuals plot outside the range of black wildebeest. Standard error for Ectorbitale to Prosthion in Figure 75 shows that the range of standard errors of the Spioenkop specimens is much smaller than that of black and blue wildebeest. The lower limit of the Spioenkop specimen standard error falls within range of the black wildebeest.

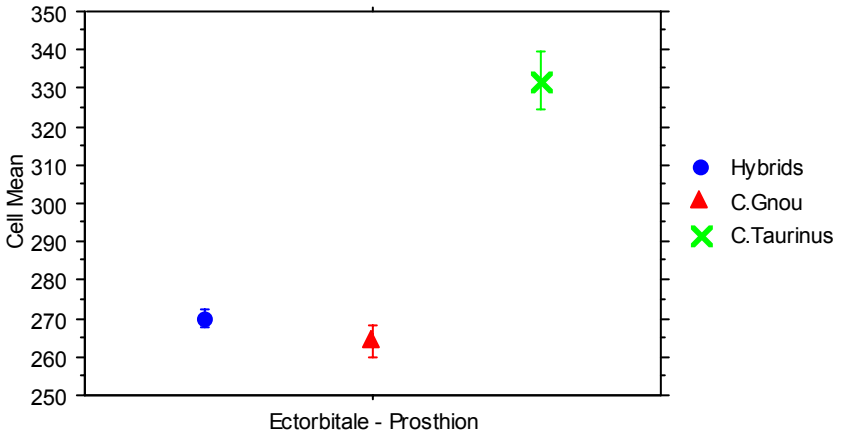

Figure 75: Standard error cell plot for the distance from the ectorbitale to the prosthion (error bars: ±1 STD error).

6.2.13 Distance from the aboral border of occipital condyle to the infraorbitale

(See Figure 3, measurement 13).

Table 16 shows a small difference in the means of black and Spioenkop wildebeest. For the Spioenkop specimens, the range and standard deviation are much larger than that of the black wildebeest. This larger range for Spioenkop specimens is seen in the minimum value that is smaller than the minimum value for black wildebeest and a maximum value, which is larger than that of the black wildebeest.

Table 16: Descriptive statistics for distance from the aboral border of the occipital condyle to the prosthion measurements.

	Aboral - Infraorbitale, Total	Hybrids	C. gnou	C. taurinus	...
Mean	265.727	253.985	251.260	295.460	
Std. Dev.	24.433	8.545	5.596	24.080	
Std. Error	4.253	2.370	1.770	7.615	
Count	33	13	10	10	
Minimum	239.700	239.700	242.300	262.600	
Maximum	334.700	267.500	260.900	334.700	
# Missing	2	0	2	0	
Range	95.000	27.800	18.600	72.100	

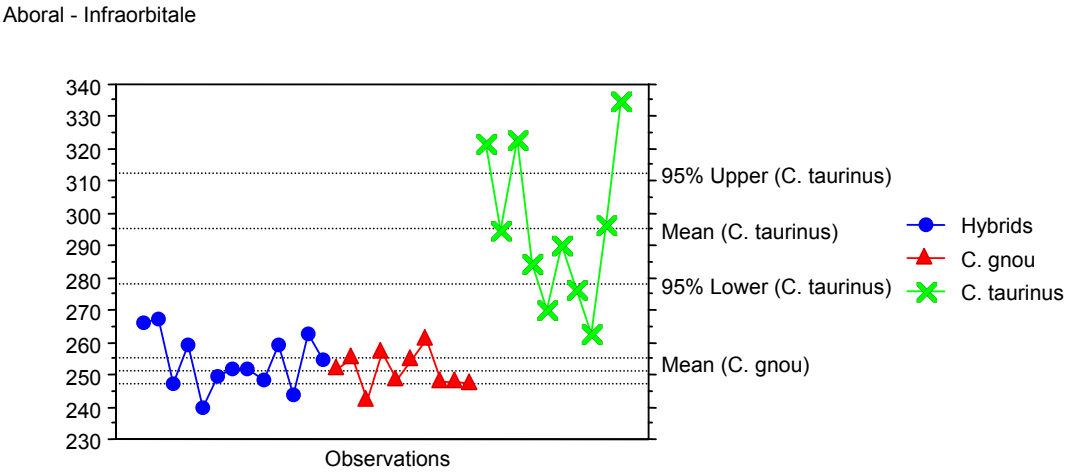

Figure 76: Univariate line plot of aboral border of occipital condyle to infraorbitale of the same side.

Figure 76 shows that both the Spioenkop and the black wildebeest have small confidence interval ranges. The measurements of black and Spioenkop individuals cluster together, while blue wildebeest have a broad range for its confidence interval. The average measurement for blue wildebeest is much larger than that of the black wildebeest. Four Spioenkop specimens fall out of range of the black wildebeest plots.

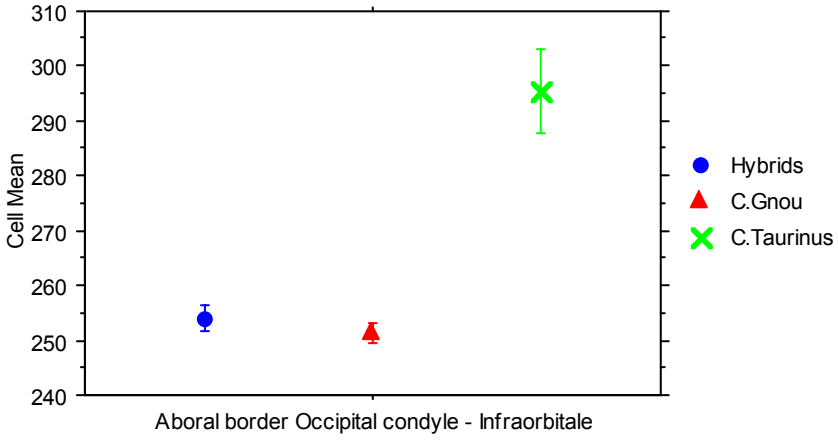

Figure 77: Standard error cell plot for occipital condyle to infraorbitale measurements (error bars: ±1 STD error).

For standard error, Figure 77 shows that all three specimen groups have a relatively narrow range for this measurement. The average standard error for the Spioenkop specimens fall outside of the range of the black wildebeest while the lower limit falls within range of the black wildebeest plot.

6.2.14 Distance from the infraorbitale to the prosthion

(See Figure 3, measurement 14).

Table 17: Descriptive statistics for the distance from the infraorbitale to the prosthion.

	Infraorbitale - Prosthion, Total	Infraorbitale - Prosthion, Hybrids	Infraorbitale - Prosthion, C.Gnou	Infraorbitale - Prosthion, C.Taurinus
Mean	139.657	132.723	130.743	154.910
Std. Dev.	13.302	4.615	5.642	11.434
Std. Error	2.429	1.280	2.132	3.616
Count	30	13	7	10
Minimum	123.200	123.200	123.600	140.900
Maximum	171.900	140.800	140.000	171.900
# Missing	5	0	5	0
Variance	176.931	21.295	31.833	130.739
Coef. Var.	.095	.035	.043	.074
Range	48.700	17.600	16.400	31.000

In Table 17, closeness in the means of both the Spioenkop specimens and black wildebeest is noted. While the standard deviation for black wildebeest is only marginally larger than the Spioenkop wildebeest, the two species share both minimum and maximum values. In Figure 78, the confidence interval range for the Spioenkop specimens is narrow and falls within the range of the black wildebeest. Only one Spioenkop individual meets the requirements of a true hybrid.

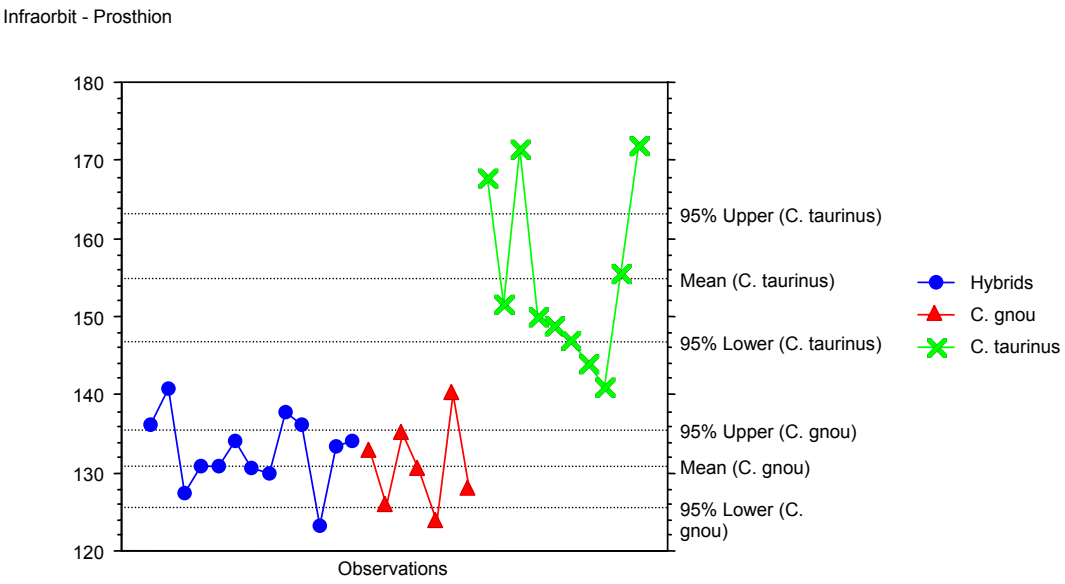

Figure 78: Univariate line plot for infraorbitale to prosthion showing the 95% confidence intervals.

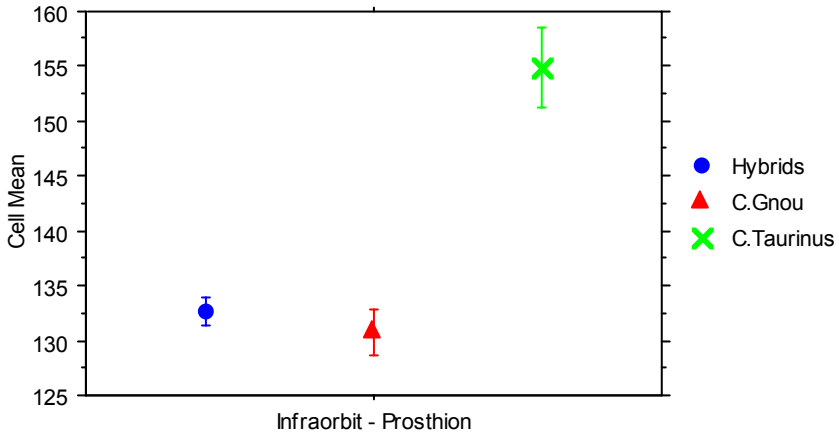

Figure 79: Standard error cell plot of infraorbitale to the prosthion (error bars: ±1 STD error).

In the standard error plot for infraorbitale to Prosthion measurements (Figure 79), the range of the black wildebeest is wider than the Spioenkop specimen range. The upper limit of the standard error for the Spioenkop specimens extends only

slightly beyond that of the black wildebeest with a larger portion of the Spioenkop specimen standard errors falling within the black wildebeest range.

6.2.15 Dental length

This measurement is taken from the postdentale to the prosthion.

(See Figure 4, measurement 15)

Table 18: Descriptive statistics for dental length.

	Dental length, Total	Dental length, Hybrids	Dental length, C.Gnou	Dental length, C.Taurinus
Mean	216.920	202.454	201.829	246.290
Std. Dev.	23.886	10.019	4.580	15.895
Std. Error	4.361	2.779	1.731	5.026
Count	30	13	7	10
Minimum	188.800	188.800	193.500	223.200
Maximum	269.900	228.600	206.500	269.900
# Missing	5	0	5	0
Range	81.100	39.800	13.000	46.700

Table 18 shows fractionally larger mean for black wildebeest when compared to Spioenkop specimens. The range of the Spioenkop specimens from the minimum to maximum value is larger than the black wildebeest. The Spioenkop wildebeest measurements extend above and below the maximum and minimum values for black wildebeest plots respectively.

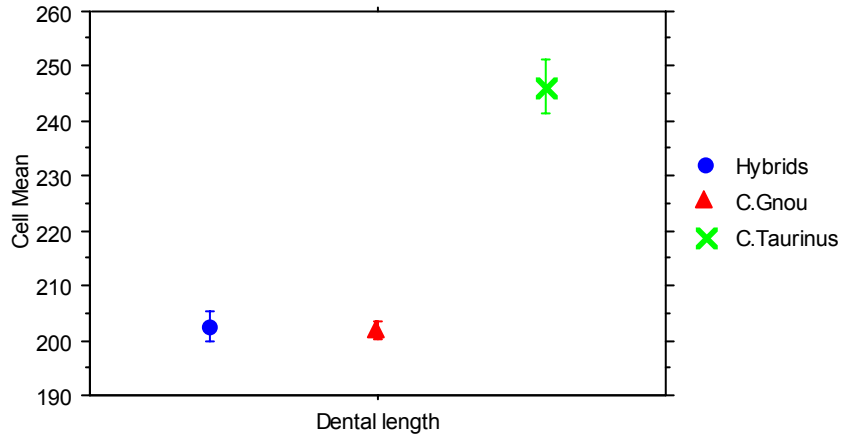

Figure 80: Standard error cell plot for dental length (error bars: ±1 STD error).

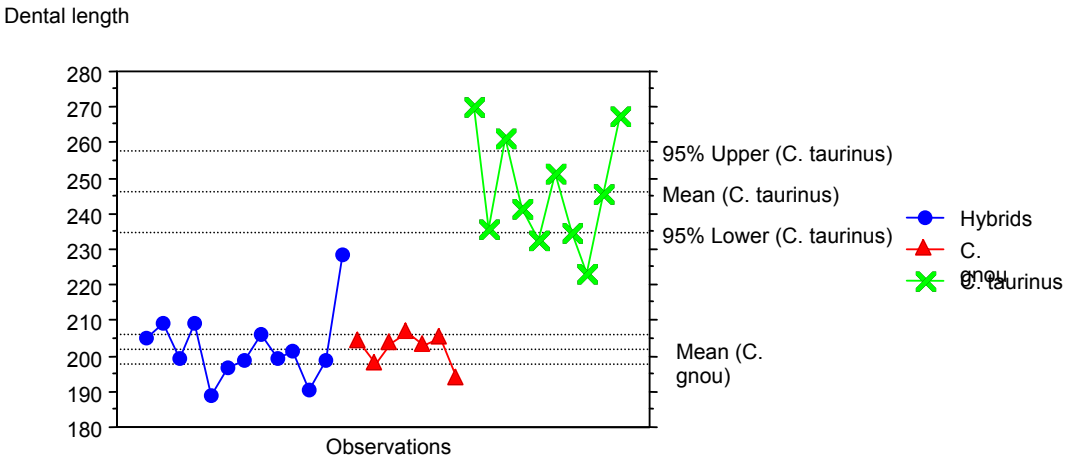

Figure 81: Univariate line plot for the dental length showing the 95% confidence intervals.

In Figure 81, the Spioenkop specimens and black wildebeest both cluster similarly. Five Spioenkop specimens lie out of the range of black wildebeest.

The standard error plot in Figure 80 shows that the Spioenkop specimens fall within the range of black wildebeest. The lower limit of the Spioenkop specimens falls slightly below that of the black wildebeest and is insignificant.

6.2.16 Oral palatal length

This measurement is taken from the palatinoorale to the prosthion.

(See Figure 4, measurement 16).

In Table 19, the Spioenkop specimens have a slightly larger mean for the oral palatal length than the black wildebeest. Black wildebeest also have a much smaller range than the Spioenkop wildebeest and blue wildebeest. The standard deviation with the Spioenkop specimens is larger than that of black. The minimum and maximum values for the Spioenkop specimens respectively fall below and above those of the black wildebeest.

Table 19: Descriptive statistics for oral palatal length.

	Oral palatal length, Total	Oral palatal length, Hybrids	Oral palatal length, C.Gnou	Oral palatal length, C.Taurinus
Mean	176.543	164.277	160.686	203.590
Std. Dev.	21.869	5.935	6.839	15.400
Std. Error	3.993	1.646	2.585	4.870
Count	30	13	7	10
Minimum	146.500	155.700	146.500	184.500
Maximum	226.100	175.000	168.400	226.100
# Missing	5	0	5	0
Range	79.600	19.300	21.900	41.600

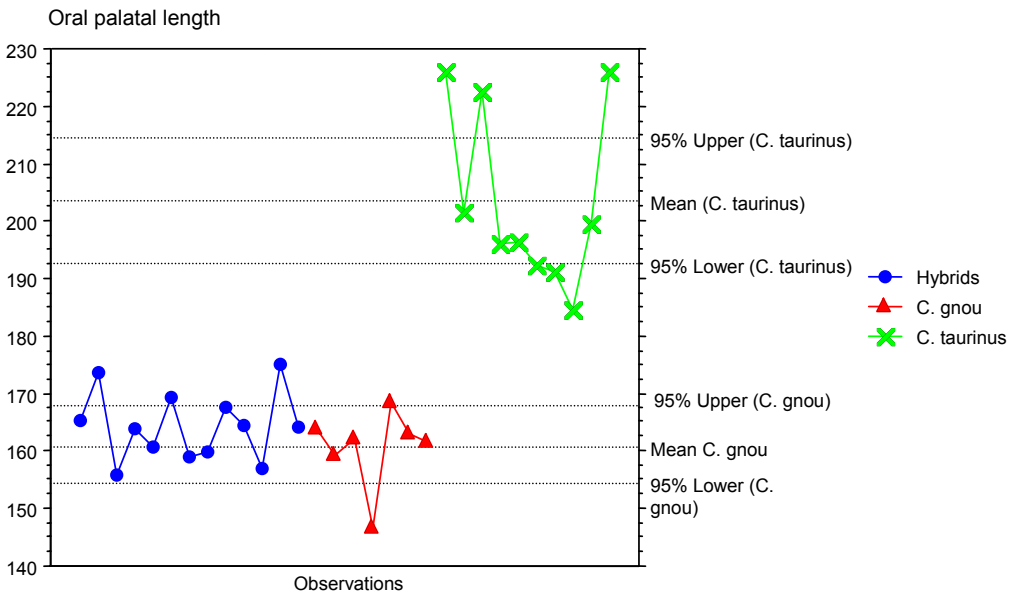

Figure 82: Univariate line plot of oral palatal length.

Figure 82 shows close relationship between black wildebeest and the Spioenkop specimens, in that the mean for the Spioenkop specimens is slightly larger than that of the black wildebeest. While the Spioenkop specimens tend to cluster similarly to the black wildebeest, the overall range is wider. Five Spioenkop specimens fall out of the range of black wildebeest.

The standard error ranges for black and Spioenkop wildebeest seen in Figure 83 are very small and overlap. However, the upper limit of the Spioenkop standard error falls outside the range of black wildebeest.

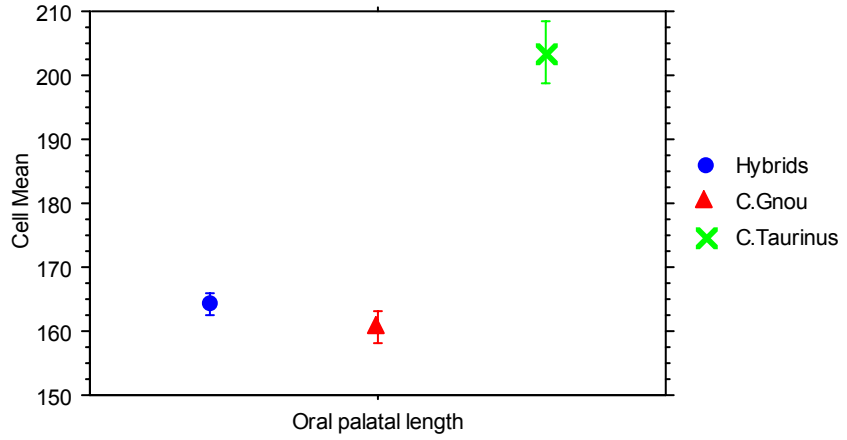

Figure 83: Standard error cell plot of oral palatal length (error bars: ±1 STD error).

6.2.17 Lateral length of premaxilla

(Nasiointermaxillare to the prosthion, see Figure 3, measurement 17).

Table 20: Descriptive statistics for nasiointermaxillare to the prosthion.

	Nasiointermax -Prosthion, Total	Nasiointermax -Prosthion, Hybrids	Nasiointermax -Prosthion, C.Gnou	Nasiointermax -Prosthion, C.Taurinus
Mean	127.921	128.785	123.933	129.190
Std. Dev.	6.355	3.464	3.097	9.531
Std. Error	1.180	.961	1.264	3.014
Count	29	13	6	10
Minimum	117.300	125.600	120.500	117.300
Maximum	144.700	136.900	127.400	144.700
# Missing	6	0	6	0
Range	27.400	11.300	6.900	27.400

Table 20 shows a significant difference in the means, minimum, maximum and range values for the black and Spioenkop wildebeest. Standard deviations for the two are almost identical. The minimum value for blue wildebeest falls within the

range of black wildebeest. In Figure 85, there is overlap in the confidence intervals of both *C. gnou* and *C. taurinus*. Black wildebeest cluster lower on the graph, while the blue wildebeest have individuals that plot from within the range of black wildebeest to past the upper interval of its own range. The Spioenkop wildebeest have a wider range than the black wildebeest. The Spioenkop wildebeest plots fall either within the upper interval for black wildebeest or above it. Seven individuals fall out of the range of the black wildebeest.

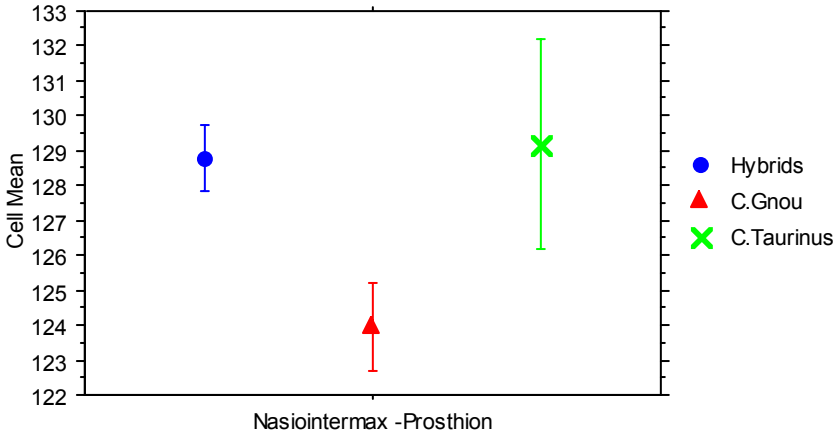

Figure 84: Standard error for nasiointermaxillare to the prosthion (error bars: ±1 STD error).

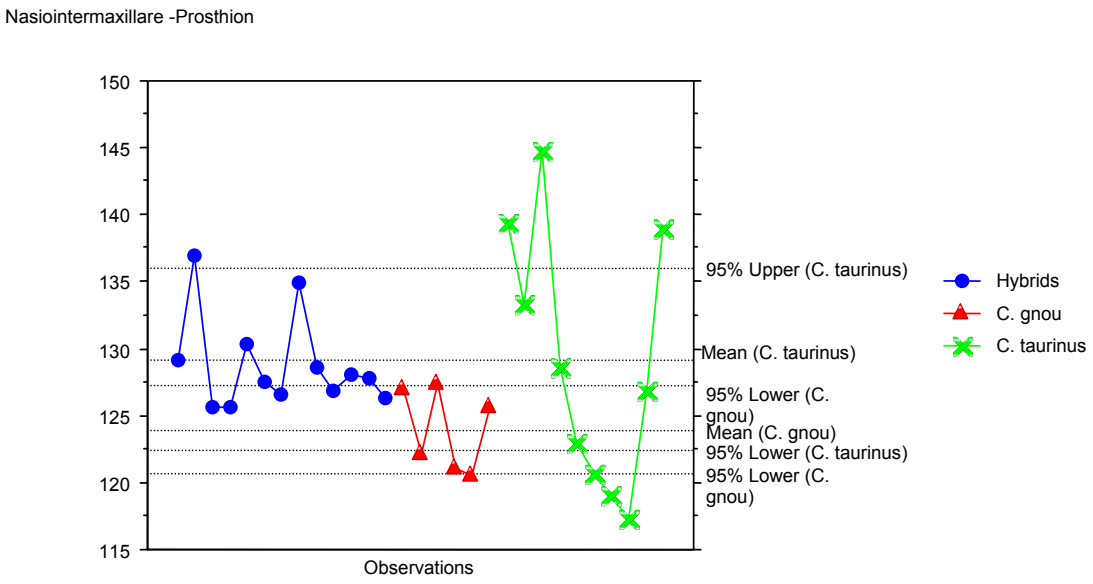

Figure 85: Univariate cell plot nasiointermaxillare to the prosthion.

Standard error for the lateral length of the premaxilla in Figure 84 shows a clear separation of the Spioenkop specimens from the black wildebeest. The average standard error and upper limit of the Spioenkop plots fall within range of the blue wildebeest, which is significantly separate from the black wildebeest.

6.2.18 Length of the cheektooth row

(See Figure 4, measurement 18).

In Table 21, the mean for the Spioenkop cheektooth-row length is smaller than that of the black wildebeest. Standard deviations for both black wildebeest and the Spioenkop specimens are the same. The range for Spioenkop specimens is slightly bigger than the black range, and the minimum and maximum values of the Spioenkop specimens fall just below those of the black wildebeest.

Table 21: Descriptive statistics for the length of the cheek tooth row.

	length cheektooth row , Total	length cheektooth row , Hybrids	length cheektooth row , C.Gnou	length cheektooth row , C.Taurinus
Mean	96.516	89.046	91.625	110.140
Std. Dev.	11.304	5.400	5.101	7.662
Std. Error	2.030	1.498	1.803	2.423
Count	31	13	8	10
Minimum	80.400	80.400	81.500	100.500
Maximum	122.000	96.800	97.100	122.000
# Missing	4	0	4	0
Variance	127.775	29.159	26.019	58.700
Coef. Var.	.117	.061	.056	.070
Range	41.600	16.400	15.600	21.500

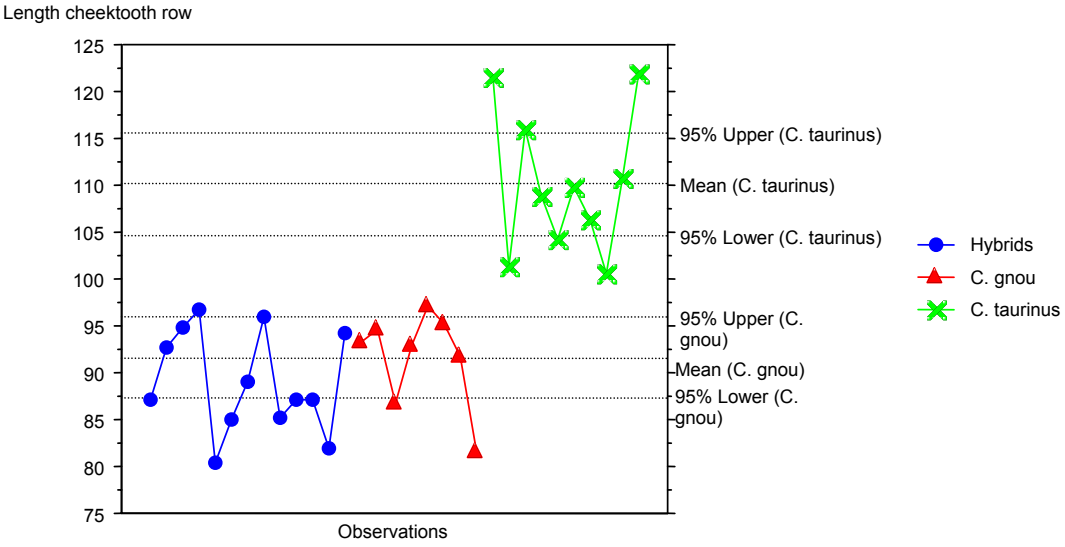

Figure 86: Univariate plot for length of the cheek tooth row.

In Figure 86, the mean of the Spioenkop specimens falls within the black wildebeest range. The spread for the black wildebeest and the Spioenkop specimens is the same. Based on the 95% confidence interval only one individual falls out of the range of the black wildebeest.

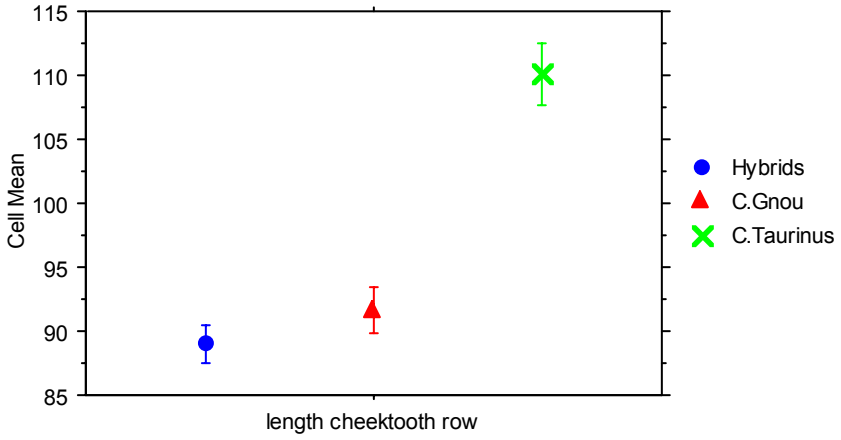

Figure 87: Standard error plot for length of cheek tooth row (error bars: ±1 STD error).

Figure 87 shows the standard error for the Spioenkop specimens falling below that of the black wildebeest. There is, however, a slight overlap of the upper limit of the Spioenkop specimens and the lower limit of the black wildebeest.

6.2.19 Length molar row

(See Figure 4, measurement 19).

Table 22: Descriptive statistics for length of molar row.

	length molar row , Total	length molar row , Hybrids	length molar row , C.Gnou	length molar row , C.Taurinus
Mean	66.690	63.015	64.713	73.050
Std. Dev.	5.656	2.230	4.325	4.188
Std. Error	1.016	.619	1.529	1.324
Count	31	13	8	10
Minimum	55.900	59.700	55.900	65.400
Maximum	81.200	67.400	67.800	81.200
# Missing	4	0	4	0
Variance	31.994	4.973	18.707	17.541
Coef. Var.	.085	.035	.067	.057
Range	25.300	7.700	11.900	15.800

Table 22, shows the mean of Spioenkop specimens is lower than the black wildebeest. Black wildebeest also have a larger range than the Spioenkop specimens. The minimum and maximum values of the Spioenkop specimens fall within the range of the black wildebeest. The blue wildebeest has a wide range, with the lower limit extended into the range of the black wildebeest. For the confidence intervals in Figure 88, the Spioenkop plots cluster close together. The confidence range of the Spioenkop plots falls within the confidence range of black wildebeest. No Spioenkop individuals fall out of the range of the black wildebeest.

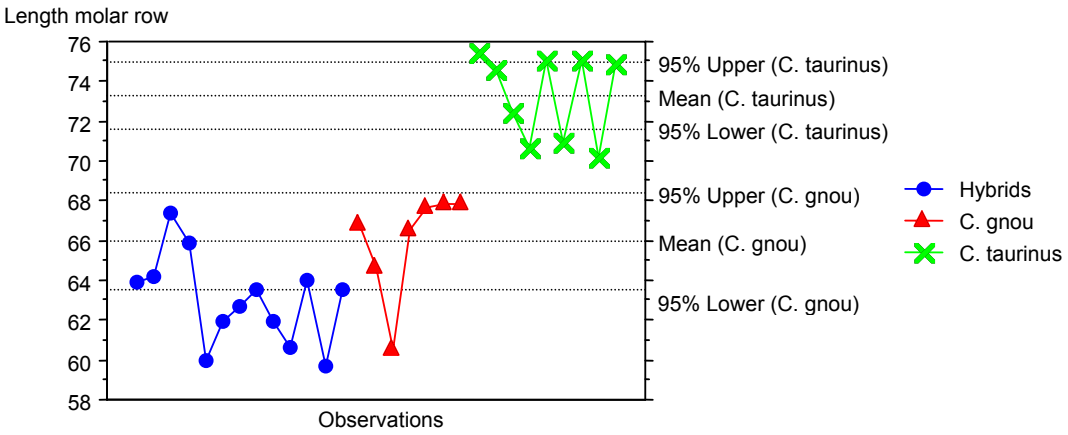

Figure 88: Univariate line plot for the length of the molar row.

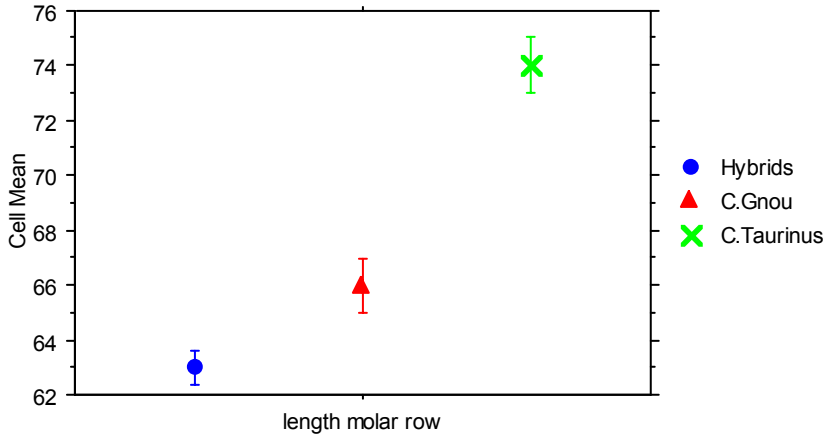

Figure 89: Standard error cell plot for length of molar row (error bars: ±1 STD error).

The standard error in Figure 89 shows the Spioenkop specimens fall below the black wildebeest. The standard error range is wider for the black than the Spioenkop specimens. The lower limit of the black wildebeest extends into the range of the Spioenkop specimens.

6.2.20 Length of premolar row

(See Figure 4, measurement 20).

Table 23: Descriptive statistics of length of premolar row.

	length premolar row , Total	length premolar row , Hybrids	length premolar row , C.Gnou	length premolar row , C.Taurinus
Mean	32.623	29.623	29.913	38.690
Std. Dev.	5.531	3.952	2.538	3.963
Std. Error	.993	1.096	.897	1.253
Count	31	13	8	10
Minimum	24.400	24.400	27.600	32.600
Maximum	45.600	35.700	34.700	45.600
# Missing	4	0	4	0
Variance	30.590	15.615	6.441	15.708
Coef. Var.	.170	.133	.085	.102
Range	21.200	11.300	7.100	13.000

Table 23 shows identical means for Spioenkop specimens and black wildebeest. The standard deviation for Spioenkop specimens is larger than that of the black. In addition, the range of the Spioenkop specimens is closer to that of the blue than the black wildebeest. The minimum value of the blue wildebeest falls within the range of black wildebeest. The univariate plot in Figure 90 shows only a few of the Spioenkop specimens falling into the confidence intervals of the black. There is no overlap in the confidence intervals of *C. gnou* and *C. taurinus.*

The black wildebeest plot close together, and the Spioenkop specimens have a wider spread. Six Spioenkop specimens fall outside of range of the black wildebeest.

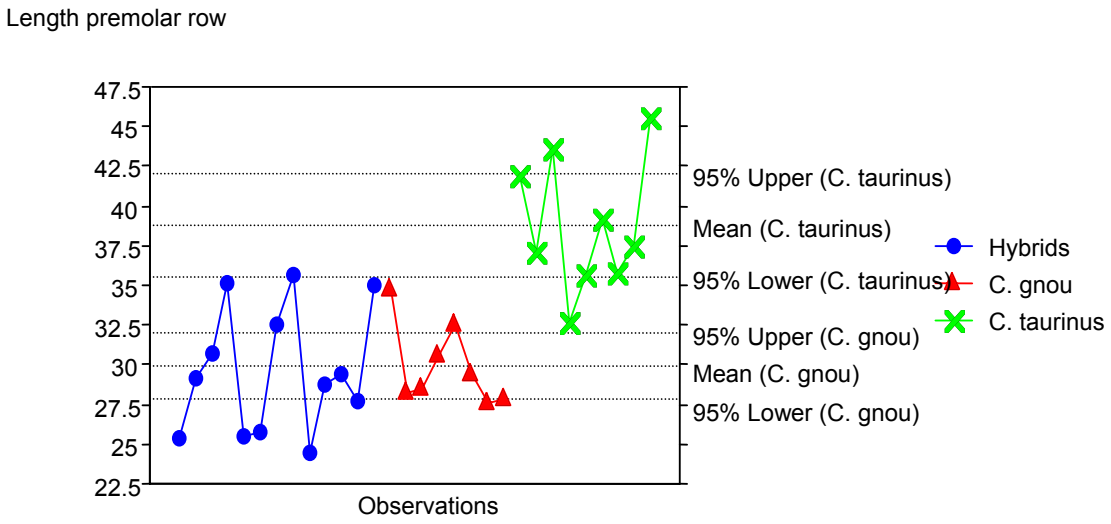

Figure 90: Univariate line plot for the length of the premolar row.

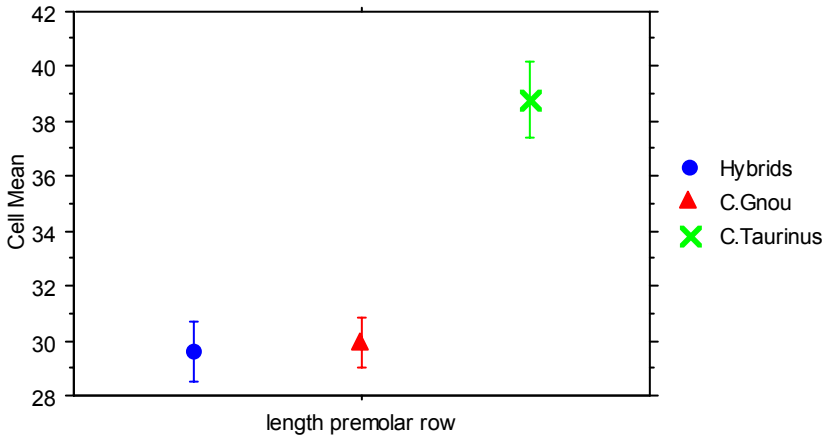

Figure 91: Standard error cell plot for length of premolar row (error bars: ±1 STD error).

The standard error for both Spioenkop specimens and black wildebeest overlap. The lower standard error of the Spioenkop specimens falls just out of the range of black wildebeest, and it considered insignificant.

6.2.21 Greatest inner length of orbit

(Ectorbitale to the entorbitale measurements, see Figure 3, measurement 21).

Table 24: Descriptive statistics for entorbitale to the ectorbitale.

	ectorbitale - entorbitale, Total	ectorbitale - entorbitale, Hybrids	ectorbitale - entorbitale, C.Gnou	ectorbitale - entorbitale, C.Taurinus
Mean	52.548	53.080	50.291	54.500
Std. Dev.	2.873	1.861	2.038	2.944
Std. Error	.516	.588	.614	.931
Count	31	10	11	10
Minimum	47.200	48.900	47.200	51.000
Maximum	59.300	55.800	53.600	59.300
# Missing	4	3	1	0
Variance	8.255	3.462	4.153	8.664
Coef. Var.	.055	.035	.041	.054
Range	12.100	6.900	6.400	8.300

In Table 24, the Spioenkop specimens have a larger mean, minimum and maximum value relative to the black wildebeest. The minimum value of the blue wildebeest falls within range of black wildebeest. The ranges of black and Spioenkop specimen wildebeest are similar, as are the standard deviations.

In Figure 92, there is a similar spread for both the Spioenkop and black wildebeest. The confidence interval of the black wildebeest has a smaller range than the blue wildebeest. Four Spioenkop specimens fall out of the range of black wildebeest and into the blue wildebeest range.

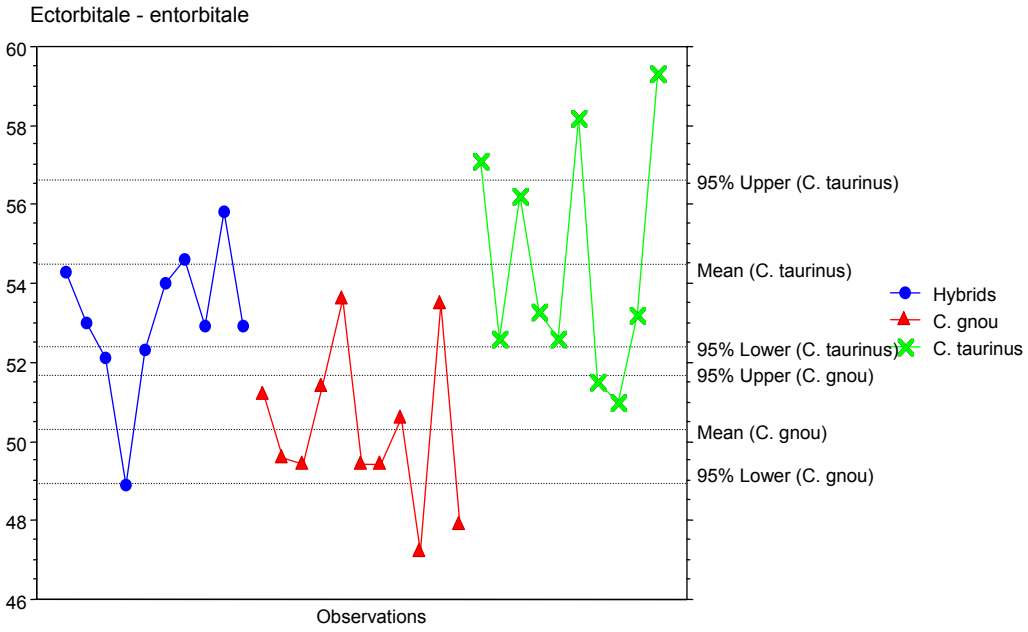

Figure 92: Univariate plot for entorbitale to the ectorbitale.

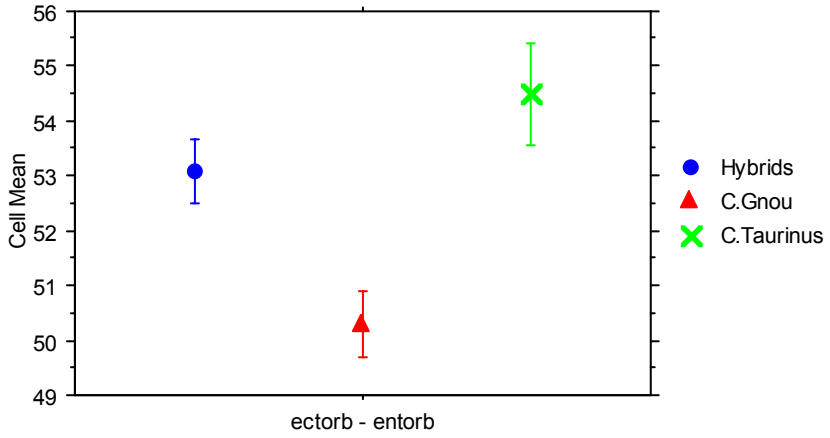

Figure 93: Standard error of ectorbitale to the entorbitale (error bars: ±1 STD error).

The standard error in Figure 93 shows that the Spioenkop specimens plot between the blue and black wildebeest, and clear of the black wildebeest range. There is a slight overlap between the upper limit of the Spioenkop specimens and the lower limit of the blue wildebeest. This overlap is insignificant.

6.2.22 Greatest inner height of the orbit

(See Figure 3, measurement 22).

Table 25 shows a similarity between all three species. The mean for the Spioenkop specimens falls between that of the blue and black wildebeest, but the difference between the three is small. The minimum and maximum values for all three species overlap, with black and blue wildebeest having identical values.

Table 25: Descriptive statistics for inner height of the orbit.

	inner height orbit, Total	inner height orbit, Hybrids	inner height orbit, C.Gnou	inner height orbit, C.Taurinus
Mean	54.888	54.875	53.964	55.920
Std. Dev.	2.764	2.160	2.398	3.585
Std. Error	.481	.624	.723	1.134
Count	33	12	11	10
Minimum	50.600	51.500	50.600	50.800
Maximum	60.800	59.800	57.100	60.800
# Missing	2	1	1	0
Variance	7.642	4.666	5.753	12.851
Coef. Var.	.050	.039	.044	.064
Range	10.200	8.300	6.500	10.000

In Figure 95, we see an overlap in the ranges of both *C. gnou* and *C. taurinus* with respect to the confidence intervals and standard error. In Figure 95, the plots are well spread for *C. gnou, C. taurinus* and the Spioenkop specimens, with the Spioenkop specimens and blue plots spreading more than the black wildebeest. Two Spioenkop individuals fall out of range of the black wildebeest.

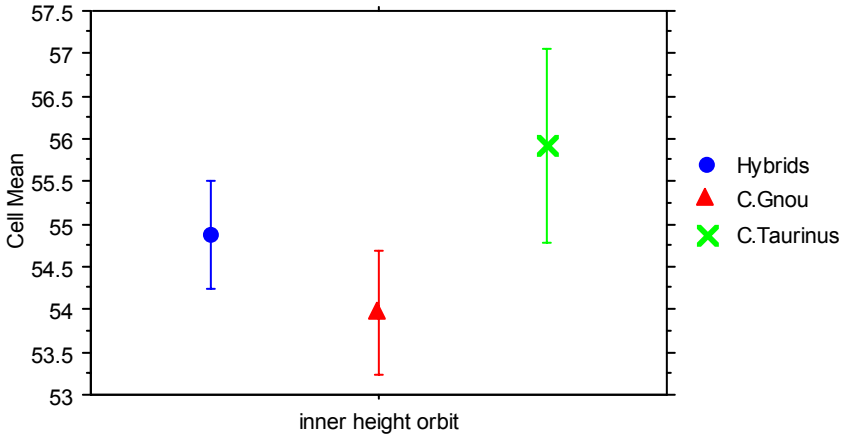

Figure 94: Standard error cell plot for inner height of the orbit (error bars: ±1 STD error).

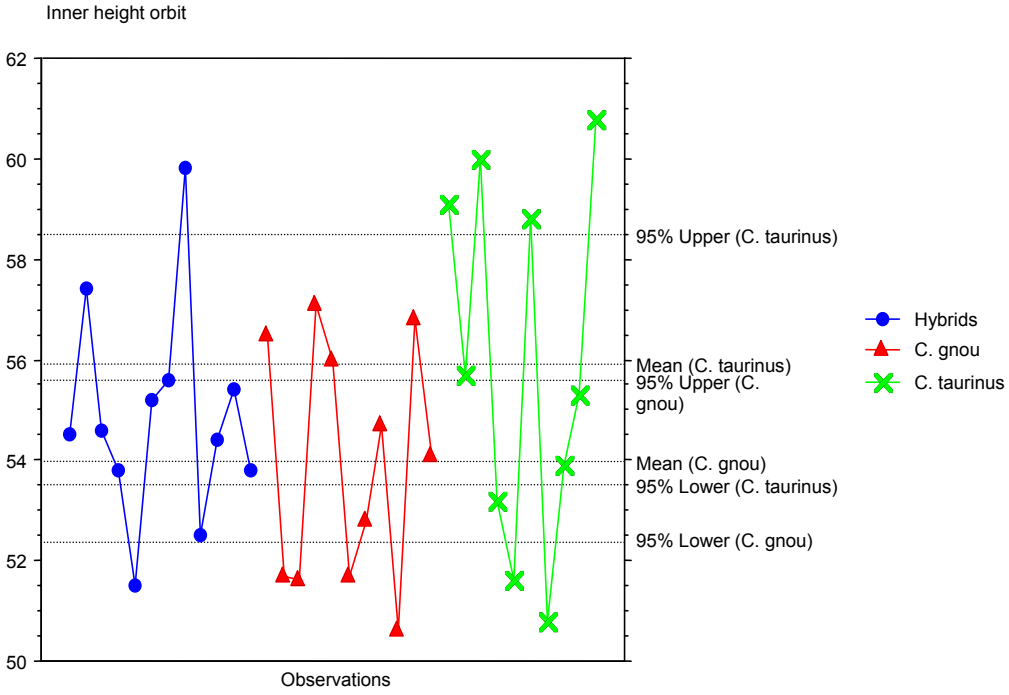

Figure 95: Univariate line plot for inner height of orbit.

6.2.23 Greatest mastoid breadth

(Otion to the otion, see Figure 2, measurement 23).

In Table 26, the mean, minimum and maximum values for Spioenkop specimens are larger than those of the black wildebeest. The Spioenkop specimens and black wildebeest have identical standard deviations and similar ranges. The minimum value of blue wildebeest falls within the range of black wildebeest.

Table 26: Descriptive statistics for otion to the otion.

	otion -otion, Total	otion -otion, Hybrids	otion -otion, C.Gnou	otion -otion, C.Taurinus
Mean	157.153	153.123	149.950	170.978
Std. Dev.	12.228	7.307	7.368	11.489
Std. Error	2.162	2.027	2.330	3.830
Count	32	13	10	9
Minimum	140.000	144.100	140.000	156.700
Maximum	193.800	167.300	159.900	193.800
# Missing	3	0	2	1
Variance	149.526	53.390	54.285	131.997
Coef. Var.	.078	.048	.049	.067
Range	53.800	23.200	19.900	37.100

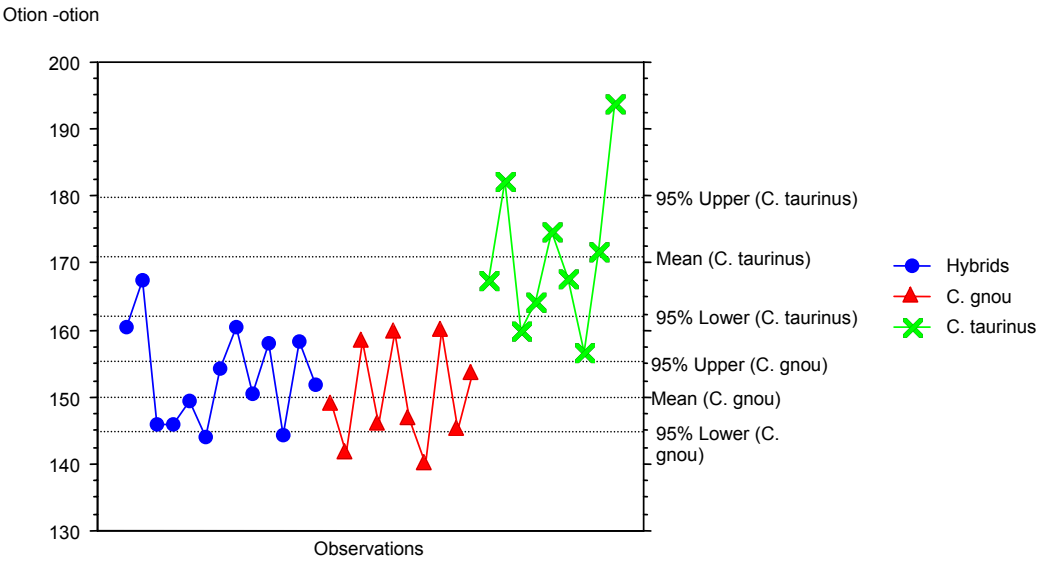

Figure 96: Univariate line plot for otion to the otion.

In Figure 96, the Spioenkop specimen plots cluster similarly to the black wildebeest plots, with similar spread. One Spioenkop specimen plots outside of the range of black wildebeest.

The standard errors in Figure 97 show that the Spioenkop specimens plot just above that of the black wildebeest. The lower limit of the Spioenkop specimen standard error falls within the range of black wildebeest.

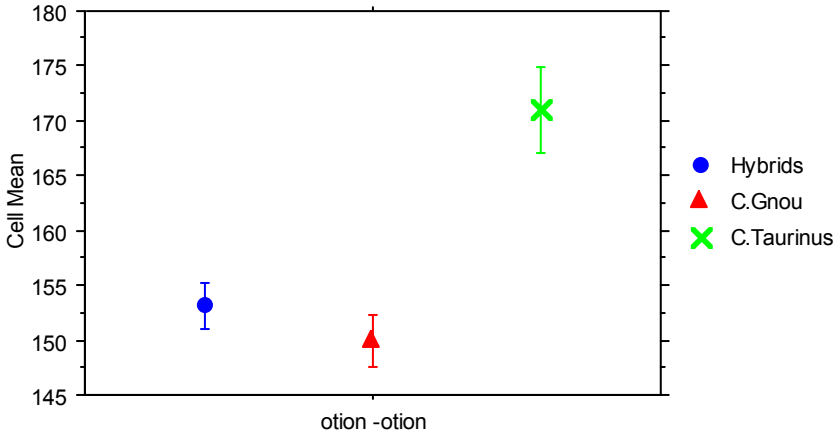

Figure 97: Standard error cell plot for otion to the otion (error bars: ±1 STD error).

6.2.24 Greatest breadth of the occipital condyles

(See Figure 2, measurement 23).

There are larger differences in the means for breadth of occipital condyle measurements. Table 27 show the mean of the Spioenkop specimens is much larger than that of the black wildebeest, and falls between *C. gnou* and *C.*

taurinus. The range of the Spioenkop specimens is slightly more than the black range, as is the standard deviation. The minimum value for the blue wildebeest falls within the range of black wildebeest.

Table 27: Descriptive statistics for greatest breadth of the occipital condyles.

	breadth occipitalcondyl, Total	breadth occipitalcondyl, Hybrids	breadth occipitalcondyl, C.Gnou	breadth occipitalcondyl, C.Taurinus
Mean	87.806	86.638	81.570	95.560
Std. Dev.	7.913	5.017	3.724	7.952
Std. Error	1.378	1.392	1.178	2.515
Count	33	13	10	10
Minimum	76.000	77.500	76.000	85.400
Maximum	108.500	92.800	88.500	108.500
# Missing	2	0	2	0
Variance	62.620	25.174	13.871	63.229
Coef. Var.	.090	.058	.046	.083
Range	32.500	15.300	12.500	23.100

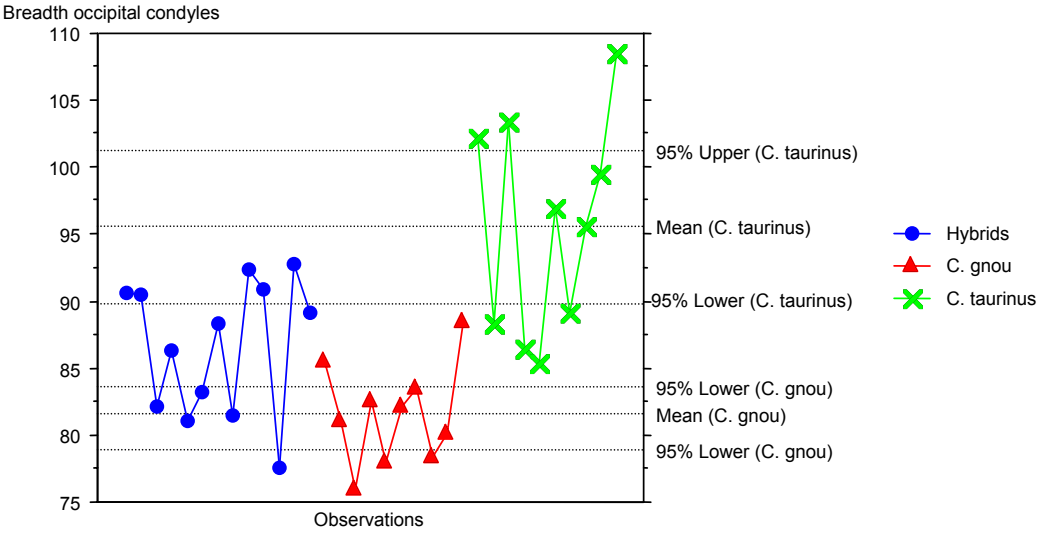

Figure 98: Univariate line plot for breadth occipital condyles.

In Figure 98, many of the Spioenkop specimen plots fall above the range of black wildebeest and into the blue wildebeest range. The confidence intervals show that

the Spioenkop plots fall inbetween the plots of *C. gnou* and *C. taurinus*. The spread of the Spioenkop plots is wide and resembles blue wildebeest spread. Six individuals fall out of the black wildebeest range.

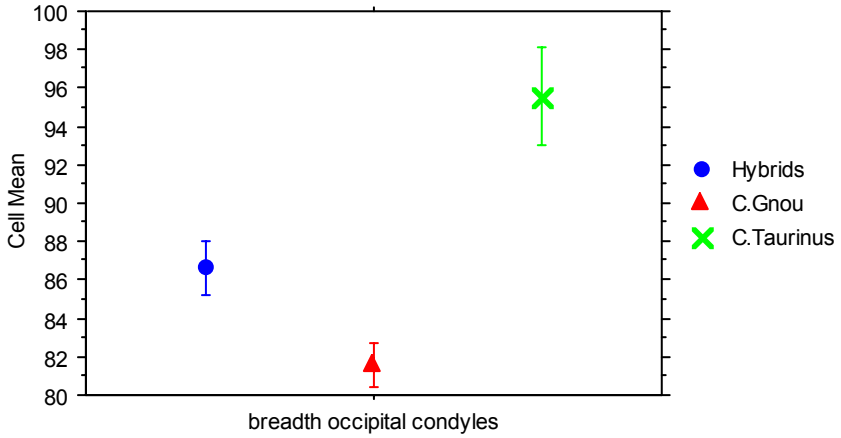

Figure 99: Standard error cell plot for greatest breadth of the occipital condyles (error bars: ±1 STD error).

In Figure 99, there is a clear separation of the standard error of the three sample groups, with the Spioenkop plots falling in between the plots of *C. gnou* and *C. taurinus*. There is no overlap in the standard errors.

6.2.25 Greatest breadth of the foramen magnum

(See Figure 2, measurement 24).

Table 28: Descriptive statistics for breadth of the foramen magnum.

	breadth foramen magnum, Total	breadth foramen magnum, Hybrids	breadth foramen magnum, C.Gnou	breadth foramen magnum, C.Taurinus
Mean	29.414	29.100	28.613	30.544
Std. Dev.	2.343	2.853	2.143	1.331
Std. Error	.435	.824	.758	.444
Count	29	12	8	9
Minimum	23.000	23.000	25.800	29.100
Maximum	32.700	32.700	30.900	32.500
# Missing	6	1	4	1
Variance	5.489	8.140	4.593	1.773
Range	9.700	9.700	5.100	3.400

Table 28 shows very little difference in the means of all the species. The standard deviation for the black and Spioenkop specimens is similar, while the standard deviation of the blue is much smaller. The Spioenkop specimens have the largest range in which both blue and black measurements fall. There is a small overlap in the ranges of blue and black wildebeest seen by the minimum value of blue, and the maximum value of black.

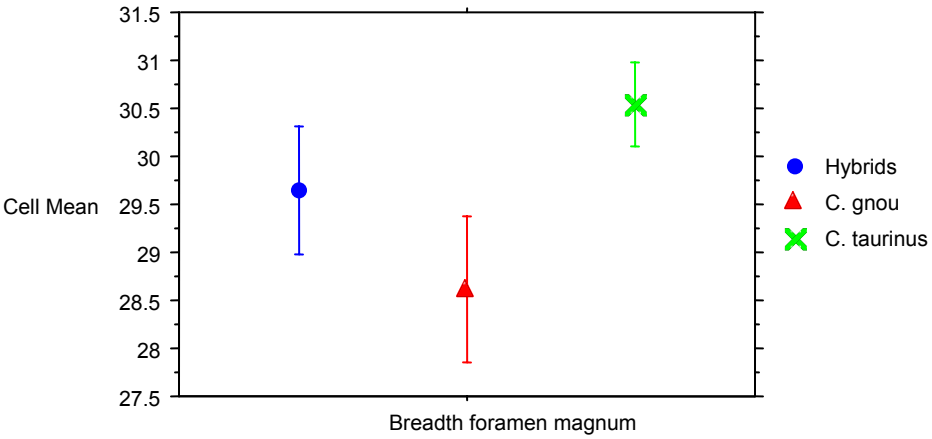

Figure 100: Standard error plot for breadth of the foramen magnum (error bars: ±1 STD error).

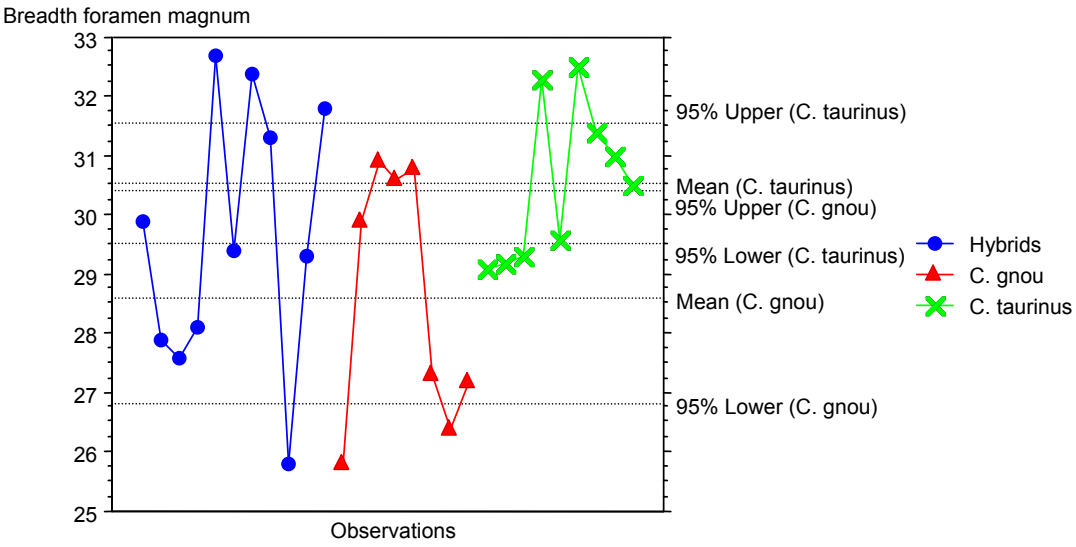

Figure 101: Univariate scatter plot for greatest breadth of foramen magnum.

In Figure 100 and Figure 101, there is overlap between the ranges of *C. gnou* and *C. taurinus*. In Figure 100, the Spioenkop wildebeest standard error overlaps with the range of the black. The upper limit and mean for the Spioenkop standard error falls just out the range of black and overlaps with the blues' lower standard error bar. Figure 101 shows that the confidence intervals of both the blue and black overlap one another. For this trait, the blue wildebeest plot clusters tightly while the black and Spioenkop plots spread across the entire confidence interval.

6.2.26 Height of foramen magnum

(From the basion to the opisthion, see Figure 2, measurement 26).

For the height of the foramen magnum, there is a large difference between the mean of the blue wildebeest and the black wildebeest (see Table 29). The Spioenkop specimen mean falls between the two, but closer to that of the black wildebeest. All three species have a small standard deviation. The ranges for black and Spioenkop wildebeest are identical. However, the Spioenkop specimens have a larger minimum and maximum value than the black.

Table 29: Descriptive statistics for height of foramen magnum.

	height foramen magnum, Total	height foramen magnum, Hybrids	height foramen magnum, C.Gnou	height foramen magnum, C.Taurinus
Mean	26.486	24.469	23.371	31.822
Std. Dev.	4.168	1.585	1.975	2.643
Std. Error	.774	.440	.746	.881
Count	29	13	7	9
Minimum	20.300	22.700	20.300	25.900
Maximum	34.600	27.700	25.600	34.600
# Missing	6	0	5	1
Variance	17.374	2.512	3.899	6.984
Coef. Var.	.157	.065	.084	.083
Range	14.300	5.000	5.300	8.700

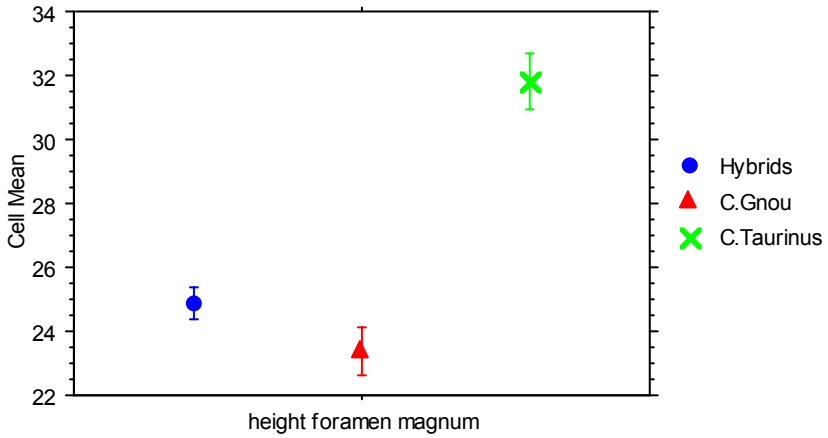

Figure 102: Standard error plot for height of the foramen magnum (error bars: ±1 STD error).

For standard error in Figure 102, the Spioenkop specimens have a small range, of which the lower limit overlaps with the upper limit of the black. This overlap is insignificant. The standard errors of the blue and black wildebeest are widely separated, with the Spioenkop specimens plotting in between the two, but closer to the black.

Only a few Spioenkop specimens plot outside the black wildebeest range in Figure 103, both the black and the Spioenkop plots have a similar spread. Many Spioenkop specimens plot in the range of black wildebeest with only three specimens outlying this range.

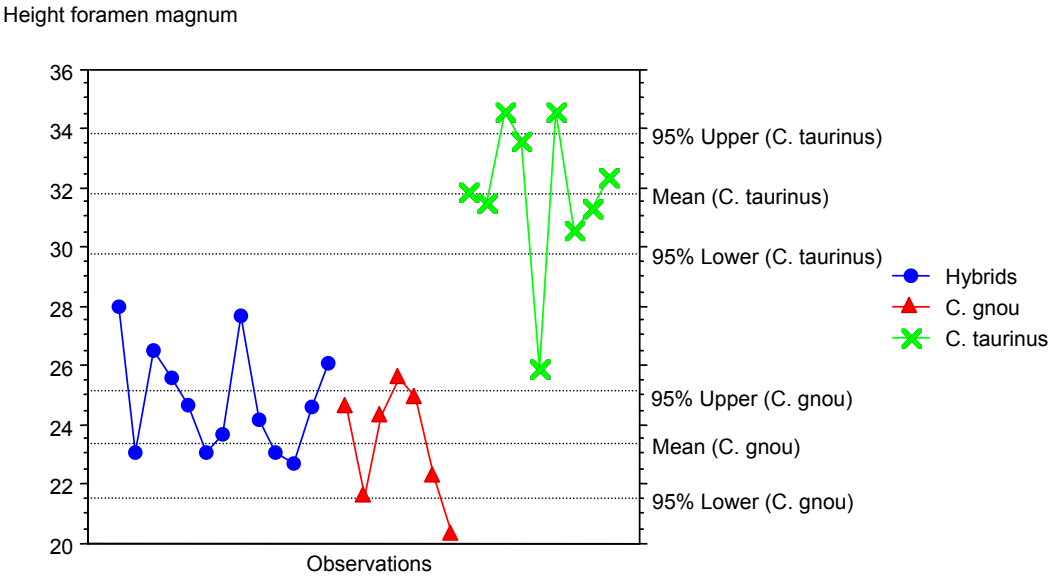

Figure 103: Univariate line plot for height of foramen magnum.

6.2.27 Least breadth between bases of the horn cores

(See Figure 1, measurement 27).

Table 30: Descriptive statistics for least breadth between the horn cores.

	Least breadth betw bases of hroncores,	... .Hybrids	C. gnou	... C. taurinus	...
Mean	42.697	22.578	33.373	74.211	
Std. Dev.	30.159	9.790	10.284	35.543	
Std. Error	5.600	3.263	3.101	11.848	
Count	29	9	11	9	
Minimum	6.100	6.100	18.700	46.200	
Maximum	160.200	36.700	52.000	160.200	
# Missing	6	4	1	1	
Range	154.100	30.600	33.300	114.000	

Table 30 shows a large difference in the means of all three species, with the Spioenkop specimens having a mean well below that of the black wildebeest. The black and Spioenkop specimens have a similar standard deviation and standard error. The minimum value of the Spioenkop specimens falls well below that of the Spioenkop specimen minimum. The black wildebeest maximum falls within the blue wildebeest range. In Figure 104, the mean of the Spioenkop specimens falls out of the confidence interval range of the black wildebeest. The black, blue and Spioenkop plots spread in a similar way. Two Spioenkop individuals plot below the black wildebeest range.

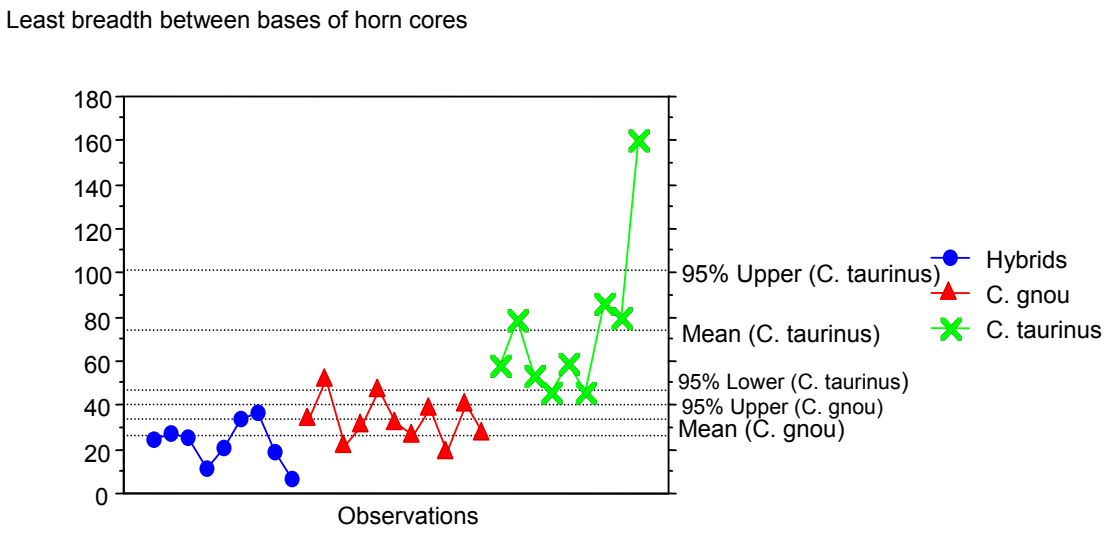

Figure 104: Univariate line plot for least breadth between bases of the horn cores.

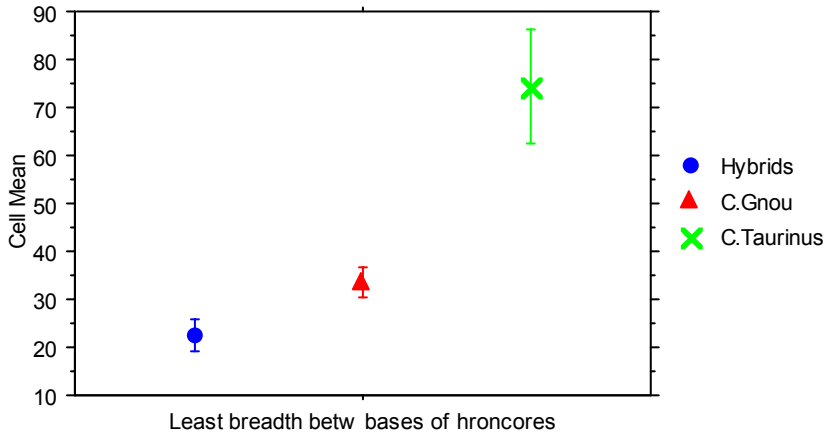

Figure 105: Standard error cell plot for least breadth between bases of horn cores (error bars: ±1 STD error).

For standard error in Figure 105, the Spioenkop specimens fall below the standard error of the black wildebeest. For this feature, the Spioenkop specimens do not plot between the blue and black wildebeest, but below the black wildebeest standard error ranges.

6.2.28 Least frontal breadth

(See Figure 1, measurement 28).

Table 31: Descriptive statistics for least frontal breadth.

	least frontal breadth, Total	least frontal breadth, Hybrids	least frontal breadth, C.Gnou	least frontal breadth, C.Taurinus
Mean	124.088	117.300	119.342	140.222
Std. Dev.	12.025	7.398	4.805	9.008
Std. Error	2.062	2.052	1.387	3.003
Count	34	13	12	9
Minimum	104.600	104.600	113.100	125.900
Maximum	152.200	126.700	128.500	152.200
# Missing	1	0	0	1
Variance	144.608	54.732	23.092	81.142
Coef. Var.	.097	.063	.040	.064
Range	47.600	22.100	15.400	26.300

In Table 31 the mean for the Spioenkop specimens is smaller than the black wildebeest mean. The Spioenkop specimens also have a larger standard deviation than the black wildebeest. The minimum value for the Spioenkop specimens falls well below the minimum of the black wildebeest, whereas the maximum value of the Spioenkop specimens falls within range of the black measurements. The minimum value of the blue wildebeest also falls within the range of black and Spioenkop wildebeest.

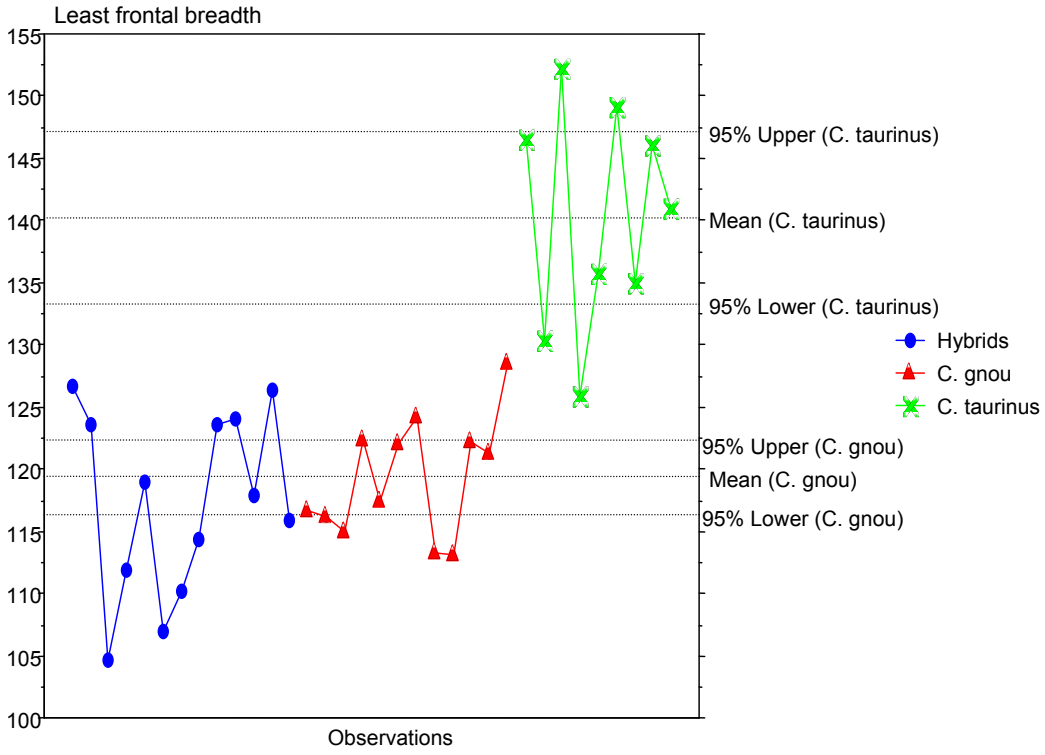

Figure 106: Univariate line plot for least frontal breadth.

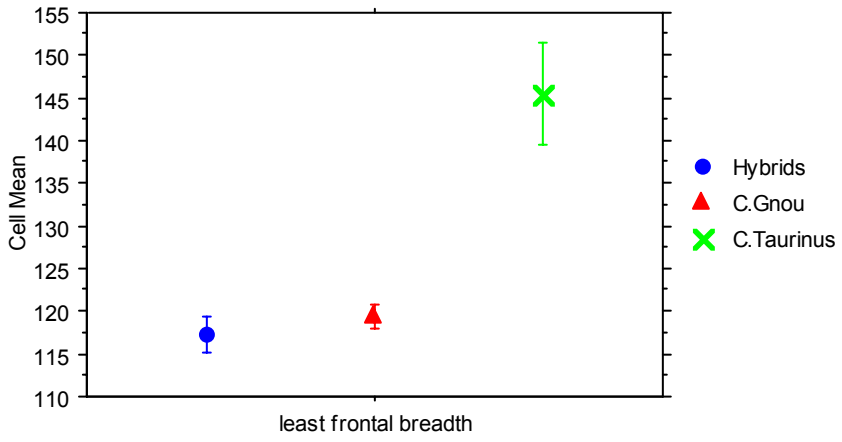

Figure 107: Standard error cell plot for least frontal breadth (error bars: ±1 STD error).

The range for black wildebeest in Figure 106 is narrow and the measurements tend to cluster closely together. The blue wildebeest measurements plot higher than the black wildebeest and are more spread than the black. The Spioenkop specimens have the same spread as the blue wildebeest. An unexpected result is that many individuals (four) fall well below the range of black wildebeest. The range of the Spioenkop specimens is larger than that of the black wildebeest. In Figure 107, the mean of the Spioenkop specimen standard error falls below the range of the black wildebeest. All three-specimen groups have a small standard error interval.

6.2.29 Greatest breadth across the orbits

(Ectorbitale to the Ectorbitale, see Figure 1, measurement 29).

In Table 32, Spioenkop specimens have a larger mean than the black wildebeest, and plot between the black and blue wildebeest. Although the ranges for black and Spioenkop wildebeest are similar, the Spioenkop maximum value falls outside the range of black. The minimum value for blue wildebeest falls in the black and hybrid wildebeest range.

Table 32: Descriptive statistics for ectorbitale to the ectorbitale measurements.

	ectorb- ectorb, Total	ectorb- ectorb, Hybrids	ectorb- ectorb, C.Gnou	ectorb- ectorb, C.Taurinus
Mean	157.382	151.050	149.609	173.530
Std. Dev.	13.752	5.632	4.401	13.968
Std. Error	2.394	1.626	1.327	4.417
Count	33	12	11	10
Minimum	142.700	143.500	142.700	153.500
Maximum	196.800	161.000	158.900	196.800
# Missing	2	1	1	0
Variance	189.123	31.717	19.367	195.118
Coef. Var.	.087	.037	.029	.080
Range	54.100	17.500	16.200	43.300

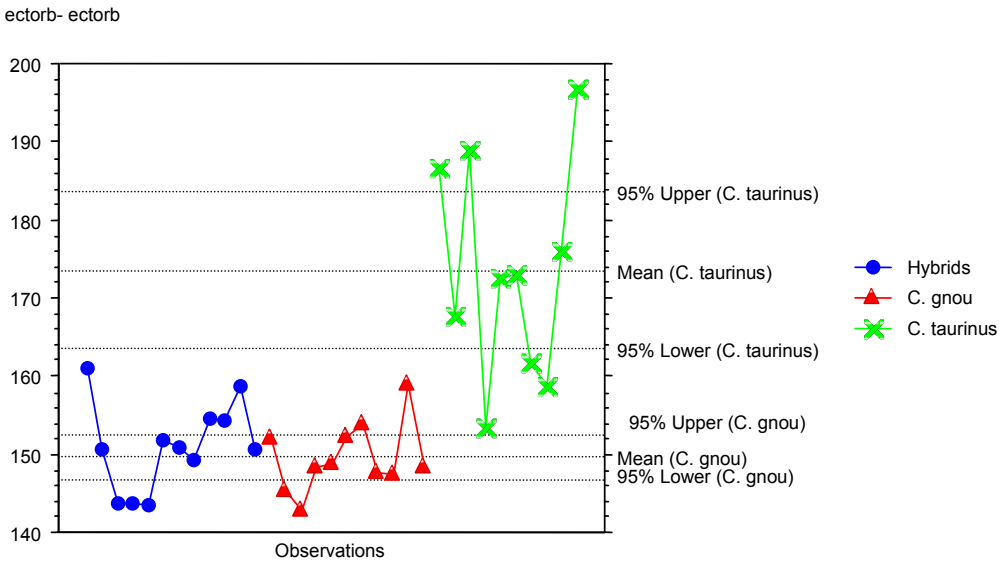

Figure 108: Univariate line plot for ectorbitale to the ectorbitale.

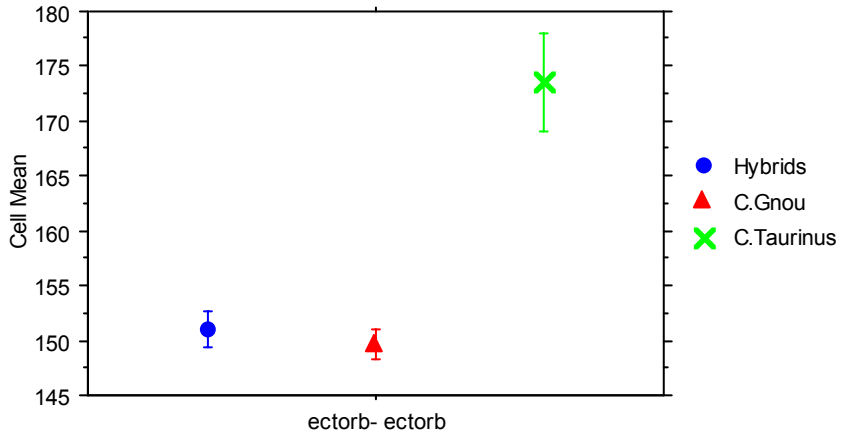

Figure 109: Standard error cell plot for ectorbitale to the ectorbitale (error bars: ±1 STD error).

Figure 108 shows a similar spread of plots for both black and Spioenkop wildebeest. Although the range of Spioenkop specimens extends past the upper limit of the black wildebeest, most individuals plot within the black wildebeest range. The blue wildebeest data are spread relative to the other two species. For the standard error plots in Figure 109, there is some overlap between the plots of black and Spioenkop wildebeest. The upper limit of the Spioenkop specimens extends past the upper limit of the black standard error. Both Spioenkop specimens and black wildebeest have narrow standard error ranges. The blue wildebeest standard error range is larger than the black wildebeest range.

6.2.30 Least breadth between the orbits

(Entorbitale to the entorbitale see Figure 1, measurement 30).

Table 33: Descriptive statistics for entorbitale to the entorbitale.

	entorb-entorb, Total	entorb-entorb, Hybrids	entorb-entorb, C.Gnou	entorb-entorb, C.Taurinus
Mean	96.974	93.669	88.473	110.620
Std. Dev.	11.952	6.905	3.232	11.732
Std. Error	2.050	1.915	.975	3.710
Count	34	13	11	10
Minimum	83.400	84.000	83.400	91.100
Maximum	126.000	106.700	92.700	126.000
# Missing	1	0	1	0
Variance	142.861	47.676	10.446	137.637
Coef. Var.	.123	.074	.037	.106
Range	42.600	22.700	9.300	34.900

The means in Table 33 are all very different, with the mean for the Spioenkop specimens falling in between the means of *C. gnou* and *C. taurinus*. Spioenkop specimens have a very large standard deviation relative to the black wildebeest standard deviation. The range of the Spioenkop specimens is much larger than the black wildebeest range. The maximum value of the Spioenkop specimens falls within the blue wildebeest range, while the minimum value falls within the black wildebeest range.

In Figure 110, many of the Spioenkop individuals plot between the parent species intervals. Black wildebeest measurement cluster over a narrow range. The blue wildebeest measurements are spread over a large range. The spread of the Spioenkop range is similar to the blue range, but not as extensive.

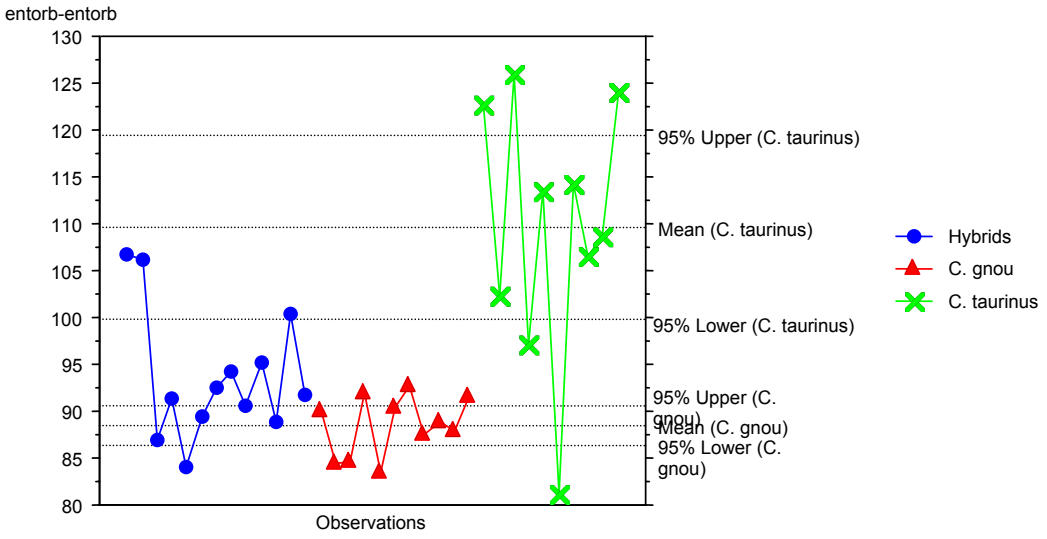

Figure 110: Univariate line plot for entorbitale to the entorbitale.

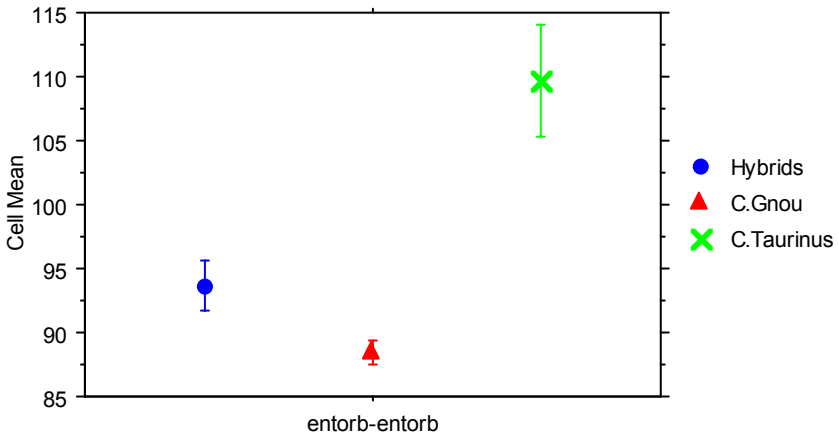

Figure 111: Standard error cell pot for entorbitale to the entorbitale (error bars: ±1 STD error).

The standard error plot in Figure 111 shows that the Spioenkop specimens plot in between the plots of black and blue wildebeest.

6.2.31 Facial breadth

(See Figure 1, measurement 31).

Table 34: Descriptive statistics for facial breadth.

	facial breadth, Total	facial breadth, Hybrids	facial breadth, C.Gnou	facial breadth, C.Taurinus
Mean	85.713	84.569	83.378	89.300
Std. Dev.	6.220	5.727	3.367	7.603
Std. Error	1.099	1.588	1.122	2.404
Count	32	13	9	10
Minimum	71.800	71.800	79.200	74.900
Maximum	101.000	94.900	88.800	101.000
# Missing	3	0	3	0
Variance	38.684	32.797	11.337	57.800
Coef. Var.	.073	.068	.040	.085
Range	29.200	23.100	9.600	26.100

Table 34 shows that while the mean for black and Spioenkop wildebeest are similar, the Spioenkop specimens are slightly larger. The Spioenkop specimens have a larger standard deviation compared to black wildebeest. Black wildebeest specimens plot over a small range, while the Spioenkop specimens have a range close to the size of blue wildebeest. The range of Spioenkop specimens extends from below the black wildebeest range and into the range of blue wildebeest.

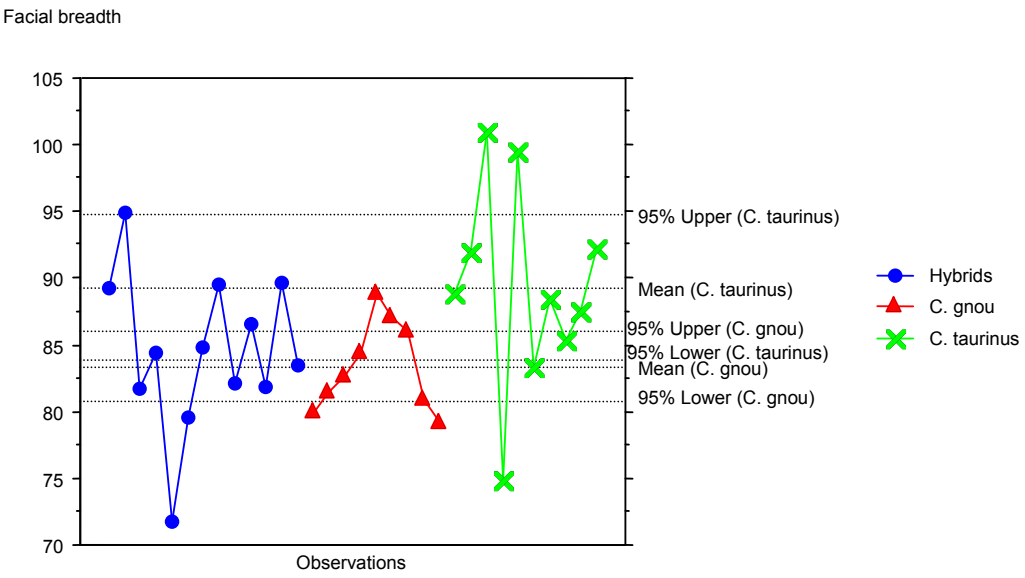

Figure 112: Univariate plot for facial breadth.

The black wildebeest plots in Figure 112 cluster and plot over a narrow range. The Spioenkop plots spread (similar to the blue wildebeest), and the range extends from just above the lower limit of black wildebeest to just under the mean of blue wildebeest.

The standard errors for all three species in Figure 113 are large. While the Spioenkop specimen upper error bar extends out of the range of the black wildebeest, there is significant overlap of the mean and lower error bar.

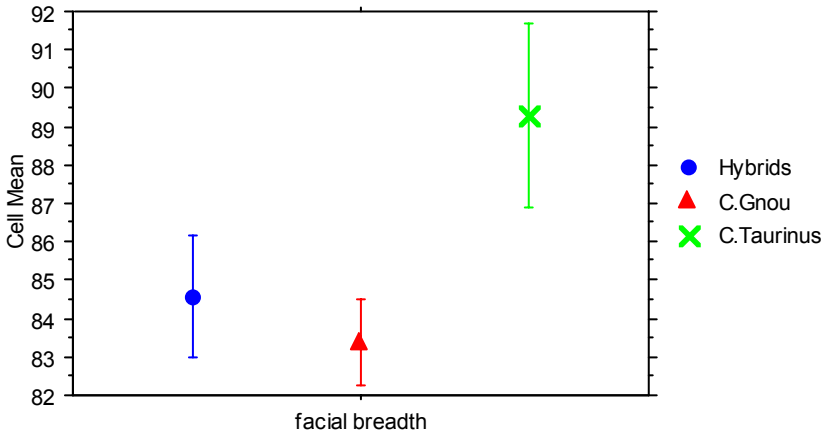

Figure 113: Standard error plot for facial breadth (error bars: ±1 STD error).

6.2.32 Greatest breath across the nasals

(See Figure 1, measurement 32).

Table 35 shows that blue wildebeest have the smallest mean of the three species, and that the Spioenkop mean plots between that of *C. gnou* and *C. taurinus*, but closer to the black mean. The black wildebeest has a narrow range while the Spioenkop range is large and similar to that of the blue wildebeest. The Spioenkop range extends from inside the blue wildebeest range (minimum) to the black wildebeest range (maximum).

Table 35: Descriptive statistics for greatest breadth across the nasals.

	grtst brdth nasal, Total	grtst brdth nasal, Hybrids	grtst brdth nasal, C.Gnou	grtst brdth nasal, C.Taurinus
Mean	41.686	43.338	44.143	36.850
Std. Dev.	4.695	3.653	2.171	4.503
Std. Error	.887	1.013	.821	1.592
Count	28	13	7	8
Minimum	30.400	38.000	40.200	30.400
Maximum	50.100	50.100	47.000	42.300
# Missing	7	0	5	2
Variance	22.046	13.348	4.713	20.277
Coef. Var.	.113	.084	.049	.122
Range	19.700	12.100	6.800	11.900

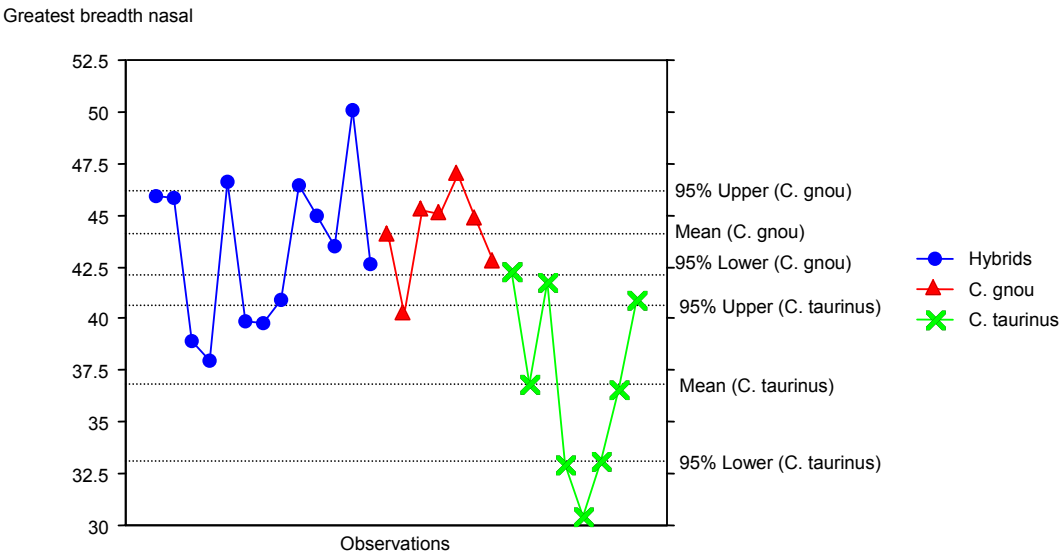

Figure 114: Univariate line plot for the greatest breadth of the nasals.

In Figure 114, the black and Spioenkop wildebeest have larger measurements than the blue. The black wildebeest measurements cluster over a small range. The range for the Spioenkop specimens is similar to that of the black. However, the data spread resembles that of the blue wildebeest.

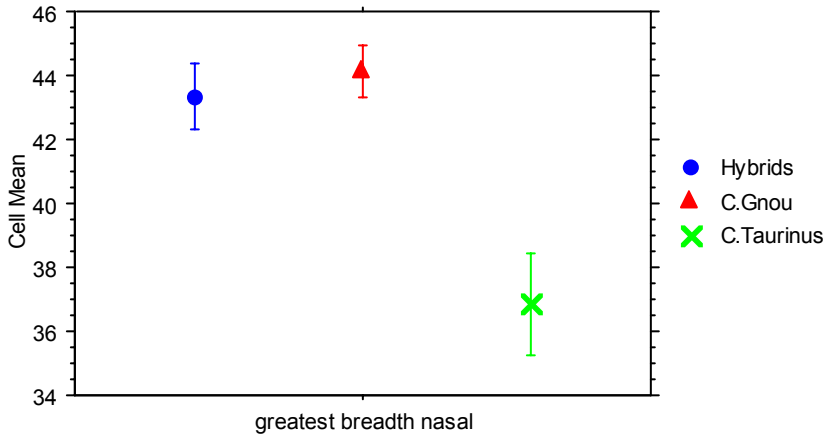

Figure 115: Standard error cell plot for greatest breadth of nasals (error bars: ±1 STD error).

The standard errors in Figure 115 are all relatively large, and there is overlap between the Spioenkop specimens and black wildebeest. The lower standard error falls out of the black range.

6.2.33 Least inner height of temporal fossa

(See Figure 3, measurement 33).

Table 36 shows identical means for Spioenkop specimens and black wildebeest, with the blue wildebeest mean being the smallest of the three. The black wildebeest have the largest range in which both blue and Spioenkop wildebeest fall. All three species have a small standard deviation.

Table 36: Descriptive statistics for inner height of temporal groove.

	hght temporal grve, Total	hght temporal grve, Hybrids	hght temporal grve, C.Gnou	hght temporal grve, C.Tauri...
Mean	40.221	40.538	40.964	38.856
Std. Dev.	3.100	2.423	3.489	3.376
Std. Error	.540	.672	1.052	1.125
Count	33	13	11	9
Minimum	32.700	35.700	33.600	32.700
Maximum	47.100	43.400	47.100	42.300
# Missing	2	0	1	1
Variance	9.610	5.871	12.175	11.395
Coef. Var.	.077	.060	.085	.087
Range	14.400	7.700	13.500	9.600

In Figure 116, the mean of *C. taurinus* falls close to the lower limits of both black and Spioenkop wildebeest. Black wildebeest have the widest confidence interval and the measurements are widely spread. Spioenkop specimens also have a wide range, which falls in between the ranges of *C. gnou* and *C. taurinus*. The standard error ranges in Figure 117 are widely spread. The black and Spioenkop specimen standard errors overlap, and the lower limit of the black wildebeest fall within the blue wildebeest standard error.

No Spioenkop specimens fall out of range of black wildebeest for this feature.

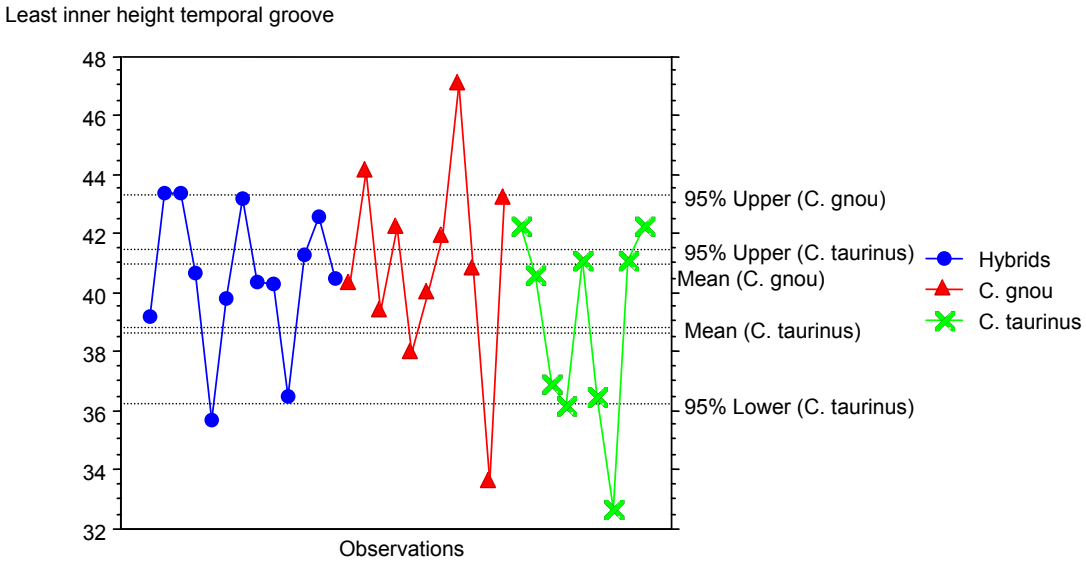

Figure 116: Univariate line plot for least inner height of the temporal groove.

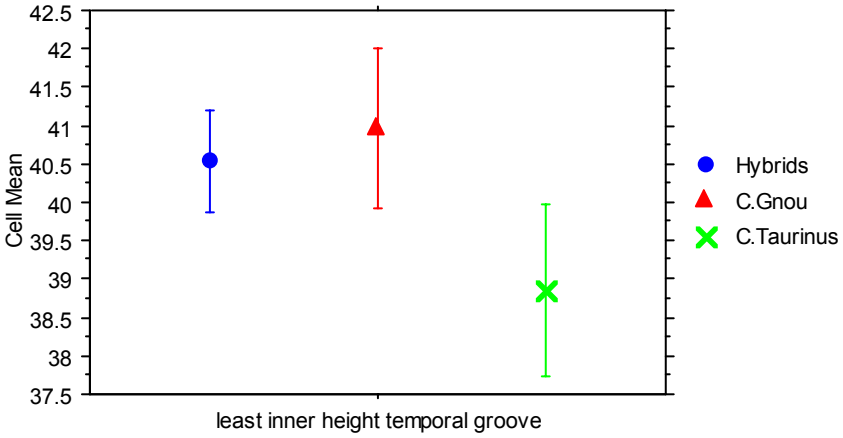

Figure 117: Standard error cell plot for least inner height of temporal groove (error bars: ±1 STD error).

6.2.34 Distance between the anterior and posterior tuberosities

(See Figure 5, measurement D).

Table 37: Descriptive statistics for distance between the anterior and posterior tuberosities.

	D, Total	D, Hybrids	D, C.Gnou	D, C.Taurinus
Mean	27.512	27.023	24.427	31.540
Std. Dev.	5.426	4.600	1.622	6.843
Std. Error	.931	1.276	.489	2.164
Count	34	13	11	10
Minimum	20.300	20.300	22.000	22.300
Maximum	44.000	37.100	26.900	44.000
# Missing	1	0	1	0
Variance	29.443	21.159	2.630	46.823
Coef. Var.	.197	.170	.066	.217
Range	23.700	16.800	4.900	21.700

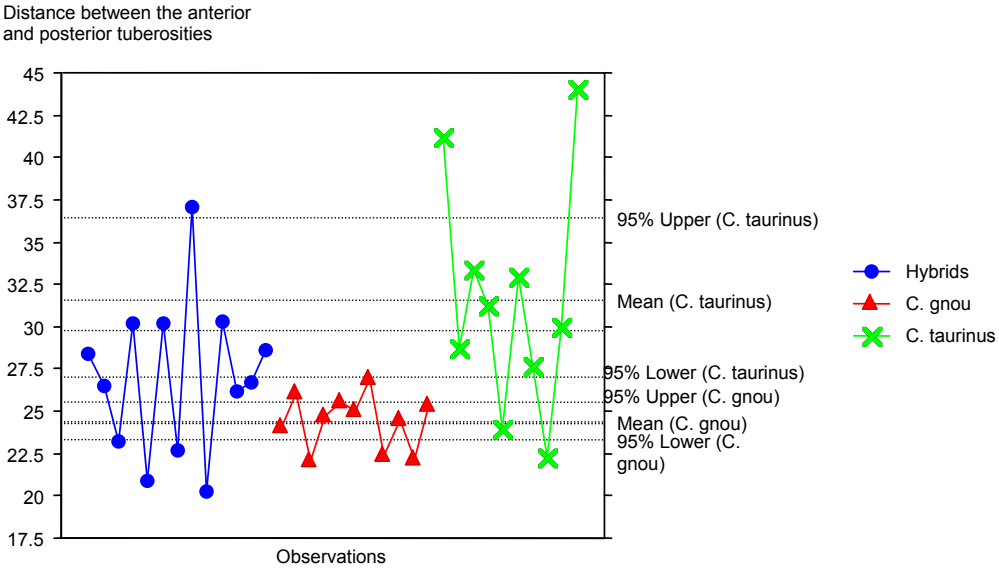

Figure 118: Univariate line plot for distance between the anterior and posterior tuberosities.

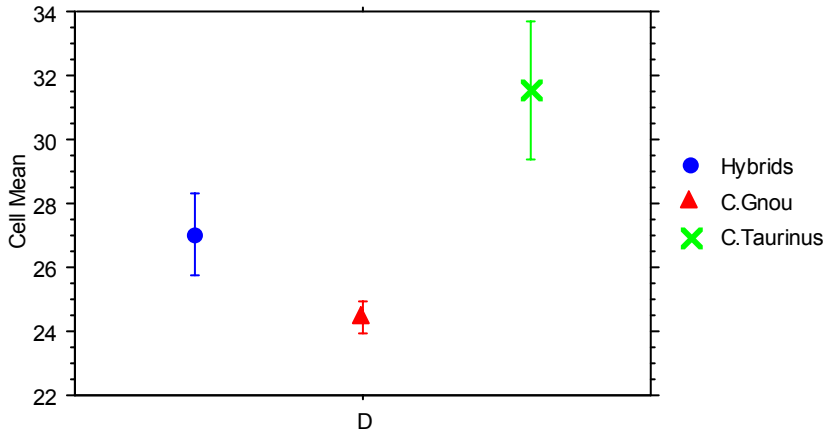

Figure 119: Standard error cell plot for distance between the anterior and posterior tuberosities (error bars: ±1 STD error).

In Table 37, the Spioenkop specimen mean falls between the mean of both black and blue wildebeest. Standard deviation of black wildebeest is small, whereas the Spioenkop specimens have a larger standard deviation similar to that of the blue wildebeest. Both the Spioenkop and blue wildebeest ranges are large, while the black has a small range. This pattern is repeated in Figure 118 where the confidence intervals of the Spioenkop specimens and blue wildebeest are large and the measurements are widely spread. The black wildebeest have a narrow range and the measurements cluster.

The standard error in Figure 119 shows the small range for black wildebeest and a large standard error (STD) range for blue wildebeest. The Spioenkop specimen standard error plots between the standard errors of *C. gnou* and *C. taurinus*, and there is no overlap between the three species.

6.2.35 Width between the anterior tuberosities

(See Figure 5, measurement Dwa).

Table 38: Descriptive statistics for the width between the anterior tuberosities.

	Dw a, Total	Dw a, Hybrids	Dw a, C.Gnou	Dw a, C.Taurinus
Mean	14.767	14.538	13.182	17.033
Std. Dev.	2.971	2.419	1.799	3.628
Std. Error	.517	.671	.543	1.209
Count	33	13	11	9
Minimum	10.500	10.800	10.500	11.500
Maximum	24.000	17.600	16.800	24.000
# Missing	2	0	1	1
Variance	8.827	5.853	3.238	13.165
Coef. Var.	.201	.166	.137	.213
Range	13.500	6.800	6.300	12.500

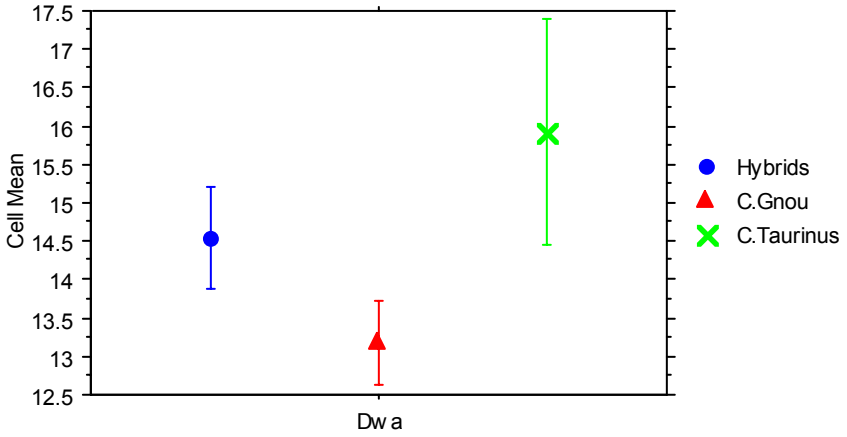

Figure 120: Standard error plot for the width between the anterior tuberosities (error bars: ±1 STD error).

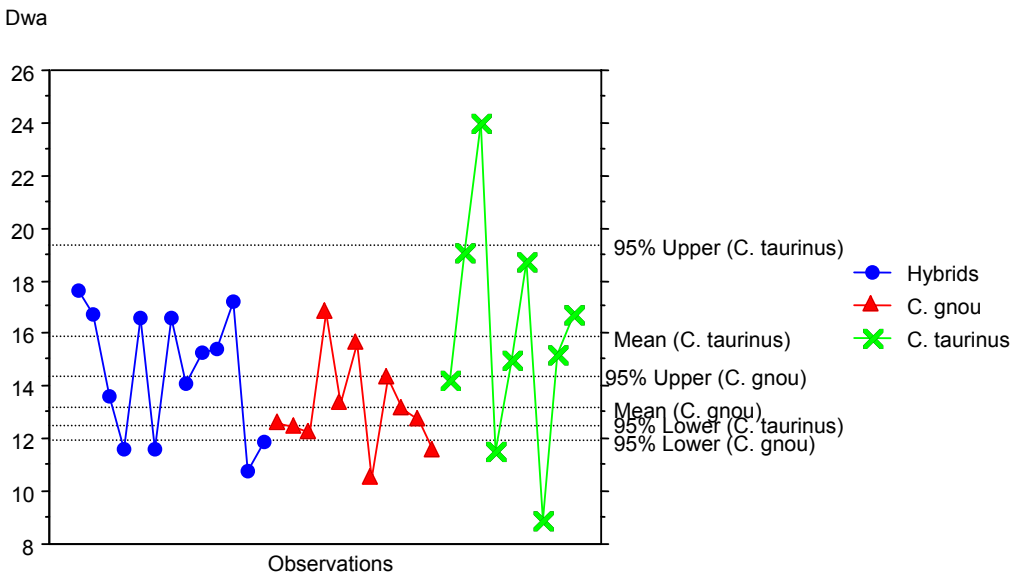

Figure 121: Univariate line plot for the width between the anterior tuberosities.

For the width between the anterior tuberosities (Dwa), Table 38 shows closeness in the means of black and Spioenkop specimens, and both species have the same range. The blue wildebeest have a larger mean and range relative to the other species in the study. Figure 120 and Figure 121 have similar patterns in that the Spioenkop specimen plots and standard error plot fall between that of the blue and black wildebeest. The lower interval of blue wildebeest and the upper interval of the black wildebeest in Figure 121 all fall within close proximity of each other. The confidence interval plots of black and Spioenkop wildebeest have similar spreads. In Figure 120, the standard error of the Spioenkop specimens plots clear of both black and blue wildebeest.

6.2.36 Width between the posterior tuberosities

(See Figure 5, measurement Dwp).

Table 39: Descriptive statistics for the width between the posterior tuberosities.

	Dw p, Total	Dw p, Hybrids	Dw p, C.Gnou	Dw p, C.Taurinus
Mean	16.288	16.954	15.073	16.811
Std. Dev.	3.675	4.168	2.606	4.052
Std. Error	.640	1.156	.786	1.351
Count	33	13	11	9
Minimum	9.400	9.400	11.200	10.800
Maximum	23.700	23.700	18.900	22.500
# Missing	2	0	1	1
Variance	13.508	17.376	6.790	16.421
Coef. Var.	.226	.246	.173	.241
Range	14.300	14.300	7.700	11.700

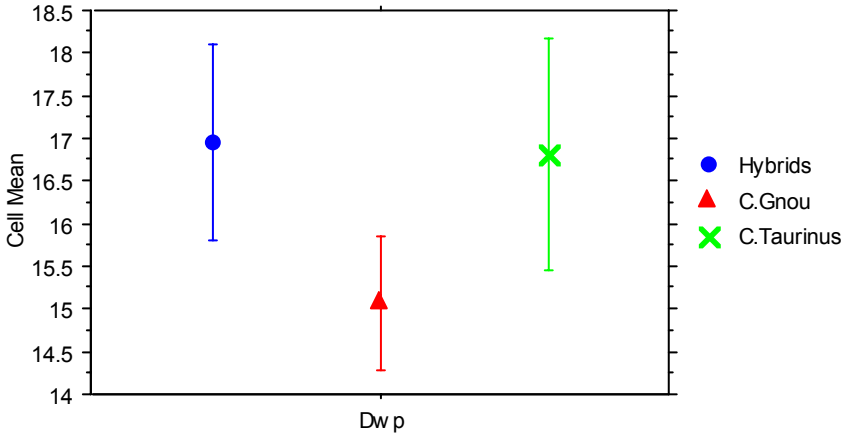

Figure 122: Standard error plots for the width between the posterior tuberosities (error bars: ±1 STD error).

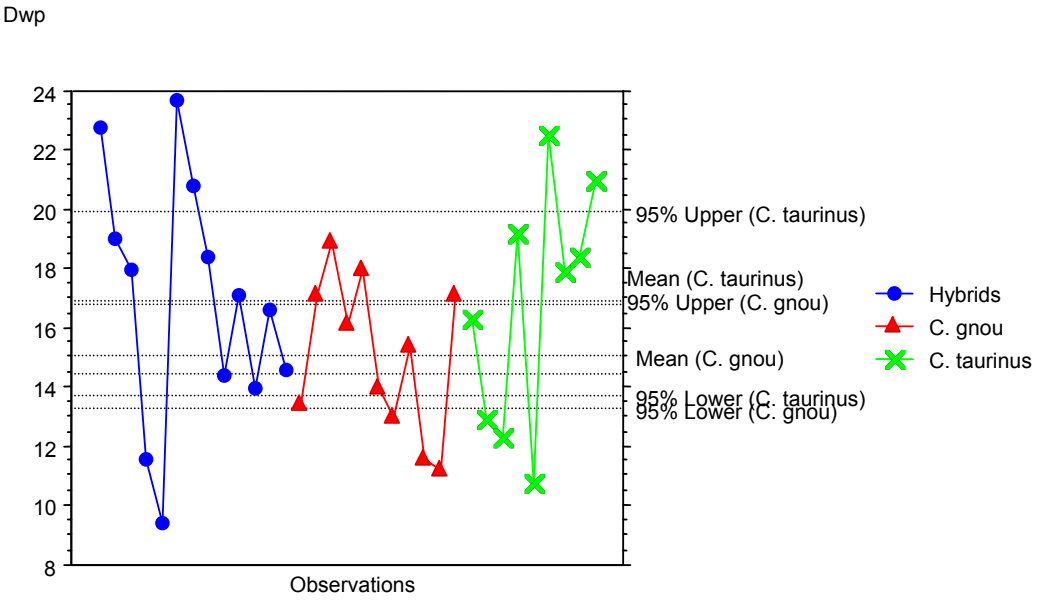

Figure 123: Univariate line plot for the width between the posterior tuberosities.

In Table 39 the mean and range for the Spioenkop specimens is larger that both blue and black wildebeest, the range for the hybrids extends from below the minimum value of blue wildebeest to past the maximum value for blue wildebeest. In Figure 122 and Figure 123 there is overlap between all three species, and the general spread for all three is wide.

6.2.37 Diameter of the earhole

Table 40: Descriptive statistics for the diameter of the earhole.

	Diameter of earhole, Total	Diameter of earhole, Hybrids	Diameter of earhole, C.Gnou	Diameter of earhole, C.Taurinus
Mean	6.748	7.385	6.070	6.600
Std. Dev.	1.012	.949	.663	.936
Std. Error	.176	.263	.210	.296
Count	33	13	10	10
Minimum	4.700	6.100	5.100	4.700
Maximum	9.000	9.000	7.200	7.500
# Missing	2	0	2	0
Variance	1.023	.901	.440	.876
Coef. Var.	.150	.129	.109	.142
Range	4.300	2.900	2.100	2.800

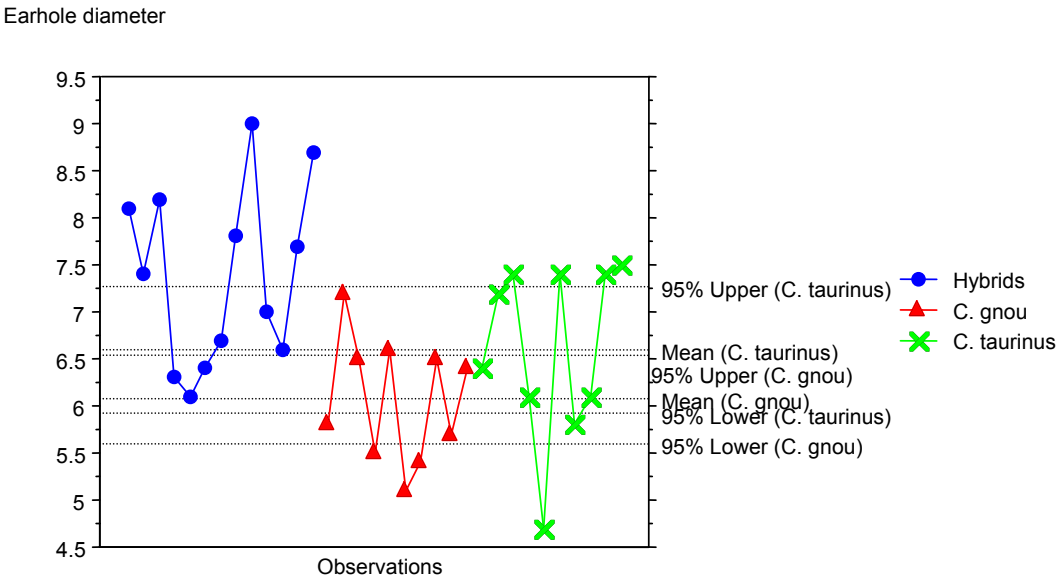

Figure 124: Univariate plot for the diameter of the earhole.

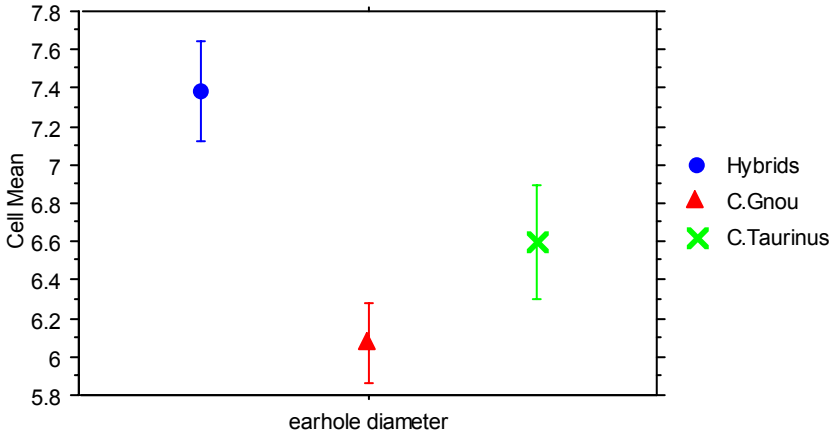

Figure 125: Standard error plot for the diameter of the earhole (error bars: ±1 STD error).

In Table 40 the mean of the Spioenkop specimens are the largest of the three. For standard deviation, standard error and range, the three species plot nearly identically. In Figure 124, there is overlap in the confidence intervals of blue and black wildebeest. The blue and black wildebeest plot in a similar way with similar spread. The Spioenkop specimens have a range that extends above that of both the blue and black wildebeest. The same pattern is seen in Figure 125, where the standard error falls well out of range of both blue and black wildebeest.

6.2.38 Auditory bullar thickness

Table 41: Descriptive statistics for the auditory bullar thickness.

	Auidtary bular, Total	Auidtary bular, Hybrids	Auidtary bular, C.Gnou	Auidtary bular, C.Taurinus
Mean	20.373	20.692	19.030	21.300
Std. Dev.	2.458	1.886	2.870	2.324
Std. Error	.428	.523	.908	.735
Count	33	13	10	10
Minimum	14.600	17.600	14.600	16.900
Maximum	24.700	23.200	24.500	24.700
# Missing	2	0	2	0
Variance	6.043	3.556	8.236	5.402
Range	10.100	5.600	9.900	7.800

In Table 41, the Spioenkop specimens have a similar mean to the blue and black wildebeest. The difference in the means is small. All three species have very small standard deviations and standard errors (Figure 100). The ranges are small for all three species, with the hybrid range plotting within the range of the blue wildebeest.

Figure 126 and Figure 127 show that the Spioenkop specimens plot similar to the both the black and blue wildebeest range. The hybrid plot is tighter than both black and blue wildebeest.

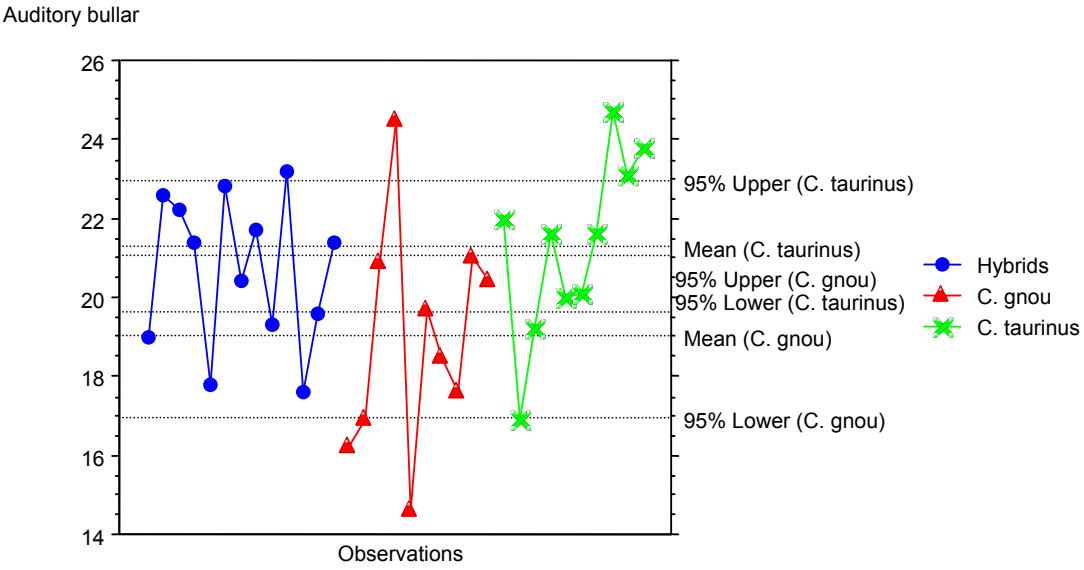

Figure 126: Univariate line plot for the auditory bullar thickness.

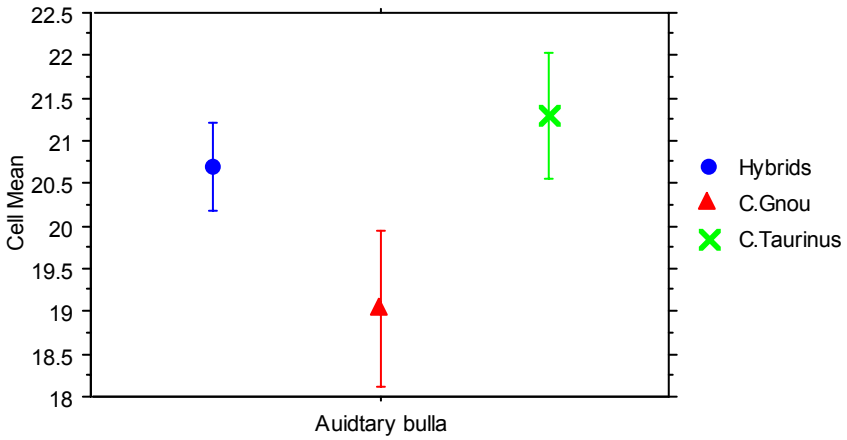

Figure 127: Standard error plot for auditory bullar thickness (error bars: ±1 STD error).

6.3 Summary univariate analysis

In this section, summary tables represent the outliers for each measurement taken on the skull. The following tables were compiled following observation of specimens individually, and in relation to the blue and black wildebeest ranges.

Table 42 shows that there are many features for which the black and blue wildebeest ranges overlap. If the overlap is greater than 30%, those features are eliminated, as metrically they are indistinguishable from one another and will not be useful in identification of hybrids as per the aims of this study. The following features were not useful in the identification of Spioenkop specimens, due to the overlap between blue and black wildebeest:

- Akrokranion to nasion
- Aboral to the entorbitale
- Greatest frontal length
- Inner height of the orbit
- Least inner height of the temporal groove

While there is overlap in the ranges of black and blue wildebeest, there are clearly a number of individuals that deviate from the black wildebeest, and are identified as possible hybrids based on the following features:

- Auditory bullar thickness: *n.* 7.

- Breadths of the foramen magnum: *n.* 5.
- Distance between anterior and posterior tuberosities: *n.* 6.
- Width between the anterior tuberosities: *n.* 2.
- Width between the posterior tuberosities: *n.* 3.
- Diameter of the earhole: *n.* 4.
- Length from the ectorbitale to the entorbitale: *n.* 9.
- Length from the entorbitale to the entorbitale: *n.* 2.
- Facial breadth: *n.* 4.
- Nasiointermaxillare to the prosthion: *n.* 7.
- Skull profile length: *n*. 3.

Table 43 shows the features in which the hybrid measurements fall within the blue wildebeest range. In this table, each specimen varies in the number of features that lie within the blue range. Hybrid specimens 12042 and 12043 have a large number of features that plot like blue wildebeest, while specimens 12047 and 12053 have no characters that lie within the blue wildebeest range.

In Table 44, the combined results are represented of features that lie within the blue range, as well as those which lie outside both *C. gnou* and *C. taurinus*. From this table we can see that all specimens have features that deviate from the black wildebeest blueprint. It is noted the features that for which Spioenkop specimens plot outside both *C. gnou* and *C. taurinus* ranges often fall well below the range

of black wildebeest. The diameter of the earhole is the only exception, in that the specimens which out lie have larger earhole diameters than both *C. gnou* and *C. taurinus*.

Statistically, hybrid specimens 12047 and 12053 show no deviation from a black wildebeest blueprint.

Table 42: Summary of the skull, showing features for which black wildebeest plot like blue wildebeest. The number one indicates that the features lie within the blue wildebeest range and a zero indicates that it does not.

Black that plot like blue													
Specimen number	M84	NMB92	NMB81	NMB96	NMB93	1930NMB	M89	M90	NMB80	Sub fossil 41464	Sub fossil C 438	c1463	SUM
Skull Measurements													
Akron-Nasion	1	0	0	1	1	0	1	1	0	0	1	0	6
Akron-Rhinion	1	0	0	0	0	0	0	1	0	0	0	0	2
Aboral-entorbitale	1	1	1	1	0	1	1	1	0	0	0	1	8
Auditory bullar thickness	0	1	1	1	1	1	0	1	1	1	1	1	10
Aboral-infraorbitale	0	0	0	0	0	0	0	1	0	0	0	0	1
Basal length of the skull	0	0	0	0	0	0	0	0	0	0	0	0	0
Breadth occipital condyle	1	0	0	0	0	0	0	0	0	0	0	1	2
Breadth foramen magnum	0	1	1	1	0	1	0	0	0	0	0	0	4
Condylobasal length of the skull	0	0	0	0	0	0	0	0	0	0	0	0	0
D	1	1	1	1	1	1	1	1	1	1	1	1	12
Dental length	0	0	0	0	0	0	0	0	0	0	0	0	0
Dwa	1	1	1	1	1	1	1	1	1	1	1	1	12
Dwp	1	1	1	1	1	1	1	1	1	1	1	1	12
Diameter earhole	1	1	1	1	1	1	1	1	1	1	1	1	12
Ectorbit-entorbit	1	0	0	1	1	0	0	0	0	1	0	0	4
Ectorbit-entorbit	0	0	0	0	0	0	1	0	0	1	0	0	2
Ectorbit-prosthion	0	0	0	0	0	0	0	0	0	0	0	0	0
Entorbit-entorbit	1	1	1	1	1	1	1	1	1	1	1	1	12
Facial breadth	1	1	1	1	1	1	1	1	1	1	1	1	12
Greatest breadth nasal	0	1	0	0	0	0	0	0	1	0	0	0	2
Greatest frontal length	1	1	1	1	1	1	1	1	1	1	1	1	12
Height foramen magnum	0	0	0	0	0	0	0	0	0	0	0	0	0
Infraorbitale-Prosthion	0	0	0	0	0	0	0	0	1	0	0	0	1
Inner height orbit	1	1	1	1	1	1	1	1	1	1	1	1	12
Least breadth btw condyles	0	1	0	0	0	0	0	0	1	0	0	0	2
Least frontal breadth	0	0	0	0	0	0	0	0	0	0	0	1	1
Least inner height of temp grve	1	0	1	1	1	1	1	0	1	1	1	0	9
Length Molar row	0	0	0	0	0	0	0	0	0	0	0	0	
Length of premolar row	1	0	0	0	0	0	0	1	0	0	0	0	2
Length of cheektooth row	0	0	0	0	0	0	0	0	0	0	0	0	0
Nasiointermax- Prosthion	1	1	1	1	1	1	1	1	1	1	1	1	12
Nasion- Prosthion	0	0	0	0	0	0	0	0	0	0	0	0	0
Nasion-rhinion	0	0	0	0	0	0	0	0	0	0	0	0	0
Oral palatal length	0	0	0	0	0	0	0	0	0	0	0	0	0
Otion-Otion	1	0	0	0	0	0	1	0	0	1	0	0	3
Premolar- Prosthion	0	0	0	0	0	0	0	0	0	0	0	0	0
Skull profile length	1	0	0	0	0	0	1	1	0	1	0	0	4
Postdentale -Aboral	1	1	0	0	0	0	0	0	0	0	0	0	2
Brdth btw base hrncres	0	1	0	0	0	1	0	0	0	0	0	0	2
Short skull length	0	0	0	0	0	0	0	0	0	0	0	0	0
SUM	20	17	14	16	14	15	16	17	15	16	13	14	
Percentage	48.8	41.5	34.1	39.0	34.1	36.6	39.0	41.5	36.6	39.0	31.7	34.1	

Table 43: Summary showing the features of the Spioenkop specimens which fall within the blue wildebeest range. 'b' indicates which features that fall within the blue wildebeest range for each specimen. There is no overlap with the black wildebeest for these outliers. The features for which there is overlap between *C. gnou* and *C. taurinus* have been removed.

Hybrids that Fall in BLUE RANGE without overlapping the Black range														
Specimen number	**12042**	**12043**	**12044**	**12046**	**12047**	**12048**	**12049**	**12050**	**12051**	**12052**	**12053**	**12054**	**12060**	**SUM**
Skull Measurements														
Akron-Rhinion	b	b	0	0	0	0	0	0	0	0	0	b	b	**4**
Aboral-infraorbitale	b	b	0	0	0	0	0	0	0	0	0	b	0	**3**
Basal length of the skull	0	b	0	0	0	0	0	0	0	0	0	0	0	**1**
Breadth occipital condyle	1	b	0	b	0	0	b	0	b	b	0	b	0	**7**
Condylobasal length	0	b	0	0	0	0	0	0	0	0	0	0	0	**1**
Dental length	0	0	0	0	0	0	0	0	0	0	0	0	b	**1**
Ectorbit-entorbit	b	0	0	0	0	0	0	0	0	0	0	0	0	**1**
Ectorbit-prosthion	0	0	0	0	0	0	0	0	0	0	0	0	0	**0**
Greatest breadth nasal	0	0	b	b	0	b	b	b	0	0	0	0	0	**5**
Height foramen magnum	b	0	b	0	0	0	0	b	0	0	0	0	b	**4**
Infraorbitale-Prosthion	0	b	0	0	0	0	0	0	0	0	0	0	0	**1**
Least breadth btw condyles	0	0	0	0	0	0	0	0	0	0	0	0	0	**0**
Least frontal breadth	b	0	0	0	0	0	0	0	0	0	0	b	0	**2**
Length of Molar row	0	0	0	0	0	0	0	0	0	0	0	0	0	**0**
Length of premolar row	0	0	0	b	0	0	b	b	0	0	0	0	b	**4**
Length of cheektooth row	0	0	0	0	0	0	0	0	0	0	0	0	0	**0**
Nasion- Prosthion	0	b	0	0	0	0	0	0	0	0	0	0	0	**1**
Nasion-rhinion	0	0	0	0	0	0	0	0	0	0	0	0	0	**0**
Oral palatal length	0	0	0	0	0	0	0	0	0	0	0	0	0	**0**
Otion-Otion	0	b	0	0	0	0	0	0	0	0	0	0	0	**1**
Premolar- Prosthion	0	0	0	0	0	0	0	0	0	0	0	0	0	**0**
Postdentale -Aboral occipital condyle	b	b	0	0	0	0	0	0	0	b	0		0	**4**
Least breadth btw base horn cores	0	0	0	0	0	0	0	0	0	0	0	0	0	**0**
Short skull length	0	b	0	b	0	0	0	0	0	0	0	0	0	**2**
SUM	**7**	**10**	**2**	**4**	**0**	**1**	**3**	**3**	**1**	**2**	**0**	**5**	**4**	

Table 44: Summary showing the features that fall outside the range of both *C. gnou* and *C. taurinus*, either above or below, and those that fall into the blue wildebeest range. '1' represents the features that lie out side both *C. gnou* and *C. taurinus*. 'b' Indicates the features that fall within the blue range. '0' indicates the features that fall within black wildebeest range.

OUT OF RANGE OF BOTH and WITHIN BLUE RANGE

Specimen number	12042	12043	12044	12046	12047	12048	12049	12050	12051	12052	12053	12054	12060	Sum '1's'	# b's	total
Skull Measurements																
Akron-Nasion	0	0	1	0	0	0	0	0	0	0	0	0	0	**1**	**0**	**1**
Akron-Rhinion	b	b	1	0	0	0	0	0	0	0	0	b	b	**1**	**4**	**5**
Aboral-infraorbitale	b	b	0	0	1	0	0	0	0	0	0	b	0	**1**	**3**	**4**
Basal length of the skull	0	b	1	0	1	0	0	0	0	0	1	0	0	**3**	**1**	**4**
Breadth occipital condyle	b	b	0	b	0	0	b	0	b	b	0	b	0	**0**	**7**	**7**
Condylobasal length	1	b	0	0	1	0	0	0	0	0	1	0	0	**3**	**1**	**4**
Distance btw tuberosities	0	0	0	0	1	0	0	0	1	0	0	0	0	**2**	**0**	**2**
Dental length	0	0	0	0	1	0	0	0	0	0	1	0	b	**2**	**1**	**3**
Dwp	1	0	0	0	1	1	0	0	0	0	0	0	0	**3**	**0**	**3**
Diameter earhole	1	0	1	0	0	0	0	1	1	0	0	1	1	**6**	**0**	**6**
Ectorbit-entorbit	b	0	0	0	0	0	0	0	0	0	0	0	0	**0**	**1**	**1**
Ectorbit-prosthion	1	0	0	1	0	0	0	0	0	1	0	0	0	**3**	**0**	**3**
Facial breadth	0	0	0	1	0	0	0	0	0	0	0	0	0	**1**	**0**	**1**
Greatest breadth nasal	0	0	b	b	0	b	b	b	0	0	0	1	0	**1**	**5**	**6**
Height foramen magnum	b	0	b	0	0	0	0	b	0	0	0	0	b	**0**	**4**	**4**
Infraorbitale-Prosthion	0	b	0	0	0	0	0	0	0	0	0	0	0	**0**	**1**	**1**
Least breadth btw condyles	0	0	0	0	1	0	0	0	0	0	0	0	1	**2**	**0**	**2**
Least frontal breadth	b	0	1	0	0	1	1	0	0	0	0	b	0	**3**	**2**	**5**
Length of molar row	0	0	0	0	0	0	0	0	0	0	0	0	0	**0**	**0**	**0**
Length of premolar row	1	0	0	b	1	1	b	b	1	0	0	0	b	**4**	**4**	**8**
Length of cheektooth row	0	0	0	0	0	0	0	0	0	0	0	0	0	**0**	**0**	**0**
Nasion- Prosthion	0	b	1	0	0	0	0	0	0	0	0	1	0	**2**	**1**	**3**
Nasion-rhinion	0	0	1	0	0	0	0	0	0	0	1	0	0	**2**	**0**	**2**
Oral palatal length	0	1	0	0	0	0	0	0	0	0	0	1	0	**2**	**0**	**2**
Otion-Otion	0	b	0	0	0	0	0	0	0	0	0	0	0	**0**	**1**	**1**
Premolar- Prosthion	1	1	0	1	0	1	1	0	1	1	1	0	0	**8**	**0**	**8**
Skull profile length	b	b	1	0	0	0	0	0	0	b	0	0	0	**1**	**3**	**4**
Postdentale -Aboral	b	b	0	0	0	0	0	0	0	b	0	b	0	**0**	**4**	**4**
Least breadth btw base horn cores	0	0	0	0	1	0	0	0	0	0	0	0	1	**2**	**0**	**2**
Short skull length	0	b	0	b	0	0	0	0	0	0	0	0	0	**0**	**2**	**2**
# of characters outlying parent	**6**	**2**	**8**	**3**	**9**	**4**	**2**	**1**	**4**	**2**	**5**	**4**	**3**			
# lying within blue	**9**	**11**	**2**	**4**	**0**	**1**	**5**	**4**	**2**	**4**	**0**	**6**	**4**			

6.4 The Lower Jaw

The measurements for *C. gnou* and *C. taurinus* were taken from Brink (2005).

6.4.1 Length of the cheektooth row

(See Figure 6, measurement 1).

Table 45: Descriptive statistics for the length of the cheektooth row.

	Length cheek tooth row , Total	Length cheek tooth row , Hybrids	Length cheek tooth row , Gnou	Length cheek tooth row , Taurinus
Mean	97.986	92.085	93.911	112.000
Std. Dev.	9.644	6.635	4.207	3.616
Std. Error	1.471	1.840	.965	1.090
Count	43	13	19	11
Minimum	84.900	84.900	88.100	106.200
Maximum	119.000	103.300	103.700	119.000
# Missing	0	0	0	0
Variance	93.008	44.026	17.702	13.076
Coef. Var.	.098	.072	.045	.032
Range	34.100	18.400	15.600	12.800

For the length of the cheektooth row in Table 45, the hybrid mean falls below both black and blue wildebeest. The Spioenkop specimens also have the larger standard deviation and range than either blue or black wildebeest. The minimum value of the hybrid is smaller than that measured for black wildebeest. The hybrid maximum, however, falls within the black wildebeest range. There is no overlap in the range of black and blue wildebeest.

In Figure 128 and Figure 129, there is a similar pattern in the plots of the black and hybrid wildebeest. Both species plots are close together and have a similar spread. For both standard error and confidence interval, black wildebeest have the narrowest range. There is clear separation between blue and black wildebeest for the confidence interval.

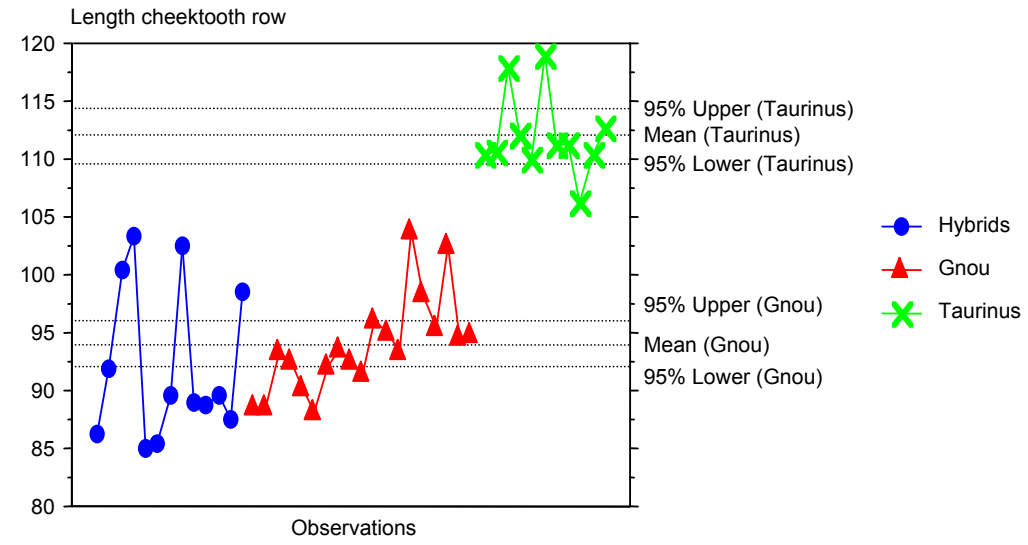

Figure 128: Univariate plot for the length of the cheektooth row.

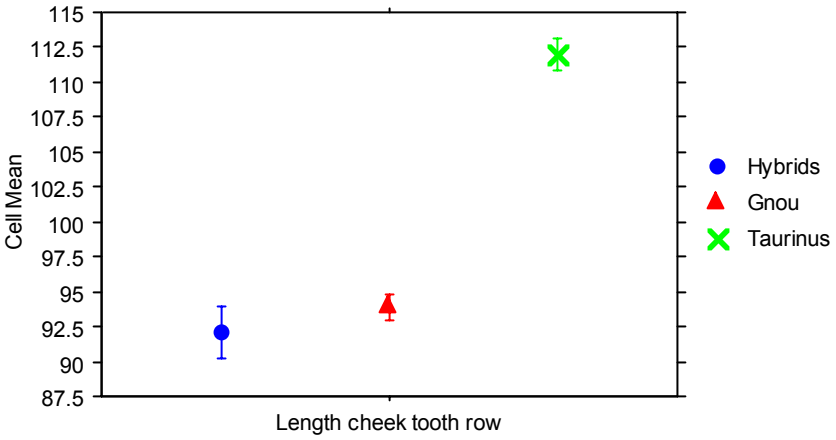

Figure 129: Standard error plot for the length of the cheek tooth row (error bars: ±1 STD error).

6.4.2 Length of the premolar row

Table 46: Descriptive statistics for the length of the premolar row.

	length premolar row , Total	length premolar row , Hybrids	length premolar row , Gnou	length premolar row , Taurinus
Mean	25.040	24.792	21.774	30.973
Std. Dev.	5.221	5.966	1.609	2.836
Std. Error	.796	1.655	.369	.855
Count	43	13	19	11
Minimum	18.500	18.500	19.100	26.100
Maximum	35.500	35.100	25.400	35.500
# Missing	0	0	0	0
Variance	27.257	35.591	2.588	8.044
Coef. Var.	.209	.241	.074	.092
Range	17.000	16.600	6.300	9.400

Table 46 shows the mean of the hybrid plotting between the means of the *C. gnou* and *C. taurinus*. The standard deviation of the Spioenkop specimens is the largest of the three groups, indicating more variability in the measurements. There is a separation in the ranges of black and blue wildebeest. The range of the Spioenkop specimens plots from below the minimum value of the black wildebeest to just below the range of blue wildebeest. In Figure 130, the same pattern repeats in that the confidence intervals of the Spioenkop specimens plots fall in-between the plots of black and blue wildebeest. For this feature, there is clear separation of the hybrid group into those that plot within the black wildebeest and those that plot in the blue wildebeest range.

There is a clear separation in the standard errors seen in Figure 131. The Spioenkop specimens have the largest standard error and plot between the standard errors of *C. gnou* and *C. taurinus*. There is no overlap between the standard errors.

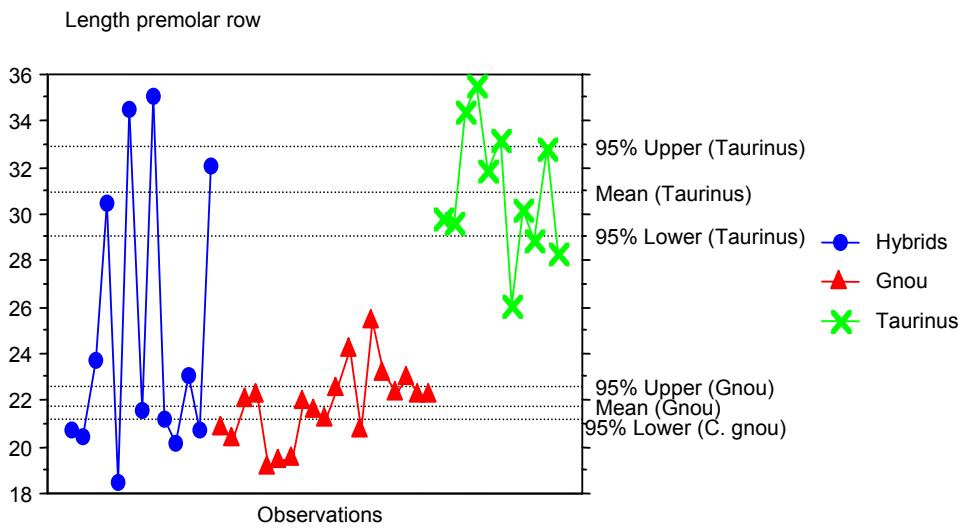

Figure 130: Univariate plot for the length of the premolar row.

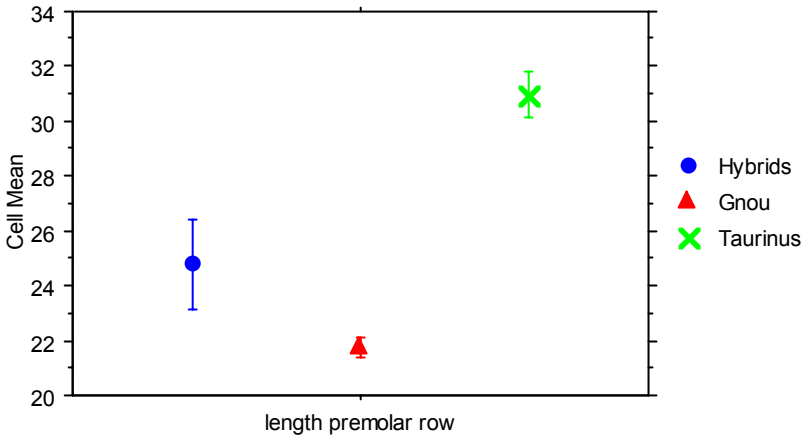

Figure 131: Standard error for length of the premolar row (error bars: ±1 STD error).

6.4.3 Length of the molar row

Table 47: Descriptive statistics for length of the molar row.

	length molar row , Total	length molar row , Hybrids	length molar row , Gnou	length molar row , Taurinus
Mean	72.912	68.023	71.668	80.836
Std. Dev.	5.698	3.046	2.620	3.127
Std. Error	.869	.845	.601	.943
Count	43	13	19	11
Minimum	64.800	64.800	67.300	76.800
Maximum	86.100	76.400	78.500	86.100
# Missing	0	0	0	0
Variance	32.465	9.275	6.866	9.779
Coef. Var.	.078	.045	.037	.039
Range	21.300	11.600	11.200	9.300

In the descriptive statistics (Table 47) for the length of the molar row, the Spioenkop specimens have the smallest mean of the three. The standard deviation and ranges of the three are similar, and there is overlap in the ranges. Figure 132 shows narrow confidence intervals for both *C. gnou* and *C. taurinus*. There is no overlap in these confidence intervals. Some hybrid plots fall below the confidence interval of the black wildebeest. This pattern repeats in the standard error plot (Figure 133), in which the Spioenkop specimens fall below the range of both blue and black wildebeest.

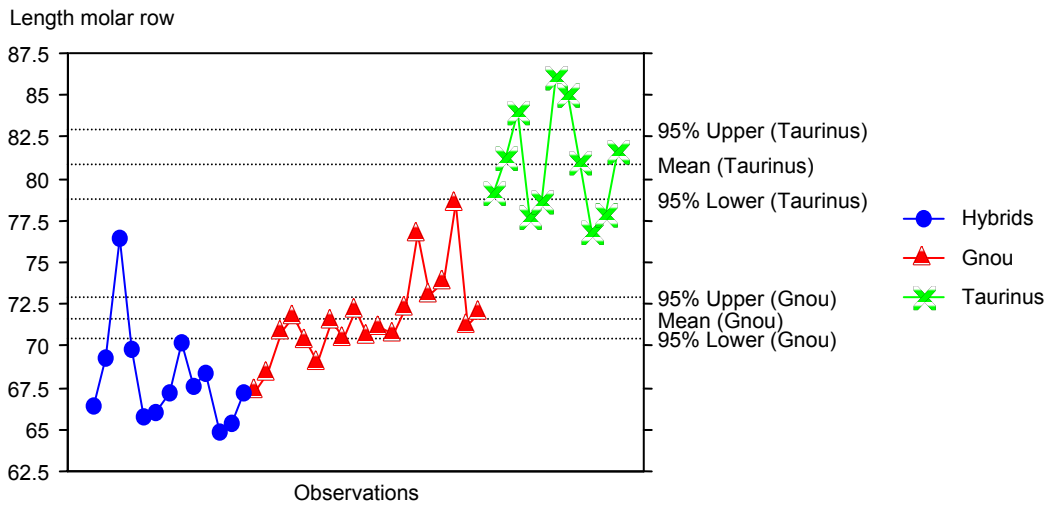

Figure 132: Univariate line plot for the length of the molar row.

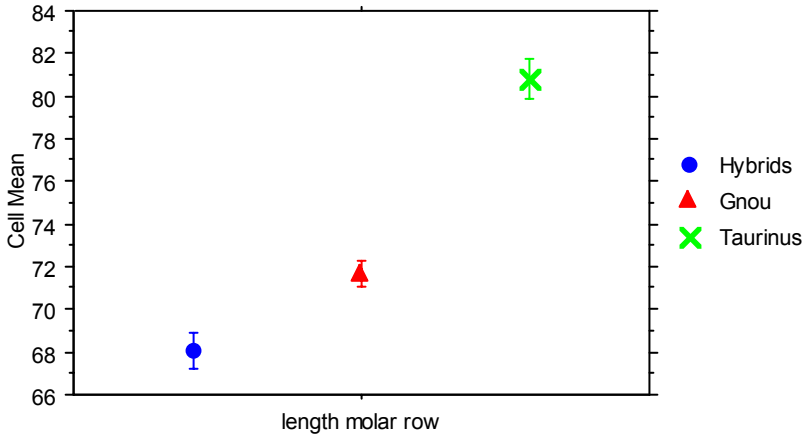

Figure 133: Standard error plot for the length of the molar row (error bars: ±1 STD error).

6.4.4 Length of the second molar (M_2)

The second molar was chosen due to the differences in the wear stages of the molars within the *Connochaetes* species. In the *Connochaetes* species, the third molar lengthens at the cost of the occlusal length of M_1 (Brink 2005). This effectively extends the functional life of the M_3 when the M_1 has become worn to the point of not being functional (Brink 2005). Due to the varying ages of the Spioenkop specimens as well as the various stages of wear on the molar, it was thought that the second molar would provide the most useful measurements out of all the molars.

Table 48: Descriptive statistics for the length M_2.

	M_2L, Total	M_2L, Hybrids	M_2L, Gnou	M_2L, Taurinus
Mean	23.177	22.092	22.305	25.964
Std. Dev.	2.225	2.096	1.199	1.188
Std. Error	.339	.581	.275	.358
Count	43	13	19	11
Minimum	20.000	20.000	20.300	23.500
Maximum	27.800	25.900	25.000	27.800
# Missing	0	0	0	0
Variance	4.949	4.394	1.437	1.411
Coef. Var.	.096	.095	.054	.046
Range	7.800	5.900	4.700	4.300

6.4.5 The descriptive statistics

The second molar was chosen due to the differences in the wear stages of the molars within the *Connochaetes* species. In the *Connochaetes* species, the third molar lengthens at the cost of the occlusal length of M_1 (Brink 2005). This effectively exyends the functional life of M_3 when the M1 has become worn to the point of not being functional (Brink 2005). Due to the varying ages of the Spioenkop specimens as

well as the various stages of wear on the molars, it is thought the the second molar would provide the most useful measurements out of the molars.

Table 48 shows no difference between the black and Spioenkop specimens, with the exception of a slightly higher standard deviation.

In Figure 134, the Spioenkop specimen plots spread over a wide range both above and below the narrow interval of the black wildebeest. There is no overlap with the blue wildebeest confidence interval. The hybrid plots show the same bimodal distribution that is seen in the measurements for the length of premolar row. Figure 135 shows the same pattern in the standard error plots, where the hybrid error range is large and extends over that of the black wildebeest.

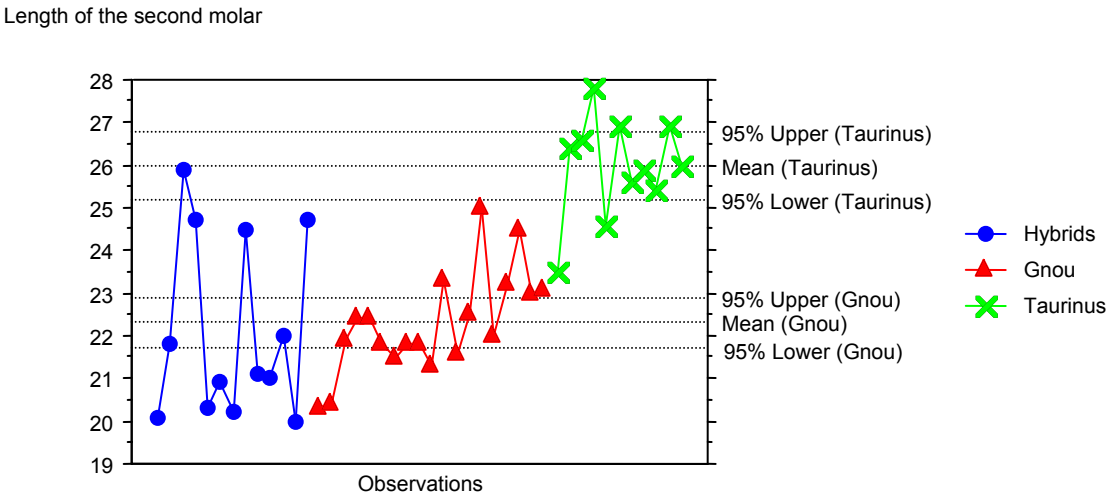

Figure 134: Univariate line plot for length of M_2.

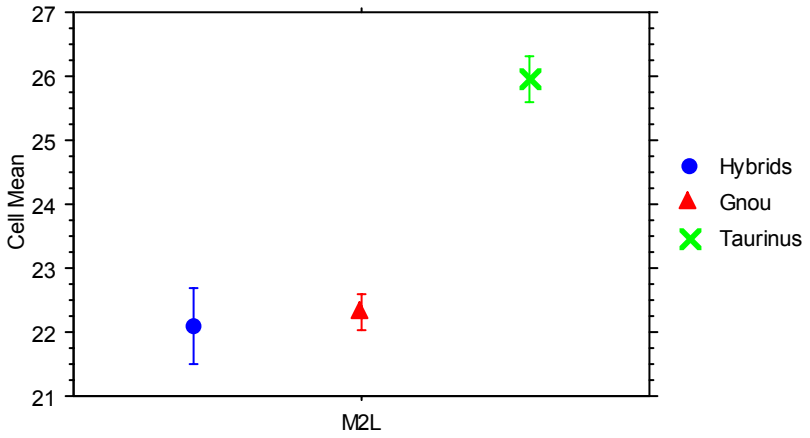

Figure 135: Standard error cell plot for length of M_2 (error bars: ±1 STD error).

6.4.6 Breadth of the second molar (M_2)

Table 49: Descriptive statistics for the breadth of M_2.

	M_2B, Total	M_2B, Hybrids	M_2B, C. gnou	M_2B, C. taurinus
Mean	11.600	11.162	11.242	12.736
Std. Dev.	.940	.695	.695	.589
Std. Error	.143	.193	.160	.177
Count	43	13	19	11
Minimum	10.000	10.100	10.000	11.800
Maximum	14.000	12.300	12.500	14.000
# Missing	0	0	0	0
Variance	.883	.483	.484	.347
Coef. Var.	.081	.062	.062	.046
Range	4.000	2.200	2.500	2.200

The descriptive statistics (Table 49) show virtually no difference between the black and Spioenkop specimens (the measurements are nearly identical with only fractional differences).

In Figure 136, black and hybrid wildebeest have a similar spread in measurements. There is no overlap between the blue and black wildebeest confidence intervals. Figure 137 shows a similar pattern in the standard error plots, where the hybrid error range overlaps the black range and extends slightly below the black standard error.

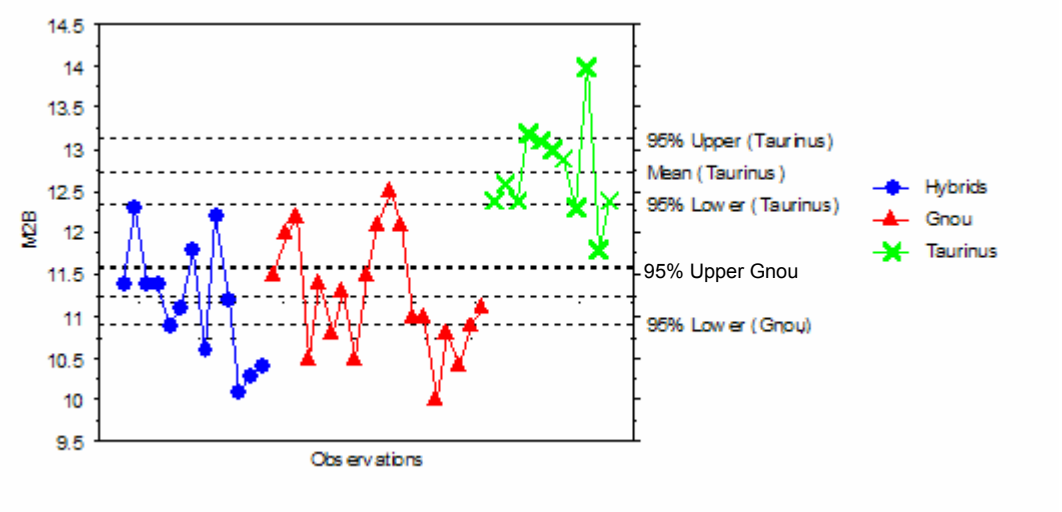

Figure 136: Univariate plot for the breadth of M_2.

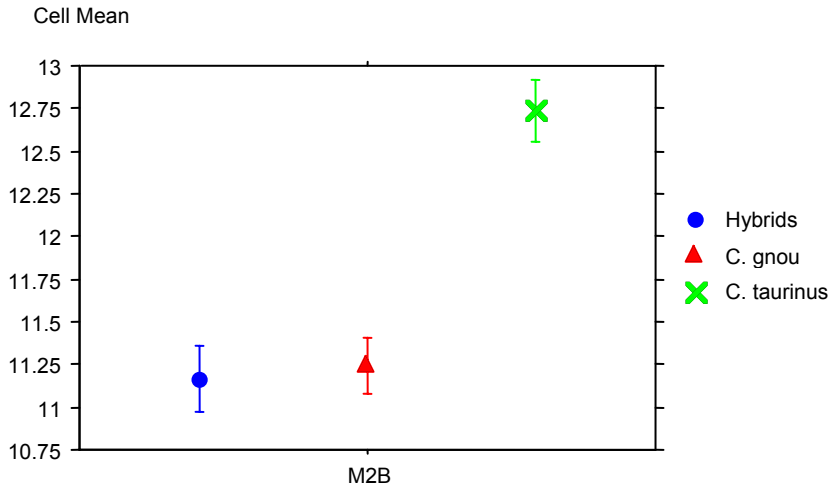

Figure 137: Standard error plot for the breadth of M2 (error bars: ±1 STD error).

6.5 Summary of the univariate analysis of the lower jaw

For the lower jaw, there are features that lie outside the ranges of both *C. gnou* and *C. taurinus*. The largest number of outliers is seen in the length of the cheektooth row and molar row. The pattern of outlying features falling below that of blue and black wildebeest (as seen in the cranium) is repeated in the lower jaw.

Table 50: Summary tables showing outlying features for the lower jaw.

A) Black wildebeest that plot like blue wildebeest

Measurement	NMB6011	A1215	A1596	NMB9411	NMB9413	NMB9408	UNK1	UNK2	UNK3	A1600	A2945	A1601	NMB9391	NMB9358	NMB8742	UNK4	NMB9870	NMB7447	NMB6029
Length of the cheektooth row	0	0	0	0	0	0	0	0	0	0	0	0	0	0	0	0	0	0	0
Length of the premolar row	0	0	0	0	0	0	0	0	0	0	0	0	0	0	0	0	0	0	0
Length of the molar row	0	0	0	0	0	0	0	0	0	0	0	0	0	b	0	0	b	0	0
Length of M2	0	0	0	0	0	0	0	0	0	0	0	0	0	b	0	0	b	0	0
Breadth of M2	0	b	b	0	0	0	0	0	0	b	b	b	0	0	0	0	0	0	0
Sum	0	1	1	0	0	0	0	0	0	1	1	1	0	2	0	0	2	0	0

B) Spioenkop specimens that fall into blue range or that lie out side of the black wildebeest range

Measurement	12042	12043	12044	12045	12046	12047	12048	12049	12050	12051	12052	12053	12054	12060
Length of the cheektooth row	1	0	0	0	0	1	0	0	0	0	0	0	0	0
Length of the premolar row	0	0	0	0	b	0	b	0	b	0	0	0	0	b
Length of the molar row	1	0	0	0	0	1	1	0	0	0	0	1	1	0
Length of M2	0	0	b	0	0	0	0	0	0	0	0	0	0	0
Breadth of M2	0	0	0	0	0	0	0	0	0	0	0	0	0	0
Sum	**2**	**0**	**1**	**0**	**1**	**2**	**2**	**0**	**1**	**0**	**0**	**1**	**1**	**1**

Table 50 B shows that a large number of features in the hybrid specimens plot in the black wildebeest range. For the length of the premolar row (Table 50 B), four Spioenkop specimens fall in the blue wildebeest range.

6.6 Axis

6.6.1 Greatest length of the corpus

(See Figure 7, measurement LCDe).

Table 51: Descriptive statistics for the length of the corpus.

	length corpus, Total	length corpus, Hybrid	length corpus, C. gnou	length corpus, *C. taurinus*
Mean	86.756	84.438	83.747	101.900
Std. Dev.	8.141	5.233	4.752	4.861
Std. Error	1.439	1.850	1.090	2.174
Count	32	8	19	5
Minimum	74.800	74.800	75.700	96.200
Maximum	108.600	93.100	96.100	108.600
# Missing	6	6	0	0
Variance	66.268	27.380	22.580	23.630
Coef. Var.	.094	.062	.057	.048
Range	33.800	18.300	20.400	12.400

The means of black and hybrid wildebeest (Figure 138 and Table 51) are slightly different in that Spioenkop specimens are marginally larger. There are similar standard deviations for the three groups. Blue wildebeest have the smallest range and the hybrid maximum value falls within the blue wildebeest range. In Figure 138, the confidence interval for black wildebeest is narrow and there is no overlap between the blue wildebeest interval range and that if the black wildebeest. In Figure 139, there is overlap in the standard errors of the Spioenkop specimens and black wildebeest.

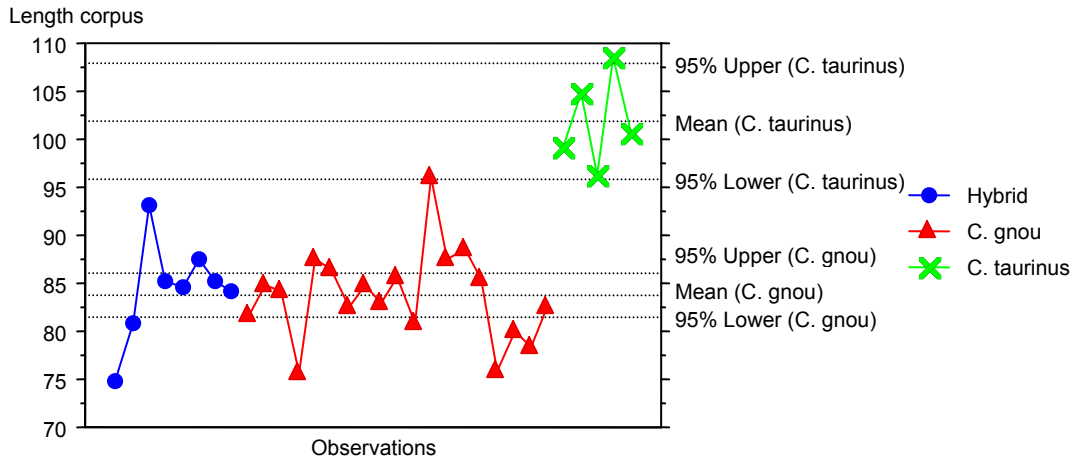

Figure 138: Univariate line plot for the length of the corpus.

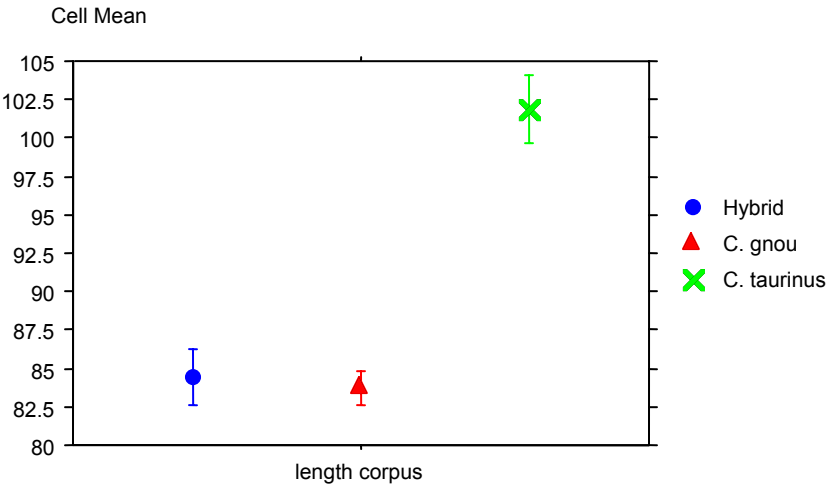

Figure 139: Standard error cell plot for the length of the corpus (error bars: ±1 STD error).

6.6.2 Greatest length of arch

Figure 140, Figure 141 and Table 52 all show that there are no marked differences between the black and hybrid wildebeest for the measurements taken on the arch of the axis. The hybrid measurements plot in a narrow range which cluster around the black wildebeest mean.

Table 52: Descriptive statistics for length of arch.

	length arch, Total	Hybrid	C. gnou	C. taurinus
Mean	76.150	73.150	73.089	92.580
Std. Dev.	10.051	5.936	6.555	11.313
Std. Error	1.777	2.099	1.504	5.059
Count	32	8	19	5
Minimum	61.500	61.500	61.700	84.500
Maximum	112.000	80.200	91.100	112.000
# Missing	6	6	0	0
Variance	101.025	35.231	42.974	127.982
Coef. Var.	.132	.081	.090	.122
Range	50.500	18.700	29.400	27.500

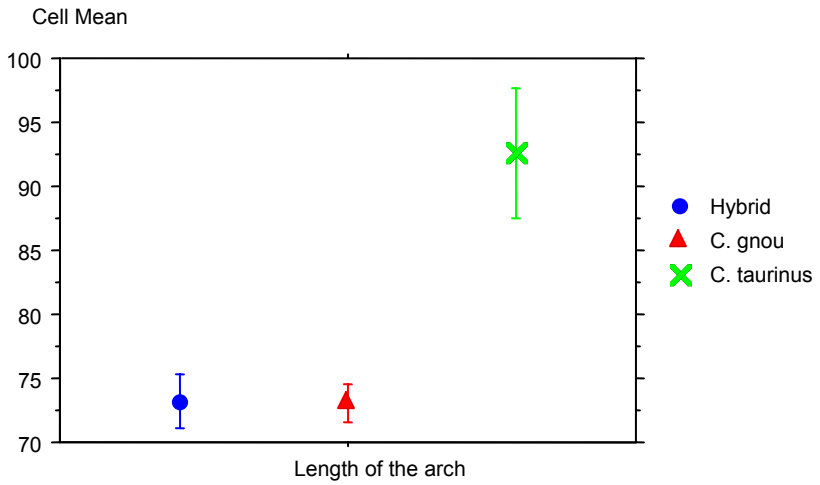

Figure 140: Standard errors for length of the arch (error bars: ±1 STD error).

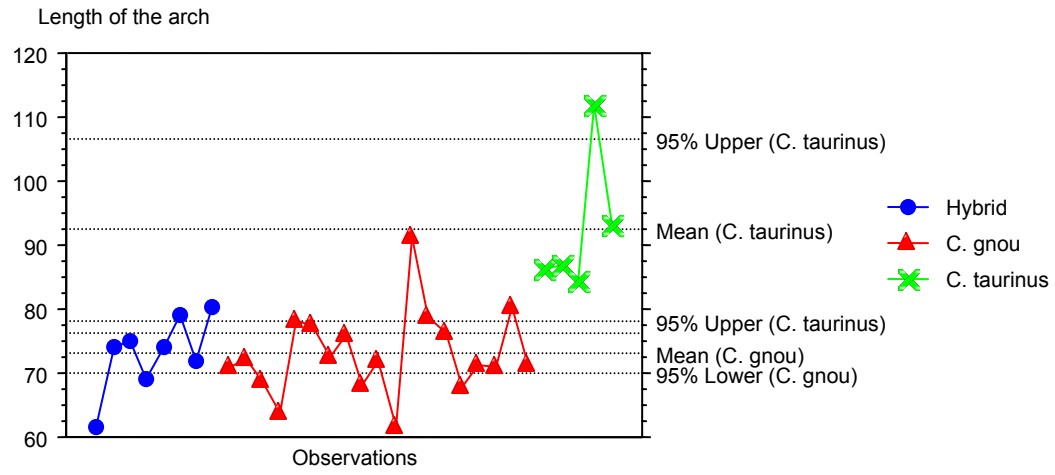

Figure 141: Univariate plot for the length of arch.

6.6.3 Greatest breadth of the cranial articular surface (BFcr)

(See Figure 7).

Table 53: Descriptive statistics for greatest breadth of the cranial articular surface.

	breadth articulares cranialis, Total	breadth articulares cranialis, Hybrid	breadth articulares cranialis, Gnou	breadth articulares cranialis, Tarinus
Mean	70.885	69.878	68.500	81.760
Std. Dev.	5.985	2.017	3.479	6.843
Std. Error	1.042	.672	.798	3.060
Count	33	9	19	5
Minimum	63.500	65.500	63.500	72.800
Maximum	92.000	72.600	74.200	92.000
# Missing	5	5	0	0
Variance	35.819	4.067	12.101	46.828
Coef. Var.	.084	.029	.051	.084
Range	28.500	7.100	10.700	19.200

Table 53 shows that the hybrid mean is slightly larger than the mean of the black wildebeest. However, the entire range of the hybrid falls within the range of the black. For the confidence interval in Figure 142, all the hybrid measurements cluster in a narrow range around the upper limit of the black wildebeest. No Spioenkop specimens plot within the blue wildebeest

confidence interval. Figure 143 shows that the hybrid standard error plots between the standard error of blue and black wildebeest, with a small overlap with the black standard error.

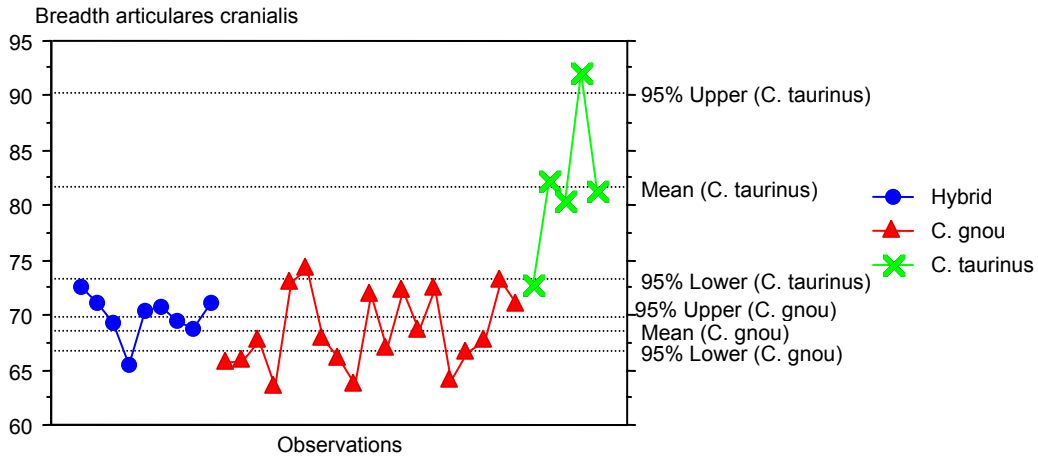

Figure 142: Univariate plots for the greatest breadth of the cranial articular surface.

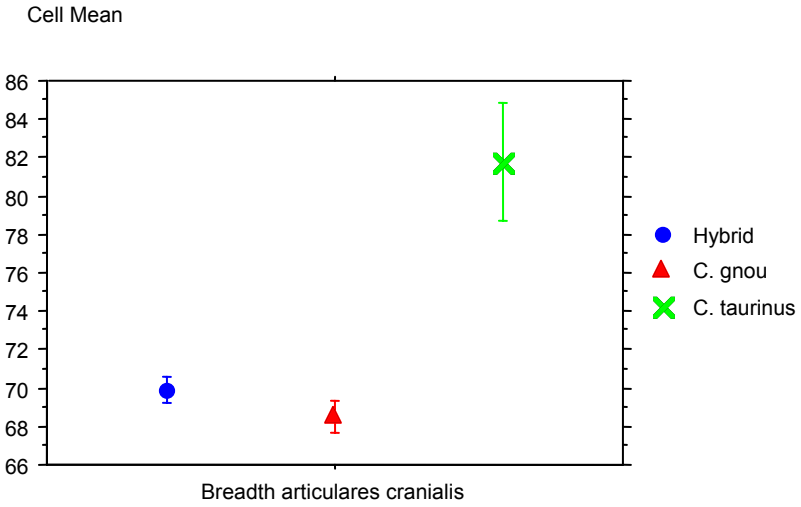

Figure 143: Standard error plot for greatest breadth of the cranial articular surface (error bars: ±1 STD error).

6.6.4 Smallest breadth of the vertebrae (SBV)

(See Figure 7).

Table 54: Descriptive statistics for smallest breadth of the vertebrae.

	smallest breadth verte, Total	smallest breadth verte, Hybrid	smallest breadth verte, Gnou	smallest breadth verte, Tarinus
Mean	42.956	42.675	42.600	44.760
Std. Dev.	2.372	1.580	2.540	2.316
Std. Error	.419	.559	.583	1.036
Count	32	8	19	5
Minimum	38.500	40.100	38.500	42.800
Maximum	50.000	44.600	50.000	48.400
# Missing	6	6	0	0
Variance	5.625	2.496	6.452	5.363
Coef. Var.	.055	.037	.060	.052
Range	11.500	4.500	11.500	5.600

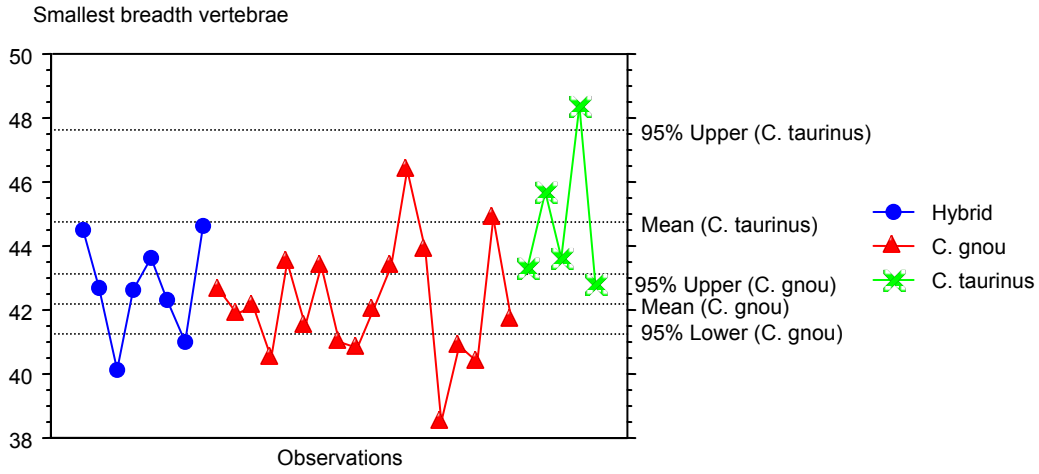

Figure 144: Univariate line plots for smallest breadth of the vertebrae.

Table 54, Figure 144 and Figure 145 all show that there are no marked differences between the black and hybrid wildebeest for measurements of the smallest breadth of the vertebrae. The hybrid measurements plot in a narrow range, which clusters around the black wildebeest mean. The black wildebeest measurements are widely spread compared to that of blue and Spioenkop samples. There is overlap in the confidence intervals of blue and black wildebeest.

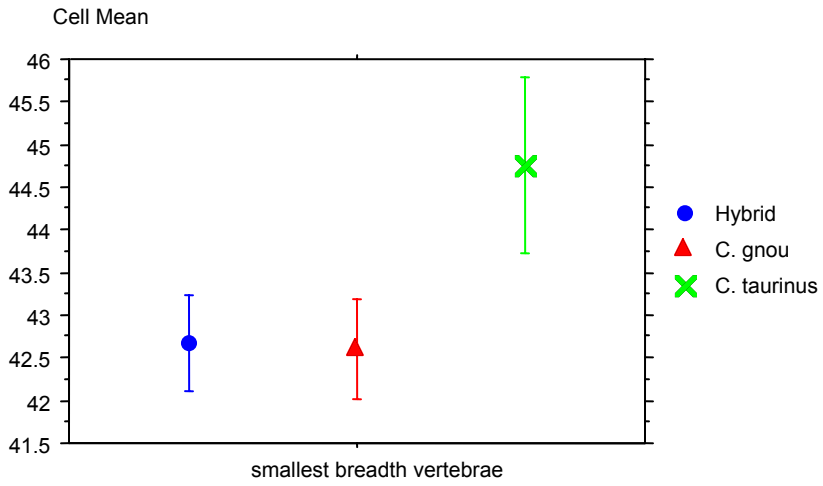

Figure 145: Standard error cell plot for smallest breadth of the vertebrae (error bars: ±1 STD error).

6.6.5 Greatest breadth of the facies terminalis caudalis (BFcd)

(See Figure 7).

Table 55: Descriptive statistics for breadth of the facies terminalis caudalis.

	BFcd, Total	BFcd, Hybrid	BFcd, C. gnou	BFcd, C. taurinus
Mean	38.036	37.411	36.868	43.600
Std...	3.357	2.168	2.593	2.112
Std. E	.584	.723	.595	.944
Count	33	9	19	5
Minim	31.500	34.700	31.500	41.400
Maxi.	46.400	40.300	42.100	46.400
# Miss	5	5	0	0
Varia.	11.272	4.701	6.726	4.460
Coef..	.088	.058	.070	.048
Range	14.900	5.600	10.600	5.000

In Table 55, the small range for the hybrid wildebeest resembles that of the blue. The narrow range for the Spioenkop specimens falls within the black wildebeest range. Standard deviation is the same in all three groups. Figure

146 shows a similar spread for both black and Spioenkop specimens. In Figure 147, there is overlap in the standard error of black and hybrid wildebeest.

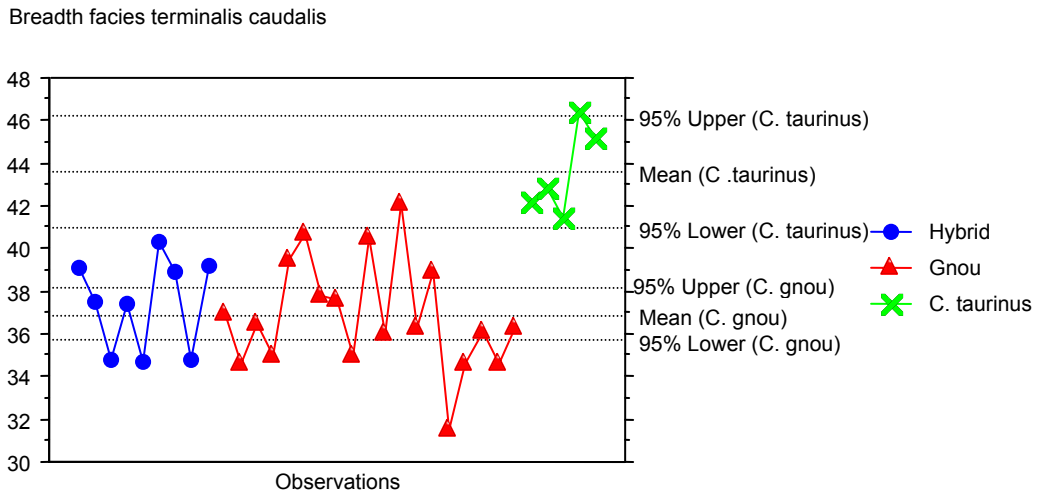

Figure 146: Univariate plot for breadth of the facies terminalis caudalis.

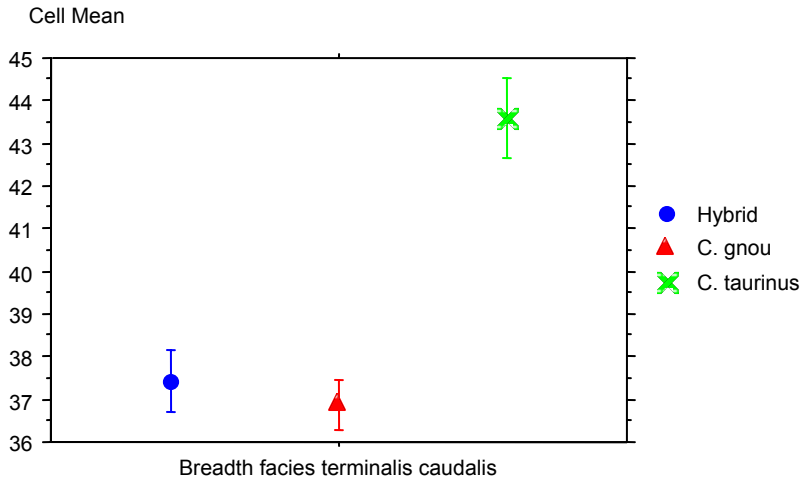

Figure 147: Standard error plot for breadth of the facies terminalis caudalis (error bars: ±1 STD error).

6.6.6 Height

(See Figure 8).

The descriptive statistics in Table 56 show that for this measurement the Spioenkop specimens have the smallest mean. The range and standard deviation also fall below those measured for black and blue. In Figure 148 the mean for the Spioenkop specimens plots close to the lower limit of the black range. The hybrid measurements do not spread as much as that of the black. In Figure 149, the standard error mean of the Spioenkop specimens falls below the black, and there is some overlap between the upper limit of the hybrid and lower limit of the black.

Table 56: Descriptive statistics for height of the axis.

	Height, Total	Hybrid	C. gnou	C. taurinus
Mean	97.277	92.875	96.279	115.333
Std. Dev.	10.479	6.385	8.840	13.051
Std. Error	1.913	2.257	2.028	7.535
Count	30	8	19	3
Minimum	84.000	84.000	85.000	103.000
Maximum	129.000	101.000	114.500	129.000
# Missing	8	6	0	2
Variance	109.812	40.768	78.137	170.333
Coef. Var.	.108	.069	.092	.113
Range	45.000	17.000	29.500	26.000

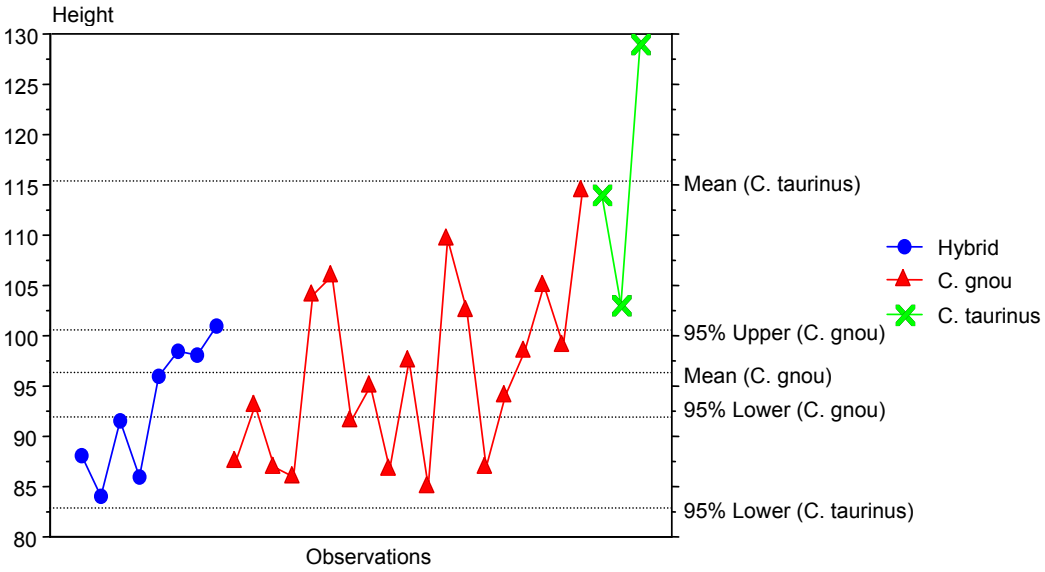

Figure 148: Univariate plot for the height of the axis.

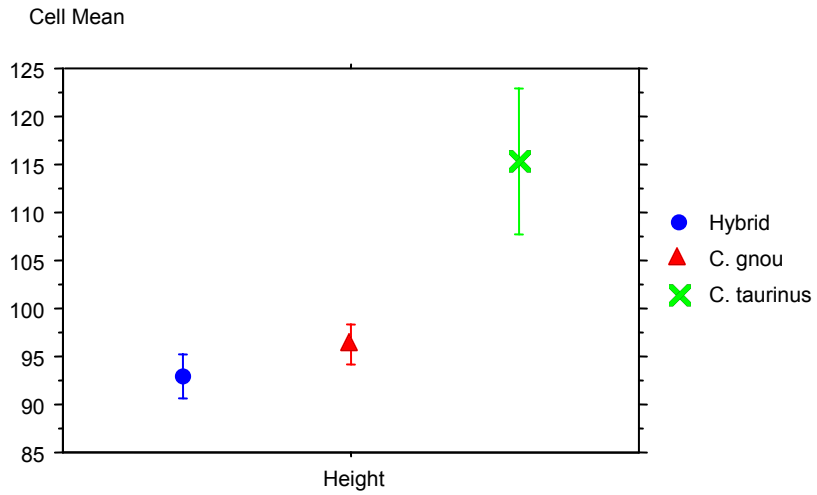

Figure 149: Standard error plot for height of the axis (error bars: ±1 STD error).

6.7 Summary of the univariate analysis of the axis

Table 57: Summary for outliers based on measurement taken on axis. '0' indicates that for this feature the Spioenkop specimens fall within the black wildebeest range and '1' indicates the specimens-that fall outside of the black wildebeest range.

Measurement	LCDe	LAPa	BFcr	SBV	BFcd	H		
Specimen Number							Sum	%'s
12042	0	0	0	0	0	0	0	0
12043	0	0	0	0	0	0	0	0
12044	1	0	0	0	0	0	1	12.5
12045	0	0	0	0	0	0	0	0
12046	0	0	0	0	0	1	1	12.5
12047	0	0	0	0	0	0	0	0
12048	0	0	0	0	0	0	0	0
12049	0	0	0	0	0	0	0	0
12050	0	0	0	0	0	0	0	0
12051	0	0	0	0	0	0	0	0
12052	0	0	0	0	0	0	0	0
12053	0	0	0	0	0	0	0	0
12054	0	0	0	0	0	0	0	0
12060	0	0	0	0	0	0	0	0
SUM	1	0	0	0	0	1		
%'s	7.1	0.0	0.0	0.0	0.0	7.1		

In Table 57, none of the specimens deviate from the measurements of black wildebeest.

6.8 Scapula

6.8.1 Greatest dorsal length (LD).

In Table 58, there is a large difference in the means, with the Spioenkop specimens having the smallest. The large standard deviations for both black and Spioenkop specimens have resulted in large ranges for both. The range of

the Spioenkop specimens extends from below the black minimum to above the black maximum. In Figure 150, the Spioenkop specimen plots fall below the black wildebeest confidence interval. In Figure 151, the standard error for the Spioenkop specimens is small and falls below the black standard error.

Table 58: Descriptive statistics for the dorsal length of the scapula.

	Dorsal length, Total	Hybrid	C. gnou	C. taurinus
Mean	141.158	135.207	140.686	170.033
Std. Dev.	14.560	9.701	6.772	13.759
Std. Error	2.972	2.593	2.560	7.944
Count	24	14	7	3
Minimum	122.500	122.500	133.600	161.400
Maximum	185.900	152.700	152.300	185.900
# Missing	1	0	1	0
Range	63.400	30.200	18.700	24.500

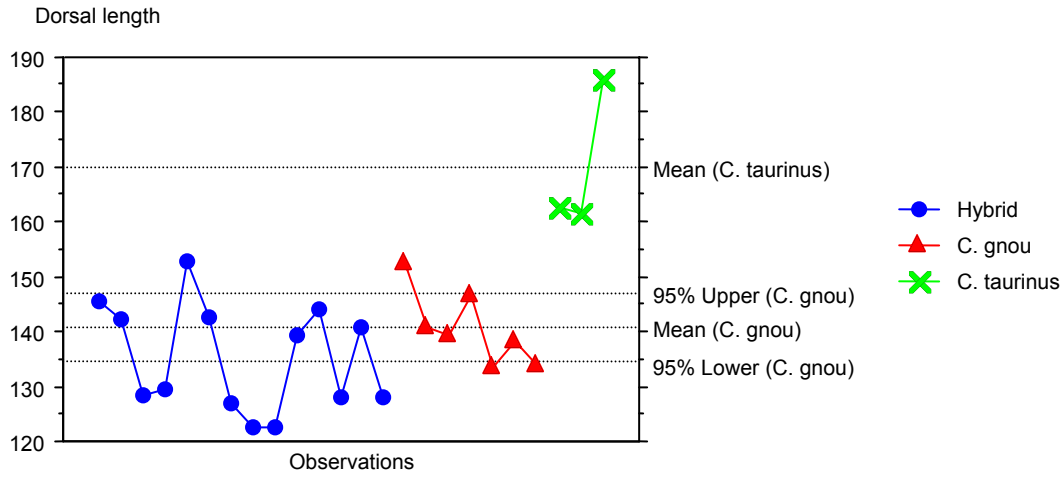

Figure 150: Univariate plot for the dorsal length of the scapula.

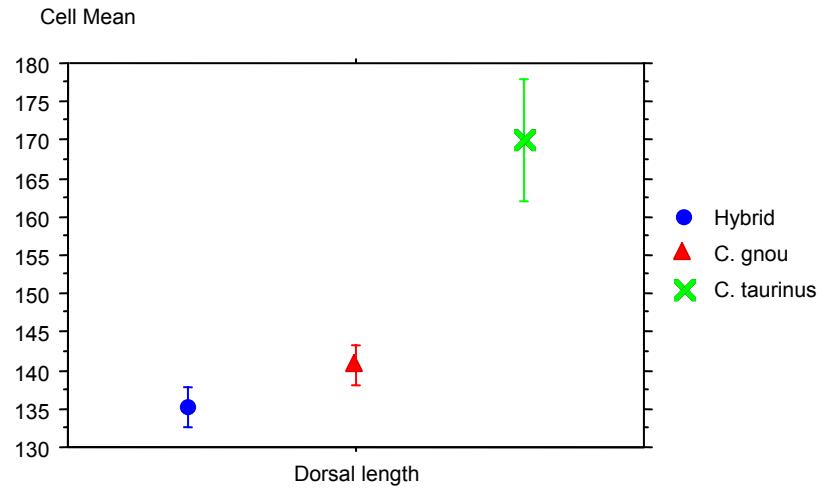

Figure 151: Standard error plot for the dorsal height of the scapula (error bars: ±1 STD error).

6.8.2 Height along spine (HS)

(See Figure 10, measurement HS).

The mean for Spioenkop specimens is much lower for this feature than the means of both blue and black wildebeest (see Table 59). All three groups have very large standard deviation is reflected in the large ranges. The range for the Spioenkop specimens extends above and below that of the black.

In Figure 152, the mean of the Spioenkop specimens coincides with the lower limit of black wildebeest. The standard error of the Spioenkop specimens in Figure 153 is small and plots below black wildebeest. There is no overlap in the standard errors of *C. gnou*, *C. taurinus* and the hybrid specimens.

Table 59: Descriptive statistics for height along the spine.

	Height along spine, Total	Height along spine, Hybrid	Height along spine, Gnou	Height along spine, Taurinus
Mean	295.696	283.943	295.200	351.700
Std. Dev.	25.218	12.565	11.870	13.857
Std. Error	5.148	3.358	4.486	8.000
Count	24	14	7	3
Minimum	271.600	271.600	276.900	337.600
Maximum	365.300	309.600	308.200	365.300
# Missing	1	0	1	0
Variance	635.941	157.867	140.897	192.010
Range	93.700	38.000	31.300	27.700

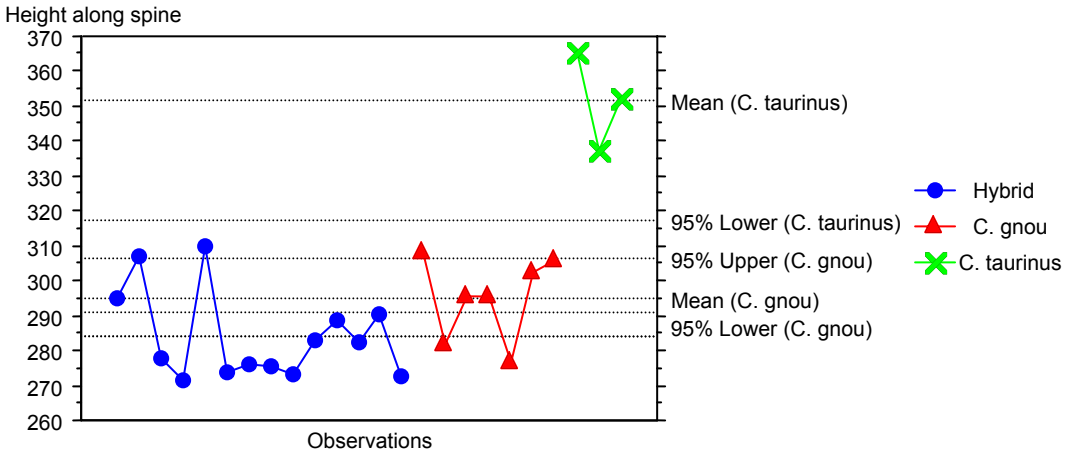

Figure 152: Univariate plot for height along spine.

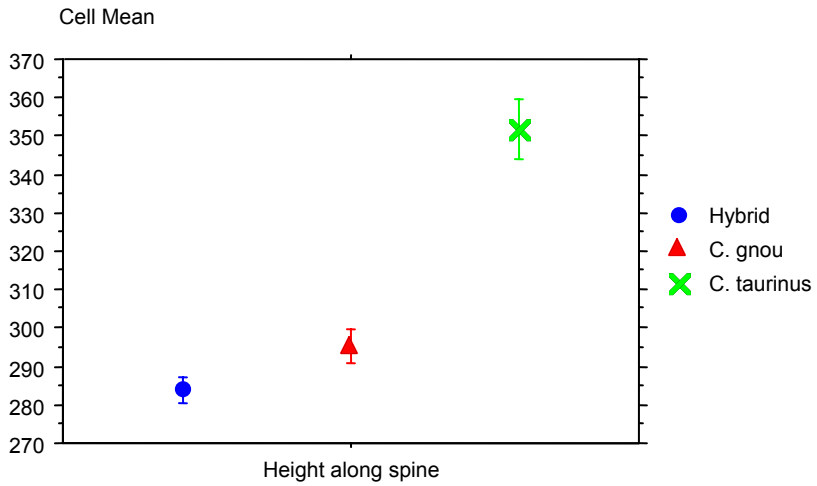

Figure 153: Standard error plot for height along spine (error bars: ±1 STD error).

6.8.3 Diagonal height (DHA)

(See Figure 10).

Table 60: Descriptive statistics for diagonal height.

	Diagonal height, Total	Hybrid	C. gnou	C. taurinus
Mean	297.483	285.014	296.883	356.867
Std. Dev.	26.617	12.097	11.428	11.673
Std. Error	5.550	3.233	4.666	6.740
Count	23	14	6	3
Minimum	273.000	273.000	279.800	343.400
Maximum	364.100	312.600	310.500	364.100
# Missing	2	0	2	0
Variance	708.451	146.338	130.602	136.263
Range	91.100	39.600	30.700	20.700

The mean for Spioenkop specimens is much lower for this feature than both the blue and black wildebeest means (see Table 60). All three groups have a very large standard deviation is reflected in the large ranges. The range for the Spioenkop specimens extends above and below that of the black.

In Figure 154, the mean of the Spioenkop specimens coincides with the lower limit of black wildebeest. The standard error of the Spioenkop specimens in Figure 155 is small, and plots below black wildebeest, with no overlap between the species.

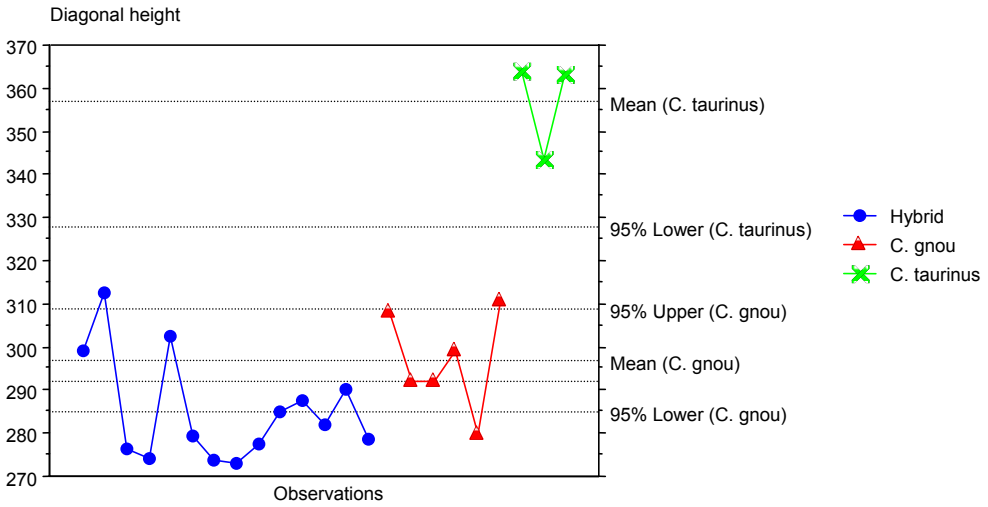

Figure 154: Univariate analysis for diagonal height.

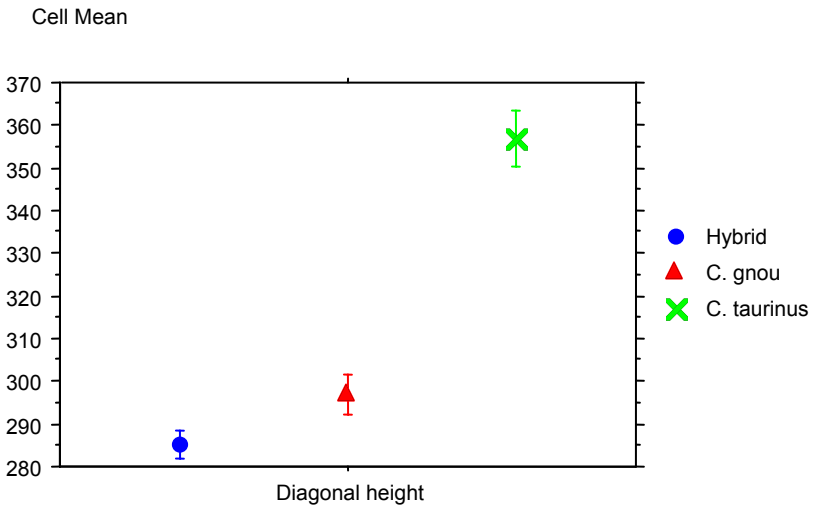

Figure 155: Standard error for diagonal height (error bars: ±1 STD error).

6.8.4 Smallest length of the collum scapulae (SLC)

(See Figure 10).

Table 61: Descriptive statistics for the smallest length of the collum scapulae.

	S.L collum scapulae, Total , Hybrid		C. gnou	C. taurinus
Mean	37.424	36.250	36.875	44.367
Std. Dev.	3.421	1.932	2.829	2.237
Std. Error	.684	.516	1.000	1.291
Count	25	14	8	3
Minimum	32.300	33.200	32.300	41.800
Maximum	45.900	40.600	41.400	45.900
# Missing	0	0	0	0
Variance	11.703	3.732	8.005	5.003
Range	13.600	7.400	9.100	4.100

Table 61, Figure 156 and Figure 157 all show that there is no marked differences between the black and hybrid wildebeest for measurements of the smallest length of the collum scapulae. The hybrid measurements plot in a small range, which cluster within the black wildebeest range. The standard error of the Spioenkop specimens falls within the range of black wildebeest.

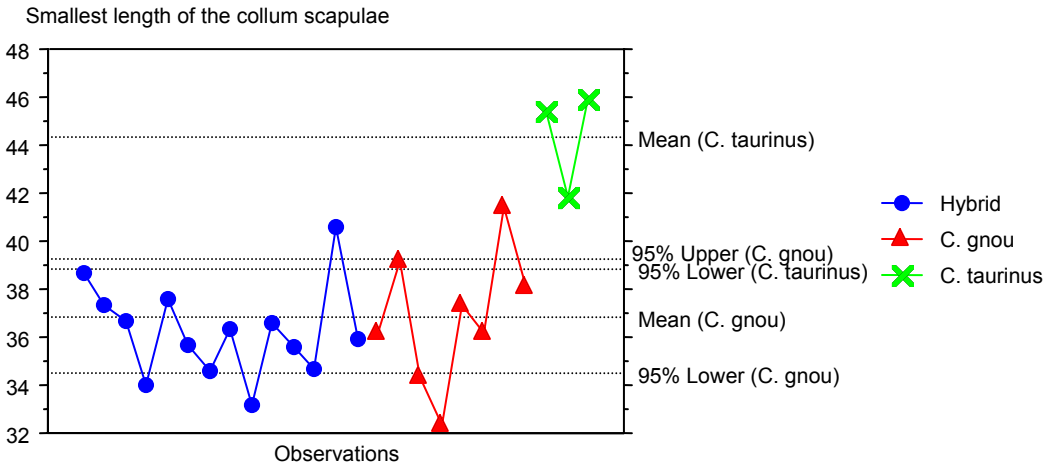

Figure 156: Univariate line plot for smallest length of the collum scapulae.

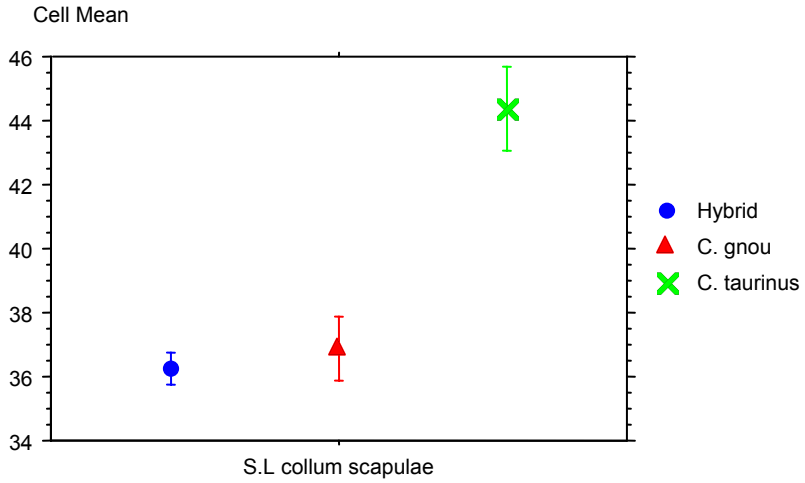

Figure 157: Standard error cell plot for smallest length of the collum scapulae (error bars: ±1 STD error).

6.8.5 Greatest length of the processus articularis (Gleniod process)

(See Figure 9 and Figure 10).

Table 62 and Figure 158 show that there are no marked differences between the black and hybrid wildebeest for measurements of the greatest length of the gleniod process. The hybrid intervals plot over a small range identical to the

black range. The measurements for the Spioenkop specimens spread more than the black. The standard error of the Spioenkop specimens (Figure 159) falls within the range of black wildebeest.

Table 62: Descriptive statistics for the greatest length of the glenoid process.

	G.L of glenoid process, Total	Hybrid	C. gnou	C. taurinus	.
Mean	61.812	60.186	60.313	73.400	
Std. Dev.	5.768	3.685	2.462	7.802	
Std. Error	1.154	.985	.870	4.504	
Count	25	14	8	3	
Minimum	52.900	52.900	56.300	65.700	
Maximum	81.300	65.500	63.800	81.300	
# Missing	0	0	0	0	
Variance	33.272	13.577	6.061	60.870	
Range	28.400	12.600	7.500	15.600	

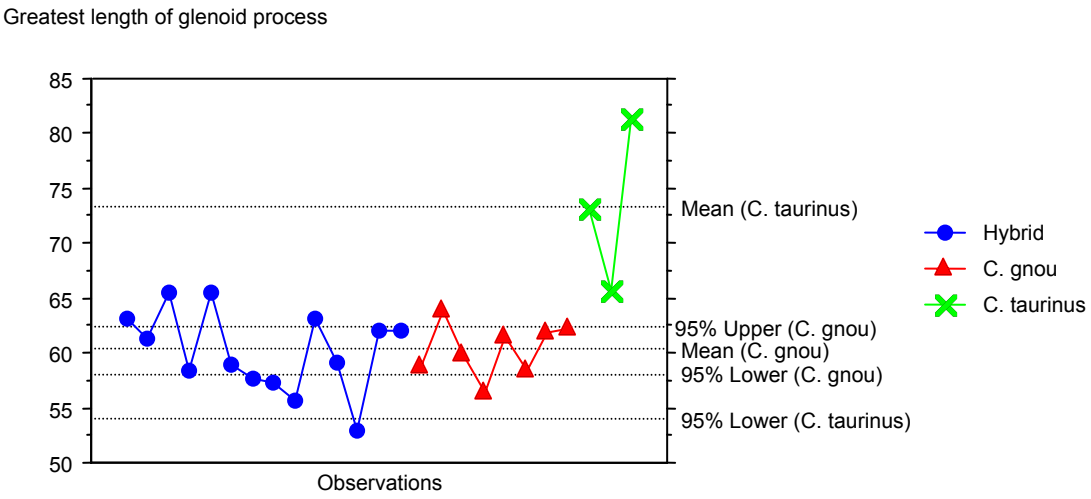

Figure 158: Univariate line plot for the greatest length of the glenoid process.

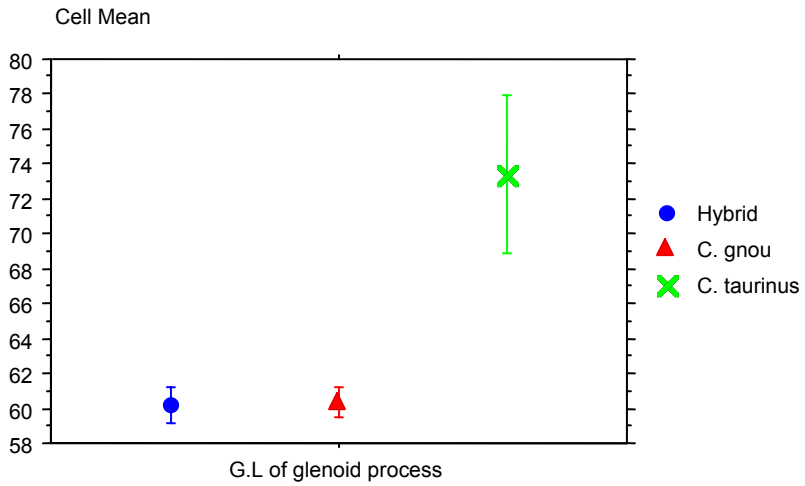

Figure 159: Standard error cell plot for greatest length of the glenoid process (error bars: ±1 STD error).

6.8.6 Length of the gleniod cavity (LG)

(See Figure 9).

Table 63: Descriptive statistics for length of the glenoid cavity.

	L glenoid cavity, Total	Hybrid	C. gnou	C. taurinus
Mean	45.264	44.271	44.113	52.967
Std. Dev.	4.049	3.059	2.647	3.190
Std. Error	.810	.818	.936	1.841
Count	25	14	8	3
Minimum	40.300	40.300	41.200	49.300
Maximum	55.100	50.500	49.000	55.100
# Missing	0	0	0	0
Variance	16.393	9.359	7.004	10.173
Range	14.800	10.200	7.800	5.800

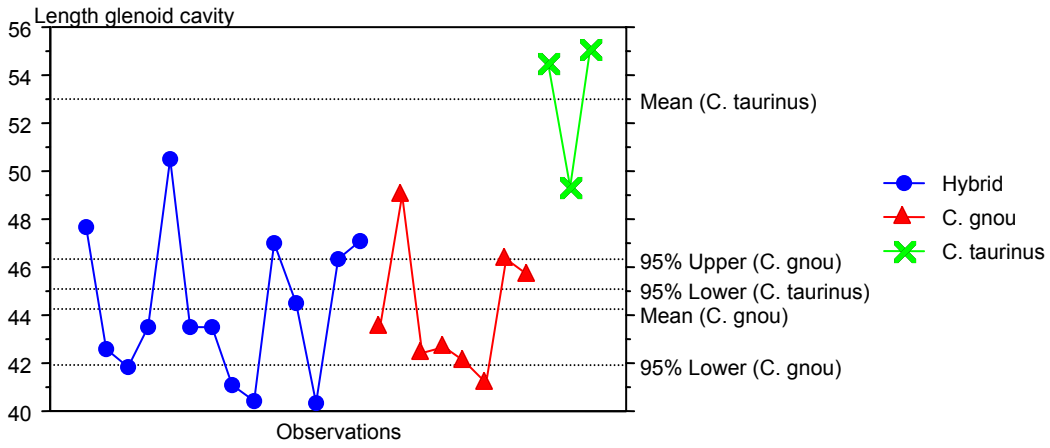

Figure 160: Univariate line plot for length of the glenoid cavity.

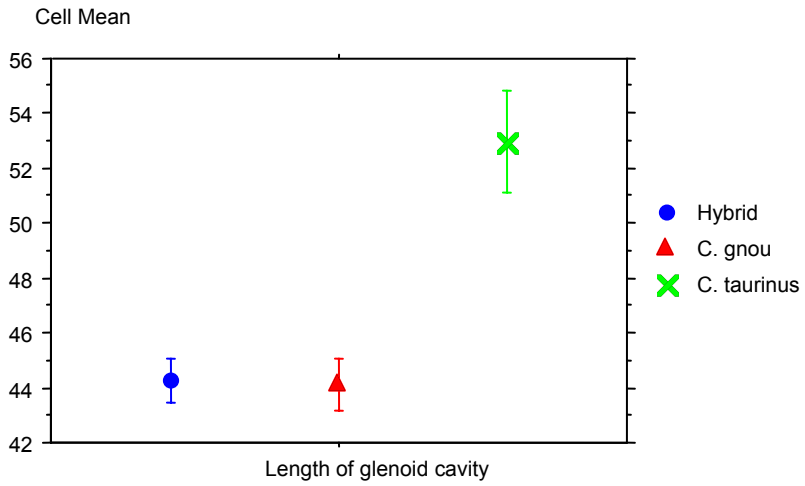

Figure 161: Standard error cell plot for length of glenoid cavity (error bars: ±1 STD error).

Table 63 and Figure 160 show that there are no marked differences between the black and hybrid wildebeest for measurements of the length of the gleniod cavity. The hybrid measurements plot in a small range, which falls within the black wildebeest range. The hybrid measurements spread more than the black, the standard error (Figure 161) of the Spioenkop specimens falls within the range of black wildebeest.

6.8.7 Breadth of the gleniod cavity (BG)

(See Figure 9).

Table 64: Descriptive statistics for breadth of glenoid cavity.

	Breadth glenoid cavity, Total	Hybrid	C. gnou	C. taurinus
Mean	39.336	38.250	38.900	45.567
Std. Dev.	3.731	2.536	3.213	4.680
Std. Error	.746	.678	1.136	2.702
Count	25	14	8	3
Minimum	34.500	34.900	34.500	40.200
Maximum	48.800	44.000	43.000	48.800
# Missing	0	0	0	0
Range	14.300	9.100	8.500	8.600

In Table 64, Figure 162 and Figure 163, there are no marked differences between the black and hybrid wildebeest for measurements of the breadth of the gleniod cavity. The hybrid measurements plot in a small range, within the black wildebeest range. Both species have a wide spread. The standard error of the Spioenkop specimens falls within the range of black wildebeest.

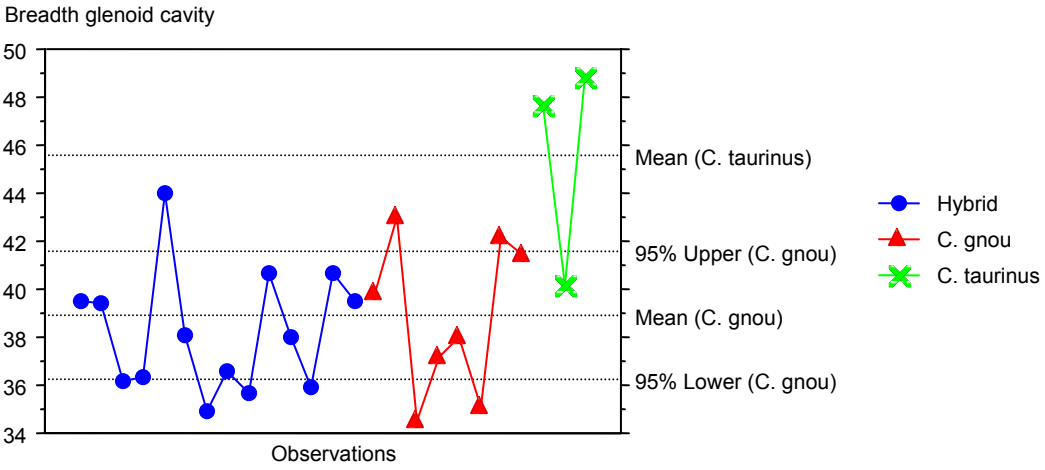

Figure 162: Univariate line plot for breadth of glenoid cavity.

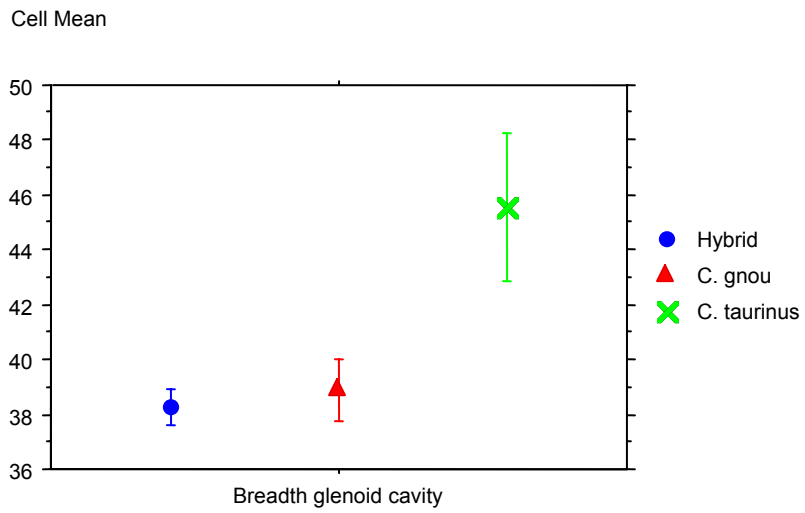

Figure 163: Standard error cell plot for the breadth of glenoid cavity (error bars: ±1 STD error).

6.9 Summary of the univariate analysis for the scapula

Table 65: Summary of outliers for the scapula measurements. '0' indicates that for this feature the Spioenkop specimens fall within the black wildebeest range and '1' indicates the specimens that fall outside of the black wildebeest range.

Measurement / Specimen Number	Ld	HS	DHA	SLC	GLP	LG	BG	SUM	%'s
12042	0	0	0	0	0	0	0	0.0	0.0
12043	1	0	1	0	0	0	0	2.0	28.6
12044	1	0	1	0	1	0	0	3.0	42.9
12045	1	1	1	0	0	0	0	3.0	42.9
12046	0	0	0	0	1	1	1	3.0	42.9
12047	0	1	0	0	0	0	0	1.0	14.3
12048	1	0	1	0	0	0	0	2.0	28.6
12049	1	0	1	0	0	0	0	2.0	28.6
12050	1	1	1	0	1	1	0	5.0	71.4
12051	0	0	0	0	0	0	0	0.0	0.0
12052	0	0	0	0	0	0	0	0.0	0.0
12053	0	0	0	0	1	1	0	2.0	28.6
12054	0	0	0	0	0	0	0	0.0	0.0
12060	0	1	0	0	0	0	0	1.0	14.3
SUM	6	4	6	0	4	3	1		
%'s	42.9	28.6	42.9	0.0	28.6	21.4	7.1		

Table 65 shows that not all individuals have features that lie outside of the black wildebeest range. Very few hybrid specimens have outlying features. The specimens with the most outlying features are:

- 12044
- 12045
- 12046
- 12050

These individuals have more than 30% of their features differing from the black wildebeest “norm”. There is little (only one hybrid falls out of range) or no difference in measurements between the Spioenkop specimens and black wildebeest for the smallest length of the collum scapulae and the breadth of the glenoid process. However, the sample sizes of blue and black wildebeest scapula are very small, making the data unreliable, as the ranges are not well-represented.

6.10 Humerus

6.10.1 Greatest length

Table 66: Descriptive statistics for greatest length of humerus.

	Greatest Length, Total	Greatest Length, Hybrid	Greatest Length, Gnou	Greatest Length, Taurinus
Mean	226.453	223.245	218.321	258.083
Std. Dev.	17.838	7.474	12.002	11.065
Std. Error	2.973	2.253	2.754	4.517
Count	36	11	19	6
Minimum	198.200	211.400	198.200	242.000
Maximum	273.000	234.200	248.500	273.000
# Missing	4	3	1	0
Variance	318.179	55.855	144.057	122.442
Range	74.800	22.800	50.300	31.000

In Table 66, the hybrid mean falls between the means of *C. gnou* and *C. taurinus*. The standard deviations of the blue and black wildebeest are larger than that of the Spioenkop specimens. The range of the Spioenkop specimens falls within the range of black wildebeest. In Figure 164, the Spioenkop specimens plot within the range of the black wildebeest.

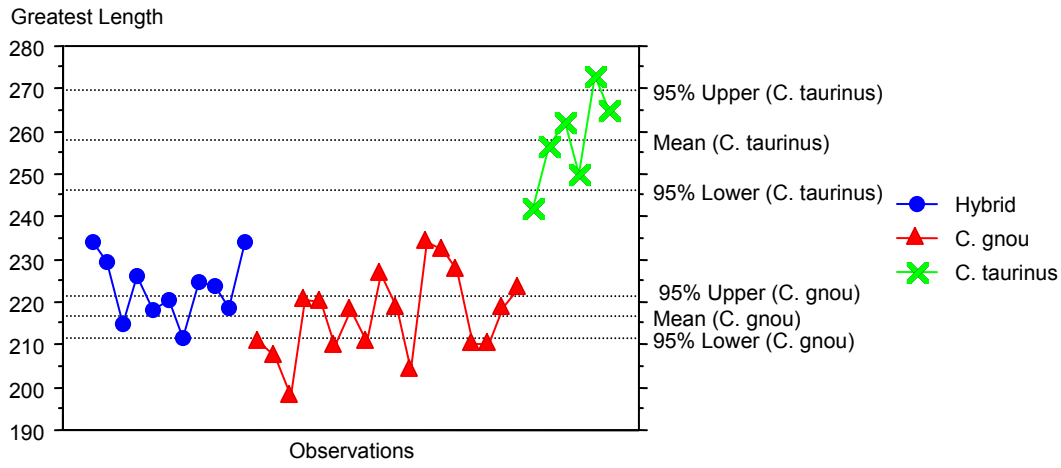

Figure 164: Univariate plot for greatest length of humerus.

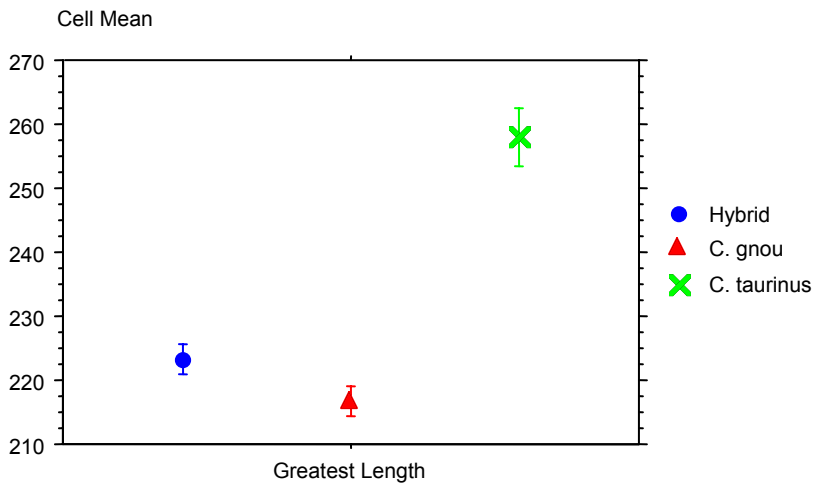

Figure 165: Standard error cell plot for greatest length of humerus (error bars: ±1 STD error).

Figure 165 shows that the Spioenkop specimen's standard error plots higher than that of the black wildebeest with a small overlap.

6.10.2 Smallest breadth of the diaphysis (SD) of the humerus

(See Figure 11).

Table 67: Descriptive statistics for smallest breadth of the diaphysis.

	breadth diaphysis, Total	Hybrid	C. gnou	C. taurinus
Mean	27.936	27.373	27.284	34.133
Std. Dev.	2.570	1.552	1.802	1.002
Std. Error	.447	.468	.413	.578
Count	33	11	19	3
Minimum	23.900	24.900	23.900	33.000
Maximum	34.900	29.500	30.400	34.900
# Missing	7	3	1	3
Variance	6.604	2.408	3.248	1.003
Coef. Var.	.092	.057	.066	.029
Range	11.000	4.600	6.500	1.900

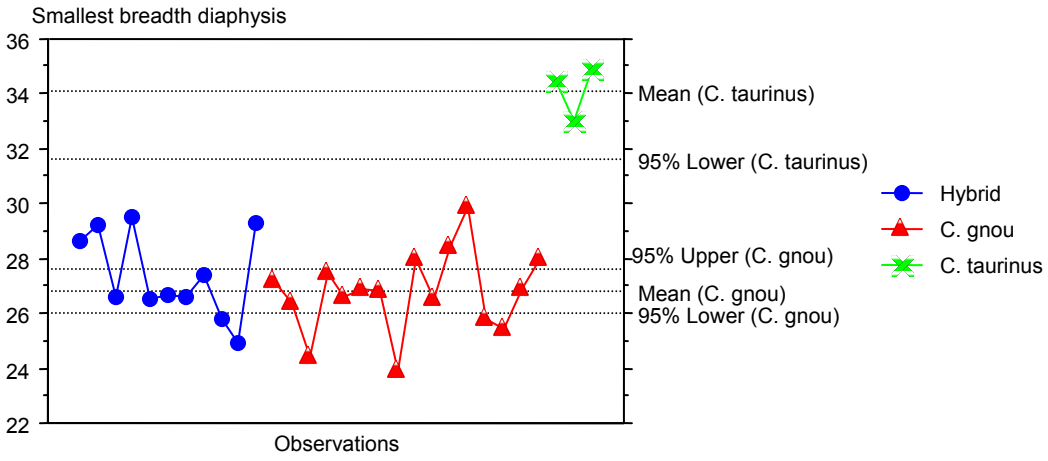

Figure 166: Univariate line plot of smallest breadth of diaphysis.

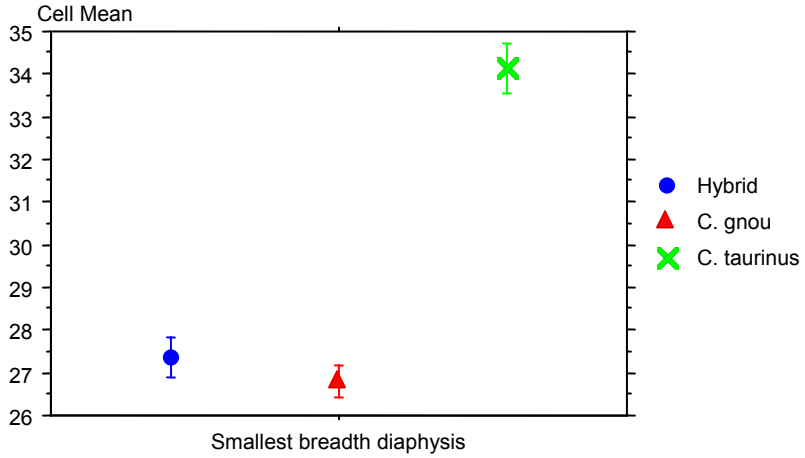

Figure 167: Standard error cell plot for smallest breadth of the diaphysis (error bars: ±1 STD error).

Table 67 and Figure 166 show that there are no marked differences between the black and hybrid wildebeest for the smallest breadth of the diaphysis. The hybrid intervals plot over a small range similar to the black range. The Spioenkop specimen measurements cluster together. The standard error of the Spioenkop specimens (Figure 167) falls within the range of black wildebeest.

6.10.3 Greatest breadth of the distal end (Bd) of the humerus

In Table 68, the mean of Spioenkop specimens is slightly larger than that of the black wildebeest. The Spioenkop specimens have a small standard deviation and range. The hybrid range falls within the black range. In there is no overlap between the blue and black wildebeest confidence intervals. In Figure 169, the standard error for the Spioenkop specimens falls out of the range of the black standard error. There is some overlap between the standard errors of black and hybrid wildebeest.

Table 68: Descriptive statistics for breadth of the distal end.

	Breadth distal end, Total	Hybrid	C. gnou	C. taurinus
Mean	57.138	56.518	55.312	63.450
Std. Dev.	4.604	2.488	4.000	4.040
Std. Error	.790	.750	.970	1.649
Count	34	11	17	6
Minimum	49.800	52.500	49.800	60.000
Maximum	70.600	60.400	62.800	70.600
# Missing	6	3	3	0
Variance	21.196	6.190	16.001	16.319
Range	20.800	7.900	13.000	10.600

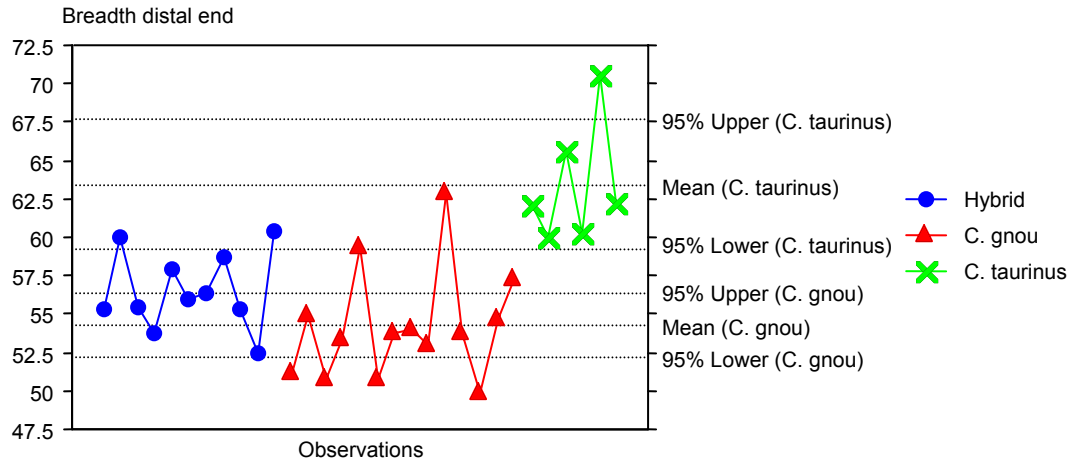

Figure 168: Univariate line plot for breadth of the distal end.

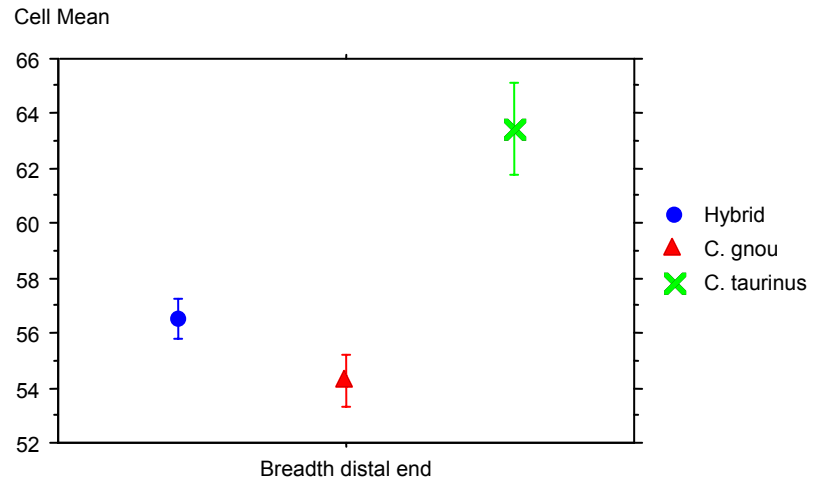

Figure 169: Standard error cell plot breadth of the distal end (error bars: ±1 STD error).

6.10.4 Greatest breadth of the trochlea (BT)

Table 69: Descriptive statistics for the breadth of the trochlea.

	Breadth of Trochlea, Total	Hybrid	C. gnou	C. taurinus
Mean	53.557	52.909	52.040	59.800
Std. Dev.	3.591	1.558	2.458	2.853
Std. Error	.590	.470	.550	1.165
Count	37	11	20	6
Minimum	47.900	51.000	47.900	55.700
Maximum	64.500	55.900	58.000	64.500
# Missing	3	3	0	0
Variance	12.897	2.427	6.044	8.140
Range	16.600	4.900	10.100	8.800

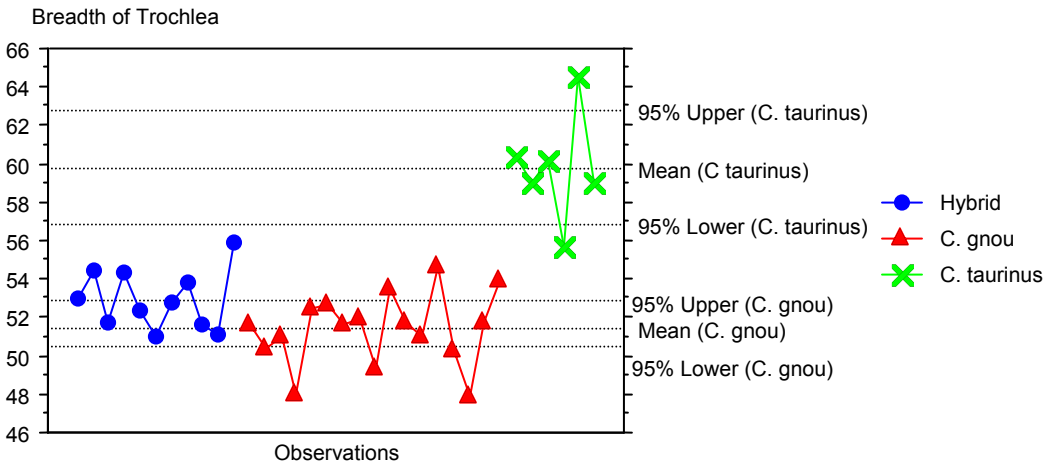

Figure 170: Univariate line plot for the greatest breadth of the trochlea.

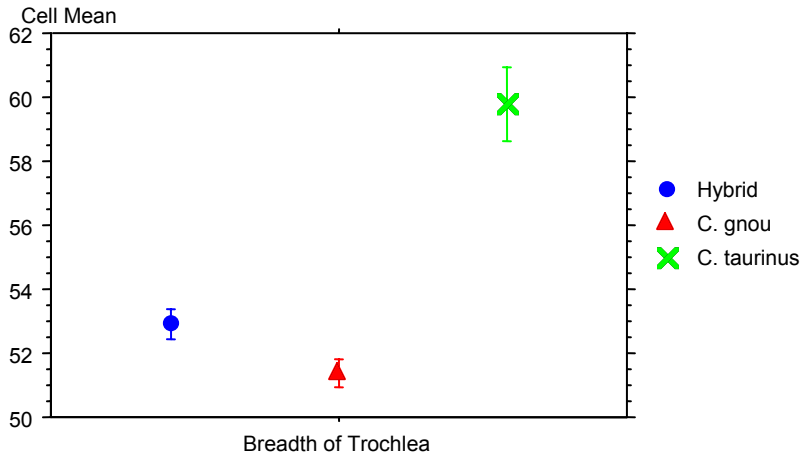

Figure 171: Standard error for the greatest breadth of the trochlea (error bars: ±1 STD error).

In Table 69, the mean of Spioenkop specimens is similar to that of the black wildebeest. The Spioenkop specimens have a small standard deviation and range that falls within the range of black wildebeest. In Figure 170, there is no overlap between the blue and black wildebeest confidence intervals and only one hybrid falls out of the black wildebeest range. In Figure 171, the standard error for the Spioenkop specimens falls out of range of the black standard error.

6.11 Summary for univariate plots for the humerus.

Table 70: Summary of outliers for the humerus measurements. '0' indicates that for this feature the Spioenkop specimens fall within the black wildebeest range and '1' indicates the specimens that fall outside of the black wildebeest range.

Measurement / Specimen Number	GL	SD	Bd	BT	SUM	%'s
12042	0	0	0	0	0	0

12043	0	0	0	0	0	0
12044	0	0	0	0	0	0
12045	0	0	0	0	0	0
12046	0	0	0	0	0	0
12047	0	0	0	0	0	0
12048	0	0	0	0	0	0
12049	0	0	0	0	0	0
12050	0	0	0	0	0	0
12051	0	0	0	0	0	0
12052	0	0	0	0	0	0
12053	0	0	0	0	0	0
12054	0	0	0	0	0	0
12060	0	0	0	1	0	0
SUM	0	0	0	1		
%'s	0	0	0	7		

From Table 70 it is seen that there are no Spioenkop specimens that plot out of the range of black wildebeest for measurements on the humerus.

6.12 Radius

For all measurements on the radius, see Figure 12.

6.12.1 Greatest length

Table 71: Descriptive statistics for the greatest length of radius.

	GL, Total	Hybrid	C. gnou	C. taurinus..
Mean	275.983	270.073	265.247	320.817
Std. Dev.	23.755	11.133	12.118	15.708
Std. Error	3.959	3.357	2.780	6.413
Count	36	11	19	6
Minimum	245.200	253.600	245.200	304.300
Maximum	343.000	284.900	287.200	343.000
# Missing	3	3	0	0
Range	97.800	31.300	42.000	38.700

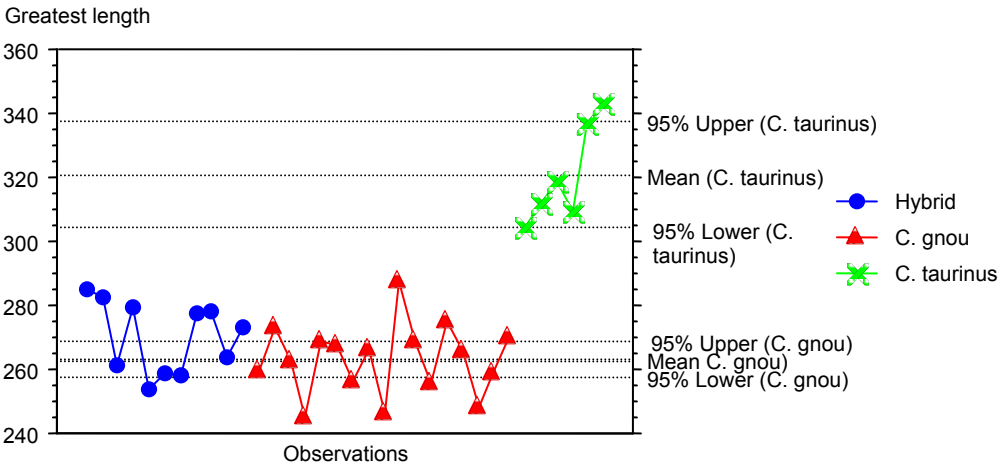

Figure 172: Univariate cell plot for greatest length of radius.

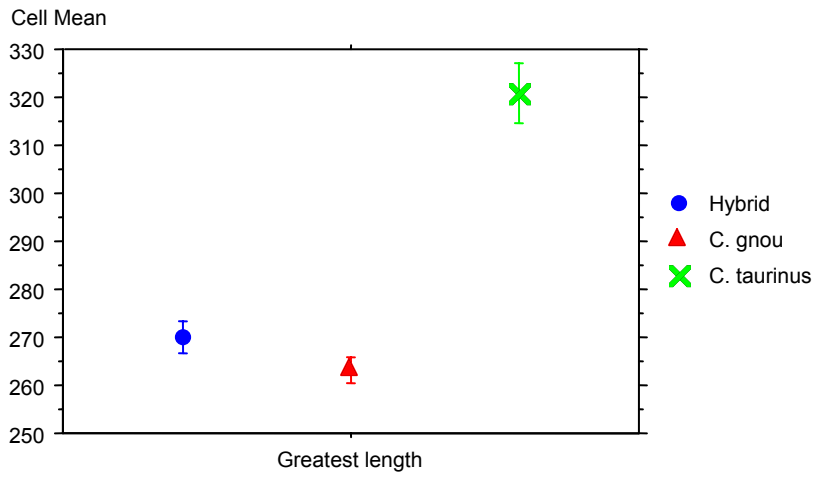

Figure 173: Standard error cell plot of greatest length of radius (error bars: ±1 STD error).

For greatest length of the radius, Table 71 shows the mean of the hybrid measurements fall between the means of blue and black wildebeest. All species have large standard deviations. Spioenkop specimens have the smallest range of the three.

In Figure 172, the mean of the hybrid coincides with the upper interval of the black wildebeest. Figure 173 shows the standard error of the Spioenkop specimens plotting above the standard error of black. There is a small overlap. There are no outlying Spioenkop specimens.

6.12.2 Breadth of the proximal end

For breadth of the proximal end of the radius, Table 72 shows the mean for Spioenkop specimens fall betweens that of the blue and black wildebeest. The

standard deviations are large for all species. Spioenkop specimens have the smallest range.

In Figure 174, the mean of the hybrids plots just above the upper interval of the black. Figure 175 shows the standard error of the Spioenkop specimens plotting above the standard error of black. There is no overlap in standard errors for any of the species.

Table 72: Descriptive statistics for breadth of the proximal end.

	Bp, Total	Hybrid	C. gnou	C. taurinus
Mean	61.086	60.436	58.437	70.667
Std. Dev.	5.335	2.292	3.209	3.734
Std. Error	0.889	0.691	0.736	1.524
Count	36	11	19	6
Minimum	54.200	56.200	54.200	67.400
Maximum	77.900	63.900	66.100	77.900
# Missing	3	3	0	0
Range	23.700	7.700	11.900	10.500

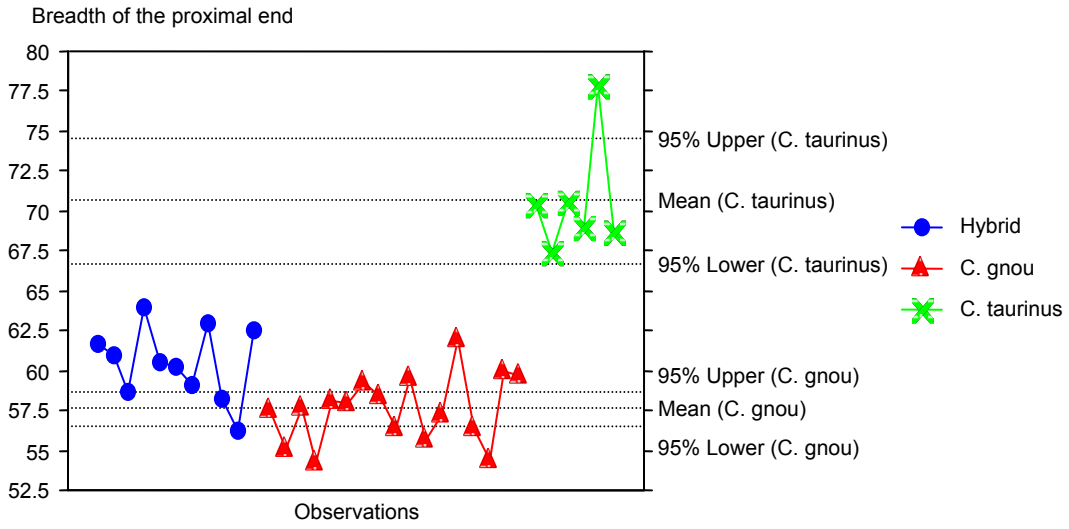

Figure 174: Univariate line plot for breadth of the proximal end.

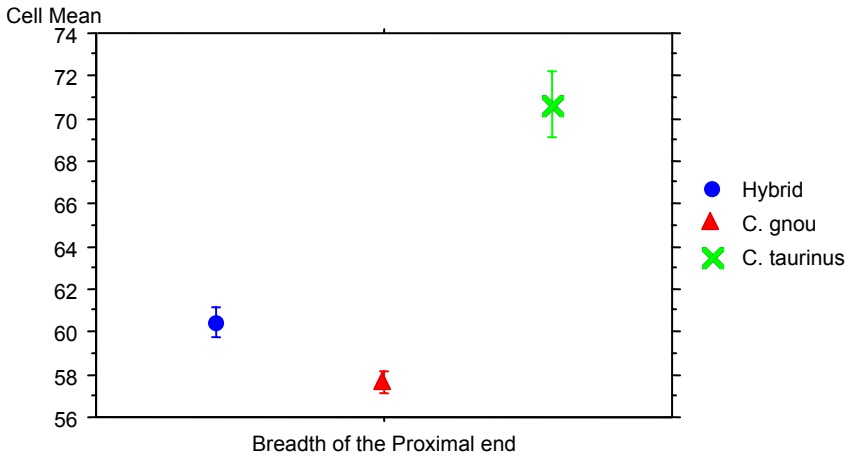

Figure 175: Standard error for breadth of the proximal end (error bars: ±1 STD error).

6.12.3 Greatest breadth of the distal end.

(See Figure 12).

Table 73: Descriptive statistics for breadth of the distal end.

	Bd, Total	Hybrid	C. gnou	C. taurinus..
Mean	50.043	45.218	49.333	61.017
Std. Dev.	6.245	3.365	2.982	3.842
Std. Error	1.056	1.015	.703	1.568
Count	35	11	18	6
Minimum	41.900	41.900	44.800	58.200
Maximum	68.700	54.500	54.600	68.700
# Missing	4	3	1	0
Range	26.800	12.600	9.800	10.500

For the breadth of the distal end Table 73 shows that the mean of the Spioenkop specimens falls below that of the blue and black wildebeest. The standard deviations of all three groups are similar. The range of the Spioenkop specimens falls below the black. Figure 176 shows the same pattern; the confidence interval for the Spioenkop specimens falls below that of the black wildebeest, as does the hybrid standard error in Figure 177.

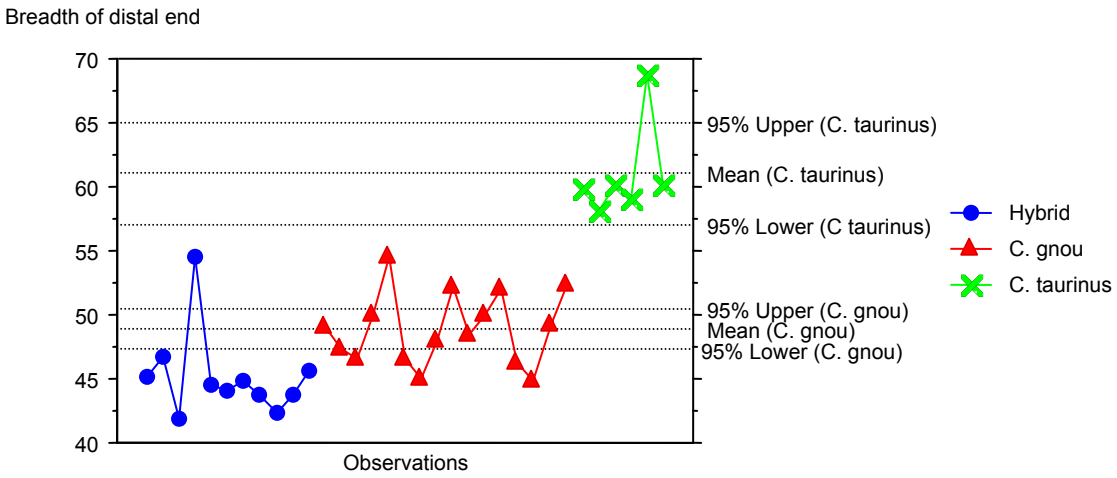

Figure 176: Univariate plot for breadth of the distal end.

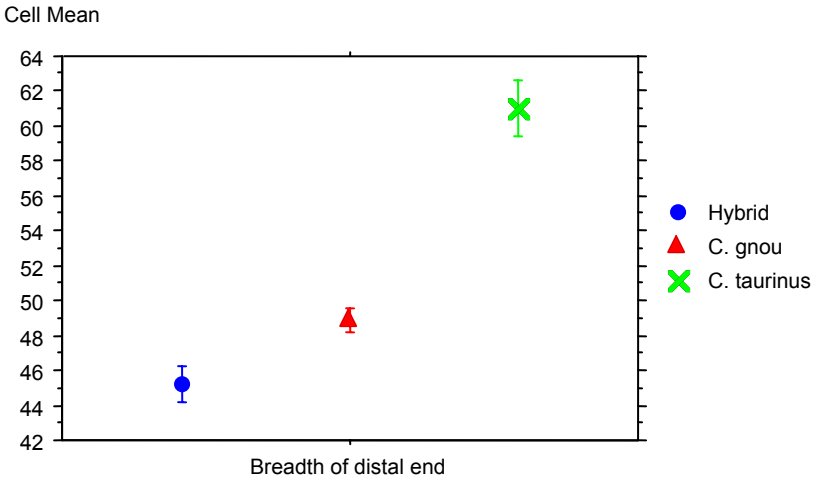

Figure 177: Standard error for the breadth of the distal end (error bars: ±1 STD error).

6.13 Summary of univariate analysis of the radius.

Table 74: Summary for outliers based on radius measurements. '0' indicates that for this feature the Spioenkop specimens falls within the black wildebeest range, and '1' indicates the specimens which fall outside the black wildebeest range.

Measurement	GL	Bp	Bd	
Specimen Number				Sum
12042	0	0	0	0
12043	0	0	0	0
12044	0	0	1	1
12045	0	0	0	0
12046	0	0	0	0
12047	0	0	0	0
12048	0	0	1	1
12049	0	0	0	0
12050	0	0	0	0
12051	0	0	1	1
12052	0	0	1	1
12053	0	0	1	1
12054	0	0	0	0
12060	0	0	0	0
SUM	0	0	5	

There is only one feature for which the Spioenkop specimen plots lie outside the black wildebeest range and that is the breadth of the distal end. For this feature, the Spioenkop specimens plot below that of the black wildebeest.

6.14 Metacarpal

6.14.1 Greatest length of the metacarpal

For the greatest length of the metacarpal, Table 75 shows that Spioenkop specimens have a mean that falls between the means of *C. gnou* and *C. taurinus*. The range of the Spioenkop specimens falls within the range of black wildebeest. In Figure 178, the confidence intervals of *C. gnou* and *C. taurinus*

do not overlap. All the Spioenkop specimens plot within the range of black wildebeest. The standard error for Spioenkop specimens in Figure 179 plots clear of the black wildebeest standard error plot.

Table 75: Descriptive statistics for greatest length of metacarpal.

	GL, Total	GL, Hybrid	GL, C.gnou	GL, C. taurinus
Mean	203.067	202.069	194.843	234.017
Std. Dev.	15.389	5.505	7.949	9.259
Std. Error	2.433	1.527	1.735	3.780
Count	40	13	21	6
Minimum	181.700	192.500	181.700	223.000
Maximum	247.500	208.700	209.700	247.500
# Missing	1	1	0	0
Variance	236.836	30.306	63.186	85.722
Range	65.800	16.200	28.000	24.500

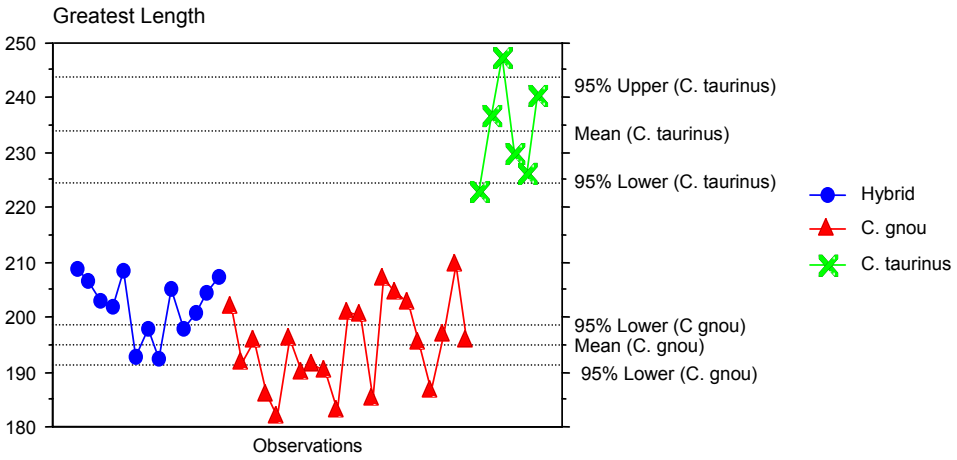

Figure 178: Univariate line plots for greatest length of metacarpal.

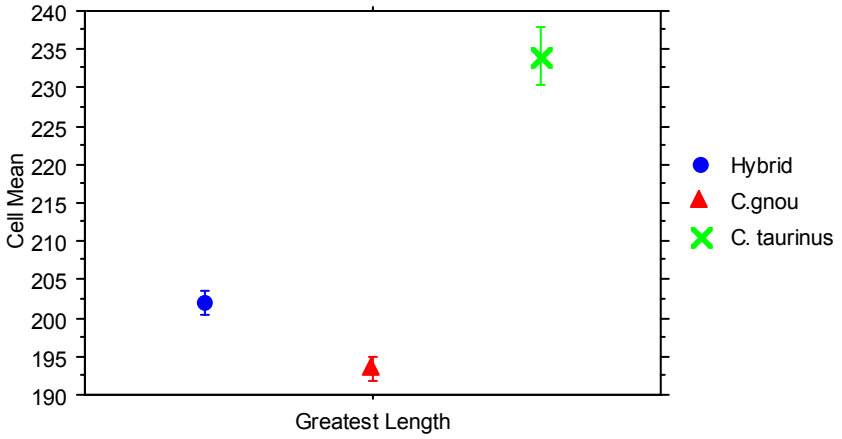

Figure 179: Standard error plot for greatest length of metacarpal (error bars: ±1 STD error).

6.14.2 Breadth of the proximal end (Bp) of the metacarpal

Table 76: Descriptive statistics for breadth of the proximal end of the metacarpal.

	Bp, Total	Bp, Hybrid	Bp, C.gnou	Bp, C. taurinus
Mean	42.429	41.750	41.443	47.467
Std. Dev.	2.804	1.445	2.031	2.266
Std. Error	.438	.386	.443	.925
Count	41	14	21	6
Minimum	36.900	39.600	36.900	45.200
Maximum	51.500	44.200	44.700	51.500
# Missing	0	0	0	0
Range	14.600	4.600	7.800	6.300

For the breadth of the proximal end of the metacarpal, Table 76 shows that Spioenkop specimens have a mean equal to the mean of the black. The range of the Spioenkop specimens falls within the range of black wildebeest. In Figure 180, the confidence intervals of *C. gnou* and *C. taurinus* do not overlap, and all the hybrid plots fall within the black wildebeest range. The standard error for Spioenkop specimens in Figure 181 plots within that of the black wildebeest standard error plot.

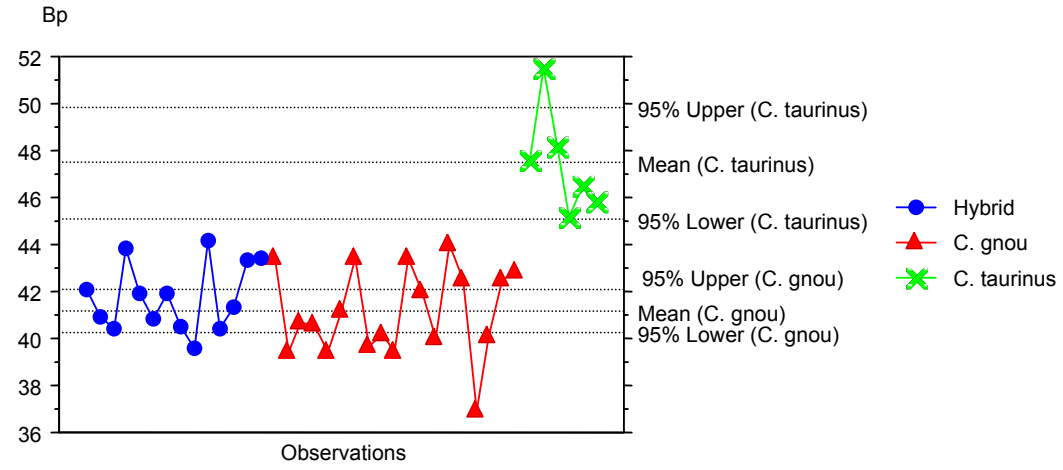

Figure 180: Univariate line plots for breadth of the proximal end of the metacarpal.

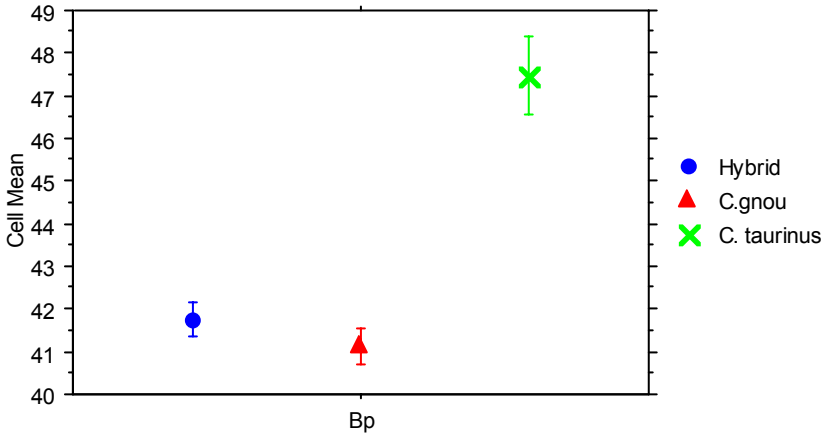

Figure 181: Standard error plot for breadth of the proximal end of the metacarpal (error bars: ±1 STD error).

6.14.3 Smallest depth of the diaphysis of the metacarpal

Table 77: Descriptive statistics for smallest depth of the diaphysis of the metacarpal.

	DD, Total	DD, Hybrid	DD, C.gnou	DD, C. taurinus
Mean	17.365	16.971	16.645	20.683
Std. Dev.	1.729	.869	.983	1.403
Std. Error	.273	.232	.220	.573
Count	40	14	20	6
Minimum	15.400	15.500	15.400	19.000
Maximum	22.500	18.500	18.500	22.500
# Missing	1	0	1	0
Range	7.100	3.000	3.100	3.500

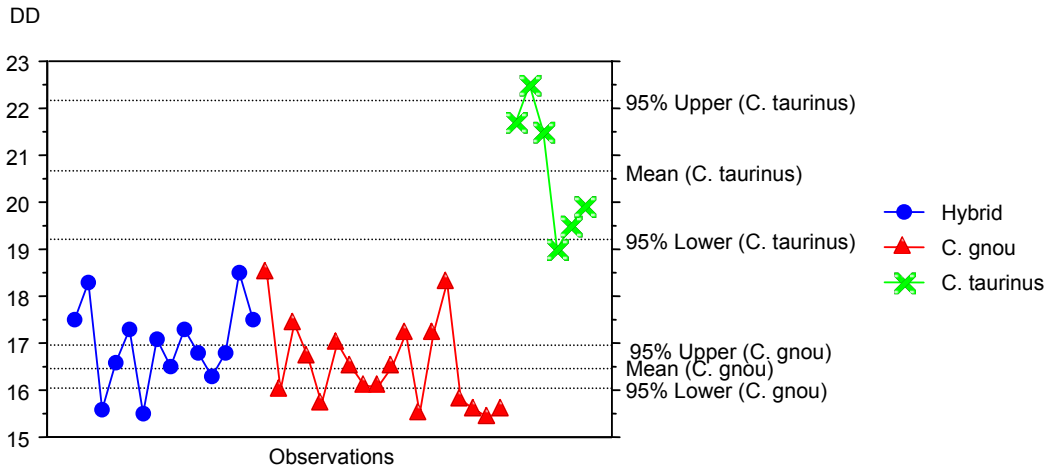

Figure 182: Univariate plot for depth of the diaphysis of the metacarpal.

For the breadth of the proximal of the metacarpal Table 77 shows that Spioenkop specimens have a mean that equals that of the black wildebeest. The range of the Spioenkop specimens falls within the range of black wildebeest. In Figure 182, there is overlap between the mean of the hybrid and the upper interval of the black, with all the hybrid plots falling within the blue

wildebeest range. The standard error for Spioenkop specimens in Figure 183 plots above that of the black wildebeest standard error plot.

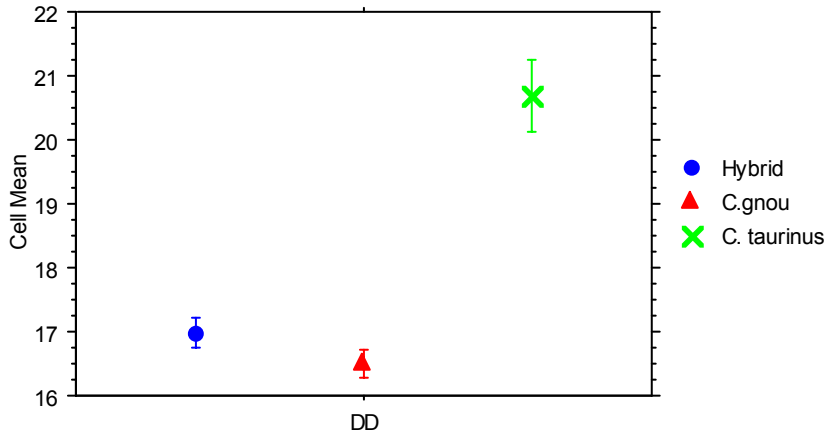

Figure 183: Standard error plot for depth of the diaphysis (error bars: ±1 STD error).

6.14.4 Smallest breadth of the diaphysis of the metacarpal

Table 78: Descriptive statistics for smallest breadth of the diaphysis.

	SD, Total	SD, Hybrid	SD, C.gnou	SD, C. taurinus
Mean	23.295	22.893	22.410	27.333
Std. Dev.	2.120	1.174	1.179	1.874
Std. Error	.331	.314	.257	.765
Count	41	14	21	6
Minimum	20.700	21.500	20.700	24.800
Maximum	30.000	24.700	24.400	30.000
# Missing	0	0	0	0
Sum	955.100	320.500	470.600	164.000

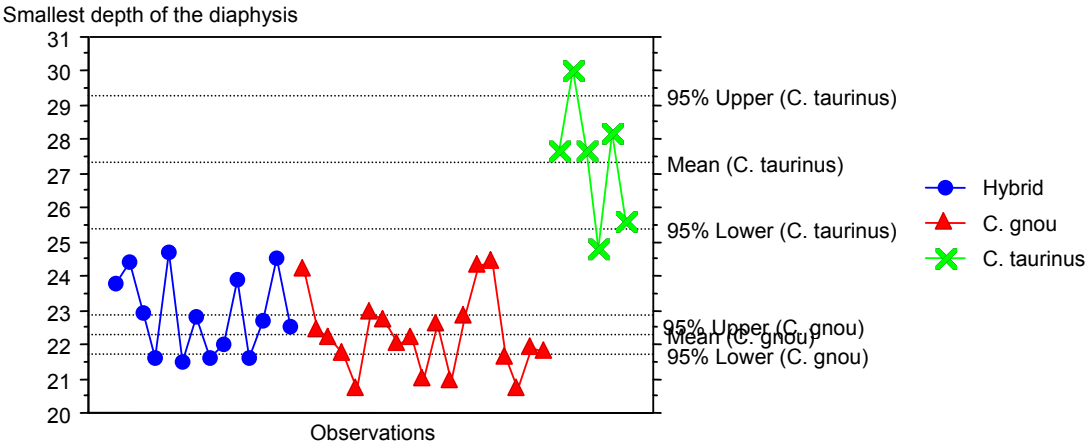

Figure 184: Univariate plot for the smallest depth of the diaphysis.

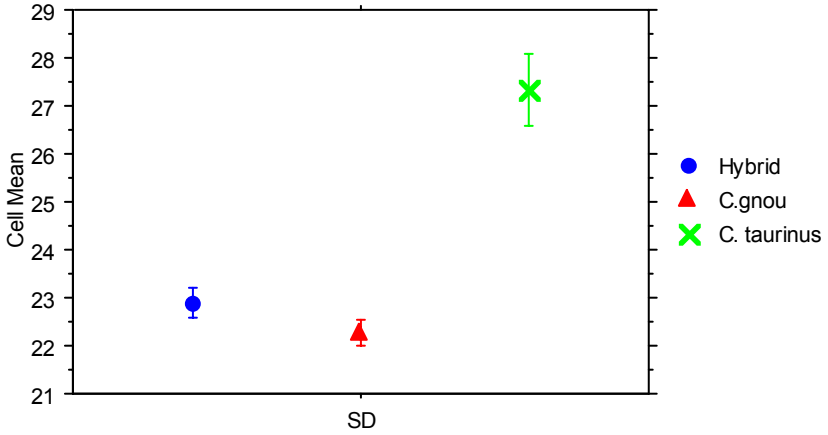

Figure 185: Standard error plot for the smallest depth of the diaphysis (error bars: ±1 STD error).

Table 78 shows that Spioenkop specimens have a mean that equals that of the black wildebeest. The range of the Spioenkop specimens falls within the range of black wildebeest. In Figure 184, there is overlap between the mean of the Spioenkop specimens and the upper interval of the black. All the Spioenkop plots fall within the black wildebeest range. The standard error for Spioenkop

specimens in Figure 185 plots above that of the black wildebeest standard error plot, with some overlap.

6.14.5 Greatest breadth of the distal end of the metacarpal

Table 79: Descriptive statistics for breadth of the distal end of the metacarpal.

	Bd, Total	Bd, Hybrid	Bd, C.gnou	Bd, C. taurinus
Mean	45.163	44.714	43.819	50.917
Std. Dev.	3.055	1.235	1.720	3.311
Std. Error	.477	.330	.375	1.352
Count	41	14	21	6
Minimum	41.000	42.700	41.000	47.200
Maximum	56.600	46.300	46.800	56.600
# Missing	0	0	0	0
Range	15.600	3.600	5.800	9.400

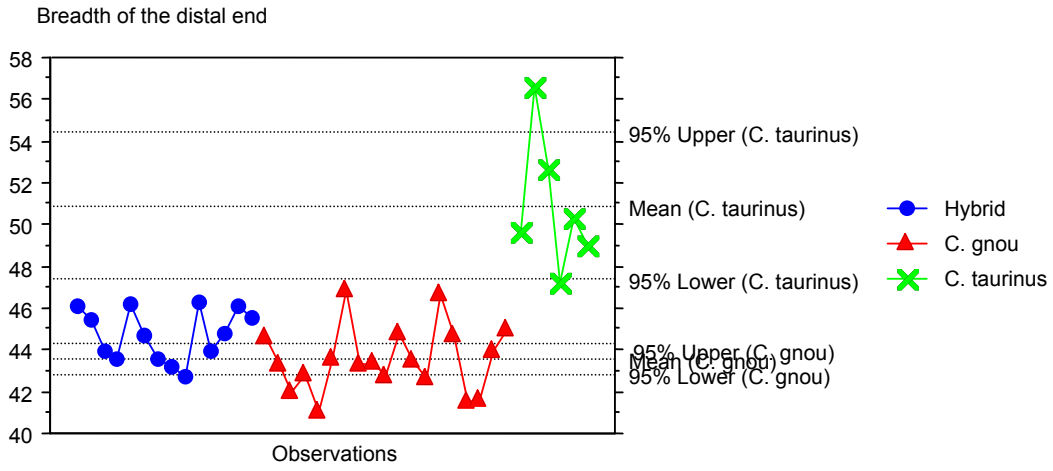

Figure 186: Univariate plots for breadth of the distal end of the metacarpal.

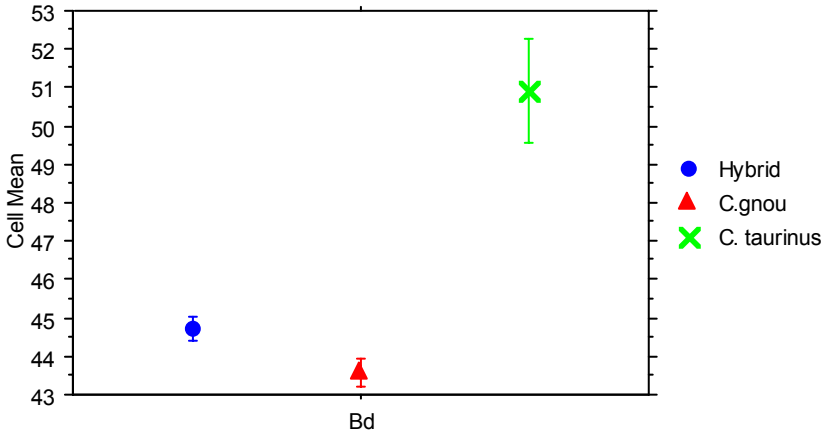

Figure 187: Standard error plot for breadth of the distal end of the metacarpal (error bars: ±1 STD error).

For the breadth of the distal of the metacarpal Table 79 shows that Spioenkop specimens have a mean that equals that of the black. The range of the Spioenkop specimens falls within the range of black wildebeest. In Figure 186, the hybrid plots all fall within the black wildebeest range. The standard error for Spioenkop specimens in Figure 187 plots above that of the black wildebeest standard error plot.

6.14.6 Depth of the achsial part of the medial condyle of the of the metacarpal

Table 80 shows that Spioenkop specimens have a mean that is slightly smaller than the black. The range of the Spioenkop specimens falls within that of black wildebeest. In Figure 188, the Spioenkop plots fall within the confidence interval of the black wildebeest. The standard error for Spioenkop specimens in Figure 189 plots within the black wildebeest standard error plot.

Table 80: Descriptive Statistics for depth of the achsial part of the medial condyle of the metacarpal.

	Dda, Total	Dda, Hybrid	Dda, C.gnou	Dda, C. taurinus
Mean	24.592	23.842	24.287	27.450
Std. Dev.	1.728	.755	1.574	1.277
Std. Error	.353	.218	.557	.638
Count	24	12	8	4
Minimum	21.600	22.700	21.600	26.500
Maximum	29.200	24.800	26.000	29.200
# Missing	17	2	13	2
Range	7.600	2.100	4.400	2.700

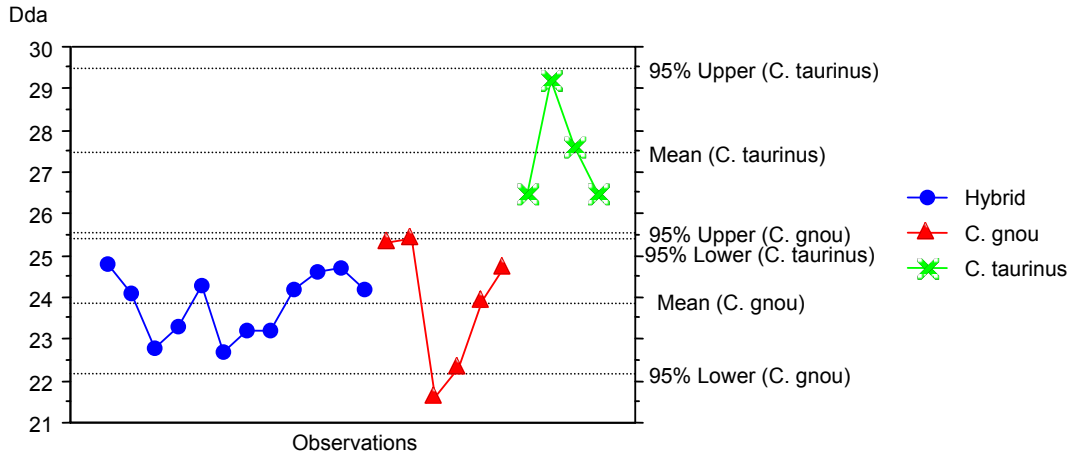

Figure 188: Univariate line plot for depth of the achsial part of the medial condyle of the metacarpal.

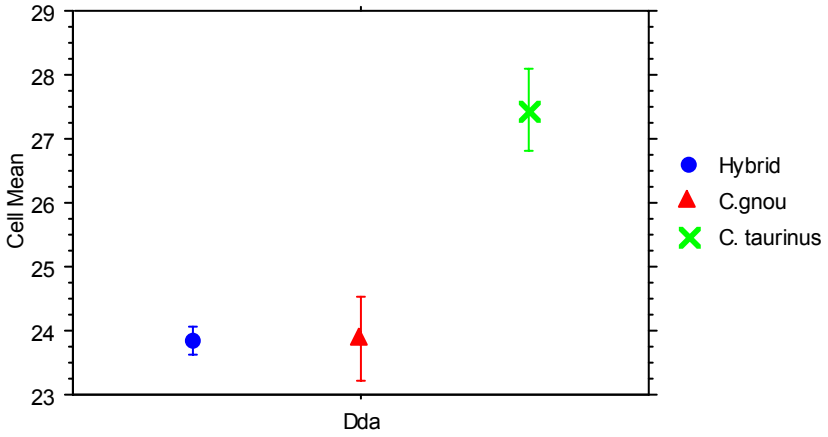

Figure 189: Standard error plot for depth of the achsial part of the medial condyle of the metacarpal (error bars: ±1 STD error).

6.14.7 Depth of the peripheral part of the medial condyle of the of the metacarpal

Table 81: Descriptive statistics for depth of the peripheral part of the medial condyle of the metacarpal.

	Ddp, Total	Ddp, Hybrid	Ddp, C.gnou	Ddp, C. taurinus
Mean	20.413	20.650	19.438	22.067
Std. Dev.	1.288	.616	1.385	1.102
Std. Error	.269	.178	.490	.636
Count	23	12	8	3
Minimum	17.700	19.600	17.700	20.800
Maximum	22.800	21.600	21.100	22.800
# Missing	18	2	13	3
Range	5.100	2.000	3.400	2.000

In Table 81, the means for all three groups are similar, with the hybrid mean being closer to the blue. All three have a small range. In Figure 190, the Spioenkop specimens plot closer to the upper confidence interval of the black wildebeest, and some plot just out of the black wildebeest range. Seven hybrid specimens fall out of the black wildebeest range. They are 12042, 12043,

12044, 12046, 12051, 12053 and 12054. The same is seen in Figure 191 with the hybrid standard error plotting between the standard errors of *C. gnou* and *C. taurinus*.

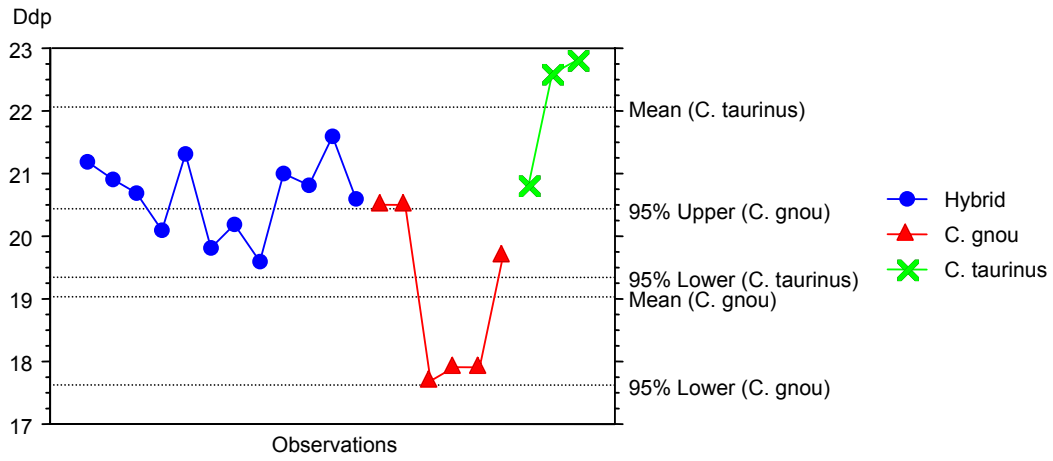

Figure 190: Univariate line graph for depth of the peripheral part of the medial condyle of the metacarpal.

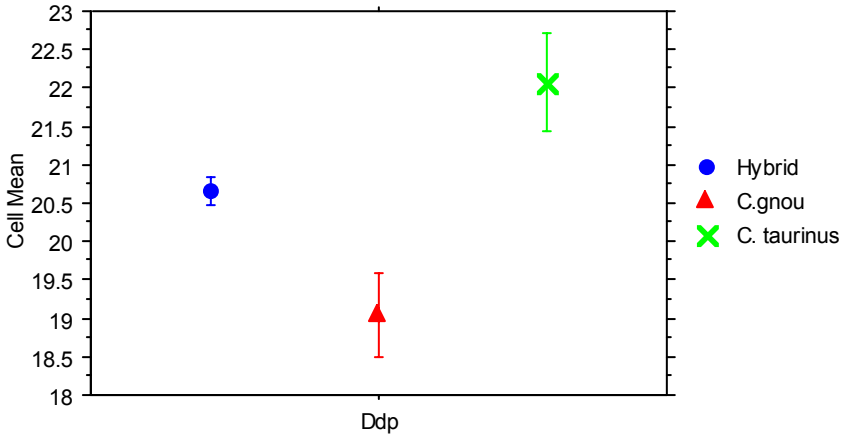

Figure 191: Standard error plot for depth of the peripheral part of the medial condyle of the metacarpal (error bars: ±1 STD error).

6.15 Summary of the univariate analysis for the metacarpal.

Table 82: Summary of the outliers for the metacarpal measurements. '0' indicates that for this feature the Spioenkop specimens falls within the black wildebeest range and '1' indicates the specimens which fall outside the black wildebeest range.

Measurement / Specimen Number	GL	Bp	Bd	SD	DD	Dda	Ddp
12042	0	0	0	0	0	0	1
12043	0	0	0	0	0	0	1
12044	0	0	0	0	0	0	1
12046	0	0	0	1	0	0	1
12047	0	0	0	0	0	0	0
12048	0	0	0	0	0	0	0
12049	0	0	0	0	0	0	0
12050	0	0	0	0	0	0	0
12051	0	0	0	0	0	0	1
12052	0	0	0	0	0	0	0
12053	0	0	0	0	0	0	1
12054	0	0	0	0	0	0	1
12060	0	0	0	0	0	0	0
SUM	0	0	0	1	0	0	7
%'s	0	0	0	7.1	0	0.0	50.0

Neither the black nor the blue range is well represented for the metacarpal. There is overlap between all three groups for most traits. There is however a trend in the Spioenkop specimens being larger than black wildebeest for depth of the peripheral part of the medial condyle of the metacarpal. This same trend is seen in the metatarsal.

6.16 Femur

For all measurements taken on the femur, see Figure 13.

6.16.1 Greatest length (GL) of the femur.

For the greatest length of femur, the mean for the Spioenkop specimens in Table 83 falls between the means of *C. gnou* and *C. taurinus*. The range and standard deviation of the Spioenkop specimens resembles that of the blue wildebeest. In Figure 192, the hybrid plots all fall with the black wildebeest confidence interval range. In Figure 193, there is no significant difference in the standard error between black and hybrid wildebeest

Table 83: Descriptive statistics for greatest length of femur.

	GL, Total	GL, Hybrid	GL, C.gnou	GL, C. taurinus
Mean	277.889	270.409	268.955	321.383
Std. Dev.	23.367	11.688	14.525	11.995
Std. Error	3.841	3.524	3.248	4.897
Count	37	11	20	6
Minimum	242.500	253.000	242.500	309.600
Maximum	343.000	284.900	300.500	343.000
# Missing	4	3	0	0
Variance	546.009	136.613	210.975	143.874
Range	100.500	31.900	58.000	33.400

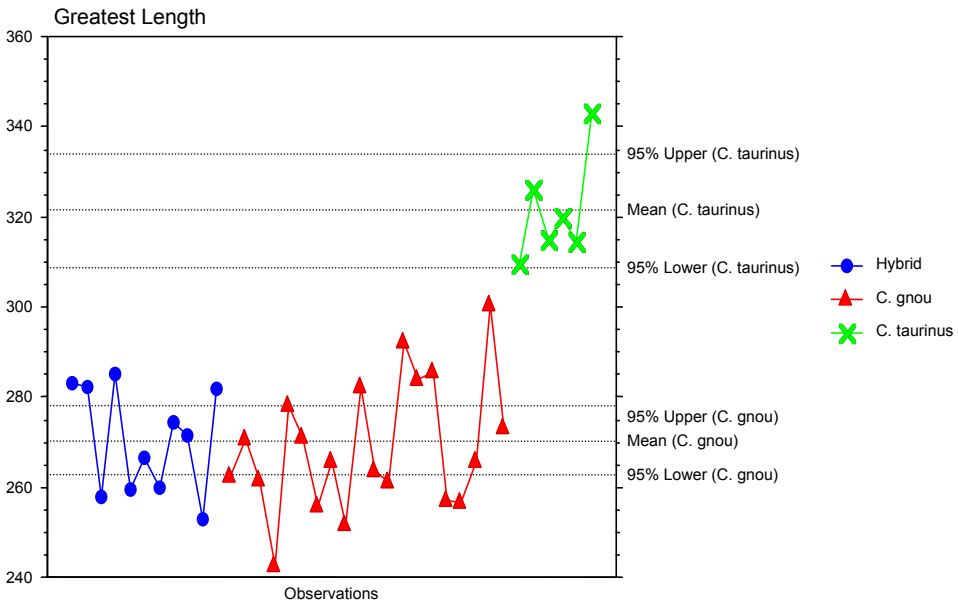

Figure 192: Univariate line plot for greatest length of the femur.

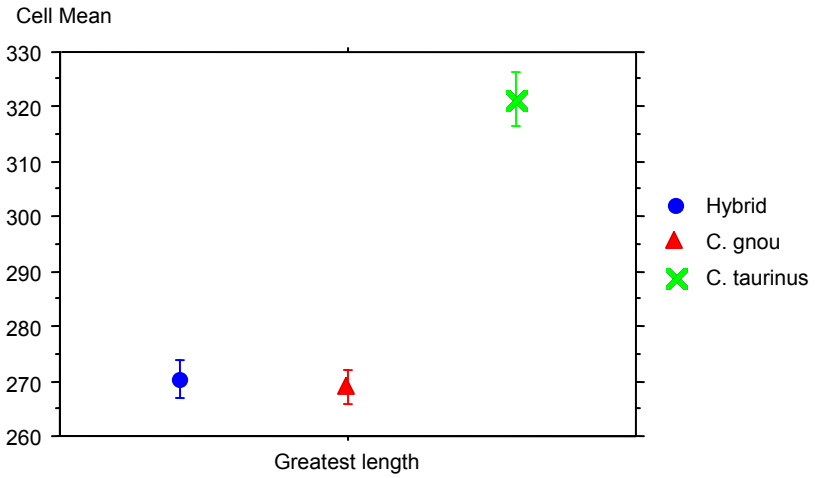

Figure 193: Standard error cell plot for greatest length of the femur (error bars: ±1 STD error).

6.16.2 Greatest breadth of the proximal end (Bp) of the femur

For breadth of the proximal end of the femur, Table 84 shows the mean for Spioenkop specimens falls between the means of the blue and black

wildebeest. The standard deviations are large for all three groups. Spioenkop specimens and black wildebeest have similar ranges for the breadth of the proximal end of the femur.

In Figure 194, the mean of the Spioenkop specimens plots just above the upper interval of the black. Almost all hybrid plots for this feature fall within the black wildebeest range. Specimens 12044 and 12054 both fall within the blue wildebeest range. There is no overlap in the confidence intervals of *C. gnou* and *C. taurinus*. Figure 195 shows the standard error of the Spioenkop specimens plotting above the standard error of black. There is some overlap in standard errors for black and Spioenkop specimens.

Table 84: Descriptive statistics for breadth of the proximal end.

	Bp, Total	Bp, Hybrid	Bp, C.gnou	Bp, C. taurinus
Mean	89.662	87.782	85.960	105.450
Std. Dev.	8.767	4.097	4.928	8.111
Std. Error	1.441	1.235	1.102	3.311
Count	37	11	20	6
Minimum	79.100	79.400	79.100	93.000
Maximum	118.000	94.400	95.600	118.000
# Missing	4	3	0	0
Range	38.900	15.000	16.500	25.000

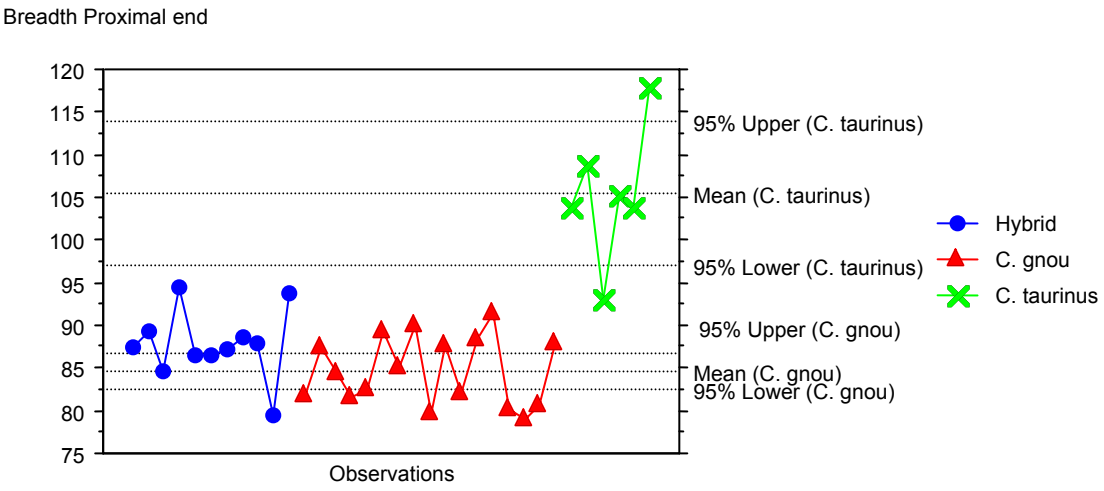

Figure 194: Univariate line plot for breadth of the proximal end.

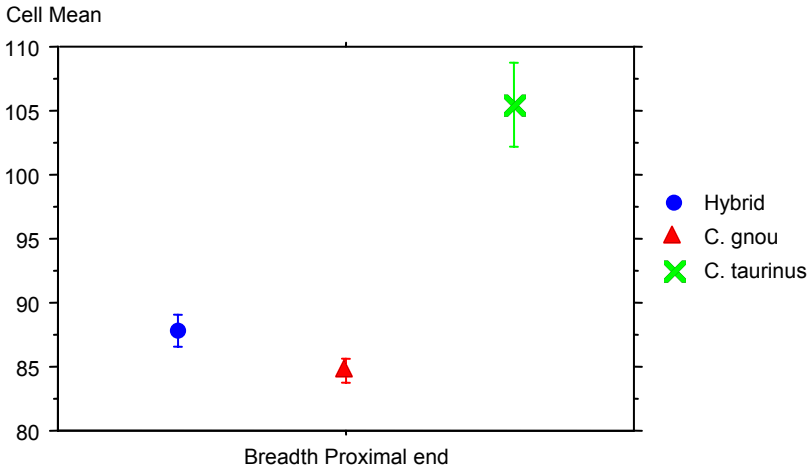

Figure 195: Standard error plot for breadth of the proximal end of the femur (error bars: ±1 STD error).

6.16.3 Smallest breadth of the diaphysis (SD) of the femur

For the smallest breadth of the diaphysis, the mean for the Spioenkop specimens in Table 85 falls between the means of blue and black wildebeest. The range and standard deviation of the Spioenkop specimens resembles that

of the blue wildebeest. In Figure 196 there is no overlap in *C. gnou* and *C. taurinus* confidence intervals. All the hybrid plots fall within the black wildebeest range. In Figure 197 there is no significant difference in the standard error between black and hybrid wildebeest.

Table 85: Descriptive statistics for the breadth of the diaphysis of the femur.

	SD, Total	SD, Hybrid	SD, C.gnou	SD, C. taurinus
Mean	27.732	26.645	26.840	32.700
Std. Dev.	2.760	1.008	2.003	1.472
Std. Error	.454	.304	.448	.601
Count	37	11	20	6
Minimum	23.100	25.500	23.100	31.000
Maximum	35.000	28.500	30.500	35.000
# Missing	4	3	0	0
Range	11.900	3.000	7.400	4.000

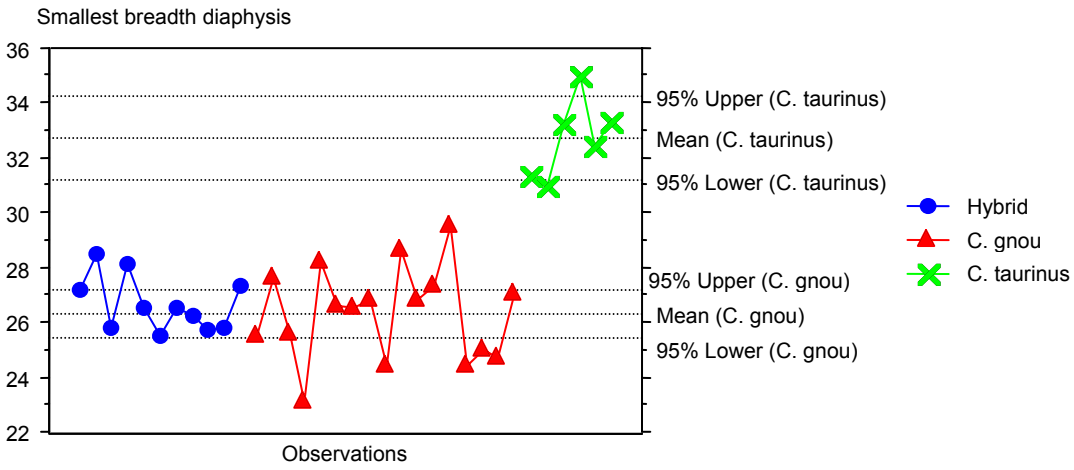

Figure 196: Univariate plots for smallest breadth of diaphysis of the femur.

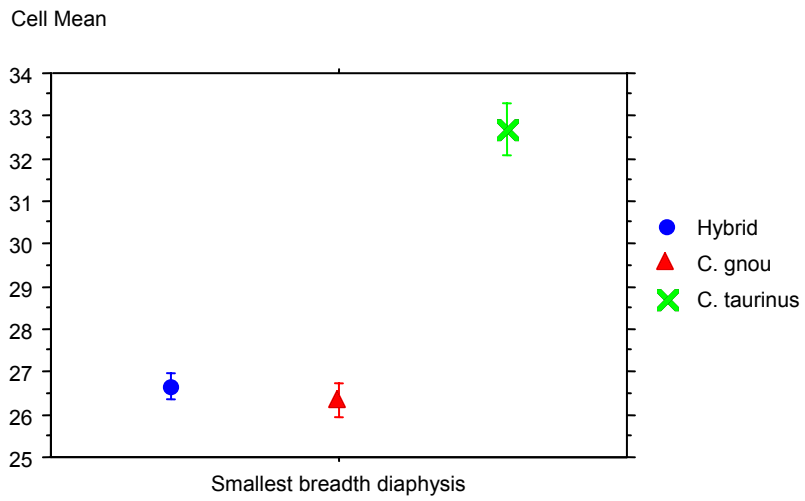

Figure 197: Standard error cell plot for breadth of the diaphysis of the femur (error bars: ±1 STD error).

6.16.4 Greatest breadth of the distal end (Bd) of the femur

For the breadth of the distal end of the femur, the mean for the Spioenkop specimens in Table 86 falls between the means of *C. gnou* and *C. taurinus.* The ranges for all the species are large and the standard deviations are small. In Figure 198, the confidence interval of the black wildebeest does not overlap with the blue. All the hybrid plots fall within the black wildebeest range. In Figure 199 there is no significant difference in the standard error between black and hybrid wildebeest.

Table 86: Descriptive statistics for the breadth of the distal end.

	Bd, Total	Bd, Hybrid	Bd, C.gnou	Bd, C. taurinus
Mean	70.740	69.267	68.765	79.533
Std. Dev.	5.616	2.884	3.821	5.776
Std. Error	.949	.961	.854	2.358
Count	35	9	20	6
Minimum	61.900	65.000	61.900	71.500
Maximum	88.700	75.500	76.500	88.700
# Missing	6	5	0	0
Range	26.800	10.500	14.600	17.200

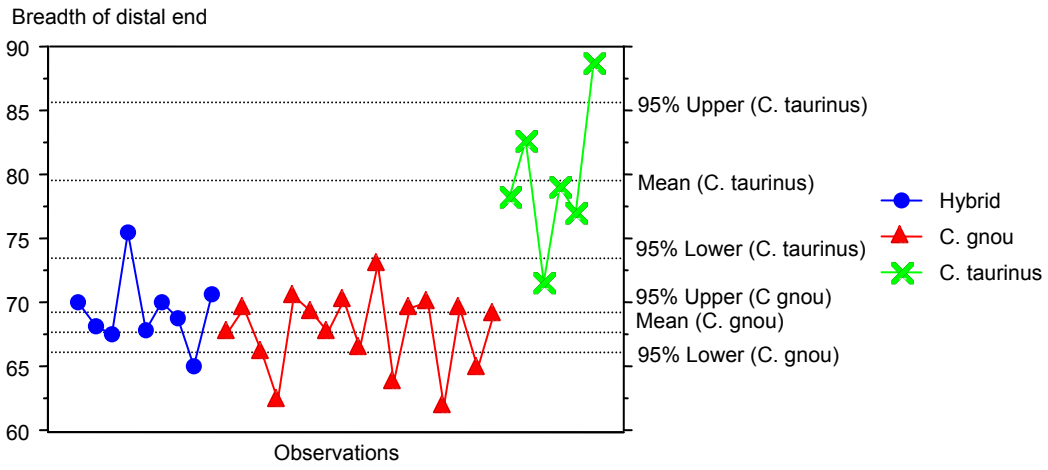

Figure 198: Univariate plot for breadth of distal end.

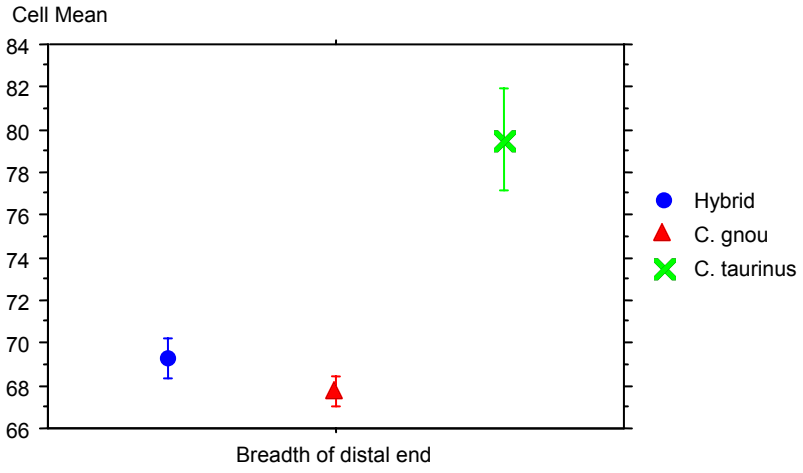

Figure 199: Standard error cell plot for breadth of distal end (error bars: ±1 STD error).

6.17 Summary of the univariate analysis of the femur.

Table 87: Summary of the outliers for measurements taken on the femur. '0' indicates that for this feature the Spioenkop specimens fall within the black wildebeest range, and '1' indicates the specimens which fall outside the black wildebeest range.

Measurement / Specimen Number	GL	Bp	Bd	SD	SUM	%'s
12042	0	0	0	0	0	0
12043	0	0	0	0	0	0
12044	1	0	0	0	0	0
12045	0	0	0	0	0	0
12046	0	0	0	0	0	0
12047	0	0	0	0	0	0
12048	0	0	0	0	0	0
12049	0	0	0	0	0	0
12050	0	0	0	0	0	0
12051	0	0	0	0	0	0
12052	0	0	0	0	0	0
12053	0	0	0	0	0	0
12054	1	0	0	0	0	0
12060	0	0	0	0	0	0
SUM	2	0	0	0		
%'s	14.2	0	0	0		

Only the greatest length has outliers for the features of the femur.

6.18 Tibia

6.18.1 Greatest length (GL) of the tibia

Table 88: Descriptive statistics for greatest length of the tibia.

	Greatest lngth, Total	Greatest lngth, Hybrid	Greatest lngth, Gnou	Greatest lngth, Taurinus
Mean	316.965	310.255	305.958	357.386
Std. Dev.	24.693	13.560	14.828	17.893
Std. Error	4.060	4.088	3.402	6.763
Count	37	11	19	7
Minimum	282.400	291.600	282.400	338.400
Maximum	386.000	326.600	335.000	386.000
# Missing	3	3	0	0
Range	103.600	35.000	52.600	47.600

In hybrid measurements, the greatest length of the tibia falls between the means of blue and black wildebeest (see Table 88). The Spioenkop specimens also show a small range which falls within the range of black wildebeest. All three groups have large standard deviations.

Figure 200 shows an overlap in the confidence intervals of the black and hybrid species. The hybrid specimens fall within the spread of the black plots. The hybrid standard error in Figure 201 has a mean that falls just outside of the standard error of the black wildebeest. The lower standard error of the Spioenkop specimens falls in the range of the black standard error.

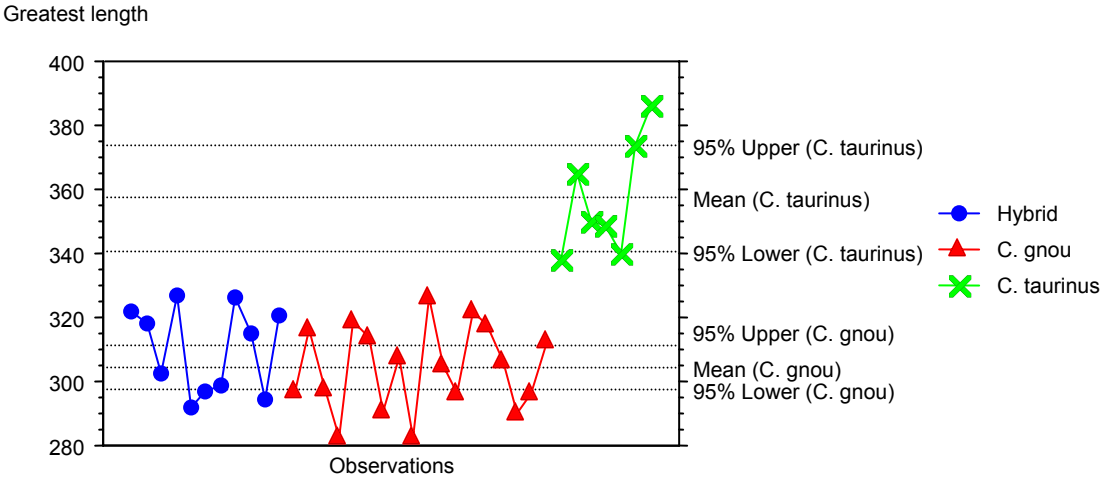

Figure 200: Univariate plot for greatest length of tibia.

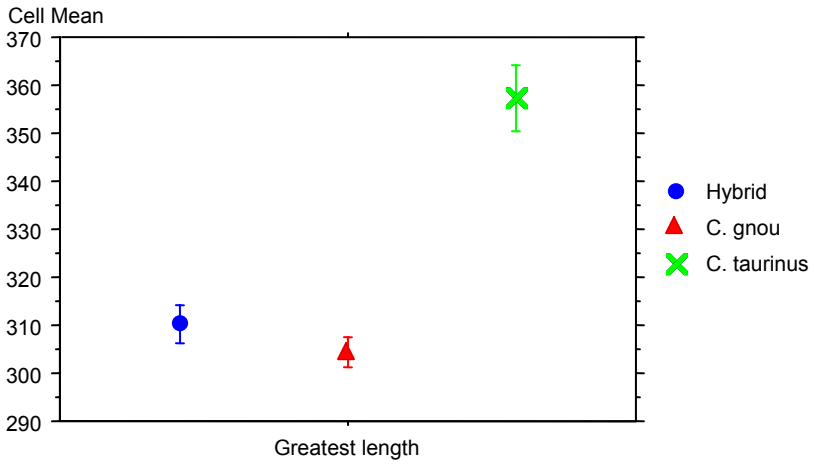

Figure 201: Standard error plot for greatest length of tibia (error bars: ±1 STD error).

6.18.2 Breadth of the proximal end of the tibia

The hybrid mean for the breadth of the proximal end of the tibia falls between the means of the blue and black wildebeest (see Table 89). The Spioenkop specimens also show a small range, which falls within the range of black wildebeest. All three groups have small standard deviations. Figure 202 the hybrid specimen plots fall within the spread of the black plots, with the exception of 12054, which falls above the range of *C. gnou*. There is no overlap in the confidence intervals of *C. gnou* and *C. taurinus*. The hybrid standard error in Figure 203 falls between the standard error of the black and blue wildebeest.

No Spioenkop specimens fall out of the range of black wildebeest for this feature.

Table 89: Descriptive statistics for the breadth of the proximal end of the tibia.

	Brdth Prox end, Total	Hybrid	C. gnou	C. taurinus
Mean	75.703	75.436	72.921	83.671
Std. Dev.	5.027	2.344	3.022	4.046
Std. Error	.826	.707	.693	1.529
Count	37	11	19	7
Minimum	67.700	71.300	67.700	80.000
Maximum	91.200	78.600	79.400	91.200
# Missing	3	3	0	0
Range	23.500	7.300	11.700	11.200

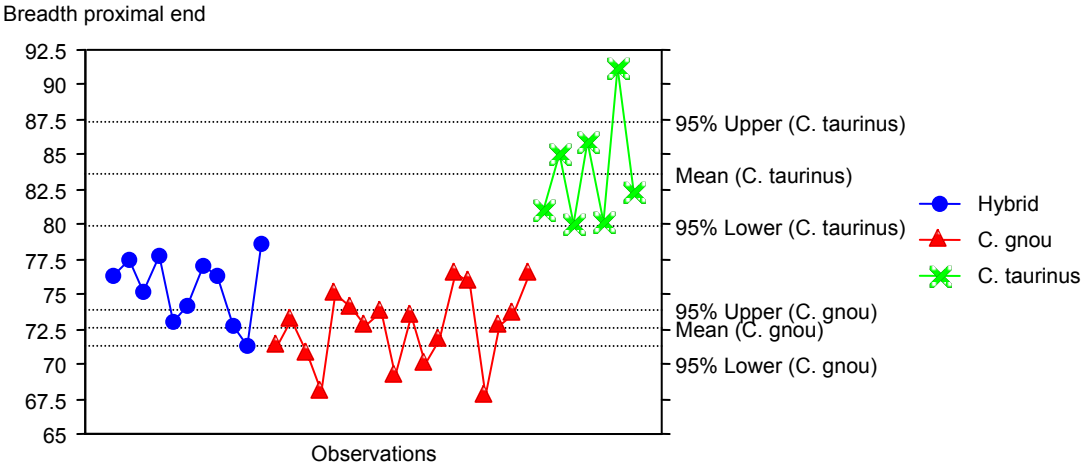

Figure 202: Univariate plots for the breadth of the proximal end of the tibia.

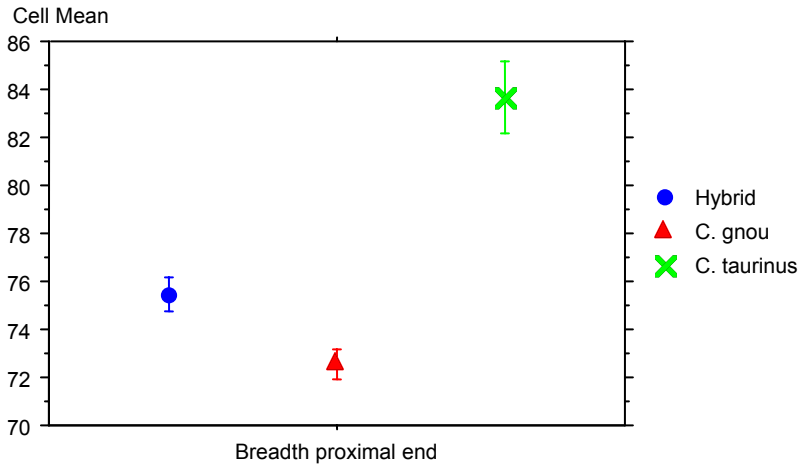

Figure 203: Standard error plot for the breadth of the proximal end of the tibia (error bars: ±1 STD error).

6.18.3 Breadth of the distal end of the tibia

The hybrid mean for the breadth of the distal end of the tibia measurements falls between the means of blue and black wildebeest (see Table 90). The Spioenkop specimens have a small range that falls within the range of black wildebeest. All three groups have small standard deviations. Figure 204 shows the hybrid specimens falling within the spread of the black wildebeest plots. The hybrid standard error in Figure 205 falls between the standard error of the black and blue wildebeest.

Table 90: Descriptive statistics for the breadth of the distal end of the tibia.

	Brdth distal end, Total	Hybrid	C. gnou	C. taurinus
Mean	46.517	45.940	44.221	53.571
Std. Dev.	4.200	1.311	2.539	2.381
Std. Error	.700	.415	.583	.900
Count	36	10	19	7
Minimum	40.300	44.500	40.300	51.600
Maximum	58.700	48.400	49.300	58.700
# Missing	4	4	0	0
Range	18.400	3.900	9.000	7.100

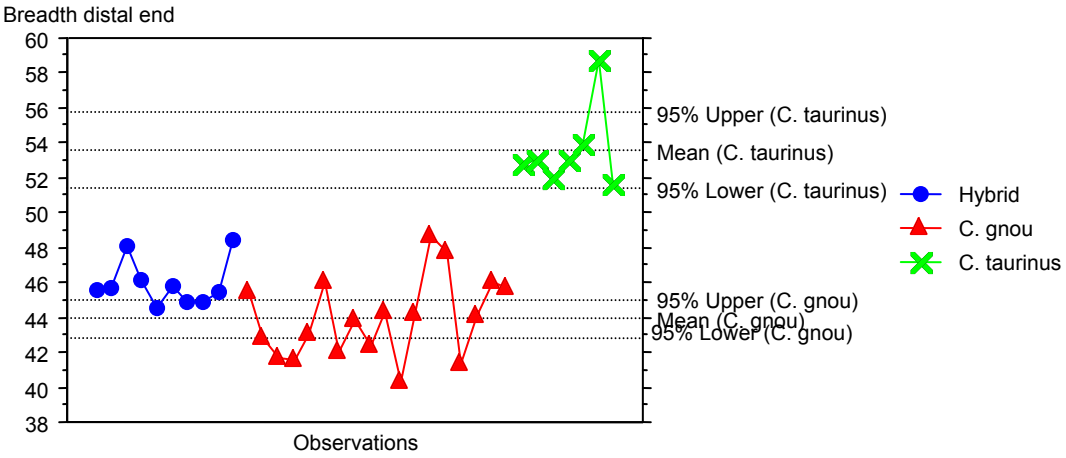

Figure 204: Univariate plot for the breadth of the distal end of the tibia.

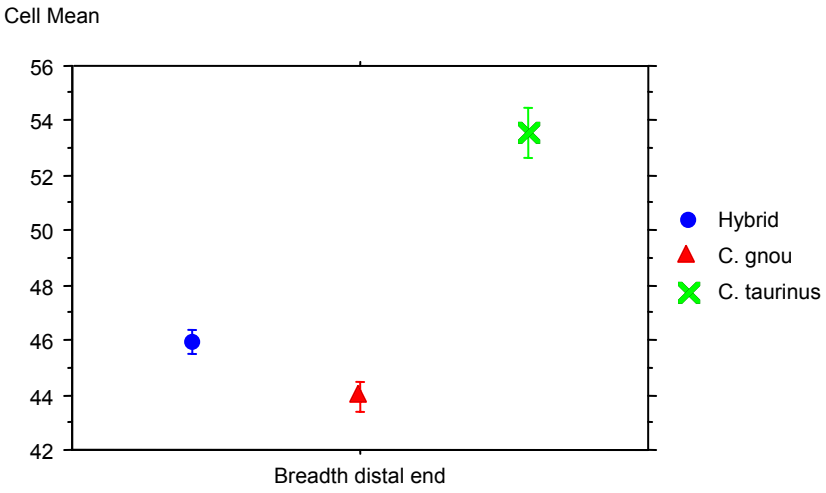

Figure 205: Standard error plot for the breadth of the distal end of the tibia (error bars: ±1 STD error).

6.19 Summary of the univariate plots for the tibia.

Table 91: Summary of the outliers for measurement s taken on the tibia. '0' indicates that for this feature the Spioenkop specimens falls within the black wildebeest range and '1' indicates the specimens which fall outside the black wildebeest range.

Measurement Specimen Number	GL	Bp	Bd
12042	0	0	0
12043	0	0	0

12044	0	0	0
12046	0	0	0
12047	0	0	0
12048	0	0	0
12049	0	0	0
12050	0	0	0
12051	0	0	0
12052	0	0	0
12053	0	0	0
12054	0	1	0
12060	0	0	0
SUM	0	1	0
%'s	0	7.142857	0

No Spioenkop specimens deviate from the black wildebeest plots for the tibia.

6.20 Metatarsal

6.20.1 Greatest length of the metatarsal

Table 92: Descriptive statistics for greatest length of metatarsal.

	Greatest length, Total	Hybrid	C. gnou	C. taurinus
Mean	228.840	227.086	220.926	253.829
Std. Dev.	14.626	5.965	10.312	7.768
Std. Error	2.313	1.594	2.366	2.936
Count	40	14	19	7
Minimum	203.000	217.900	203.000	245.000
Maximum	266.000	236.100	237.000	266.000
# Missing	0	0	0	0
Range	63.000	18.200	34.000	21.000

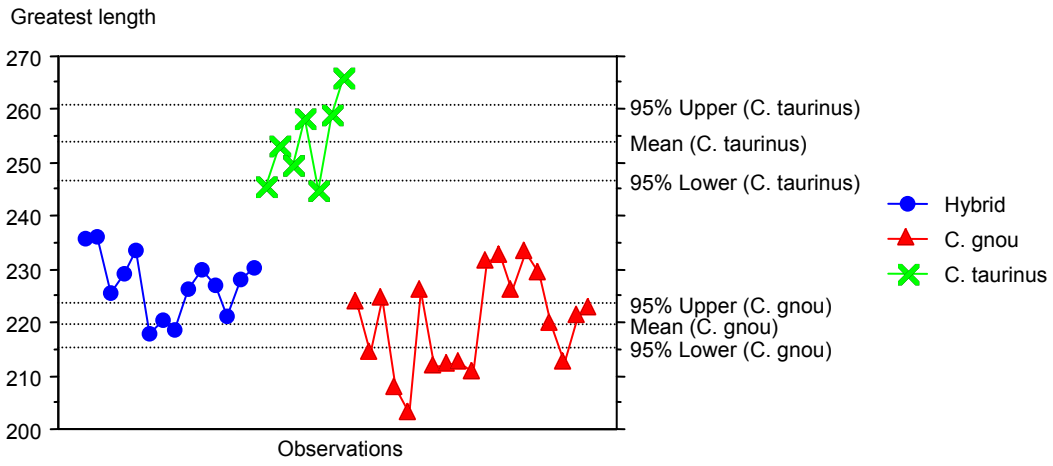

Figure 206: Univariate line plot for greatest length of metatarsal.

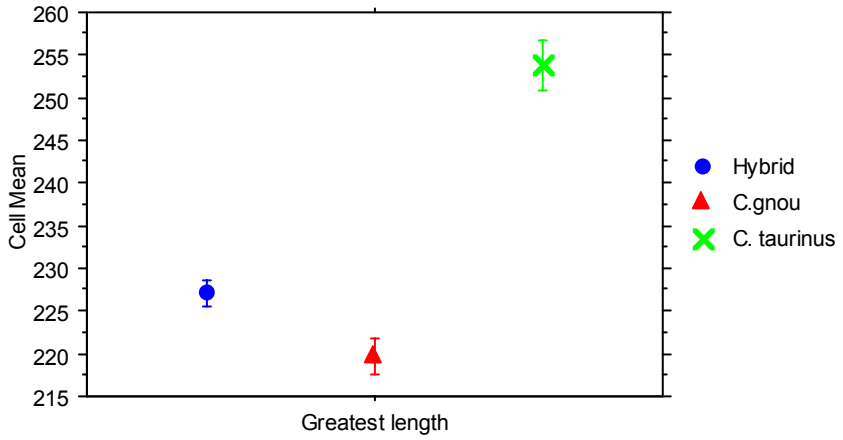

Figure 207: Standard error cell plot for greatest length of metatarsal (error bars: ±1 STD error).

For the greatest length of the metatarsal, Table 92 shows differences between the means of all three groups. The Spioenkop specimens mean plots between that of *C. gnou* and *C. taurinus*. The Spioenkop specimens have the smallest standard deviation. Black wildebeest have a very large range that repeats in the confidence intervals shown in Figure 206. The black wildebeest plots spread, and the Spioenkop wildebeest fall within the black range. Specimens 12042 and 12043 lie out side the black wildebeest range. There is no overlap

in the standard errors (Figure 207), with all three species having small standard errors, with the Spioenkop specimens plotting between the standard error plots of *C. gnou* and *C. taurinus*.

6.20.2 Greatest breadth of the proximal end of the metatarsal

Table 93: Descriptive statistics for greatest breadth of the proximal end for the metatarsal.

	Breadth Proximal, Total	Breadth Proximal, Hybrid	Breadth Proximal, C.gnou	Breadth Proximal, C. taurinus
Mean	37.110	36.329	36.258	40.986
Std. Dev.	2.412	1.254	1.830	1.763
Std. Error	.381	.335	.420	.666
Count	40	14	19	7
Minimum	33.200	34.600	33.200	38.600
Maximum	43.600	38.500	39.700	43.600
# Missing	0	0	0	0
Range	10.400	3.900	6.500	5.000

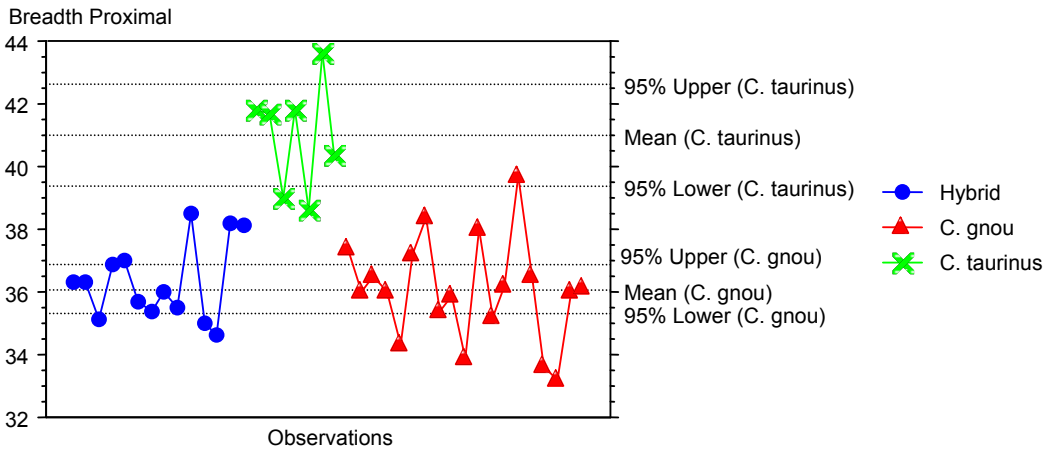

Figure 208: Univariate plot for the breadth of the proximal end of the metatarsal.

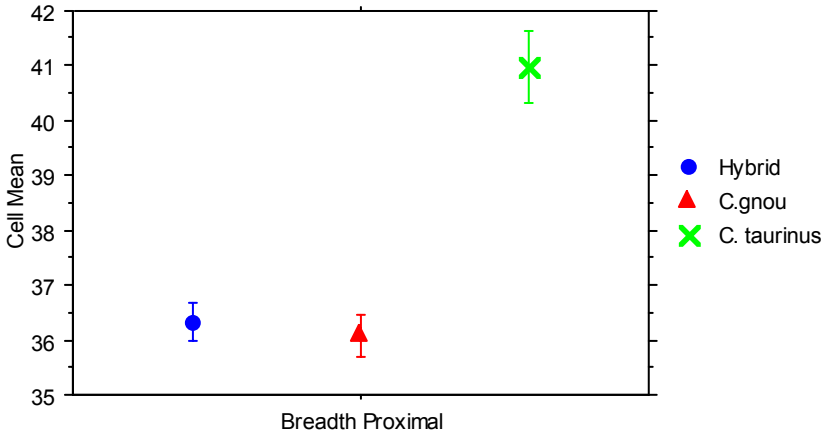

Figure 209: Standard error plot of the breadth of the proximal end of the metatarsal (error bars: ±1 STD error).

In Table 93, the means of the Spioenkop specimens and black are identical, and blue plot just above. This repeats in the confidence interval plots (Figure 208). In this graph black and Spioenkop specimens, share a mean, and all the hybrid measurements fall within the black wildebeest range. This graph has a similar pattern to the plots of greatest length. Figure 209 shows the standard error for Spioenkop specimens, plotting with the black.

6.20.3 Smallest breadth of the diaphysis of the metatarsal

In Table 94, the means of all three groups are all similar, with Spioenkop specimens and black having identical means, and blue being slightly larger. All three groups have small ranges for the breadth of the diaphysis. This repeats in the confidence interval plots (Figure 210). In this graph black and Spioenkop specimen means plot close together, the Spioenkop specimens have a small range that overlap with both *C. gnou* and *C. taurinus*. The cluster of the data for the Spioenkop specimens is similar to blue wildebeest. Figure 209

shows the standard error for Spioenkop specimens plotting with the blue standard error plot.

Table 94: Descriptive statistics for breadth of the diaphysis of the metatarsal.

	SD, Total	SD, Hybrid	SD, C.gnou	SD, C. taurinus
Mean	20.005	19.350	19.058	23.886
Std. Dev.	2.145	.904	1.144	1.669
Std. Error	.339	.242	.262	.631
Count	40	14	19	7
Minimum	16.400	17.400	16.400	21.000
Maximum	25.800	20.900	20.900	25.800
# Missing	0	0	0	0
Range	9.400	3.500	4.500	4.800

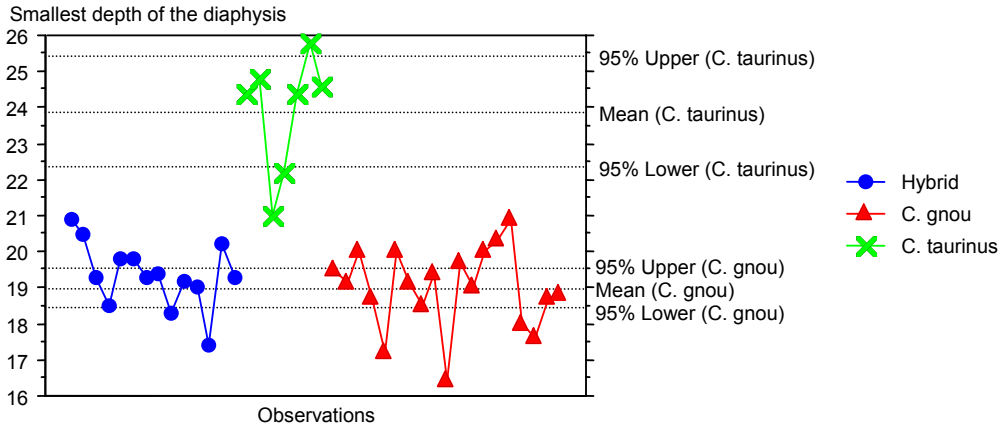

Figure 210: Univariate line plot for smallest breadth of the diaphysis of the metatarsal.

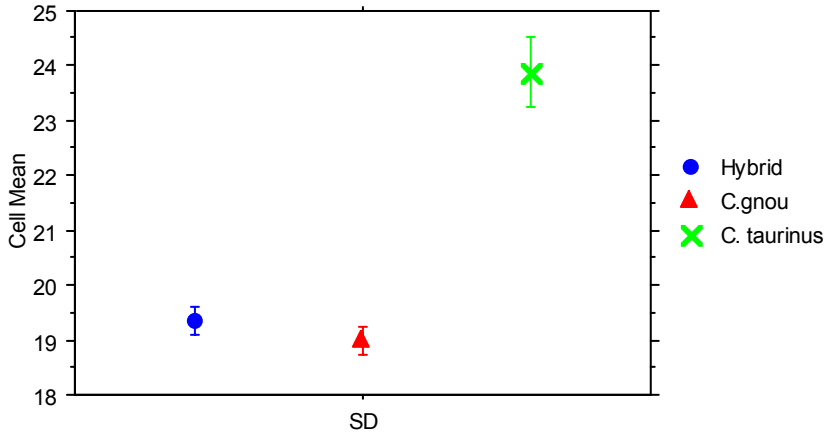

Figure 211: Standard error plot for the smallest breadth of the diaphysis of the metatarsal (error bars: ±1 STD error).

6.20.4 Greatest breadth of the distal end of the metatarsal

Table 95: Descriptive statistics for breadth of the distal end of the metatarsal.

	Breadth distal, Total	Breadth distal, Hybrid	Breadth distal, C.gnou	Breadth distal, C. taurinus
Mean	41.055	40.272	39.468	46.929
Std. Dev.	3.191	1.012	1.682	2.412
Std. Error	.504	.270	.386	.912
Count	40	14	19	7
Minimum	36.600	38.800	36.600	44.000
Maximum	51.700	41.900	42.700	51.700
# Missing	0	0	0	0
Range	15.100	3.100	6.100	7.700

In Table 94, the means of the Spioenkop specimens and black species are all similar, with hybrid mean falling between the means of *C. gnou* and *C. taurinus*, and black having the smallest mean. All three have small ranges, the hybrid range falls within the black wildebeest range. This repeats in the confidence interval plots (Figure 212). In this graph black and Spioenkop specimens share a mean and there is no overlap between the blue wildebeest confidence interval and the black. The cluster of the data for the Spioenkop

specimens is similar to black wildebeest. Figure 209 shows that the standard error for Spioenkop specimens plots just above the black wildebeest.

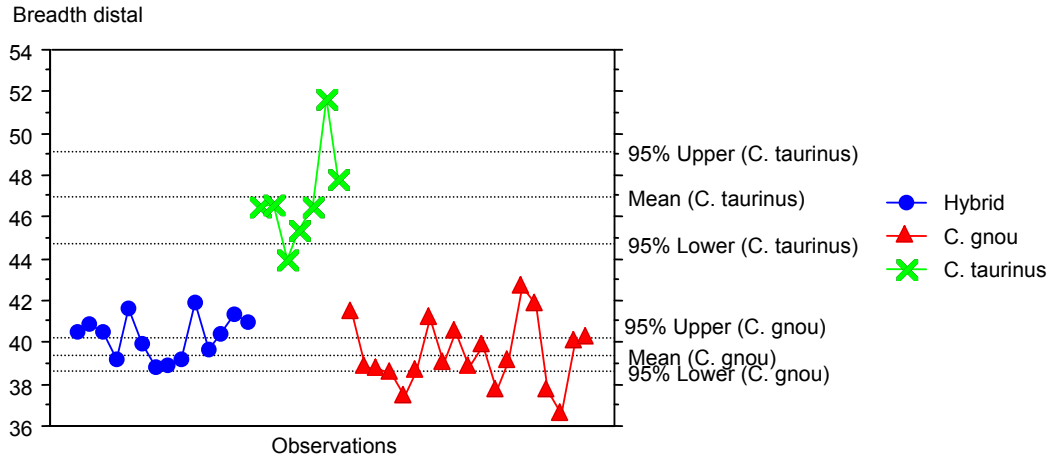

Figure 212: Univariate plot for breadth of the distal end of the metatarsal.

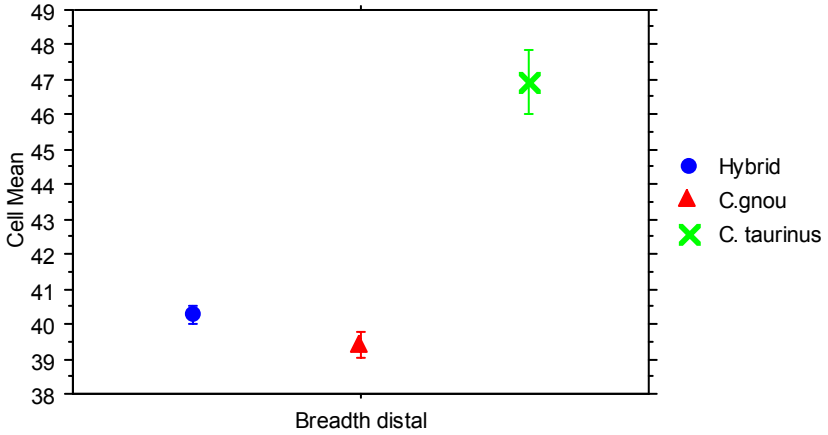

Figure 213: Standard error for breadth of the distal end of the metatarsal (error bars: ±1 STD error).

6.20.5 Smallest depth of the diaphysis (DD) of the metatarsal

Table 96: Descriptive statistics for smallest depth of the diaphysis of the metatarsal.

	DD, Total	DD, Hybrid	DD, C. gnou	DD, C. taurinus
Mean	18.769	18.162	17.863	22.357
Std. Dev.	1.917	.819	.840	1.183
Std. Error	.307	.227	.193	.447
Count	39	13	19	7
Minimum	16.700	16.700	16.700	20.800
Maximum	24.200	19.600	19.300	24.200
# Missing	1	1	0	0
Range	7.500	2.900	2.600	3.400

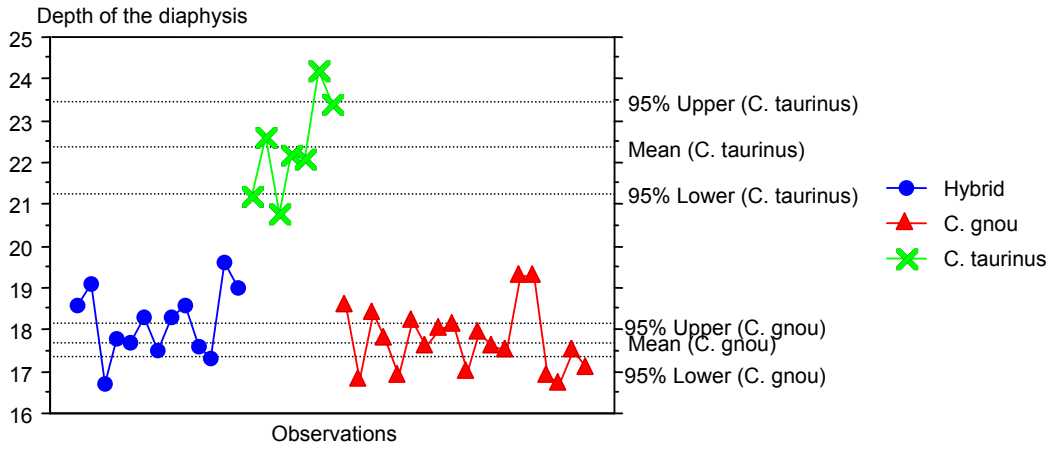

Figure 214: Univariate plot for the depth of the diaphysis of the metatarsal.

In Table 96, the mean of the Spioenkop specimens falls between that of *C. gnou* and *C. taurinus*, and black wildebeest have the smallest mean. All three have small ranges, however, the hybrid range falls within the black wildebeest range. This repeats in the confidence interval plots (Figure 214). In this graph, black and Spioenkop specimen means are similar, and there is no overlap with the blue wildebeest confidence interval. The cluster of the data for the Spioenkop specimens is similar to black wildebeest. Figure 215 shows the

standard error for hybrid species having some overlap with the black standard error.

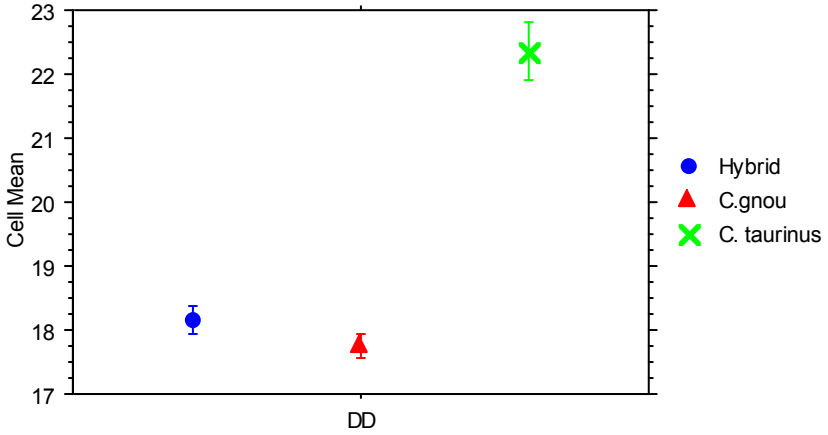

Figure 215: Standard error plot for depth of the diaphysis of the metatarsal (error bars: ±1 STD error).

6.20.6 Depth of the achsial part of the medial condyle of the metatarsal (Dda)

Table 97: Descriptive statistics for depth of the achsial part of the medial condyle of the metatarsal.

	Dda, Total	Dda, Hybrid	Dda, C.gnou	Dda, C. taurinus
Mean	23.843	23.167	23.400	27.433
Std. Dev.	1.807	.871	1.137	1.607
Std. Error	.394	.251	.464	.928
Count	21	12	6	3
Minimum	21.800	22.100	21.800	25.600
Maximum	28.600	25.100	24.600	28.600
# Missing	19	2	13	4

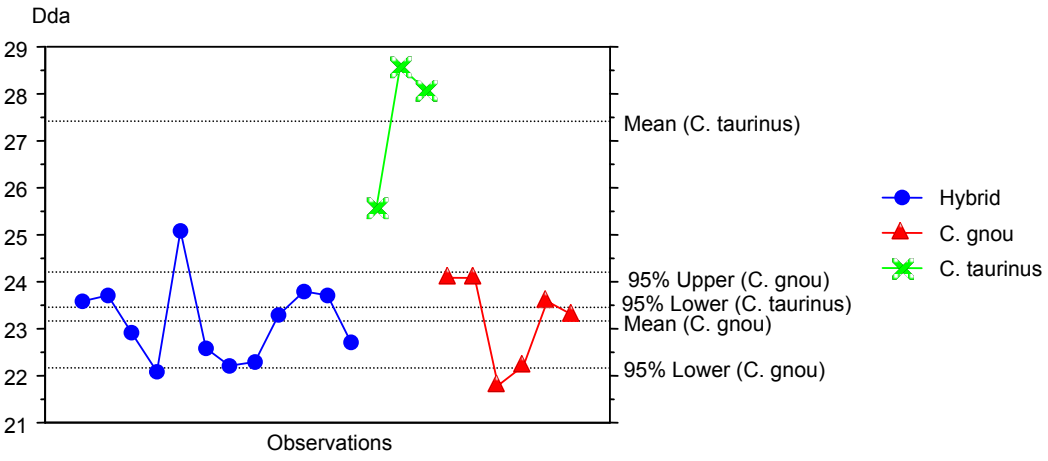

Figure 216: Univariate plot for depth of the achsial part of the medial condyle of the metatarsal.

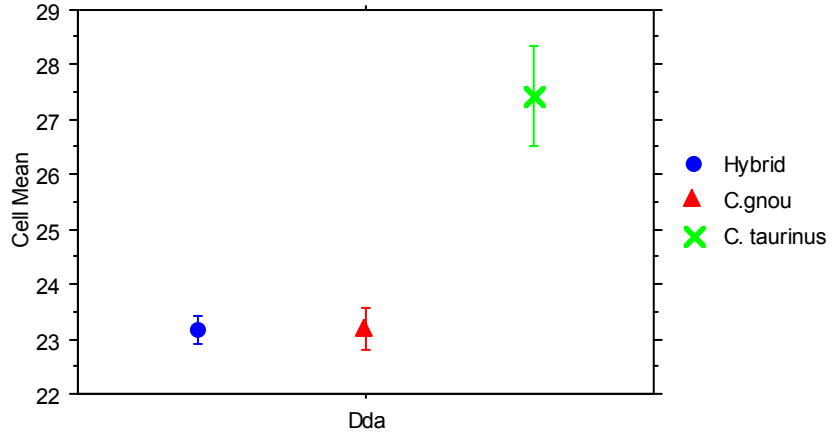

Figure 217: Standard error plot for depth of the achsial part of the medial condyle of the metatarsal (error bars: ±1 STD error).

In Table 97, the means of the Spioenkop specimens and black species are similar, the hybrid mean falls between the mean of *C. gnou* and *C. taurinus*. All three have small ranges, the hybrid ranges fall within the black wildebeest range. This repeats in the confidence interval plots (Figure 216). In this graph, black and Spioenkop specimens means are similar. There is overlap with the blue and black wildebeest confidence intervals but due to the small sample

size for blue wildebeest, this overlap is insignificant. The cluster of the data for the Spioenkop specimens is similar to black wildebeest. Figure 217 shows the standard error for hybrid species in which there is some overlap with the black.

6.20.7 Depth of the peripheral part of the medial condyle of the metatarsal (Ddp)

Table 98: Descriptive statistics for depth of the peripheral part of the medial condyle of the metatarsal.

	Ddp, Total	Ddp, Hybrid	Ddp, C.gnou	Ddp, C. taurinus
Mean	19.871	20.150	18.283	21.933
Std. Dev.	1.461	.796	.928	1.137
Std. Error	.319	.230	.379	.657
Count	21	12	6	3
Minimum	16.900	19.000	16.900	21.000
Maximum	23.200	21.400	19.600	23.200
# Missing	19	2	13	4
Range	6.300	2.400	2.700	2.200

In Table 98, the means for all three groups are similar, the hybrid mean being closer to the blue. All three have a small range. In Figure 218, a large number of the hybrid plots fall out of the black wildebeest confidence interval. These specimens are 12042, 12043, 12044, 12046, 12047, 12051, 12052 and 12054. The same is seen in Figure 219, with the hybrid standard error plotting between the standard errors of *C. gnou* and *C. taurinus*.

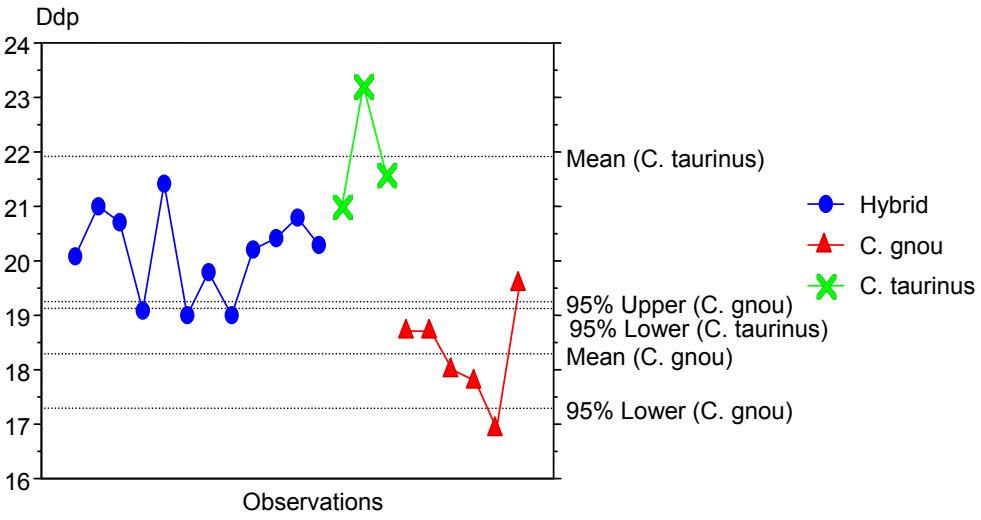

Figure 218: Univariate plot for depth of the peripheral part of the medial condyle of the metatarsal.

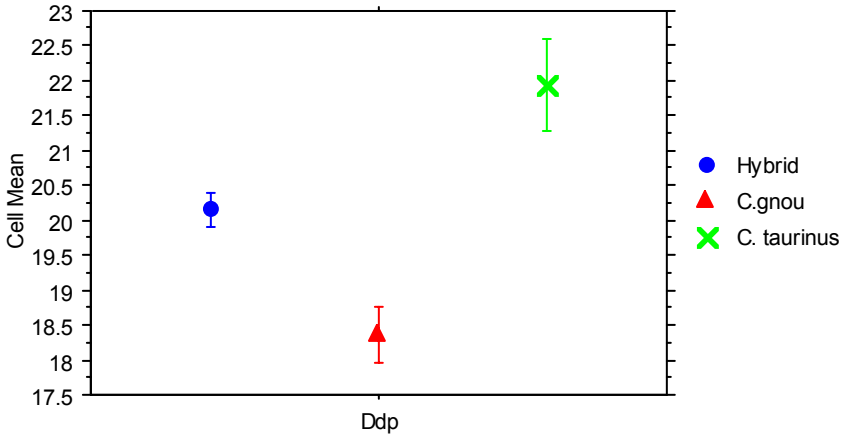

Figure 219: Standard error cell plot for depth of the peripheral part of the medial condyle of the (error bars: ±1 STD error).

6.21 Summary of the univariate analysis for the metatarsal.

Table 99: Summary of measurements taken on the metatarsal. '0' indicates that for this feature the Spioenkop specimens fall within the black wildebeest range, and '1' indicates the specimens which fall outside the black wildebeest range.

Measurement / Specimen Number	GL	Bp	Bd	SD	DD	Dda	Ddp
12042	0	0	0	0	0	0	1
12043	0	0	0	0	0	0	1
12044	0	0	0	0	0	0	1
12045	0	0	0	0	0	0	0
12046	0	0	0	0	0	1	1
12047	0	0	0	0	0	0	1
12048	0	0	0	0	0	0	0
12049	0	0	0	0	0	0	0
12050	0	0	0	0	0	0	0
12051	0	0	0	0	0	0	1
12052	0	0	0	0	0	0	1
12053	0	0	0	0	0	0	0
12054	0	0	0	0	0	0	1
12060	0	0	0	0	0	0	0
SUM	0	0	0	0	0	1	8
%'s	0	0	0	0	0	7.1	57.1

From Table 99 it is evident that the Spioenkop specimens only differ from black wildebeest in one measurement, depth of the peripheral part of the medial condyle of the metatarsal. This trait is consistent throughout most of the individuals. Even with *C. gnou* and *C. taurinus* having small sample sizes, there is a definite trend for a larger depth in the peripheral part of the medial condyle in the Spioenkop specimens.

7 DISCUSSION AND CONCLUSION

This study aimed to test whether it is possible to identify hybrid wildebeest based on morphology and metric comparison with pure blue and black wildebeest. To this end, 14 skeletons of modern hybrid *Connochaetes taurinus* and *Connochaetes gnou,* from more than one post-hybridisation generation from the Spioenkop reserve, were morphologically and metrically compared with a sample comprising 15 modern blue and 15 black wildebeest. This goal was achieved using a comparative morphological and statistical approach.

This chapter focuses on features in Spioenkop specimens that exhibit statistical and morphological deviation from modern blue and black wildebeest. The identification of these features as characteristic to hybrids is discussed.

7.1 Hybridisation effects

7.1.1 Statistical analysis of the skull

At the start of this study, it was assumed that some the Spioenkop Specimens would be hybrids. It was hypothesised that the measurements would plot between the measurements of the parent species due to the size differences between *C. gnou* and *C. taurinus*. In each case, the hybrids should theoretically be bigger than the black wildebeest. The evolution of the black

wildebeest is characterised by a general reduction in body size (Brink 1993), with some varying morphological features (see chapter 2) and changes in horn morphology. This is confirmed in the bivariate plots where black and blue wildebeest plot along a straight line for many of the features (Brink 2005).

The following features in the crania of some Spioenkop hybrids plotted below the range of black wildebeest:

- Basal length of the skull
- Condylobasal length
- Distance between the posterior tuberosities
- Length of the premolar row
- Premolar to the Prosthion

Statistical plots also show many features for the Spioenkop specimens falling into the blue range. These include:

- Akrokranion to the rhinion
- Breadth of the occipital condyle
- Ectorbitale to the entorbitale
- Greatest breadth of the nasal
- Height of the foramen magnum
- Length of the premolar row
- Postdentale to the aboral boarder of the occipital condyle.

For these features, there was little or no overlap between *C. gnou* and *C. taurinus*. This suggests that potential hybrids in the sample are in fact true

hybrids. Spioenkop specimens 12042, 12043 and 12054 have a high number of features that fall in the blue range. This could indicate an early generation of hybrid, where blue genes may be dominant. The rest of the Spioenkop group has features that plot (in varying degrees) in the blue range. This could be due to introgressing black wildebeest males. There is a large degree of variation within the sample.

Statistically the following features were found to be useful in identifying hybrids:

- Breadth of the occipital condyles
- Greatest breadth of the nasal

The above features were chosen because five or more individuals from the hybrid population plotted in the blue wildebeest range. A large number of individuals have this trait, which consistently outlies the black wildebeest range, even after many generations and possible introgression. This indicates the start of permanent change in the hybrid skull size and morphology relative to black wildebeest.

Also noted is a general trend to an increase in the size of the skull. Although many of the Spioenkop specimens plotted within the black wildebeest range, the standard error plots show a trend for larger means in this population.

Based on statistical results alone, specimens 12047 (female) and 12053 (male) can be considered as belonging to black wildebeest, as they consistently fall

within the black wildebeest range. This is not, however, the case with the morphological observations, as they display unusual morphology.

There are apparently permanent changes occurring in the hybrid sample. The features for which a consistent trend is seen, presumably over many generations, are as follows: for the breadth of the occipital condyle, the Spioenkop sample shows a tendency for a greater breadth, similar to the blue wildebeest. For the measurement of the greatest breadth of the nasal, the hybrid measurements indicate a trend towards a narrower nasal breadth than the black wildebeest. The auditory bullae throughout the Spioenkop sample are deformed. The Spioenkop specimens have earhole diameters which are larger than that of the blue wildebeest.

7.1.2 Morphology of the skull

Morphological differences in the Spioenkop specimens were great.

Inconsistent horn curvature was seen throughout the sample, with some individuals having horns that form wider angles than the black wildebeest relative to the skull, and others with unusual bends in the horns. Unusual horn morphology is thus a good indicator of hybridisation in wildebeest.

Excessive bone growth and fusion of all the sutures in the Spioenkop sample may be interpreted as an over-compensation against the blue gene, which codes for unfused sutures. Most of the Spioenkop specimens have deformed auditory bullae, a trait that is consistent over many generations of these

hybrids, and is therefore a useful indicator of hybridisation. All fourteen of the Spioenkop specimens have morphological differences in the skull, and are therefore interpreted as hybrids. This contradicts the statistical results which showed that two of the specimens plotted the same as the black wildebeest.

7.1.3 Statistical analysis of the post crania

Statistically, there was little difference in the post crania of the Spioenkop specimens and black wildebeest. The standard error plots did, however, show that while the Spioenkop specimens plotted within the black wildebeest range, there was a general trend for a larger size in the Spioenkop specimens. There is the exception of the scapula and distal radius, in which the trend in the hybrids was to be smaller than the black wildebeest, changes in the dimensions of the medial condyles of the metacarpal and metatarsal are also noted.

7.1.4 Morphological deviation in the post crania

Morphologically, there were many differences in the post crania of the Spioenkop specimens and black wildebeest. Excessive bone growth on postcranial elements was found on all the Spioenkop specimens in varying degrees, and is a good indicator that these individuals are hybrids. The deformities on the articular facets of some of the axes may be due to strain on the point of articulation between the axis and atlas. The wear pattern on the

trochlea of the femur caused by friction with the patella is also unusual and unique to the Spioenkop specimens. The fusion of the radius and ulna is a good indication of hybrid morphology, as this does not occur in either the blue or the black wildebeest. Specimens 12042, 12047, 12048, 12052 and 12054 have fusion of both the radius and ulna. This makes excessive fusion in the Spioenkop specimens an important indicator of hybridisation. Plots for the medial condyle of the metatarsal and metacarpal are unusual, as the achsial part trends towards being smaller than the black is, while the peripheral part trends towards being larger.

Morphological and metric deviations are more common in the skulls of the Spioenkop sample than in the postcrania. The large number of morphological deviations seen in the skull may be due to plasticity in the genes coding for the skull. When hybridisation occurs, features in the skull may be easier to change than the post crania.

The fact that there are more changes in the skull than the post crania may be considered significant, and can be understood in the context of the evolutionary process of the black wildebeest from a blue wildebeest ancestor (Brink 2005). In this process, skull and horn characters were the first to change, while morphological changes in the postcrania were less marked, and lagged behind the cranial changes (Brink 2005). This suggests that the cranium of the black wildebeest was of primary importance in the process of speciation. Therefore, the implication of the frequent differences in the crania

of the Spioenkop sample is that it reflects the evolutionary process of the black wildebeest (Brink pers comm. 2007).

7.1.5 Species concepts

The wildebeest hybrids pose interesting questions regarding species concepts. According to the the concepts discussed (evolutionary, mate recognition and ecological), black wildebeest could be thought of as a sub-species of the blue wildebeest. However, with regards to the biological species concept, it is no longer thought that fertile offspring can only result from conspecific parents (Brink pers. Comm. 2007). The split between the two species occurred relatively recently (1Ma) and there has been complete reproductive isolation in natural populations of wildebeest this was until human intervention. Black wildebeest is a stable independent species. Blue and black wildebeest are morphologically and behaviourally distinct, so while there has been geographic overlap of these species in the past, hybridization has not occurred. This hybridisation has only occurred due to artificial management. Therefore, the validity of *Connochaetes gnou* and *Connochaetes taurinus* as possible sub-species should not be based on a man-made problem. It must be considered that if these two species were left in their natural environment without human interference, there would most likely be no interbreeding (as there has been no evidence of this occurring in the past (Brink pers comm., 2006)) and the validity of the two as separate species would not be under question.

7.2 Conclusion

This study has proved successful in using a statistical as well as a comparative morphological approach to identify modern hybrids. For some features, the presumed hybrid Spioenkop specimens exceed the normal variation observed in black wildebeest, and shows overlap with the blue wildebeest range.

The extent of metric deviation or increased variability in the Spioenkop specimens in relation to black wildebeest is large, and is interpreted as the result of hybridisation. According to Internet reference 1, first generation hybrids show a high statistical deviation and are morphologically easily identifiable. From the statistics conducted in this study, specimens 12042 and 12043 are most likely first generation hybrids due to the high number of deviations from the black wildebeest. Specimens 12047 and 12053 were considered black wildebeest based on statistical analysis, but from the comparative morphology study, it is clear that all 14 specimens from the Spioenkop sample are hybrids. This demonstrates that identification of hybrids based on measurements alone may be deceiving, and that morphology must be considered. In the Spioenkop sample, unique traits are found that occur over many generations this indicates permanent changes occurring within the hybrid population.

There is no consistency in the deviations of the hybrid specimens. There is no middle ground for the hybrids. Plots are unpredictable and random for most features, and no certain range can be given for any measurement taken on the

Spioenkop specimens. Thus, any deviation seen from black wildebeest morphology can be considered due to hybridisation. The morphology seen in the hybrid specimens is unnatural, and the deformities and unusual wear patterns may be an indication that these animals are under genetic stress.

According to this study, hybrid wildebeest can be identified by an increase in body size relative to black wildebeest. This size increase cannot be given a quantitative scale as the pattern appears to be random in the Spioenkop hybrid plots but from the statistical analyses done it is fair to conclude that there is a general trend for an increase in body size in the Spioenkop sample. Hybrids can also be identified by an unnatural horn morphology and excessive bone growth around the basal bosses. From the statistical analyses, it is clear that the Spioenkop hybrids show a trend towards larger size in both the crania and post crania. Future studies will provide a better indication of whether traits identified as diagnostic/characteristic of wildebeest hybrids, are also present in other hybrid populations.

REFERENCES

ALEXANDER, G., 2004. *Island Biogeography*. Unpubl. Lecture notes APES 205. July-September.

BOESSNECK, J., & VON DEN DRIESCH, A., 1978. The significance of measuring animal bones from archaeological sites. In R.H. Meadow & M. Zeder (eds.) *Approaches to Faunal Analysis in the Middle East.* Peabody Museum Bulletin 2.

BRINK, J.S., 1993. Postcranial evidence for the evolution of the black wildebeest, *Connochaetes gnou*: an exploratory study. *Palaeontologia africana* **30:** 61-69.

BRINK, J.S., 2005. *The Evolution of the Black Wildebeest, Connochaetes Gnou, and Modern Large Mammal Faunas in Central Southern Africa*. Unpublished PhD Thesis, University of Stellenbocsh.

BRINK, J.S., BERGER, L.R. & CHURCHILL, S.E., 1999. Mammalian fossils from erosional gullies (dongas) in the Doring River drainage, central Free State province, South Africa. In Becker C., Manhart H., Peters J. & Schibler J., (Eds). *Historium animalium ex ossibus. Beitrage zur Palaoanatomie, Archaologoe, Agyptologie, Ethnologie und Geschichte der Tiermedizin: Festschrift fur Angela von den Driesch.* Verlag Leidorf M., Rahden/Westf., pp 79-90.

BROOM, R., 1913. Man contemporaneous with extinct animals in South Africa. *Annals of the South African Museum* **12**:13-16.

BROWN, J.D., 1988. *Understanding Research in Second Language Learning: a Teachers Guide to Statistics and Research Design*. London, Cambridge University Press.

CORBET, S.W., GRANT, W.S., & ROBINSON, T.J., 1994. Genetic divergence in South African wildebeest: analysis of allozyme variability. *Heredity* **82**(6): 479-483.

DOBZHANSKY, T., 1937. *Genetics and the Origins of Species*. Reprinted ed., 1982. Columbia University Press, New York.

EISENMANN, V., & BRINK, J. S., 2000. Koffiefontein “quaggas” and the true Cape quaggas: the importance of basic skull morphology. *South African Journal of Science* **96**:529-533.

ELDREDGE, N., 1993. What, if anything, is a species? In Kimbel, W.H. & Martin, L.B., (Eds). *Species, Species Concepts and Primate Evolution*. Plenum press, New York, pp 3-19.

ESTES, R.D., 1991. *The Behaviour Guide to African Mammals*. Russell Friedman, Johannesburg.

FABRICIUS, C., LOWRY, D. & VAN DEN BERG, P., 1988. Fecund black wildebeest x blue wildebeest. *South African Journal of Wildlife Research* **18:** 35-37.

GENTRY, A.W., 1978. Bovidae. In Maglio, V. & Cooke, H.S.B., (Eds). *Evolution of African Mammals.* Harvard University Press, Cambridge, pp. 540-572.

GENTRY, A. W., 1992. The subfamilies and tribes of the family bovidae. *Mammal Review* **22:** 1-32.

GENTRY, A.W., & GENTRY, A., 1978. Fossil bovidae (mammalia) of Olduvai Gorge, Tanzania. Part I. *Bulletin of the British Museum (Natural History)* **29:** 290-446.

GROBLER, J.P., HARTL, G.B., GROBLER, N., KOTZE, A., BOTHA, K. & TIEDMANN, R., 2005. The genetic status of an isolated black wildebeest (*Connochaetes gnou*) population from the Abe Bailey Nature Reserve, South Africa: micro satellite data on a putative past hybridisation with blue wildebeest (*Connochaetes taurinus*). *Mammalian Biology* **70:** 35-45.

HARRIS, J.M., 1991. Family Bovidae. In Harris, J.M., (Ed). *Koobi For a Research Project. The Fossil Ungulates: Geology, Fossil Artiodactyls and Palaeoenvironments,* 3. Clarendon Press, Oxford. Pp139-320.

KAPPELMAN, J., PLUMMER, T.W., BISHOP, L., DUNCAN, A. & APPLETON, S., 1997. Bovids as indicators of plio-pleistocene palaeo-environments in East Africa. *Journal of Human Evolution* **32**: 229-256.

KOK, O., & VRAHIMIS, S., 1995. Black wildebeest territorial clearings. *Journal Of African Zoology* **109**: 231-237.

LANGLEY, N., 1995. Black wildebeest x blue wildebeest hybrid at Spioenkop Nature Reserve. Unpublished Natal Parks Board report, pp 6.

MAYR, E., 1942. *Systematics and the Origins of Species*. Reprinted ed. 1982. Columbia University Press, New York.

MAYR, E., 1963. *Animal Species and Evolution*. Oxford University Press.

PATTERSON, H.E.H., 1985. The recognition concept of species. In Vrba, E.S., (Ed). *Species and Speciation.* Transvaal Museum Monograph No. 4. Transvaal museum, Pretoria. pp 21-29.

PLUG, I., & BADENHORST, S., 2001. *The distribution of macromammals in southern Africa over the past 30 000 years as reflected in animal remains from archaeological sites.* Transvaal Museum Monograph No. 12.

PLUG, I., & ENGELA, R., 1992. The macrofaunal remains from recent excavations at Rose Cottage cave, Orange Free State. *South African Archaeological Bulletin* **47:** 16-25.

PLUG, I., & PETERS, J., 1991. Osteomorphological differences in the appendicular skeleton of *Antidorcas marsupialis* (Zimmerman 1780) and *Antidorcas bondi* (Cooke & Wells, 1951) (Mammalia: Bovidae) with notes on the osteometry of *Antidorcas bondi. Annals of the Transvaal Museum* **35**(17): 253-263.

PLUMMER, T. W., & BISHOP, L.C., 1994. Hominid palaeo-ecology at Olduvai Gorge, Tanzania as indicated by antelope remains. *Journal of Human Evolution* **27:** 47-75.

RHYMER, J.M., & SIMBERLOFF, D., 1996. Extinction by hybridisation and introgression. *Annual Review of Ecological Systematics* **27:** 83-109.

SIMPSON, G.G., 1951. The species concept. *Evolution* **5:** 285-298.

SMITHERS, R.H.N., 1986. *Land mammals of southern Africa, a field guide*. Macmillan South Africa, Johannesburg. pp 154-158.

SZALAY, F.S., 1993. Species concepts the tested, the untestable and the redundant. In Kimbel W. H., & Martin L. B., (Eds). *Species, Species Concepts and Primate Evolution*. Plenum press, New York, pp 25-39

TOWNSEND, J., 2002. *Practical Statistics for Environmental and Biological Scientists.* John Wiley & Sons, Ltd.

VON DEN DRIESCH, A., 1976. A guide to the measurement of animal bones from archaeological sites. *Peabody Museum Bulletin* **1**: 1-136.

VON RICHTER W., 1974. Connochaetes gnou. *Mammalian Species*. **50**:1-6.

VRBA, E.S., 1985. Introductory comments on species and speciation. In Vrba E.S., (Ed). *Species and Speciation*. Transvaal museum Monograph No. 4. Transvaal museum, Pretoria, pp ix-xvii.

VRBA, E.S., 1979. Phylogentic analysis and classification of fossil and recent Alcelaphini Mammalia: Bovidae. *Biological Journal of the Linnean Society* **11**:207-228.

Internet references

1) Black wildebeest and blue wildebeest hybridisation. *Current Issues Wildebeest Hybridisation.* [Online]. Available from: http://www.kznwildlife.com/WildebeestDetail.htm. [Cited 6 November 2006].
2) Species concepts. [online] Available from: http://163.238.8.180/~fburbrink/Courses/Evolution/Evolution%2018.ppt#261,6,EvolutionarySpeciesConcept(ESC) [cited 25 November 2006].

APPENDIX

Table 100: Measurements of the skull, part A.

Species	Specimen Number	Profile Length	Condylobasal Length	Basal Length	Short Skull Length	Premolare-Prosthion	Nasion - Prosthion	Akron - nasion	greatest frontal length	Akron - Rhinion	Nasion - Rhinion	Arboral -enorbit	Ectorb - Prosthion	Aboral - Infraorbital	Infraorbit - Prosthion	Dental length
Spioenkop	**12042**	418.4	395.8	369.5	254.5	116.9	236.5	.	230	357.3	157.7	202.9	278.8	266.2	136.1	205
Spioenkop	**12043**	432.5	398.6	377.8	258.8	119.4	250.2	.	.	365.8	.	.	.	267.5	140.8	209.3
Spioenkop	**12044**	377.4	371	245	243.2	104.3	225.8	168	185.5	313.7	145.3	186.4	254.1	247.2	127.4	199.4
Spioenkop	**12046**	393	386.8	362.9	259.2	114.5	232	184.1	198.5	337.7	155.2	185.3	276.4	259.2	130.9	209.4
Spioenkop	**12047**	392.5	365.7	342.1	232.8	110.1	234.2	189.7	209.8	344.9	155.7	180.3	261.1	239.7	130.9	188.8
Spioenkop	**12048**	389.5	373.3	350.9	243.4	114.6	241.9	175	199.6	330.4	158.5	182.6	269.2	249.7	134.1	196.9
Spioenkop	**12049**	391.2	379.3	354.7	240.7	116.2	231.3	181.5	197	331.6	152.3	190.8	268.3	252	130.7	198.6
Spioenkop	**12050**	396.8	378.4	353.9	242.6	112.5	236.3	194.5	207	341.9	155.6	190.4	271.6	252	130	205.9
Spioenkop	**12051**	407.7	384.7	357.2	240.8	116.4	239	.	.	347.2	150.6	.	268.1	248.2	137.8	199.2
Spioenkop	**12052**	401.4	392.3	368.1	252.2	115.4	233.4	187.8	207.2	341.4	150.4	193.9	276.7	259	136.2	201.5
Spioenkop	**12053**	384.5	366.6	341.5	236.3	106.3	231.8	178	199.4	321.4	144.9	174.7	260	243.7	123.2	190.6
Spioenkop	**12054**	419.1	393.9	364.6	254.4	120.2	245.6	.	202.7	364.8	157.6	.	281	262.7	133.3	198.7
Spioenkop	**12060**	405.5	383.7	358.3	245	113.8	241.2	195.9	210.3	357.5	166.2	191.4	272.8	254.7	134	228.6
C. gnou	**M84**	402.3	390.2	355.5	243.6	113	233.8	193.8	202.4	348.5	154.4	185.5	270.5	251.6	132.6	203.9
C. gnou	**NMB92**	393.4	376.3	350	247	103.7	229.4	174.6	191.2	322.1	150.4	183.3	245.6	255.2	125.8	197.7
C. gnou	**NMB81**	.	.	.	231.2	.	.	177	207.4	.	.	186	.	242.3	.	.
C. gnou	**NMB96**	.	.	.	250.7	.	.	193.3	202.1	343.7	150.8	192.4	.	257.1	.	.
C. gnou	**NMB93**	.	.	.	.	.	.	184.1	204.6	.	.	.	.	.	.	.
C. gnou	**1930NMB**	385.1	377.1	354.9	243.8	110.5	240.1	172.6	187.9	330.3	161.3	180.8	268.8	248.2	135	203.2
C. gnou	**M89**	406	380.4	361.8	250	111.7	235.4	189.3	196.4	345.9	155.1	188.5	272.5	254.4	130.3	206.5
C. gnou	**M90**	412	379.3	356.8	249.7	108.3	238	186.8	201.2	353.2	166.1	184.8	269	260.9	123.6	203
C. gnou	**NMB80**	393.3	376.4	353.8	246	108.7	233	176.5	197.3	326.8	150.6	177.7	273	248	140	205
C. gnou	**SUBFOSS41464**	401.9	370.2	349.9	248.4	102	.	.	.	.	.	172.9	249.1	247.6	127.9	193.5
C. gnou	**SUBFOSS c438**	.	.	.	241.4	.	.	182.2	.	.	.	180	.	247.3	.	.
C. taurinus	**NMB57**	493.8	483.2	452.2	304.7	148	334	202.9	209.1	448.3	251.1	218.3	358.4	321.8	167.7	269.9
C. taurinus	**NMB12172**	441.5	437.6	410.2	271.6	140	290.7	195.8	206.4	413	212.3	190.4	333.3	295	151.6	235.6
C. taurinus	**NMB77**	496.9	481.6	452.9	304.7	147.5	316.9	229.1	238.2	449	228.9	215.4	359.6	322.8	171.5	261.5
C. taurinus	**NMB12209**	438.6	423.8	398.5	266.5	132.6	286.1	200.6	229	399	209.7	190.2	326.6	284.3	150	241.3
C. taurinus	**NMB12088**	415.3	412.1	385.4	266.8	129.6	261	180	184.9	355.1	179.3	189	309.5	270	148.8	232.4
C. taurinus	**NMB9355**	427.6	431.6	400.1	259	142.1	259.2	201.4	213	378.2	278.3	290.6	312.6	290.2	147.1	251.4
C. taurinus	**NMB12066**	419.4	416.1	389.1	257.7	130.3	269	194	221.8	382.2	201.8	186	310.5	276.6	144	234.5
C. taurinus	**NMB12064**	403.4	401.7	371.3	258.8	124.6	251.7	185.5	190.5	350.1	.	183.5	298.3	262.6	140.9	223.2
C. taurinus	**NMBF64**	457	446.2	415.8	280	135.3	281	.	225.5	419.5	206.2	197.7	345.8	296.6	155.6	245.5
C. taurinus	**NMB73**	511.2	494.6	.	.	149.9	332	226.4	242.4	470.1	250.7	222	365.6	334.7	171.9	267.6

Table 101: Measurements of the skull, part B.

Species	Specimen Number	Oral palatal length	Nasiointermax -Prosthion	length chktooth row	length mol row	length premolar row	ectorb - entorb	inner height orbit	otion - otion	breadth occicondyles	breadth foram mag	height foram mag	least breadth btw condyles	least frontal breadth	ectorb-ectorb	entorb-entorb
Spioenkop	**12042**	165.3	129.1	87.2	63.9	25.4	54.3	54.5	160.4	90.6	23	28	.	126.7	161	106.7
Spioenkop	**12043**	173.5	136.9	92.7	64.2	29.2	.	.	167.3	90.5	29.9	23.1	24.3	123.5	.	106.1
Spioenkop	**12044**	155.7	125.6	94.9	67.4	30.7	53	57.4	145.9	82.2	27.9	26.5	26.9	104.6	150.7	86.9
Spioenkop	**12046**	164	125.6	96.8	65.9	35.1	52.1	54.6	146	86.3	27.6	25.6	24.9	111.9	143.7	91.3
Spioenkop	**12047**	160.6	130.4	80.4	60	25.5	48.9	53.8	149.3	81	28.1	24.7	11.7	119	143.6	84
Spioenkop	**12048**	169.3	127.5	85	61.9	25.7	52.3	51.5	144.1	83.2	.	23.1	20.2	107	143.5	89.4
Spioenkop	**12049**	159.1	126.6	89	62.7	32.5	54	55.2	154.2	88.3	32.7	23.7	33.9	110.1	151.8	92.5
Spioenkop	**12050**	159.9	134.9	95.9	63.5	35.7	54.6	55.6	160.3	81.5	29.4	27.7	36.7	114.3	50.9	94.2
Spioenkop	**12051**	167.7	128.6	85.2	61.9	24.4	.	59.8	150.5	92.4	32.4	24.2	18.5	123.6	149.3	90.5
Spioenkop	**12052**	164.3	126.9	87.1	60.6	28.8	.	52.5	157.9	90.9	31.3	23.1	.	124	154.5	95.2
Spioenkop	**12053**	157.1	128	87.2	64	29.4	52.9	54.4	144.4	77.5	25.8	22.7	.	117.9	154.3	88.9
Spioenkop	**12054**	175	127.8	81.9	59.7	27.7	55.8	55.4	158.4	92.8	29.3	24.6	.	126.4	158.6	100.3
Spioenkop	**12060**	164.1	126.3	94.3	63.5	35	52.9	53.8	151.9	89.1	31.8	26.1	6.1	115.9	150.7	91.7
C. gnou	**M84**	163.9	127	93.3	66.8	34.7	51.2	56.5	148.9	85.5	25.8	24.6	33.6	116.6	151.9	90
C. gnou	**NMB92**	159.4	122.1	94.6	64.7	28.2	49.6	51.7	141.7	81	29.9	21.6	52	116.2	145.4	84.4
C. gnou	**NMB81**	.	.	86.7	60.5	28.5	49.4	51.6	.	76	30.9	24.3	21.3	114.9	142.7	84.6
C. gnou	**NMB96**	.	.	.	.	.	51.4	57.1	158.2	82.6	30.6	25.6	.	122.4	148.4	92
C. gnou	**NMB93**	.	.	.	.	.	53.6	56	.	.	.	.	30.6	117.4	148.7	83.4
C. gnou	**1930NMB**	162	127.4	92.9	66.5	30.6	49.4	51.7	145.9	78	30.8	.	46.6	122.1	152.3	90.3
C. gnou	**M89**	146.5	121	.	.	.	49.4	52.8	159.5	82.1	27.3	24.9	31.8	124.2	153.8	92.7
C. gnou	**M90**	168.4	120.5	97.1	67.7	32.5	50.6	54.7	146.7	83.5	.	.	26.4	113.2	147.7	87.5
C. gnou	**NMB80**	163	125.6	95.1	67.8	29.4	47.2	50.6	140	78.4	26.4	22.3	38.7	113.1	147.5	88.8
C. gnou	**SUBFOSS41464**	161.6	.	91.8	67.8	27.6	53.5	56.8	159.9	80.1	27.2	20.3	18.7	122.2	158.9	87.9
C. gnou	**SUBFOSS c438**	.	.	81.5	55.9	27.8	47.9	54.1	145.2	.	.	.	40.3	121.3	148.4	91.6
C. gnou	**C1463**	.	.	.	.	.	.	.	153.5	88.5	.	.	27.1	128.5	.	.
C.taurinus	**NMB57**	226.1	139.4	121.6	81.2	41.9	57.1	59.1	.	102.2	29.1	31.9	58.1	146.6	186.6	122.7
C.taurinus	**NMB12172**	201.4	133.3	101.3	65.4	37.1	52.6	55.7	167.5	88.3	29.2	31.5	79	130.3	167.6	102.3
C.taurinus	**NMB77**	222.5	144.7	115.9	74.6	43.6	56.2	60	182.3	103.4	29.3	34.6	53.2	152.2	189	126
C.taurinus	**NMB12209**	196	128.6	108.9	72.4	32.6	53.3	53.2	160	86.5	32.3	33.6	46.2	125.9	153.5	97.1
C.taurinus	**NMB12088**	196.4	123	104.2	70.7	35.7	52.6	51.6	164.3	85.4	29.6	25.9	58.7	135.8	172.5	113.4
C.taurinus	**NMB9355**	192.4	120.7	109.9	75.1	39.2	58.2	58.8	174.8	97	32.5	34.6	46.3	149.2	172.9	81.1
C.taurinus	**NMB12066**	191.3	119.1	106.3	70.9	35.8	51.5	50.8	167.7	89.2	31.4	30.6	86.7	135	161.8	114.3
C.taurinus	**NMB12064**	184.5	117.3	100.5	75.1	27.9	51	53.9	156.7	95.6	31	31.3	79.5	146	158.6	106.6
C.taurinus	**NMBF64**	199.4	126.8	110.8	70.2	37.5	53.2	55.3	171.7	99.5	30.5	32.4	.	141	176	108.6
C.taurinus	**NMB73**	225.9	139	122	74.9	45.6	59.3	60.8	193.8	108.5	.	.	160.2	193	196.8	124.1

Table 102: Measurements of the skull, part C.

Species	Specimen Number	facial breadth	greatest breadth nasal	least inner height temp	Dwa	Dwp	Dcbo	D
Spioenkop	**12042**	89.2	45.9	39.2	17.6	22.8	104.4	28.4
Spioenkop	**12043**	94.9	45.8	43.4	16.7	19	106.2	26.5
Spioenkop	**12044**	81.7	38.9	43.4	13.6	18	94.1	23.2
Spioenkop	**12046**	84.4	38	40.7	11.6	11.6	97.6	30.2
Spioenkop	**12047**	71.8	46.6	35.7	16.6	9.4	88.9	20.9
Spioenkop	**12048**	79.5	39.9	39.8	11.6	23.7	98.7	30.2
Spioenkop	**12049**	84.8	39.8	43.2	16.6	20.8	89.4	22.7
Spioenkop	**12050**	89.5	40.9	40.4	14.1	18.4	94.5	37.1
Spioenkop	**12051**	82.1	46.4	40.3	15.3	14.4	83.4	20.3
Spioenkop	**12052**	86.6	45	36.5	15.4	17.1	100.8	30.3
Spioenkop	**12053**	81.9	43.5	41.3	17.2	14	85.8	26.2
Spioenkop	**12054**	89.6	50.1	42.6	10.8	16.6	100.4	26.7
Spioenkop	**12060**	83.4	42.6	40.5	11.9	14.6	104.3	28.6
C. gnou	**M84**	80	44	40.3	12.6	13.4	87.8	24.1
C. gnou	**NMB92**	81.4	40.2	44.1	12.4	17.1	98	26.1
C. gnou	**NMB81**	82.6	.	39.4	12.2	18.9	94.9	22
C. gnou	**NMB96**	.	45.2	42.2	16.8	16.1	100.9	24.7
C. gnou	**NMB93**	84.4	.	38	.	.	.	.
C. gnou	**1930NMB**	88.8	45.1	40	13.3	18	91.1	25.5
C. gnou	**M89**	87.1	47	41.9	15.6	14	114.4	25
C. gnou	**M90**	.	44.8	47.1	10.5	13	93.3	26.9
C. gnou	**NMB80**	86	42.7	40.8	14.3	15.4	93.9	22.4
C. gnou	**SUBFOSS41464**	80.9	.	33.6	13.1	11.6	.	24.5
C. gnou	**SUBFOSS c438**	79.2	.	43.2	12.7	11.2	93.4	22.2
C. gnou	**C1463**	.	.	.	11.5	17.1	.	25.3
C. taurinus	**NMB57**	88.9	42.3	42.3	14.2	16.3	113.5	41.2
C. taurinus	**NMB12172**	92	36.8	40.6	19.1	12.9	99.9	28.7
C. taurinus	**NMB77**	101	41.8	36.9	24	12.3	106.9	33.4
C. taurinus	**NMB12209**	74.9	32.9	36.2	11.5	19.2	.	31.2
C. taurinus	**NMB12088**	99.5	30.4	41.1	15	10.8	94.6	24
C. taurinus	**NMB9355**	83.3	.	36.5	18.7	22.5	103.4	32.9
C. taurinus	**NMB12066**	88.4	33.1	118.2	8.9	17.9	94	27.7
C. taurinus	**NMB12064**	85.3	.	32.7	15.2	18.4	100.8	22.3
C. taurinus	**NMBF64**	87.5	36.6	41.1	16.7	21	97.7	30
C. taurinus	**NMB73**	92.2	40.9	42.3	.	.	.	44

Table 103: Measurements of the lower jaw.

Species	Specimen number	Lngth Chktth row	lngth molar row	lngth premolar row	M2L lower	M2B lower
Spioenkop	12042	86.3	66.4	20.7	20.1	11.4
Spioenkop	12043	91.8	69.3	20.4	21.8	12.3
Spioenkop	12044	100.4	76.4	23.7	25.9	11.4
Spioenkop	12046	103.3	69.8	30.5	24.7	11.4
Spioenkop	12047	84.9	65.7	18.5	20.3	10.9
Spioenkop	12048	85.4	66	34.5	20.9	11.1
Spioenkop	12049	89.5	67.2	21.6	20.2	11.8
Spioenkop	12050	102.4	70.2	35.1	24.5	10.6
Spioenkop	12051	88.9	67.6	21.2	21.1	12.2
Spioenkop	12052	88.7	68.4	20.2	21	11.2
Spioenkop	12053	89.5	64.8	23.1	22	10.1
Spioenkop	12054	87.5	65.3	20.7	20	10.3
Spioenkop	12060	98.5	67.2	32.1	24.7	10.4
C. gnou	NMB-F6011	88.5	67.3	20.8	20.3	11.5
C. gnou	A1215	88.5	68.3	20.3	20.4	12
C. gnou	A1596	93.4	70.8	22	21.9	12.2
C. gnou	NMB-F9411	92.4	71.8	22.2	22.4	10.5
C. gnou	NMB-F9413	90.2	70.3	19.1	22.4	11.4
C. gnou	NMB-F9408	88.1	69	19.4	21.8	10.8
C. gnou	UNK1	92	71.5	19.5	21.5	11.3
C. gnou	UNK2	93.6	70.5	21.9	21.8	10.5
C. gnou	UNK3	92.5	72.2	21.6	21.8	11.5
C. gnou	A1600	91.5	70.6	21.2	21.3	12.1
C. gnou	A2945	96	71.1	22.5	23.3	12.5
C. gnou	A1601	95	70.7	24.2	21.6	12.1
C. gnou	NMB-F9391	93.3	72.3	20.7	22.5	11
C. gnou	NMB-F9358	103.7	76.7	25.4	25	11
C. gnou	NMB-F8742	98.3	73.1	23.2	22	10
C. gnou	UNK4	95.5	73.8	22.3	23.2	10.8
C. gnou	NMB-F9870	102.5	78.5	23	24.5	10.4
C. gnou	NMB-F7447	94.5	71.2	22.2	23	10.9
C. gnou	NMB-F6029	94.8	72	22	23.1	11.1
C. taurinus	NMB-F 8732	110.4	79.2	29.8	23.5	12.4
C. taurinus	NMB-F 9356	110.7	81.2	29.6	26.4	12.6
C. taurinus	A1039	118	84	34.4	26.6	12.4
C. taurinus	NMB -F9357	112	77.7	35.5	27.8	13.2
C. taurinus	A2840	110	78.7	31.9	24.6	13.1
C. taurinus	Unk1	119	86.1	33.2	26.9	13
C. taurinus	A1438	111.3	85	26.1	25.6	12.9
C. taurinus	NMB-F9310	111.2	81	30.2	25.9	12.3
C. taurinus	A1441a	106.2	76.8	28.9	25.4	14
C. taurinus	A1441b	110.5	77.9	32.8	26.9	11.8
C. taurinus	Unk2	112.7	81.6	28.3	26	12.4
C. taurinus	Unk3	110.5	79.2	34	26.1	11.6

Table 104: Measurements of the axis.

Species	Specimen number	LCDe	LAPa	BFcr	SBV	BFcd	H
Spioenkop	12042	.	.	72.6	44.5	39.1	.
Spioenkop	12043	.	.	.	.	.	.
Spioenkop	12044	74.8	61.5	71.1	42.7	37.5	88
Spioenkop	12045	.	.	.	.	.	.
Spioenkop	12046	80.9	74.2	69.3	.	34.8	84
Spioenkop	12047	93.1	75.1	65.5	40.1	37.4	91.5
Spioenkop	12048	.	.	.	.	.	.
Spioenkop	12049	85.2	69	70.3	42.6	34.7	86
Spioenkop	12050	.	.	.	.	.	.
Spioenkop	12051	84.5	74.1	70.7	43.6	40.3	96
Spioenkop	12052	87.6	79.2	69.5	42.3	38.9	98.5
Spioenkop	12053	85.2	71.9	68.7	41	34.8	98
Spioenkop	12054	84.2	80.2	71.2	44.6	39.2	101
Spioenkop	12060	.	.	.	.	.	.
Gnou	SAM39121	81.6	71	65.7	42.6	36.9	87.5
Gnou	SAM39318	84.8	72.2	65.9	41.9	34.6	93
Gnou	SAM39233	84.2	68.9	67.6	42.1	36.5	87
Gnou	SAM38249	75.7	63.8	63.5	40.5	35	86
Gnou	SAM36660	87.5	78	72.9	43.5	39.5	104
Gnou	SAM36675	86.4	77.4	74.2	41.5	40.7	106
Gnou	SAM38783	82.6	72.5	67.8	43.4	37.8	91.5
Gnou	SAM37090	84.7	75.9	66	41	37.6	95
Gnou	SAM35619	83	68	63.6	40.8	35	86.7
Gnou	SAM35853	85.7	72	71.8	42	40.5	97.5
Gnou	SAM36710	80.9	61.7	67	43.4	36	85
Gnou	NMB-F8708	96.1	91.1	72.3	46.4	42.1	109.6
Gnou	NMB-F9779	87.5	78.7	68.5	43.9	36.3	102.5
Gnou	NMB-F8742	88.5	76.1	72.4	50	38.9	87
Gnou	NMB-F8741	85.4	67.8	64.1	38.5	31.5	94
Gnou	NMB-F7439	75.8	71.2	66.5	40.9	34.6	98.5
Gnou	NMB-F8736	80.1	71	67.6	40.4	36.1	105
Gnou	NMB-F9358	78.3	80.3	73.2	44.9	34.6	99
Gnou	NMB-F7447	82.4	71.1	70.9	41.7	36.3	114.5
Taurinus	SAM36108	99.2	86.4	72.8	43.3	42.2	114
Taurinus	NMB9352	104.8	87	82.2	45.7	42.8	103
Taurinus	NMB9356	96.2	84.5	80.4	43.6	41.4	129
Taurinus	NMB8737	108.6	112	92	48.4	46.4	.
Taurinus	AZ563	100.7	93	81.4	42.8	45.2	.

Table 105: Measurements of the scapula.

	Specimen Number	Ld	HS	DHA	SLC	GLP	LG	BG
Spioenkop	**12042**	145.4	294.7	299	38.7	63.2	47.7	39.5
Spioenkop	**12043**	142.3	307.2	312.6	37.3	61.3	42.6	39.4
Spioenkop	**12044**	128.3	277.9	276.3	36.7	65.5	41.8	36.2
Spioenkop	**12045**	129.4	271.6	274	34	58.4	43.5	36.3
Spioenkop	**12046**	152.7	309.6	302.3	37.6	65.5	50.5	44
Spioenkop	**12047**	142.6	273.7	279.2	35.7	58.9	43.5	38.1
Spioenkop	**12048**	126.9	276	273.6	34.6	57.6	43.5	34.9
Spioenkop	**12049**	122.5	275.5	273	36.3	57.3	41.1	36.6
Spioenkop	**12050**	122.5	273.3	277.3	33.2	55.7	40.4	35.7
Spioenkop	**12051**	139.4	282.7	284.8	36.6	63.1	47	40.7
Spioenkop	**12052**	144.2	288.4	287.4	35.6	59.1	44.5	38
Spioenkop	**12053**	128	282.1	282	34.7	52.9	40.3	35.9
Spioenkop	**12054**	140.8	290.1	290.1	40.6	62.1	46.3	40.7
Spioenkop	**12060**	127.9	272.4	278.6	35.9	62	47.1	39.5
Gnou	**NMB7447**	/	/	/	36.2	58.7	43.5	39.8
Gnou	**NMB8708**	152.3	308.2	308	39.2	63.8	49	43
Gnou	**NMB6029**	140.7	282	292	34.3	59.9	42.4	34.5
Gnou	**NMB12394**	139.4	295.4	292	32.3	56.3	42.7	37.2
Gnou	**NMB9779**	146.7	295.6	299	37.3	61.4	42.1	38
Gnou	**NMB8741**	111.3	265.2	269	31.6	52.6	39.8	35.2
Gnou	**NMB8736**	133.6	276.9	279.8	36.2	58.3	41.2	35.1
Gnou	**NMB9358**	138.2	302.3	310.5	41.4	61.8	46.3	42.2
Gnou	**NMB9870**	133.9	306	/	38.1	62.3	45.7	41.4
Taurinus	**NMB8737**	162.8	365.3	364.1	45.4	73.2	54.5	47.7
Taurinus	**NMB9352**	161.4	337.6	343.4	41.8	65.7	49.3	40.2
Taurinus	**NMB9356**	185.9	352.2	363.1	45.9	81.3	55.1	48.8
	Specimen Number	**Ld**	**HS**	**DHA**	**SLC**	**GLP**	**LG**	**BG**

Table 106: Measurements of the humerus.

Species	Specimen number	GL	Bd	SD	BT
Spioenkop	12042	234.2	55.3	28.6	53
Spioenkop	12043	229.4	60	29.2	54.4
Spioenkop	12044	214.7	55.4	26.6	51.7
Spioenkop	12045	.	.	.	.
Spioenkop	12046	226.1	53.8	29.5	54.3
Spioenkop	12047	218	57.9	26.5	52.4
Spioenkop	12048	220.5	56	26.7	51
Spioenkop	12049	211.4	56.4	26.6	52.8
Spioenkop	12050	.	.	.	.
Spioenkop	12051	224.7	58.7	27.4	53.8
Spioenkop	12052	223.9	55.3	25.8	51.6
Spioenkop	12053	218.6	52.5	24.9	51.1
Spioenkop	12054	234.2	60.4	29.3	55.9
Spioenkop	12060	.	.	.	.
Gnou	SAM 39122	210.4	.	27.2	51.6
Gnou	SAM 39311	.	51.1	.	50.4
Gnou	SAM 39231	207.3	54.9	26.4	51
Gnou	SAM 38249	198.2	50.8	24.4	48
Gnou	SAM 36660S	220.6	53.4	27.5	52.5
Gnou	SAM 36675	220	59.4	26.6	52.7
Gnou	SAM 38783	209.5	.	26.9	51.6
Gnou	SAM 37090	218	.	26.8	51.9
Gnou	SAM 35619	210.8	50.8	23.9	49.3
Gnou	SAM 35853	226.5	53.8	28	53.5
Gnou	SAM 36239	218.5	54	26.5	51.7
Gnou	SAM 36710	204.2	53	28.4	51
Gnou	NMB 8708	234	60.7	29.7	56
Gnou	NMB 9779	232	60.9	30.4	53.2
Gnou	NMB 8742	227.6	62.8	29.9	54.6
Gnou	NMB 8741	210	53.8	25.8	50.3
Gnou	NMB 7439	210	49.8	25.4	47.9
Gnou	NMB 8736	218.5	54.7	26.9	51.7
Gnou	NMB 7447	223.5	57.3	28	53.9
Gnou	NMB 9358	248.5	59.1	29.7	58
Taurinus	TMAZ 563	242	62.1	34.5	60.4
Taurinus	SAM 36064	256.5	60	33	59
Taurinus	SAM36108	262	65.6	34.9	60.2
Taurinus	NMB 9352	250	60.2	.	55.7
Taurinus	NMB 9356	273	70.6	.	64.5

Table 107: Measurements of the radius.

Species	Specimen number	G.L	Bp	Bd
Spioenkop	12042	284.9	61.6	45.1
Spioenkop	12043	282.2	60.9	46.7
Spioenkop	12044	261.1	58.6	41.9
Spioenkop	12045	.	.	.
Spioenkop	12046	279.5	63.9	54.5
Spioenkop	12047	253.6	60.5	44.6
Spioenkop	12048	259	60.3	44.1
Spioenkop	12049	258.2	59.1	44.9
Spioenkop	12050	.	.	.
Spioenkop	12051	277.2	63	43.8
Spioenkop	12052	278.1	58.2	42.4
Spioenkop	12053	263.6	56.2	43.8
Spioenkop	12054	273.4	62.5	45.6
Spioenkop	12060	.	.	.
Gnou	SAM39121	259.3	57.5	49
Gnou	SAM39318	273.3	55.1	.
Gnou	SAM39233	262.4	57.6	47.3
Gnou	SAM38249	245.2	54.2	46.5
Gnou	SAM36660	269	58.1	50
Gnou	SAM36675	267.8	58	54.6
Gnou	SAM38783	256	59.2	46.6
Gnou	SAM37090	266	58.4	45
Gnou	SAM35619	246.5	56.4	47.9
Gnou	SAM35853	287.2	59.5	52.2
Gnou	SAM36239	268.6	55.7	48.4
Gnou	SAM36710	255.5	57.2	50
Gnou	NMB8708	282	66.1	53
Gnou	NMB9779	284	65	52.8
Gnou	NMB8742	274.9	62	52.1
Gnou	NMB8741	265.5	56.4	46.2
Gnou	NMB7439	248	54.3	44.8
Gnou	NMB8736	258.7	59.9	49.2
Gnou	NMB7447	269.8	59.7	52.4
Taurinus	TMAZ563	304.3	70.4	59.9
Taurinus	M	312	67.4	58.2
Taurinus	SAM36108	319	70.6	60.1
Taurinus	NMB9352	309.6	69	59
Taurinus	NMB9356	337	77.9	68.7

Table 108: Measurements of the metacarpal.

Species	Specimen number	GL	Bp	Depth of prox end	Smllst brdth diaphysis	DD	Bd	Dda	Ddp
Spioenkop	12042	208.7	42.1	30	23.8	17.5	46.1	24.8	21.2
Spioenkop	12043	206.6	40.9	27.1	24.4	18.3	45.4	24.1	20.9
Spioenkop	12044	202.9	40.4	27.5	22.9	15.6	43.9	22.8	20.7
Spioenkop	12045	201.9	43.8	27.7	21.6	16.6	43.6	23.3	20.1
Spioenkop	12046	208.3	41.9	28.6	24.7	17.3	46.2	24.3	21.3
Spioenkop	12047	192.8	40.8	28.6	21.5	15.5	44.7	22.7	19.8
Spioenkop	12048	197.7	41.9	28.4	22.8	17.1	43.6	23.2	20.2
Spioenkop	12049	192.5	40.5	26.4	21.6	16.5	43.2	23.2	19.6
Spioenkop	12050	.	39.6	26.3	22	17.3	42.7	.	.
Spioenkop	12051	205.2	44.2	29	23.9	16.8	46.3	24.2	21
Spioenkop	12053	197.7	40.4	26.8	21.6	16.3	43.9	.	.
Spioenkop	12052	200.9	41.3	27.4	22.7	16.8	44.8	24.6	20.8
Spioenkop	12054	204.4	43.3	29.8	24.5	18.5	46.1	24.7	21.6
Gnou	SAM38981	201.8	43.4	27.9	24.2	18.5	44.6	.	.
Gnou	SAM39122	191.5	39.4	26.4	22.4	16	43.3	.	.
Gnou	SAM39311	195.8	40.7	.	22.2	17.4	42	.	.
Gnou	SAM39233	186	40.6	26.8	21.7	16.7	42.8	.	.
Gnou	SAM38249	181.7	39.4	26	20.7	15.7	41	.	.
Gnou	SAM36660	196.1	41.2	28.1	22.9	17	43.6	.	.
Gnou	SAM36675	190	43.4	30.4	22.7	16.5	46.8	.	.
Gnou	SAM38783	191.4	39.7	25	22	16.1	43.3	.	.
Gnou	SAM37090	190.1	40.2	27	22.2	16.1	43.4	.	.
Gnou	SAM35619	183	39.4	27.7	21	16.5	42.7	.	.
Gnou	SAM35853	200.9	43.4	28.2	22.6	17.2	44.8	.	.
Gnou	SAM36239	200.5	42	27	20.9	.	43.5	.	.
Gnou	SAM36710	185	40	27.4	22.8	15.5	42.6	.	.
Gnou	NMB8708	206.9	44	29.8	23.3	17.8	45.6	25.1	20.2
Gnou	NMB9779	204.4	44	27.2	24.3	17.2	46.7	25.3	20.5
Gnou	NMB8742	202.5	42.5	27.4	24.4	18.3	44.7	25.4	20.5
Gnou	NMB8741	195.2	36.9	26.3	21.6	15.8	41.5	21.6	17.7
Gnou	NMB7439	186.7	40.1	25.3	20.7	15.6	41.6	22.3	17.9
Gnou	NMB8736	196.8	42.5	27	21.9	15.4	43.9	23.9	17.9
Gnou	NMB9358	209.7	44.7	29.3	24.3	18	46.8	26	21.1
Taurinus	NMB9352	223	47.6	27.9	27.7	21.7	49.7	26.5	20.8
Taurinus	NMB9356	237	51.5	32.4	30	22.5	56.6	29.2	22.6
Taurinus	NMB8737	247.5	48.2	31	27.7	21.5	52.7	27.6	22.8
Taurinus	SAM36061	229.8	45.2	29	24.8	19	47.2	.	.
Taurinus	TM563	226.4	46.5	29	28.2	19.5	50.3	26.5	.
Taurinus	SAM36101	240.4	45.8	30.7	25.6	19.9	49	.	.

Table 109: Measurements of the femur.

Species	Specimen number	GL	Bp	SD	Bd
Hybrid	12042	283	87.4	27.2	70
Hybrid	12043	282	89.2	28.5	68.2
Hybrid	12044	258	84.5	25.8	67.5
Hybrid	12045	.	.	.	.
Hybrid	12046	285	94.4	28.1	75.5
Hybrid	12047	259	86.5	26.5	.
Hybrid	12048	266	86.4	25.5	67.8
Hybrid	12049	260	87.3	26.5	70
Hybrid	12050	.	.	.	.
Hybrid	12051	274	88.7	26.2	.
Hybrid	12052	271	88	25.7	68.8
Hybrid	12053	253	79.4	25.8	65
Hybrid	12054	282	93.8	27.3	70.6
Hybrid	12060	.	.	.	.
Gnou	SAM39121	262	81.9	25.5	67.7
Gnou	SAM39318	270	87.4	27.6	69.6
Gnou	SAM39233	261	84.4	25.6	66.1
Gnou	SAM38249	242	81.6	23.1	62.4
Gnou	SAM36660	278	82.6	28.2	70.4
Gnou	SAM36675	271	89.3	26.6	69.2
Gnou	SAM38783	256	85	26.5	67.6
Gnou	SAM37090	266	90.1	26.8	70.2
Gnou	SAM35619	252	79.8	24.4	66.4
Gnou	SAM35853	282	87.6	28.6	73
Gnou	SAM36239	263	82	26.8	63.8
Gnou	SAM36710	261	88.3	27.3	69.6
Gnou	NMB8708	292	94	30.5	76.5
Gnou	NMB9779	284	90.4	29.2	73.8
Gnou	NMB8742	286	91.3	29.5	70
Gnou	NMB8741	257	80.1	24.4	61.9
Gnou	NMB7439	256	79.1	25	69.5
Gnou	NMB8736	266	80.7	24.7	64.9
Gnou	NMB 9358	300	95.6	29.5	73.6
Gnou	NMB7447	273	88	27	69.1
Taurinus	TMAZ563	310	103.8	31.3	78.3
Taurinus	TMAZ1272	326	108.8	31	82.7
Taurinus	SAM36064	315	93	33.2	71.5
Taurinus	SAM36108	320	105.2	35	79
Taurinus	NMB9352	314	103.9	32.4	77
Taurinus	NMB9356	343	118	33.3	88.7

Table 110: Measurements of the tibia.

Species	Specimen number	GL	Bp	Bd
Spioenkop	12042	321.6	76.3	45.6
Spioenkop	12043	318.2	77.5	45.7
Spioenkop	12044	302.3	75.1	48.1
Spioenkop	12045	.	.	.
Spioenkop	12046	326.6	77.7	46.1
Spioenkop	12047	291.6	73	44.5
Spioenkop	12048	297.1	74.2	45.8
Spioenkop	12049	298.6	77	44.9
Spioenkop	12050	.	.	.
Spioenkop	12051	326.5	76.3	44.9
Spioenkop	12052	315.2	72.8	45.4
Spioenkop	12053	294.2	71.3	.
Spioenkop	12054	320.9	78.6	48.4
Spioenkop	12060	.	.	.
Gnou	SAM39121	296.6	71.3	45.4
Gnou	SAM39318	316	73.2	42.8
Gnou	SAM39233	297.7	70.8	41.7
Gnou	SAM38249	282.4	68	41.6
Gnou	SAM36660	319	75	43
Gnou	SAM36675	314	74	46
Gnou	SAM38783	290.6	72.8	42
Gnou	SAM37090	307.4	73.8	43.8
Gnou	SAM35619	282.5	69.2	42.4
Gnou	SAM35835	326	73.4	44.3
Gnou	SAM36239	305	70	40.3
Gnou	SAM36710	296	71.8	44.2
Gnou	NMB8708	335	79.4	49.3
Gnou	NMB9779	322	76.4	48.6
Gnou	NMB8742	317.5	75.9	47.7
Gnou	NMB8741	306.5	67.7	41.3
Gnou	NMB7439	290	72.8	44.1
Gnou	NMB8736	296.5	73.6	46
Gnou	NMB7447	312.5	76.4	45.7
Taurinus	TMAZ563	338.4	81	52.8
Taurinus	TMAZ1272	364.8	85.1	53
Taurinus	SAM36064	350	80	52
Taurinus	SAM36108	349	85.9	53
Taurinus	NMB9352	340	80.2	53.9
Taurinus	NMB9356	373.5	91.2	58.7
Taurinus	NMB8737	386	82.3	51.6

Table 111: Measurements of the metatarsal.

Species	Specimen Number	GL	Bp	Dp	SD	DD	Bd	Dda	Ddp
Spioenkop	12042	235.8	36.3	38.7	20.9	18.6	40.5	23.6	20.1
Spioenkop	12043	236.1	36.3	35.9	20.5	19.1	40.9	23.7	21
Spioenkop	12044	225.4	35.1	35.9	19.3	16.7	40.5	22.9	20.7
Spioenkop	12045	229.1	36.9	39.8	18.5	17.8	39.2	22.1	19.1
Spioenkop	12046	233.6	37	37.2	19.8	.	41.6	25.1	21.4
Spioenkop	12047	217.9	35.7	35.6	19.8	17.7	39.9	22.6	19
Spioenkop	12048	220.3	35.4	35.8	19.3	18.3	38.8	22.2	19.8
Spioenkop	12049	218.6	36	36	19.4	17.5	38.9	22.3	19
Spioenkop	12050	226.2	35.5	32.7	18.3	18.3	39.2	.	.
Spioenkop	12051	229.8	38.5	38.9	19.2	18.5	41.9	23.3	20.2
Spioenkop	12053	221.2	34.6	37	17.4	17.3	40.4	.	.
Spioenkop	12052	226.9	35	37.1	19	17.6	39.7	23.8	20.4
Spioenkop	12054	228.1	38.2	35.9	20.2	19.6	41.3	23.7	20.8
Spioenkop	12060	230.2	38.1	38.4	19.3	19	41	22.7	20.3
C. gnou	SAM38989	223.8	37.4	40.6	19.5	18.6	41.4	.	.
C. gnou	SAM39121	214.1	36	39.4	19.1	16.8	38.8	.	.
C. gnou	SAM39318	224.6	36.5	39.4	20	18.4	38.7	.	.
C. gnou	SAM39233	207.5	36	41.8	18.7	17.8	38.5	.	.
C. gnou	SAM38249	203	34.3	40	17.2	16.9	37.4	.	.
C. gnou	SAM3660	225.8	37.2	41.4	20	18.2	38.6	.	.
C. gnou	SAM36675	211.8	38.4	41	19.1	17.6	41.2	.	.
C. gnou	SAM38783	211.9	35.4	38.8	18.5	18	39	.	.
C. gnou	SAM37090	212.4	35.9	41.7	19.4	18.1	40.5	.	.
C. gnou	SAM35619	210.5	33.9	39	16.4	17	38.8	.	.
C. gnou	SAM35835	231.2	38	38.4	19.7	17.9	39.8	.	.
C. gnou	SAM36239	232.5	35.2	39	19	17.6	37.7	.	.
C. gnou	SAM36710	225.8	36.2	39.4	20	17.5	39.1	.	.
C. gnou	NMB8708	237	39.5	38.8	20	19.3	41.6	24.6	18.7
C. gnou	NMB9779	233.2	39.7	37.7	20.3	19.3	42.7	24.1	18.7
C. gnou	NMB8742	229.2	36.5	36.1	20.9	19.3	41.8	24.1	18
C. gnou	NMB8741	219.7	33.6	33.1	18	16.9	37.7	21.8	17.8
C. gnou	NMB7439	212.8	33.2	33.2	17.6	16.7	36.6	22.2	16.9
C. gnou	NMB8736	221.3	36	36.4	18.7	17.5	40	23.6	19.6
C. gnou	NMB9358	241	37	38.1	20.6	19.4	41.9	25.5	21.2
C. gnou	NMB7447	222.5	36.1	36.2	18.8	17.1	40.2	23.3	19.1
C.taurinus	TMAZ563	245.5	41.8	44.3	24.4	21.2	46.5	.	.
C.taurinus	TMAZ1272	253.4	41.7	44.7	24.8	22.6	46.6	.	.
C.taurinus	SAM36064	249.5	39	44.5	21	20.8	44	.	.
C.taurinus	SAM36108	258.4	41.8	44.4	22.2	22.2	45.4	.	.
C.taurinus	NMB9352	245	38.6	39	24.4	22.1	46.5	25.6	21
C.taurinus	NMB9356	259	43.6	43.3	25.8	24.2	51.7	28.6	23.2
C.taurinus	NMB8737	266	40.4	40	24.6	23.4	47.8	28.1	21.2